2016

POLYMER NANOPARTICLES IN ELECTROKINETIC CHROMATOGRAPHY

Jesse Samuel Hyslop
University of Montana, Missoula

POLYMER NANOPARTICLES IN ELECTROKINETIC CHROMATOGRAPHY

By

JESSE SAMUEL HYSLOP

Bachelor of Science, Northwest Nazarene University, Nampa, Idaho, 2009

Dissertation

presented in partial fulfillment of the requirements
for the degree of

Doctor of Philosophy
in Analytical Chemistry

University of Montana
Missoula, MT

August 2016

Approved by:

Scott Whittenburg, Dean of The Graduate School
Graduate School

Christopher Palmer, Chair
Department of Chemistry and Biochemistry

Michael DeGrandpre
Department of Chemistry and Biochemistry

Mark Cracolice
Department of Chemistry and Biochemistry

Kent Sugden
Department of Chemistry and Biochemistry

Nicholas Natale
Department of Biomedical & Pharmaceutical Sciences

POLYMER NANOPARTICLES IN ELECTROKINETIC CHROMATOGRAPHY

Advisor: Christopher Palmer

Chairperson: Michael DeGrandpre

Electrokinetic chromatography (EKC) is a prevalent analytical separation technique first introduced by Terabe *et al.* in 1984. EKC is a modification of capillary electrophoresis in which analytes are separated via selective interactions between analytes and an ionic pseudostationary phase (PSP) dispersed in the background electrolyte (BGE) buffer which fills the capillary. Application of an electric field of several hundred volts per cm on the capillary induces electroosmotic flow (EOF) of the BGE and mobility of the PSP. Various ionic PSPs are capable of fast, selective, and efficient analytical separations.

Latex nanoparticle (NP) PSPs consisting of amphiphilic block copolymers produced through Reversible Addition-Fragmentation chain Transfer (RAFT) controlled polymerization have shown promising results as PSPs. These NPs are self-assemblies of the amphiphilic copolymers less than 150 nm in diameter, consisting of copolymers with ionic moieties on one end of the polymer and hydrophobic moieties on the other. The RAFT synthetic approach allows unprecedented control over ionic head group chemistry, hydrophobic core group chemistry, degree of polymerization of hydrophilic and hydrophobic polymer blocks, and overall size of the NP. Control of NP architecture and chemistry have been predicted to provide access to unique PSP selectivities and allow optimization of NP performance.

Motivated by a desire to gain greater fundamental understanding of the structure-performance relationships for these NP PSP materials, the RAFT synthetic approach was refined and utilized to study the effects of these parameters on NP PSP performance. Many novel NPs were synthesized utilizing 2-acrylamido-2-methylpropane sulfonic acid (AMPS) monomer to form the ionic shell and butyl-, ethyl-, and methyl- acrylate to generate the hydrophobic core.

This dissertation reports the mobility, methylene selectivity, efficiency, linear solvation relationship (LSER) parameters, and practical chromatographic performance of a large set of NP PSPs and develops the first empirical relationships between NP architecture and chromatographic performance of NP PSPs in EKC.

It is found that under typical EKC conditions ionic block chemistry has little effect on performance for 5-10 mer blocks. Solute-PSP interactions appear to be localized on the hydrophobic block of the copolymer with the length of alkyl chains on the hydrophobic block controlling the cohesively and hydrophobicity of the PSP. Small (<50 nm) NPs provide higher efficiency than do large (>100 nm) NP PSPs with small hydrophobic NP PSPs providing the best overall performance.

This work provides the fundamental understanding of the behavior of RAFT polymerized NP PSPs essential for their further development and application in electrokinetic chromatography.

Acknowledgements

Thanks are due first of all to my advisor, Chris Palmer, whose guidance and assistance throughout this research has been invaluable. Thanks also to my committee for overseeing my progression through the degree and kindly allowing me office space to hide from my other responsibilities in while writing!

The support and confidence of my family through all the years of graduate school has given me a firm anchor through all the uncertainties and trials of grad school. I am grateful in particular for the confidence of my Grandmother, Julie, and her investment in my undergraduate education that has enabled me to continue that education as far as I have wished.

This work would not be possible without the contributions of the many undergraduates I have had the pleasure to work with through the years. Throughout this dissertation nanoparticles are labeled LH, HNC, and KH. Each occurrence illustrates a major contribution they have made to my research. Leah Hall's dedicated work through years of synthetic development has made much of the results reported here possible. More than that, her friendship and good humor through the vicissitudes of instruments (and their computers) helped make research much better than working! The contributions of Hungngai Chuk, Kyle Hall, and Rayel Brown have built on this base to answer fascinating questions and fill in gaps I never would have had time to pursue on my own.

The Palmer research group has also been of constant assistance from my first lab work with Andre Umansky to my continuing collaboration with Julie and Stan McGettrick.

Collaborators both within the University and without have contributed to this work as well. My EAPSI host advisor Emily Hilder and Dario Arrua, then at the University of Hobart in Tasmania, provided me not only with access to world class instrumentation and facilities, but more importantly, access to a better understanding of what it means to be a scientist. Closer to home Bill Gleason at Montana Tec and Fanny Astruc-Diaz at UMT have made their dynamic light scattering instruments available, and Earle Adams has provided both the expertise and boundless enthusiasm needed for NMR spectroscopy.

I come to Brittany Busby last, for it is the place of honor. Through all these years of struggles and stress, through countless deadlines and homework assignments, through every presentation and lecture, even when I was on the other side of the world, Brittany has steadfastly supported me through this all these years. Her counsel and comradery are reflected not only in my work but have shaped who I aspire to be.

With deepest thanks,

Jesse Hyslop

Contents

Table of Figures

List of Tables

List of Equations

List of Abbreviations

ACROSS	Australian Center For Research on Separations Science		MALDI	Matrix Assisted Laser Desorption/ionization
AMPS	2-Acrylamido-2-methylpropane sulfonic acid		mCTA	Macro Chain Transfer Agent
ANC	Acetonitrile		MEKC	Micellar Electrokinetic Chromatography
APCI	Atmospheric Pressure Chemical Ionization		MS	Mass Spectroscopy
BGE	Background Electrolyte		N	Efficiency in theoretical plates
CD	Cyclodextrin		N	Number of measurements
CE	Capillary Electrophoresis		NMR	Nuclear Magnetic Resonance Spectroscopy
CTA	Chain Transfer Agent		NP	Nanoparticle
DLS	Dynamic Light Scattering		OD	Outer Diameter
EKC	Electrokinetic Chromatography		PAH	Polyaromatic Hydrocarbon
EOF	Electroosmotic Flow		PSP	Pseudostationary Phase
ESI	Electrospray Ionization		RAFT	Reversible Addition-Fragmentation Chain Transfer
GC	Gas Chromatography		TOF	Time of Flight
HPLC	High Performance Liquid Chromatography		UV-VIS	Ultra Violet - Visible Spectroscopy
ID	Inter Diameter		V-501	4,4'-Azobis (4-cyanovaleric acid)
LC	Liquid Chromatography		VDC	Volts Direct Current
LSER	Linear Solvation Energy Relationship			

Chapter 1 Introduction

Once upon a time a man by the name of Mikhail Tswett recorded an experiment in which a mixture of chemicals were separated from one another. Using a tube filled with sand he washed a mixture of pigments extracted from tree leaves through the sand, separating the pigments from one another. The pigments that stuck to the sand most strongly washed through slowest, and so the mixture of pigments separated out into bands of color in the tube according to the stickiness of the pigments on the sand. Tswett coined the term chromatography to describe the process using the Greek words *chroma*, color, and *graphein*, to write[1]. We still use the same word to describe a system of separating compounds from one another: Chromatography [1].

Tswett first utilized what would come to be known as normal phase adsorption chromatography at the beginning of the twentieth century. By the beginning of the twenty first century, the field of chromatography encompassed a vast array of techniques utilized to separate innumerable compounds for both analysis and production. Chromatography has become one of the great enabling sciences that is utilized in almost all other fields of physical science, and many fields of biology and engineering.

1.1 Types of Chromatography
Chromatography techniques are broadly classified by either the phase in which they operate or by the primary type of interaction they utilize to induce a separation. Three fundamental types are noted here to introduce the underlying principles and terms:

1.1.1 Gas Chromatography
In gas chromatography (GC) volatile analytes are carried through the system by an inert carrier gas. Hydrogen and helium are the most common and best performing gasses for GC. The separation is induced by molecular interactions between the analytes in the carrier gas and a thin film deposited on the interior surfaces of the tube or "column" through which the carrier gas flows. Because the film is fixed to the column, it is referred to as the "stationary phase" of the system. The stickiness, or "retention," of the stationary phase towards a given analyte is determined by the difference in free energy of solvation of an analyte in the two phases. An analyte's solvation energy is the Gibbs free energy of solvation (G) of the specific analyte at a specific pressure and temperature in a specific phase as shown in Equation 1-1:

$$G_{(p,T)} = H - TS \qquad \text{1-1}$$

Intermolecular interactions between an analyte and the stationary phase are considered by the enthalpy of the interaction (H). These are dependent on the type and strength of intermolecular interactions. The influence of the entropy term (S, the tendency toward

---

[1] He also effectively named the process after himself; his name is the Russian word for color.

energy dispersal, influences the ability of the analyte to diffuse into a less ordered configuration of particles) is described in conjunction with the temperature (T) of the system. When an analyte particle is adsorbed into the stationary phase it will be restricted in available energy states and orientations and S will be relatively low; therefore the free energy of solvation will be dominated by the enthalpy of the intermolecular interactions between the analyte and stationary phase described by the H term. However, when the volatile analyte is in the carrier gas, the inert gas will provide no intermolecular interactions, and H will equal zero. The molecule has relatively few restrictions on movement, providing more states to disperse energy amongst, and the entropy will be relatively high. The free energy of solvation in the mobile phase will, therefore, only depend on the entropy and temperature.

Employing these principles the chromatographer can configure the GC system to separate an analyte of interest from unwanted species: operating at higher temperatures will increase the entropic contribution and lead to lower free energy in the carrier gas. Selecting a stationary phase chemistry that provides unique enthalpies of interaction for the analyte(s) or matrix will cause the analyte(s) to be retained in the stationary phase to different degrees. These effects cause analytes to elute at different times based on the amount of time each analyte is retained in the stationary phase rather than being moved through the column by the carrier gas.

This is the mechanism of Partition Chromatography. During its elution through the column, analytes will partition between the stationary phase and carrier gas a vast number of times. The time an analyte requires to elute is therefore the time it spends in the carrier gas plus the time it spends in the stationary phase, and the greater the free energy of solvation in the stationary phase, the greater the time that the analyte will stay in that phase. Therefore, greater enthalpy in the intermolecular interactions between the stationary phase and the analyte result in greater analyte retention in the column.

Gas chromatography most often employs micrometer thick hydrophobic stationary phase coatings on fused silica (SiO_2) capillary columns. Columns are thirty meters long or more to provide sufficient time for even very slight differences in enthalpy to result in the complete separation of small volatile molecules as they elute at different rates. The entire system is maintained at a few hundred degrees Celsius to maintain the volatility of the analyte(s). High sensitivity detectors such as mass-spectroscopy and flame-ionization-detectors are employed to detect and characterize analytes as they elute from the capillary column.

1.1.2 Liquid Chromatography

The same chromatography principles based on free energy of solvation apply to liquid chromatography (LC), the other ubiquitous chromatographic technique. However, as the name implies, LC utilizes a liquid carrier for analytes, called the mobile phase. This results in several fundamental differences. First, the enthalpy of interactions between an analyte and the mobile phase is no longer zero and can be controlled by changing the composition of the mobile phase. Second, the greater viscosity of liquids means diffusion

cannot be relied on to transport analytes as great of distances within the mobile phase to reach a stationary phase surface as that of gas chromatography. Third, the temperature range in which most liquids can be manipulated is very limited compared to GC; LC is generally held constant at, or near, room temperature.

Utilizing these differences allows chromatographers to control the intermolecular interactions at the heart of chromatography in even more ways. The low operating temperature mitigates the potential for thermal degradation of the analyte that can be problematic in GC. Liquid mobile phases also allow for analysis of high molecular mass and nonvolatile analytes, allowing a broad range of compounds to be analyzed or purified by LC that cannot be analyzed by GC because they are nonvolatile or unstable.

The reduced rate of diffusion in the liquid mobile phase necessitates that columns have very narrow flow paths to ensure that analytes consistently interact with the stationary phase and are not marooned in the middle of a flow channel where they cannot physically interact with the stationary phase. This is achieved by packing a tubular column with porous or semi-porous particles of 1 µm to 10 µm diameter, much as Tswett packed the glass tubes he used with sand, to provide a massive surface area on the particles and narrow flow paths between particles.

The surface of sand (and silica oxide, SiO_2, its more homogenous modern replacement) is naturally functionalized by acidic silanol sites that provide dipole-dipole, hydrogen bonding, and ionic interactions for analyte molecules. Often, a thin layer of water adsorbs to the silica surface, providing an aqueous stationary phase. In this system analytes are separated based on their polarity, and hydrophobic mobile phases like hexane are used to contrast the polar stationary phase. This system of polar stationary phase and non-polar mobile phase has become known as "Normal" phase chromatography, as it was the original system developed.

The inverse system of a polar mobile phase and a non-polar stationary phase was therefore named "Reversed" phase chromatography. In reversed phase chromatography the silica particles in the column are generally modified with alkyl hydrocarbon chains. The resulting hydrophobic coating provides analyte interactions through London dispersion forces. This allows reversed phase chromatography to be a more general technique as all molecules interact to some level with London dispersion forces, while not all molecules are susceptible to polar interactions.

The relative strength of the interactions can be selected in two ways: by alkyl chain length and mobile phase polarity. Functionalizing the column packing with alkyl chains two carbon links long (C2 chain) provides minimal interaction strength, while C18 functionalized columns (chains eighteen carbon atoms long) provide the maximum potential hydrophobic interactions [2], [3].

The greatest asset of reversed phase chromatography though is the ease with which the free energy of solvation can be adjusted through the mobile phase. Water is the most

common reversed phase mobile phase; its high polarity contrasts well against the non-polar stationary phase. By modifying the aqueous mobile phase with less polar, more organic, additives the overall polarity of the mobile phase can be precisely selected to provide the desired analyte retention. The pH of the mobile phase and the use of additives such as ion pairing reagents can also have significant impacts on retention and selectivity.

The improved control of chromatographic selectivity provided by LC and wider range of analytes that can be separated by it, are balanced by a few intrinsic limitations. The narrow flow paths in packed columns and viscous mobile phases generate large back pressures that require high-pressure pumps, sample injection systems, and plumbing to operate at the flow rates required for timely analysis of a sample. Analytes with solubility extremes towards either organic/hydrophobic or aqueous/polar phases prove problematic: some proteins are infamous for permanently adsorbing onto reversed phase columns, rendering the column useless.

However, the advantages of LC are more than great enough to justify the effort and expense required to overcome the limitations. For example, High Performance Liquid Chromatography (HPLC) systems typically employ pumps capable of operating at 9000 psi (600 atm) to drive water/acetonitrile mobile phases through columns several mm wide and several cm long packed with 3-10 µm particles coated with C18 alkyl chains. Almost every known detection system has been used with HPLC, but the most common are UV-Vis, mass-spectroscopy, and refractive index detectors.

1.1.3 Capillary Electrophoresis
Capillary Electrophoresis (CE) is unique from other systems in two ways: first, CE separates charged analytes based on their mobility in an electric field rather than by their retention in a stationary phase, and second, capillary electrophoresis utilizes electroosmotic flow rather than pressure-driven flow to carry analytes through the column. This provides a number of intrinsic advantages, although CE on its own is limited to the separation of ionic compounds.

Fundamental principles
In a typical CE instrument a 20,000-30,000 Volts Direct Current (VDC) potential is applied across a 30-90 cm long fused silica capillary as illustrated in Figure 1. The resulting 200-1000 V cm^{-1} electric field along the capillary causes ions in the solution to migrate towards one of the potentials based on the charge and size of the ion: Cations (+ charged ions) migrate toward the cathode (- potential), and anions (- charged ions) migrate towards the anode (+ potential).
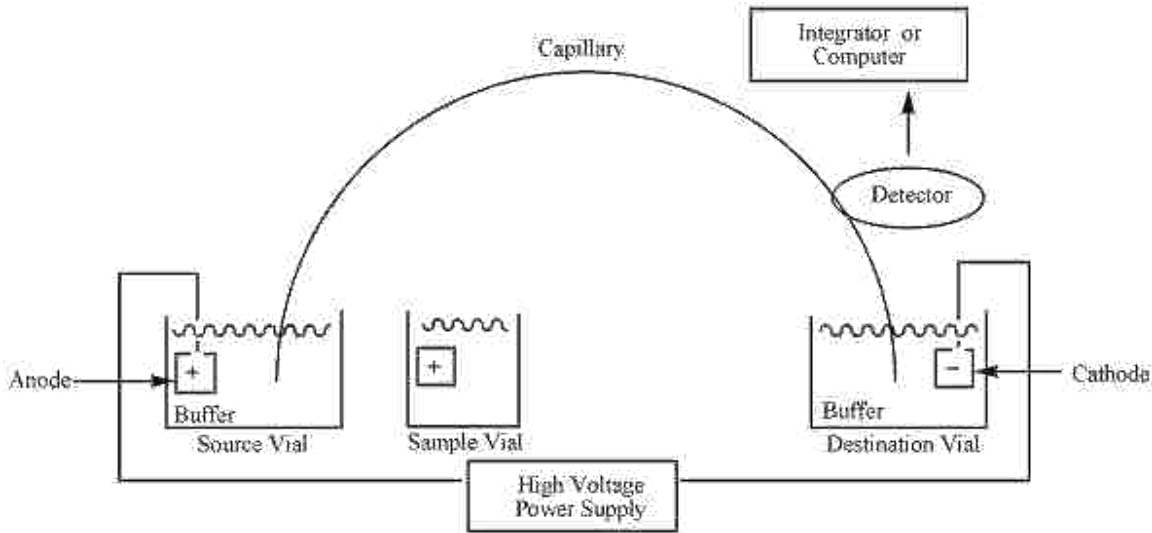
Figure 1 Capillary Electrophoresis instrumental layout [4].

The mobility of an ion (μ_{ep}) is based on the sum of the electrostatic attraction of the ion towards an electrode and the opposing force of drag the ion experiences as it migrates through the solution in the capillary. The resulting function contains terms for the overall charge of the ion (z), the viscosity of the solution (η), and the Stokes radius of the ion (r) as seen in Equation 1-2.

$$\mu_{ep} = \frac{z}{6\pi\eta r}$$

1-2

The Stokes radius is based in turn on the experimentally determined diffusion coefficient of the ion (D), the temperature (T) and Boltzmann constant (k_B), along with the viscosity of the solution (η) as given in Equation 1-3.

$$r = \frac{k_B T}{6\pi\eta D}$$

1-3

From these equations the velocity (v) of an ion in an electric field (E) can be shown to be a linear function of the field strength, the charge of the ion, and the diffusion coefficient at a given energy ($k_B T$) as seen in Equation 1-4.

$$v_{ep} = E\mu_{ep} = \frac{EzD}{k_B T}$$

1-4

Equation 1-4 shows the fundamental properties that underlay CE chromatography. First, CE will only separate ions, and the velocity of ions will increase with their charge (z). Any neutral compounds (z=0) will elute together, having no electrophoretic mobility of their own and a v_{ep} of zero. Second, the size of the analytes will determine their electrophoretic velocity. The diffusion coefficient increases with decreasing mass, so

1-5

smaller ionic analytes will migrate with higher velocity than larger ions of the same charge. Third, the velocity of migration is directly related to the electric field strength; higher field strength results in higher velocities. Higher velocities generally result in shorter analysis times.

In addition to the velocity of the ions arising from their own mobility in the electric field, the potential induces a bulk flow in the capillary as well. This Electroosmotic Flow (EOF) arises from charges on the wall of the capillary. Under non-acidic conditions the terminal silanol sites on the surface of the SiO_2 fused silica capillary are deprotonated. These anionic sites provide a negative zeta potential on the walls of the capillary, attracting a diffuse layer of cations in the 10-20 nm of solution incident to the capillary wall (See Figure 2B). This diffuse layer of cations has mobility towards the cathode when a potential is applied, and they sweep the rest of the bulk solution along with them as shown in Figure 2A.
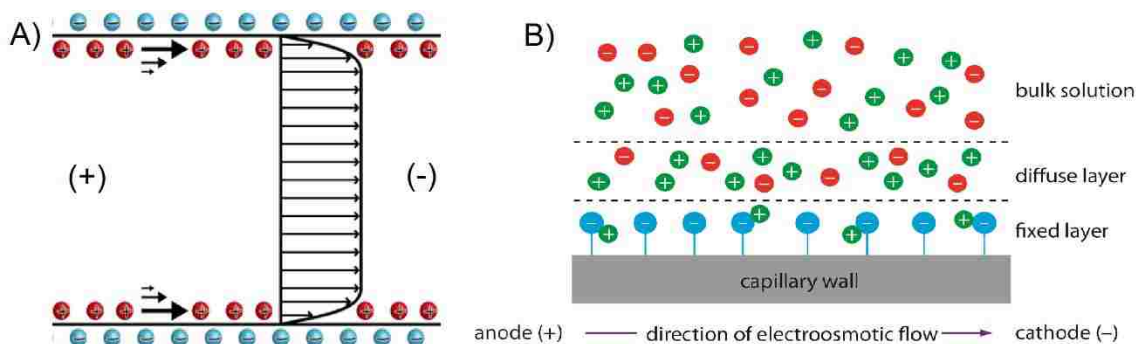
Figure 2 Electroosmotic Flow profile. A) Mobility at the capillary wall induces linear flow across the entire capillary (adapted from [5]*). B) The mobility at the capillary wall arises from a diffuse layer 10-20nm thick of cation rich solution (figure adapted from* [6]*).*

Because the bulk solution is being swept along by the solution in the diffuse layer at the walls of the capillary, the effects of drag from the wall is restricted to the diffuse layer. The rest of the solution migrates with a linear flow profile, meaning that there is no radial velocity gradient. The effects of the velocity gradient in the diffuse layer are negligible, as it only comprises a few thousandths of the diameter of the capillary.

This flat flow profile of EOF provides a great advantage over pressure driven flow. In a pressure driven system friction between the wall and the bulk solution induces a parabolic flow profile where the velocity varies from zero at the wall to twice the average velocity in the center of the channel (Figure 3). In pressure driven systems the peak broadening that results from this non-uniform flow must be accepted as part of the process, but in EOF driven systems this source of broadening is eliminated, allowing better resolution separations.
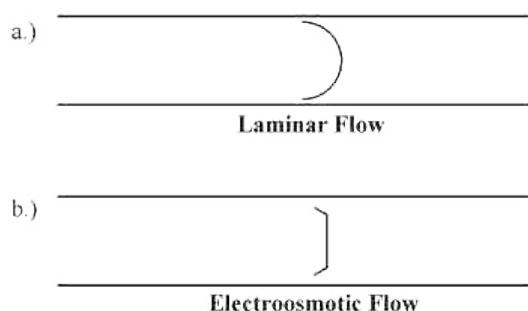
Figure 3 Flow velocity profiles for a) pressure driven flow and b) EOF.

The velocity of the analytes in the capillary will be the sum of the velocity of the analyte (v_{ep}) and the velocity of the EOF (v_{eof}) as shown in Figure 4. For cations injected at the anode end of the capillary, this means that they will rapidly elute through the capillary, allowing for rapid analysis. However, anions will migrate away from the detector. If the EOF is great enough, they may be swept past the detector eventually, but many small, highly charged anions have greater mobility than the EOF, and will elute out of the capillary at the anode. Simply reversing the potential on the capillary would allow anions with high mobility to elute past a detector on the capillary, however, the system would be inefficient as long analysis times would be required for even very high mobility anions to migrate against the EOF.
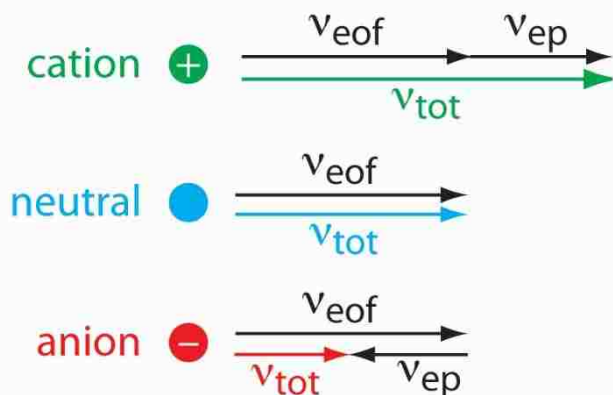
Figure 4 Mobility in CE is additive. Cations elute at the velocity of the EOF (v_{eof}) plus the velocity provided by their own mobility (v_{ep}). Neutral analytes have no intrinsic mobility and are therefore swept along at the velocity of the EOF. Because the mobility of anionic analytes is in the opposite direction from the EOF (v_{ep}) they will elute at the difference in their velocities (v_{tot}). Reproduced from [6].

To analyze anions it is therefore necessary to reverse the velocity of the EOF by switching the zeta potential of the capillary walls from anionic to cationic. This is often achieved by adsorbing a layer of cationic liposome or polymer onto the capillary wall. The cationic material binds to the wall through ionic interactions on one side of the material, and provides cationic zeta potential on the other side, attracting anions to

provide the diffuse layer, and reversing the direction of the EOF to flow towards the anode.

Types of analysis

Recalling the layout of a CE system from Figure 1, a typical CE separation can now be understood: the capillary is flushed with a buffer to ensure a uniform zeta potential on the capillary walls; a sample of ions is typically injected into the anode end of the capillary; a potential is applied, inducing EOF of the buffer and migration of the ions; the ions are detected with on-capillary detection by UV-VIS or conductivity detectors, or by post-column detection with mass spectrometry; and finally, the capillary is flushed with fresh buffer to prepare it for the next run.

Analysis of cations is conducted with normal EOF and anions with reversed EOF by coating the capillary with cationic material. Atomic and small molecular ions in simple low ionic strength matrixes are often analyzed by on-column conductivity detection. However, CE really shines as a preliminary separation for analysis of larger molecules by mass spectrometry (MS). A number of devices have been employed to interface CE with MS. Electrospray Ionization (ESI) is the most widely used MS interface. This is further developed in the 5.6.3 Detector Compatibility section on page 5-105. The incredible power of CE-ESI-MS as an analytical detection/ characterization technique will be seen to motivate much of the work in Chapter 2 - The Development of the PSP.

Limitations

The obvious limitation of CE is that it is only applicable to ions. Neutral, uncharged, analytes are swept through the capillary by the EOF, but CE on its own provides no mechanism to separate them from one another.

CE also utilizes injection volumes as small a few nL: this small injection volume is typically an advantage because less sample is required, but it does mean that high sensitivity detectors must be employed to detect the extremely small amounts of analyte that are separated by CE. The zeta potential of the capillary is effected by the pH of the buffer as well, so the operational pH may be limited to a particular range to provide the desired EOF or analyte ionization.

1.2 Electrokinetic Chromatography

To recap, Capillary Electrophoresis (CE) provides a number of significant advantages over other LC techniques even with the few limitations it has; the separations are generally very fast, very little sample is needed, no complicated (and expensive) pumps or valves are required, and the system is both very rugged and amenable to miniaturization as a field-portable device. In laboratory settings the ability to pair CE with many detection systems and extremely fast reconditioning time between runs is valuable. Another intrinsic advantage is the linear flow profile provided by the EOF. This allows CE to reach levels of separation efficiency far above even the best HPLC systems. However, CE is unable to separate neutral analytes.

In 1984 Shigeru Terabe and coworkers at Kyoto University, Japan, introduced Electrokinetic Chromatography (EKC) as a technique to separate neutral analytes using a CE instrument [7]. The technique Terabe demonstrated employs anionic micelles (discussed in detail on page 2-20) to provide hydrophobic selectivity for neutral analytes. The charged micelles in turn provided electrophoretic mobility to retained analytes. As illustrated in Figure 5, the anionic micelles migrate against the EOF with about half the velocity of the EOF. This results in the micelles being swept towards the cathode.

This velocity difference is translated to neutral analytes based on the fraction of the time they spend in the micelle (partition coefficient) between the buffer and the micelles: analytes that do not interact with the micelle are swept out of the capillary at the velocity of the EOF, while analytes with high affinity for the hydrophobic micelle cores are retained in the micelles, and elute at the slower velocity of the micelle.
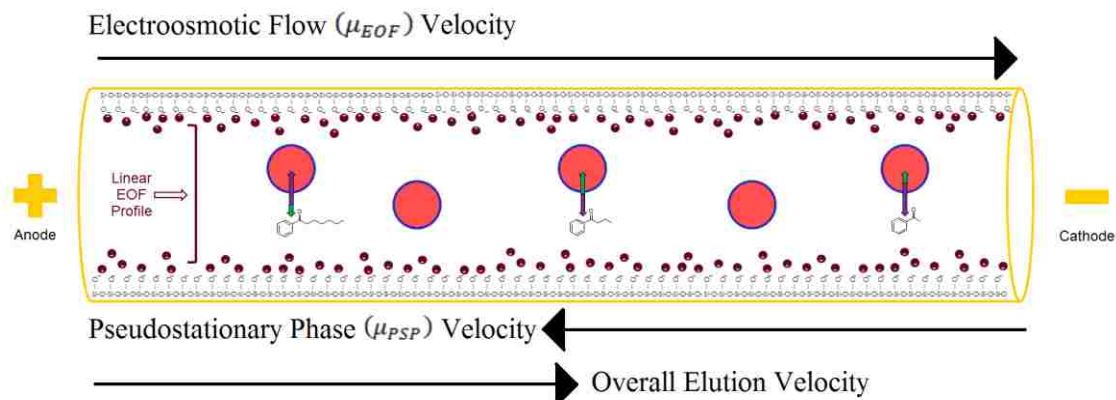
Figure 5 Electrokinetic Chromatography with anionic PSP. Bulk EOF caries analytes and PSP towards the cathode with velocity μ_{EOF} while the mobility of the PSP provides a velocity μ_{PSP} towards the anode. The overall elution velocity of the PSP is thus $\mu_{EOF} - \mu_{PSP}$. Analytes will elute at velocities between that of the EOF and PSP based on their affinity to the PSP.

Because the micelle produces a separation by retaining and slowing analytes, it is analogous to the stationary phase in LC. However, unlike LC stationary phases, the micelles are not fixed to a stationary surface; while they elute at a reduced velocity, they still elute from the capillary. For this reason the phase is called a Pseudo Stationary Phase (PSP).

1.2.1 Fundamental principles
EKC separates analytes by differences in elution velocity. The fastest velocity a neutral analyte can have is that of the EOF, while the slowest velocity is that of the PSP. While most compounds have some retention in the PSP, a few, such as acetone, methanol, and dimethyl sulfoxide, have such weak interactions that they can be considered to migrate at the velocity of the EOF and are therefore used to mark the elution time of the EOF. This time is referred to as t_0.

The minimum velocity can be measured directly by observing the elution time of a compound that is very highly retained by the PSP such as naphthalene or Sudan III, or by iterative numerical methods from a homologous series of analytes (see 4.1.2 Chromatographic characterization on page 4-56). Both methods give t_{PSP}, the elution time of the PSP. These times are denoted on the chromatogram in Figure 6.
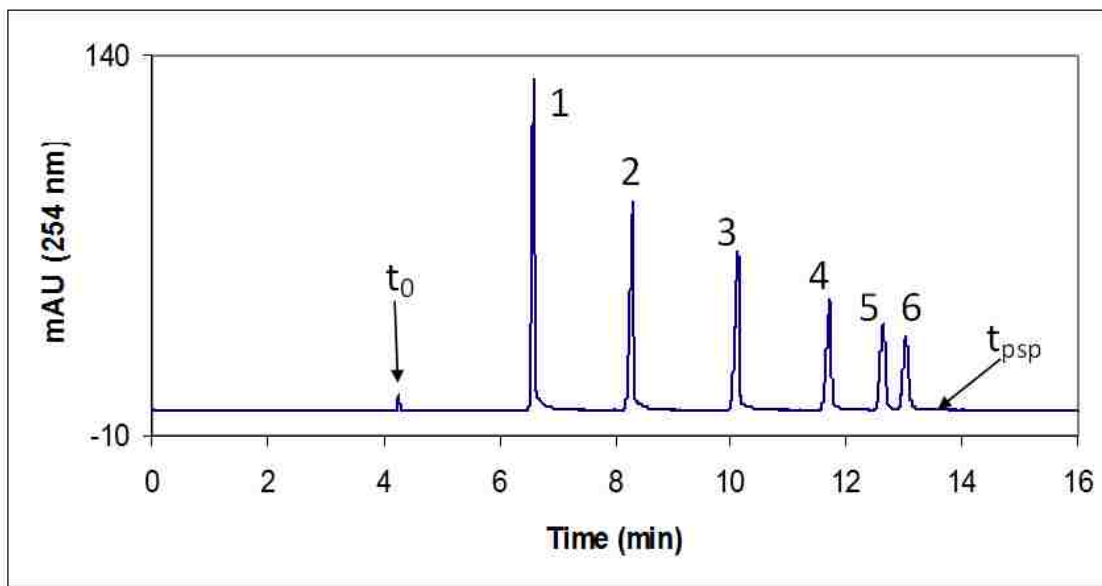
Figure 6 EKC separation of six phenones reproduced from [8]. t_0 is acetone, 1. acetophenone (k=1.1), 2. propiophenone (k=2.4), 3. butyrophenone (k=5.4), 4. valerophenone (k=12), 5. hexanophenone (k=30), 6. heptanophenone (k=72). 50 mM SDS in 20 mM TRIS buffer at pH 7.0.

The velocity, and thus the retention time (t_r), of any neutral analyte is therefore based on the fraction of time the analyte spends in the background electrolyte vs the time it spends in the PSP. This fraction is measured by the retention factor (k) given in Equation 1-5.

$$k = \frac{t_r - t_0}{t_0 \left(1 - \frac{t_r}{t_{PSP}}\right)}$$

1-5

All of the times measured to determine the retention factor in Equation 1-5 include the effects of the EOF velocity, and the EOF is highly dependent on the zeta potential of the capillary. The zeta potential is known to vary enough to significantly impact results from run to run. Unfortunately it is not practical to measure t_{PSP} on every run to normalize for these variations in potential. To mitigate this, chromatographers determine the mobilities of each component of the system and calculate retention factor from the mobilities.

The mobility of the PSP is independent of the EOF and only depends on the charge and size of the PSP (Equation 1-2). It is typically about half the magnitude of the EOF and in the opposite direction. Once the mobility of the PSP (μ_{PSP} in Equation 1-7) is determined from an accurate measurement of t_0 and t_{PSP} from the same run, the μ_{PSP} can be

considered constant in that specific buffer system. The apparent "mobility" of the neutral analytes is a function of the μ_{PSP} and the retention factor of the analyte in the PSP arising from the difference in the free energy of solvation between the buffer and PSP (Equation 1-1).

$$\mu_{EOF} = \frac{L_D \cdot L_t}{V \cdot t_0 \cdot 60} \cdot 10^4 \qquad \text{1-6}$$

$$\mu_{PSP} = \left(\frac{L_D \cdot L_t}{V \cdot 60}\right)\left(\frac{1}{t_{PSP}} - \frac{1}{t_0}\right) \cdot 10^4 \qquad \text{1-7}$$

$$\mu_r = \frac{L_D \cdot L_t}{V \cdot t_r \cdot 60} \cdot 10^4 \qquad \text{1-8}$$

Term	Value	Units
μ_r	Mobility of an analyte	$10^{-4}(cm^2/V \cdot s)$
L_D	Capillary length to detector	cm
L_t	Total capillary length	cm
V	Voltage applied	VDC

Table 1 Mobility units and factors.

This means that by describing t_r and t_{PSP} in terms of their mobilities, the variations in EOF can be fully quantified by measurement of only t_0. Although variations in t_0 from fluctuation in zeta potential will appear in the t_r used in Equation 1-8 as well, the μ_r term experiences co-dependent variance with the μ_{EOF}, effectively accounting for the variation in t_r. The retention factor can thus be defined in terms of mobility in Equation 1-9.

$$k = \frac{\mu_{EOF} - \mu_r}{\mu_r - (\mu_{EOF} + \mu_{PSP})} \qquad \text{1-9}$$

By using the retention factor, selectivity between different analytes can be quantified by the ratio between their retention factors. This is the selectivity term (α) given in Equation 1-10 where k_1 is the retention factor of the less-retained analyte, and k_2 is that of the more strongly retained and later eluting analyte. This convention assures that α will always be greater than one. This begs the question "how much selectivity is needed to separate two analytes?" To answer this, efficiency and resolution must be introduced.

$$\alpha = \frac{k_2}{k_1} \qquad \text{1-10}$$

While selectivity quantifies the separation between two compounds, efficiency (N) considers how wide of a band the analyte has diffused into at the point of measurement. This can be measured in a number of ways in units of time or distance, but what the different forms shown in Equation 1-11 all share is that they measure of how far the compound has moved as measured by the length of the capillary to the detector (L_D) or retention time (t_r) divided by how wide the concentration band has become. This width can be described by the variance (σ^2), product of diffusion and time ($D t_r$), or by the width of the peak (w).

1-11

$$N = \frac{L_D^2}{\sigma^2} = \frac{L_D^2}{2Dt_r} = 16\left(\frac{t_r}{w}\right)^2 \qquad \text{1-11}$$

Efficiency is one of the terms that begins to illustrate the power of CE based separations. High efficiency means that analytes with even very small differences in selectivity can be resolved from one another because the analytes remain in narrow bands that only require slight separation to no longer overlap one another. While GC can have an efficiency of N ≥ 100,000 in a few minute separation, CE and EKC can do the same in a liquid phase in the same time or less. This eclipses HPLC that typically can only generate an efficiency of 20,000 in a normal ten-minute run.

The separation between two bands of analyte can be quantified by using these chromatographic terms in the master resolution equation (1-12). A resolution value of zero means the compounds are not separated from one another at all, while a resolution of 1.5-2 means there is just base line resolution between the peaks (ex. between peaks 5 and 6 in Figure 6). To achieve an R_s of 1.5 or above, Equation 1-12 shows there must be some retention ($k{\neq}0$), some difference between k_1 and k_2 ($\alpha{\neq}1$), and as little broadening as can be achieved (N>>0).

$$R_s = \frac{\sqrt{N}}{4} \cdot \frac{\alpha - 1}{\alpha} \cdot \frac{k}{k - 1} \qquad \text{1-12}$$

The master resolution equation must be modified for EKC however. In traditional affinity chromatography increasing retention factor always increases retention time. However, in EKC, no matter how great the retention factor becomes, the retention time can never exceed the t_{PSP}. This means that another term must be added to the master resolution equation to relate the maximum retention that can be achieved in EKC to the mobility of the PSP as shown in Equation 1-13.

$$R_s = \frac{\sqrt{N}}{4} \cdot \frac{\alpha - 1}{\alpha} \cdot \frac{k_2}{k_2 - 1} \cdot \frac{1 - \dfrac{t_0}{t_{PSP}}}{1 + \left(\dfrac{t_0}{t_{PSP}}\right)k_1} \qquad \text{1-13}$$

The consequence of this fourth term can be seen when the product of the third and fourth terms are plotted in Figure 7 as a function of k for various ratios of t_{PSP}/t_0. In the case of a true stationary phase $t_{PSP} = \infty$ (it never elutes) and Equation 1-13 reduces to Equation 1-12. The contribution of retention to overall resolution in this case is given by the red line in Figure 7. Beyond a retention factor of ~ k = 10 (the analyte spends ten times more time in the PSP than the mobile phase) there is limited contribution to resolution from increasing k.
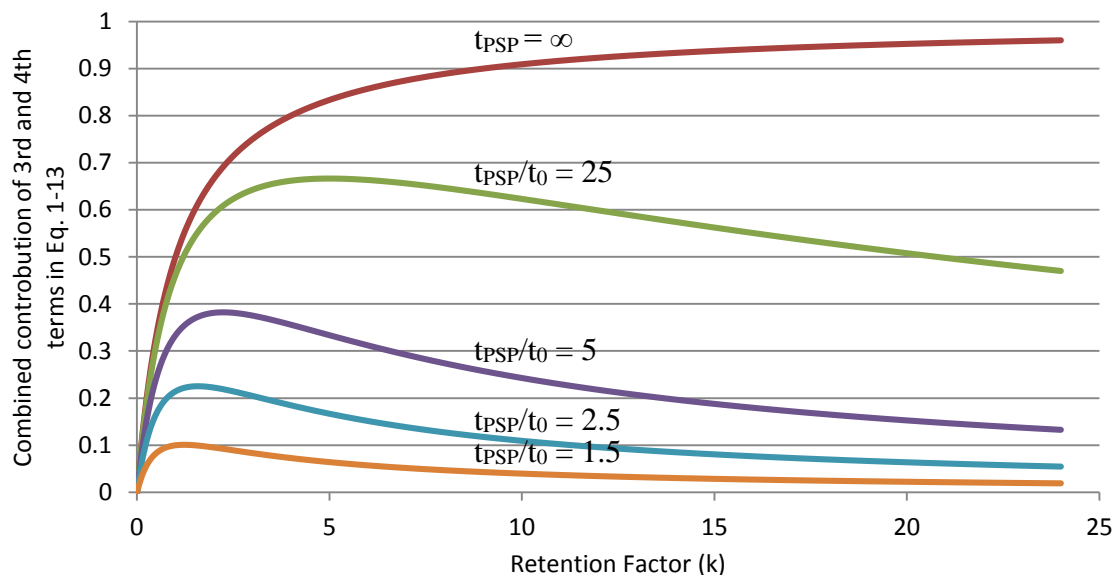
Figure 7 Contribution of third and fourth terms of Equ 1-13 plotted as a function of retention factor (k).

However, for an EKC system where $t_{PSP} \neq \infty$, increasing retention factor beyond an optimum value will decrease the resolution of the separation as the highly retained analytes begin to clump together against the end of the separation window at t_{PSP}. Therefore, for EKC there exists an optimum retention factor that places the analyte in the middle of the separation window between t_0 and t_{PSP} and maximizes the retention factor contribution to the overall resolution of the separation. Figure 7 also illustrates that increasing the mobility of the PSP, thus increasing the t_{PSP}/t_0 ratio, enables a greater contribution to the overall resolution to be achieved. This illustrates an advantage provided by PSPs with high mobility relative to the EOF.

In addition, Figure 7 illustrates the advantages that changing mobile phase composition in LC and EKC can provide: by adding more organic non-polar solute to the mobile phase the retention factor for analytes can be controlled to provide optimum retention for fast separations. While the overall contribution of the retention term can be maximized through controlling the retention factor, higher mobility PSPs will also provide a wider separation window that will provide better resolution at the cost of increased analysis time.

The effect of the selectivity term is straightforward: the greater the difference in selectivity, the greater the difference in analyte elution velocities, and the further apart the resulting peaks will be on a chromatogram. In context of the master resolution equation, the main question chromatographers are interested in is how little selectivity can still provide a baseline resolution of $R_s = 1.5$? This is significant because differences in retention factors, and thus selectivity, arise from differences in chemical structures of the analytes that provide differing levels of free energy of solvation. Thus the less

selectivity that is needed to achieve a resolution of 1.5, the less differences there must be in the analytes to separate them by chromatography.

Thus we see that the master resolution equation allows us to correlate how the chromatographic performance terms inter-relate and impact one another. From this framework the design objectives for a PSP can now be described. The ability of the PSP to perform chromatography will depend on these four terms (μ_{PSP}, k, α, and N) for a given set of analytes.

1.3 Pseudostationary phase properties
To chemically govern the chromatographic terms μ_{PSP}, k, α, and N chromatographers may use a number of techniques; modifying the mobile phase with an organic solvent to govern the retention factor is one of the examples already noted.

An ideal PSP will be compatible with all such techniques and the capability of the PSP can be broadly described by its performance in seven categories.

1. Mobility – μ_{PSP} is a function of the charge on the PSP. A PSP with highly ionized moieties that remain ionized over a wide pH range enables the pH of the mobile phase to be changed to facilitate separations. Increasing PSP mobility also improves the t_{PSP}/t_0 ratio.
2. Stability – The stability of the PSP in organic modifiers and detectors effects the level of control that can be exerted on retention factor and may enable or preclude the use or some detectors such as ESI-MS.
3. Conductivity – The impact of the PSP on the overall conductivity of the solution in the capillary is the primary limiting factor of the electric field strength that can be employed, and thus, of the overall speed of EKC. Excessive conductivity leads to Joule heating that cases loss of efficiency [9].
4. Mass Transfer – Mass transfer of analytes between the PSP and mobile phases must be rapid and consistent to avoid peak broadening [10].
5. Mono-dispersity – The PSP must be uniform in terms of mobility, stability, and permeability; the presence of two phases of PSP with inconsistent behavior could result in broadening and loss of efficiency [10].
6. Detector compatibility – The PSP must be compatible with the desired detectors. For UV-Vis the PSP must not contain chromophores or scatter light; for mass spectroscopy detectors the PSP should not suppress analyte ionization or interfere with detection.
7. Selectivity – The PSP must be able to solvate the analyte and provide unique solvation energy based on analyte structure.

1.3.1 Mobility

The mobility of the PSP arises from acidic or basic moieties on the PSP that are ionized under EKC conditions. For anionic PSPs theses are often carboxylic acids or sulfonic acids and for cationic PSPs ammonium moieties are most often employed. When considering or designing a material for use as PSP, care must be taken that the material will remain ionized at the intended operational pH; ideally it will remain ionized over a very broad pH range so one PSP material may be employed in a variety of EKC conditions. For example, the low pKa of sulfonic acid moieties allows PSPs with such chemistry to operate from basic conditions to moderately acidic pH without loss of mobility from protonation of the acid.

1.3.2 Stability

One of the advantages of liquid based chromatography is the control of retention factor it affords chromatographers through changing the composition of the mobile phase. This is an advantage as it allows one stationary phase material to be used in the separations of analytes with vastly different enthalpies of interaction with the stationary phase by simply adjusting the composition of the mobile phase to provide comparable enthalpies towards the mobile phase as needed from one analyte to the next. The same can be done with EKC only if the PSP is stable in the organic modifiers that are employed.

Stability also affects the types of detectors that can be used with EKC. Because the PSP elutes through the detector in EKC, unstable PSPs can interfere with the operation of some detectors or contaminate the detected spectra. Surface active surfactant based PSPs in particular can suppress ionization and may interfere with detection in electrospray ionization mass spectroscopy (ESI-MS) detectors. The lack of structural stability for these PSPs limits them from being used with MS detectors.

1.3.3 Conductivity

The conductivity of the buffer solution provides the primary limit on the electrical potential that can be applied to the capillary, and thus to the maximum velocities in the system. As conductivity in the capillary increases the power dissipated from the capillary as heat must also increase based on the power law. Beyond some point the capillary can no longer dissipate the heat fast enough to maintain a uniform temperature throughout the capillary. When this occurs, a radial temperature gradient is formed with elevated temperatures in the core of the capillary, impacting the partition coefficient of the analyte towards the PSP, as well as the viscosity of the mobile phase. This causes analytes to experience different elution velocities depending on their radial location in the capillary, leading to significant band broadening and loss of efficiency [9].

This effect is called Joule Heating and it effectively limits the maximum electrical field strength that can be successfully applied to an EKC separation. The requirement for low conductivity therefore favors PSPs with a strong affinity for analytes as they can function at low concentrations so they have less impact on the overall conductivity. This also means that PSPs that do not introduce excess counter ions or highly conductive monomers are also preferred.

1.3.4 Mass Transfer

Mass transfer describes the ability of analytes to partition in and out of a PSP. The PSP should allow an analyte to rapidly transition from the mobile phase to the PSP and back again relative to the time scale of its axial movement through the capillary. Slow analyte partitioning results in loss of efficiency as discussed in greater detail in on page 5-87. The ionic moieties should also not inhibit the movement of analytes between the phases.

1.3.5 Mono-dispersity

Mono-dispersity in PSP performance and analyte interactions (measured by the variance in chromatographic terms μ_{PSP}, k, α, and N) is required to provide uniform behavior. This is most directly achieved by reducing polydispersity in PSP size and ensuring uniform chemical composition of the PSP. Large variance coupled with poor permeability can result in large magnitudes of band broadening and poor peak shape [10].

1.3.6 Detector compatibility

As discussed above in stability, surface active and surfactant based PSPs have serious compatibility concerns with ESI-MS detection. Detector compatibility is a broader concept than just which detectors can or cannot be used however. For UV-Vis detectors the intensity of light passing through the capillary, and therefore the PSP too, must be accurately measured. Therefore PSPs should not contain chromophores that interfere with the absorption spectra of the analytes. In addition, the PSPs must be small enough to avoid Mie scattering of light in the UV region of the spectrum. This effectively limits PSP particle diameters to 150 nm or less.

1.3.7 Selectivity

The final characteristic of a PSP considered here is selectivity. The desired selectivity for a PSP is determined by the nature of the analyte, or type of analytes, that the PSP is to be used to separate by EKC. The conceptual goal of chromatographic selectivity is to provide moderate retention to the analyte of interest and either no retention or very high retention to everything else that may be present. This would cause any impurities or matrix that impedes identification and quantification of the analyte to elute before or after the analyte, allowing measurement of the pure analyte without interference.

More realistically though, chromatographers typically wish to separate and quantify a mixture of many analytes simultaneously. To do so by EKC the PSP must provide retention to all the analytes of interest, but that retention must vary just enough from analyte to analyte to allow them to be separated from one another, as well as from the sample matrix. The most broadly applicable type of interaction is van der Waals forces present between molecules. These are most noticeable in neutral hydrophobic compounds where there are no stronger types of interactions, like hydrogen bonding, available to over-shadow them. Van der Waals forces include dipole-dipole interactions, dipole-induced dipole, and London dispersion forces from instantaneously induced dipoles.

So for exactly the same reasons as reversed phase LC, EKC employs hydrophobic PSPs to separate analytes in an aqueous mobile phase. The hydrophobic PSP interacts with analytes through van der Waals forces while generally avoiding stronger interactions with the analytes.

1.4 Advantages and applications of EKC

Electrokinetic Chromatography shows promise for a large number of the areas HPLC chromatography is employed in. Although a great deal of excitement and attention was focused on EKC for more than a decade after its 1984 introduction, EKC remains one of the lesser known chromatographic tools. The excitement was due to the many chromatographic advantages EKC offers, while the limited application EKC has experienced is primarily a result of irreproducibility in the technique that has proven extremely difficult to overcome.

Still, EKC offers unique capabilities that are advantageous for specific applications and for several developing fields of chromatography. The relatively simple CE instrument can be highly robust and lends itself well to miniaturization. This is of particular value for security applications such as explosives detection or drug analysis in the field. Miniaturization can go as far as etching flow paths onto glass slides to provide separations on a system a few cm in size as in lab-on-a-chip applications.

The high efficiency of EKC enables separations to typically be conducted much faster than in HPLC, and for compounds with less selectivity. This is possible through the elimination of many of the mechanisms of band broadening that exist in HPLC. For example, a consequence of the linear flow profile provided by EOF is the elimination of band broadening from pressure-driven flow. This is an immense advantage as the primary source of band broadening that remains in EKC is expected to be analyte diffusion. The elimination of any additional "plumbing" between the injection of a sample at one end of a capillary and the detection at the other eliminates extra-column band broadening from fittings and valves that are required in HPLC.

The relatively high speed of EKC separations makes them particularly useful for near real-time monitoring or for high throughput environments where large numbers of samples must be analyzed.

Samples are injected by filling the inlet end of the capillary with a mm-to-cm long plug of sample solution. EKC capillaries are 25-75 µm in diameter so the volume of sample injected is measured in nL. These incredibly small injection volumes can provide a great advantage for the analysis of extremely small samples such as individual cells [11] or micro-scale synthesis products.

These advantages have led to the use of EKC in the pharmaceutical industry for rapid analysis of synthetic products and qualification of final products; security services look to CE and EKC for detection and identification of explosives and controlled substances, often in mobile, field based labs; environmental analysis of pollutants and natural

systems continues to be researched; and recently the newer fields like metabolomics have begun to employ EKC and CE as preparatory separations for analysis by MS.

However, the limited separation "window" between t_0 and t_{PSP} does limit the peak capacity of EKC and the diversity of analytes that can be separated in a single run. Thus, the real power of EKC is in the rapid separation of around ten analytes of similar structure and chemistry.

1.5 Limitations

Despite the many advantages of EKC, the technique has seen limited application in industry. The primary limitation of EKC is the poor reproducibility of the technique in comparison to the existing standard of HPLC. Because the velocity of both the EOF and PSP are related to their degree of charge (Equations 1-2 and 1-4) the retention time of an analyte is heavily influenced by the buffer conditions; even subtle variations in pH or ionic strength of the buffer from run to run result in significant variations in retention times for t_0, t_r, and t_{PSP}. Under optimum conditions a run-to-run retention factor RSD of at more than one percent is typical, and five or even ten percent RSD is not uncommon for analytes with either very high or low retention factors.

To mitigate this, chromatographers calculate apparent mobilities for analytes rather than using retention times to identify species. This accounts for variations in the EOF from changing zeta potential on the capillary wall, but it does not account for variations in the mobility of the PSP (μ_{PSP}) as discussed with Equation 1-9. To minimize this effect the PSP must be designed to be relatively insensitive to its chemical environment. Even with stable PSP chemistry, EKC should be expected to have some variability in EOF and μ_{PSP} from run to run.

The variability in elution velocities excludes retention time alone as the method of identifying analytes as is typical in HPLC. This variability further recommends the use of highly selective detectors (like MS detectors) for use with CE and EKC as the selective detector can be relied on to definitively identify the analytes despite the variability in apparent mobility. Unfortunately, coupling an instrument valued for its simplicity and robustness (CE) with the most complex and expensive detectors on the market (MS) is not an optimum solution; the disadvantages of the detector void many of the advantages of the instrument.

Finally, CE is a purely analytical instrument. Unlike HPLC that can be scaled up to preparatory scale separations of grams or even kg of a sample, CE based techniques are intrinsically limited to ng scales of sample due to the minute volume of the capillary column.

1.6 Conclusions

Separations are one of the cornerstones of scientific investigation in physical science and fields as diverse as engineering and cosmetics. The same fundamental principles of retention based on free energy of solvation apply to the various techniques that are utilized to separate mixtures of analytes either to purify a particular compound or to allow the identification and quantification of the compounds present in the sample.

Among the many techniques, CE is particularly suited to rapid analysis of ions. CE provides extremely high separation efficiency because of the linear flow profile generated by the EOF. On-column detection with UV-Vis or conductivity detectors further maintains the high efficiency of the technique by eliminating extra-column band broadening sources. CE can also be paired with MS detectors to provide high sensitivity and high selectivity detection. These advantages make CE-MS a valuable tool for some of the most challenging separations undertaken today in proteomics and metabolomics, although it is not applicable for in-field or miniaturized analyses.

EKC extends the advantages of CE to analysis of neutral analytes while simultaneously providing alternate selectivity to charged analytes as well. At the heart of EKC is the PSP. The chemistry and behavior of the PSP determine the contrast in free energy of solvation between the mobile phase and the PSP which elute at alternate velocities. The properties the PSP should possess or provide can be summarized in the seven terms discussed above: mobility, stability, conductivity, mass transfer, mono-dispersity, detector compatibility, and selectivity.

The need for PSPs that can simultaneously perform well in all seven categories has always been the greatest challenge facing EKC. Chapter 2 provides a history of the development and refinement of PSPs through the last thirty years of literature leading to this work in which the behavior and performance of the most advanced generation of PSP yet is reported.

Chapter 2 The Development of the PSP

The pseudo stationary phase is the heart of electrokinetic chromatography. From the introduction of EKC in 1984 to the present, PSP development has remained the core area of research, and the fundamental source of limitations, for EKC. To fully understand the motivations and significance of this work, this chapter will review the evolution of PSP technology over the last thirty years that culminates in this investigation of the fundamental relationships between PSP architecture and performance in the most advanced PSPs yet developed.

Many reviews have been published detailing the incremental development of PSPs [8], [12]–[17] and MS detectors and applications [18]. In this chapter the developments will be set out by each class of PSP to better illustrate the progressive nature of those developments and the way each as leveraged the successes of the earlier generations of PSPs.

2.1 Micelles

The original report of EKC by Terabe and coworkers utilized micelles of sodium dodecylsulfate (SDS) surfactant as the PSP to conduct what is called micellar electrokinetic chromatography (MEKC) [7]. Above the critical micelle concentration (CMC) surfactants (such as SDS) aggregate to form micelles in aqueous solutions. This aggregation is driven by the favorable change in free energy experienced by the hydrophobic tails of the surfactant molecules when segregated from water in the core of a micelle, rather than in the bulk aqueous solution, as illustrated in Figure 9. This favorable free energy change is opposed by the electrostatic and/or steric repulsion between the ionic/polar head groups of the surfactant and their associated water [19].
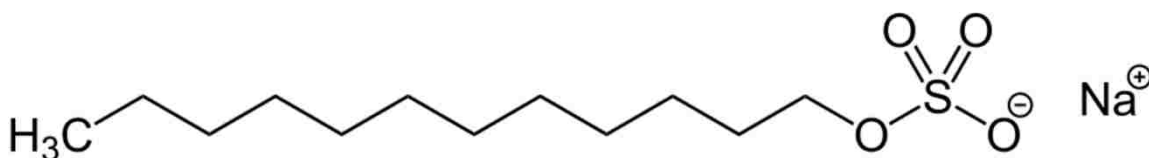
Figure 8. SDS surfactant.

The core of the micelle is a dynamic, hydrocarbon-like, volume of randomly oriented and intertwined hydrocarbon groups. However, the viscosity of this hydrophobic core may be ten times that of a neat sample of a similar mass hydrocarbon [20]. The "shell" of the micelle contains the polar moieties, bound counterions, and associated water. This "shell" is also a dynamic environment: the net charge on an ionic micelle is less than the aggregation number (number of surfactant molecules in the micelle), indicating that a significant fraction of counterions remain associated with the micelle.

Features of this zone have been described by a number of researchers using a number of terms: some terms are defined here. The Stern layer is comprised of the counterions associated with the micelle and extends from the counterions bound to the ionic groups of

the surfactant to the hydrodynamic shear surface defined by the interface between water molecules that move with a micelle through the bulk solvent and the water that does not migrate with a moving micelle. The Gouy-Chapman layer extends further, containing all the counterions needed to maintain electrical neutrality.
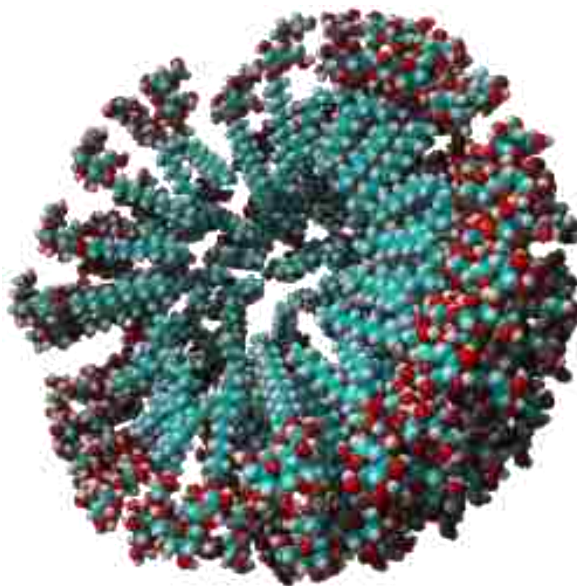
Figure 9. Micelle of surfactants aggregate to self-solvate their hydrophobic moieties in the micelle core with ionic "shell" on exterior. Generated from [21].

For SDS in water the CMC is ~5.5 mM [22] with some variation based on the ionic strength of the solution. Above this concentration adding further SDS will cause the additional SDS to aggregate into micelles. However, as with any micellar system, there will always be a background concentration of free surfactant in solution equal to the CMC. In water the aggregation number is typically around 65-95 [23], [24] but is strongly impacted by the ionic strength of the solution; more counterions provide increased shielding of the ionic head groups of the surfactant, allowing tighter packing of the surfactant and higher aggregation numbers.

Terabe used a 50 mM SDS solution for his original MEKC work and this has remained the standard to which all other PSPs are compared. The reason for this is that SDS is a remarkably good PSP that is readily available in high purity and low at cost, and it is difficult to improve upon it. In chapter 1 the seven properties of PSP performance were introduced (pg. 1-14): mobility, stability, conductivity, permeability, mono-dispersity, detector compatibility, and selectivity.

Describing the performance of SDS in these terms, the sulfate ionic groups provide outstanding mobility (-4.05×10^{-4} cm^2 V^{-1} s^{-1} [25]) and remain ionized to relatively low pH. The stability of micellar PSPs however is poor in both organic modifiers and in ESI-MS detectors. The presence of organic modifiers in a micellar solution reduces the

difference in the free energy of solvation for the hydrophobic moiety of the surfactants by increasing the solubility of the free surfactant in solution. This raises the CMC at which micelles begin to form as shown in Figure 10.
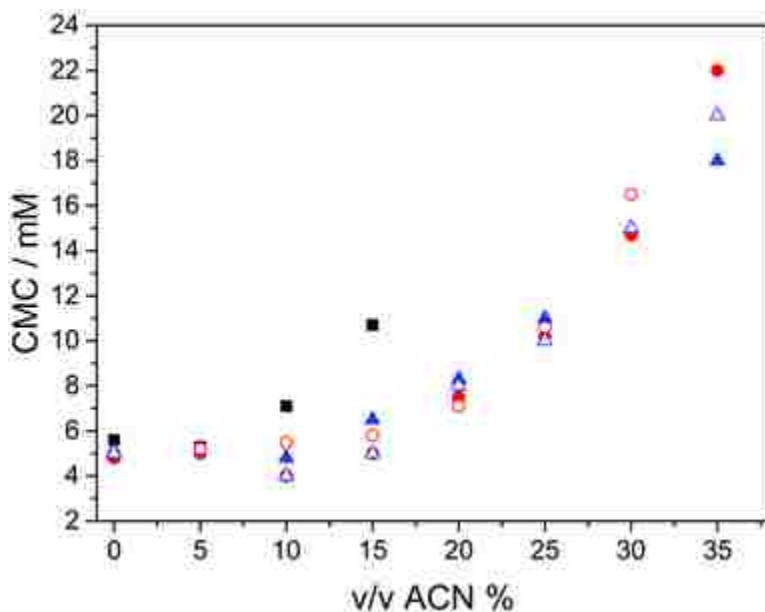
Figure 10. Increase in the CMC of SDS as acetonitrile modifier content increases. Reproduced from [22]. "Shape of the symbol corresponds to the method of determination; squares: conductivity measurements; solid circles: mobility of naphthalene; transparent circles: mobility of the system peak; solid triangles: intensity of coumarin 153; transparent triangles: fraction of rhodamine 123."

The sensitivity of SDS to organic modifiers marks the first limitation of SDS as a PSP. The CMC defines the amount of free surfactant in solution, and that free surfactant directly affects the conductivity.

A second limitation of SDS stability is that in ESI, surface active surfactants like SDS interfere with droplet nucleation and ion transfer to the analytes, suppressing ionization. For this reason micellar PSPs are incompatible with ESI-MS detection unless complicated partial-filling or filtering techniques are employed to prevent the PSP from eluting into the detector [26]–[29].

The third parameter, conductivity, is among the most significant limitations of micellar PSPs. The conductivity of the system is based on the total concentrations of ions, including free surfactant. For surfactant based PSPs, like SDS, with moderate to high CMC, the contribution to conductivity from the PSP is often much greater than the contribution of the BGE. For example, a typical 10 mM borate or tris BGE buffer will conduct ~7.5 µA through a 50 µm by 50 cm capillary with applied potential of 20 kV. The same buffer with 50 mM SDS will conduct ~35 µA. The mechanism by which conductivity limits EKC performance is called Joule Heating, and its effect on efficiency in EKC has been extensively researched by Davis et al. in several papers [9], [30].

During the run the power conducted through the capillary must be dissipated as heat from the capillary. Above ~0.2 W/m the capillary cannot dissipate the heat fast enough to maintain a uniform temperature profile across the capillary. With active cooling this can be improved to ~1 W/m. However, at some point the resulting radial temperature gradient begins to affect the behavior of the interaction between the analytes and the PSP. The variation in temperature results in a variation in the partition factor of the analytes between the mobile phase and PSP as a function of radial position in the capillary, meaning that analytes are less retained by the PSP in the hotter core of the capillary than they are near the cooler walls of the capillary. Less retention translates to faster migration velocities, causing band broadening as analytes in different domains of the capillary migrate at different velocities. The solution in the different temperature domains also undergoes convective mixing, further broadening the analyte concentration bands as shown in Figure 11.
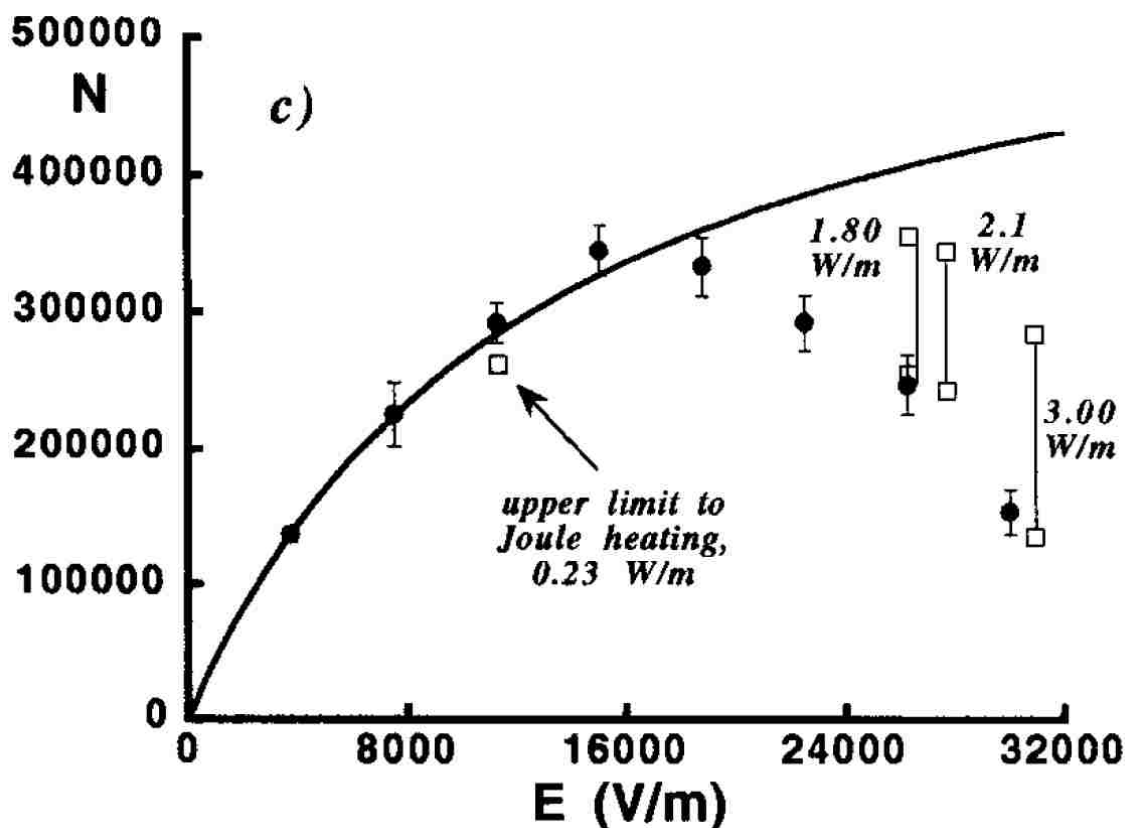
Figure 11. The effect of Joule Heating on efficiency of MEKC. Reproduced from work of Joe Davis [9]. Black dots show the peak efficiency (N) for perylene as number of theoretical plates vs. electric field strength (E). The black line denotes modeled efficiency without Joule Heating, open squares show modeled efficiency considering Joule Heating.

To avoid the severe impact Joule Heating has on the efficiency of the separation, the power dissipated by the capillary must be limited to prevent Joule Heating from occurring. This can only be done by either limiting the voltage applied to the capillary (and thus limiting the overall speed of separation) or by limiting the conductivity of the

BGE (primarily determined by the PSP). Micellar PSPs like SDS contribute a large fraction of overall conductivity through the free surfactant in the BGE, effectively limiting MEKC to lower electrical potentials and slower runs. Thus the contribution of the PSP to overall conductivity indirectly defines the maximum separation speed in MEKC.

Rates of mass transfer of analyte partitioning into and out of micellar PSPs are outstanding, with estimates suggesting that analytes partition 10 – 100 times faster than necessary to avoid measurable band broadening relative to the intrinsic band broadening from analyte diffusion [10]. Where exactly solutes interact with the micelle remains an open question. A number of techniques have been employed to determine the site of interaction: thermodynamic modeling and X-Ray diffraction, spectroscopic (absorption and fluorescence), and NMR [31]–[35]. In reality solutes can rapidly diffuse between the aqueous BGE, polar/ionic shell, and anhydrous hydrophobic core. In consequence the "site" of interaction is a temporal average of the solute's location. Unsurprisingly, hydrophobic saturated hydrocarbons are generally found in the core while polar solutes are more often found in the shell.

Because micellar PSPs have dynamic structures even the most strongly solvated solutes will be obliged to partition between the bulk BGE phase and the micellar PSP. The average residence time of a surfactant in a micelle is reported to be a millisecond or less [20], and the lifetime of individual micelles is thus limited, ensuring solute exchange between micelles [36]–[38]. The primary chromatographic limitation in this category is that the generally small size of micellar PSPs may be unable to fully solvate very large analytes, leading to diminishing applicability towards large solutes.

Micellar PSPs also provide good monodispersity and spherical architecture at concentrations from the CMC to at least ten times CMC [20]. The surfactant can generally be purchased in a pure form as in the case of SDS, or purified before use, further enabling uniformity of the resulting micelles. Polydispersity arises in MEKC at high concentrations or from the effects of organic additives or electrolytes. Under these conditions variation in the micellar architecture into rods, dumbbells, and the like result in variation of the aggregation number, or the total number of surfactants that aggregate to compose a micelle. For SDS, micelles become ellipsoidal around 70 mM and change to rods if the concentration of salts is above 70 mM as well. For higher SDS concentrations the salt threshold is lower [39].

Micellar PSPs provide ideal detector compatibility with UV-Vis detection, but are generally incompatible with MS detectors. Most surfactants utilized for MEKC do not contain chromophores and are much smaller than the wavelengths of light used for detection, providing low background interference and little to no Mie scattering in UV-Vis detectors. However, most CE instruments employ on-column detection, which eliminates extra-column band broadening and possible sources of contamination at the cost of reduced path length: MEKC generally utilizes 50 µm ID capillaries resulting in a very short path length. Although bubble cells can be used to increase sensitivity by

increasing path length, this comes at the cost of reducing resolution between peaks. This results in a limit of detection (LOD) of several ppm to several hundred ppm depending on the absorptivity of the analyte.

Micellar surfactants complicate the interfacing of EKC with electrospray ionization (ESI) and MS detection due to ionization suppression [40] and interference in the m/z range of many analytes. The direct coupling of MEKC with SDS to ESI-MS for the analysis of basic analytes has been reported, but strong background ions like $[(SDS)_n +Na]^+$ are observed along with ionization suppression of 90% or more at typical SDS concentrations [41]–[43]. For neutral analytes that require the PSP for MEKC separation, the limit of detection can be above 20 µM, eliminating much of the sensitivity advantage of MS detection [18]. At higher SDS concentrations of 2.33% w/w (81 mM) no peaks can be detected at all for an injection of 20 µg/mL doping agents [44].
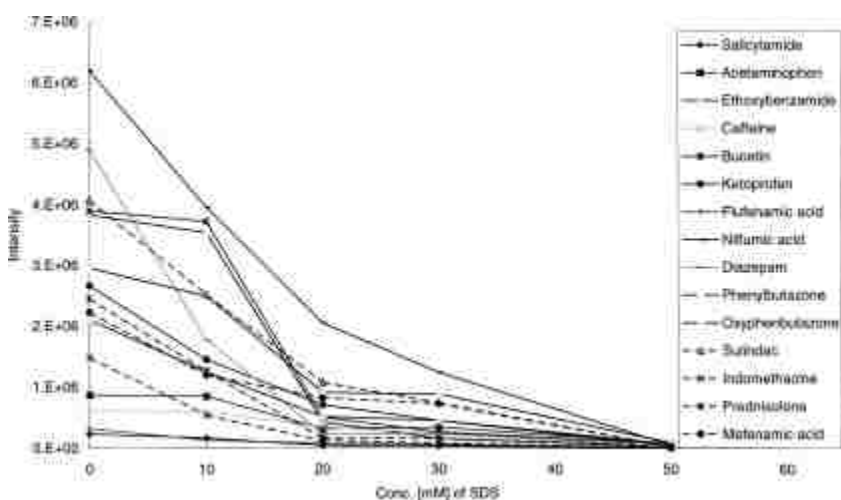
Figure 12 ESI suppression by SDS. Reproduced from [41].

Because of this, attempts to employ micellar PSPs with MS detection typically require complex techniques such as partial filling [26]–[29], [45], where only part of the capillary is filled with PSP to prevent elution of the PSPs alongside the analytes, or reverse-migrating micelles [46].

Selectivity is the final category of micellar PSP performance to consider. As defined in Equation 1-10 on page 1-11, selectivity is measured as the ratio between the retention factors of two solutes. The goal of the chromatographer is often to achieve sufficient selectivity to separate analytes with similar structure and inter-molecular interactions. In MEKC this requires the free energy change of solvation in the PSP to be quite sensitive to subtle variations in analyte structure and chemistry. Micelles provide some limited control over the relative strengths of solvation interactions by changing the chemical environment of the shell, but generally offer little control over the actual types of interactions offered by the PSP [47], [48].

2-25

Increasing the ionic strength of the BGE or using stronger counterions increase the shielding on the ionic surfactant groups in the micelle shell. This reduces the electrostatic repulsion between surfactants and allows the micelle to become denser and more hydrophobic. Additionally, increasing the surfactant concentration creates a greater number concentration of micelles that exert electrostatic pressure on fellow micelles, further compacting the micelles in the solution.

The increased density impacts the hydrophobicity and cohesively of the micelle as well as reducing the strength of ionic and polar interactions with the shell due to the increased shielding. However, the concentrations of surfactant and salts needed to produce these structural changes is so high relative to normal MEKC operating conditions that the impacts of the increased ionic strength on efficiency through Joule Heating and increased analysis time would dominate any observed changes in practical chromatographic performance or selectivity of the system.

Micelle structure and selectivity has also been demonstrated to be significantly altered by fluorination of the alkyl chain of the surfactant. Work with lithium perfluorooctanesulphonate (LiPFOS) has shown significantly different selectivity from other micellar PSPs [49]–[51] with LiPFOS micelles exhibiting more structured and less organic-like behavior than other surfactants [49]. One of the unique selectivities of the fluorinated LiPFOS PSP is that the highly electronegative fluorine atoms results in unusually strong interactions with polar and polarizable solutes compared to all other PSPs. The PSP has even been shown to provide stronger polar interactions than water in one of the studies [49]. This behavior suggests that even though the core of the micelle is very difficult to modify, it also has a significant impact on the selectivity of the micellar PSP.

2.2 Molecular micelles
The limited stability of surfactant-based PSPs in MEKC has driven the development of a number of alternate PSPs. One of the first steps in mitigating these limitations was to polymerize of the core of a micelle to obtain a PSP with a CMC of zero. By using surfactants with vinyl groups on the end of their hydrophobic chain, the surfactants could be covalently bound to one another, eliminating free surfactant in solution. This was first reported by Palmer and McNair in 1992 utilizing sodium-10-undecylenate (SUA) surfactants [52], [53].

The work employed a significant body of research on the polymerization of SUA [54]–[61] that enable the facile aggregation of SUA surfactants in aqueous media followed by thermal initiation by potassium persulfate to polymerize the ten or so surfactants in each micelle into a single micelle-like oligomer as depicted in Figure 13.
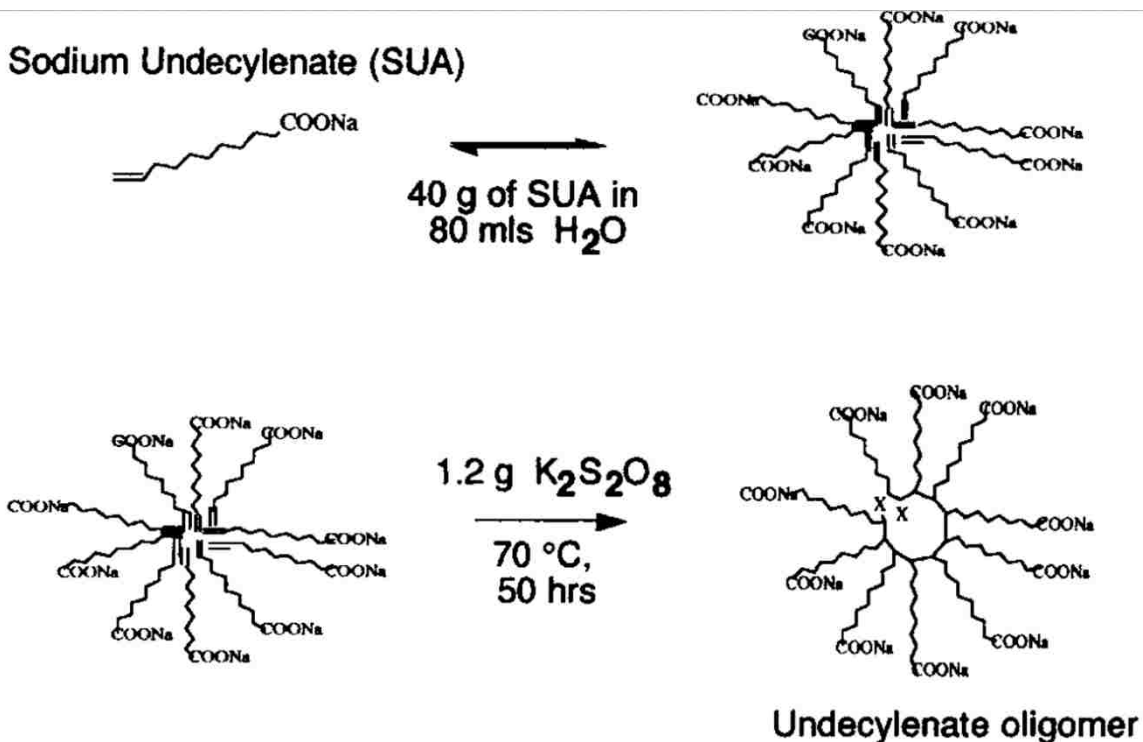
Figure 13 Synthesis of sodium undecylenate (SUA) molecular micelles. Reproduced from [53]. *SUA aggregates in aqueous media and is polymerization is induced by potassium sulfate.*

The resulting molecular micelles (or micellar polymers as they were initially known) were shown to solve the stability difficulties intrinsic to traditional micelles. Separations of polyaromatic hydrocarbons (PAH) in acetonitrile concentrations as high as 40% have been demonstrated [53], and their performance for PAH separations has been demonstrated to be superior to several other PSPs in organically modified solutions [62].

Unfortunately, the carboxylic acid head groups of the SUA proved susceptible to loss of ionization and lacked the mobility over wide pH ranges afforded by SDS. This was addressed by the second generation of molecular micelles developed by Palmer and Terabe in 1996 [63], [64]. This set employed sodium undecenyl sulfate (SUS) surfactants in the same synthetic processes to yield oligomers with sulfate head groups analogous to SDS.

The SUS PSPs were found to provide analogous methylene selectivity and improved mobility, even over SDS micelles. The SUS molecular micelles particularly shone in terms of their stability in systems with high organic modifier content. The SUS PSPs were also demonstrated to provide alternate selectivity from SDS as illustrated by the elution order of substituted benzene and naphthalene compounds shown in Figure 14.
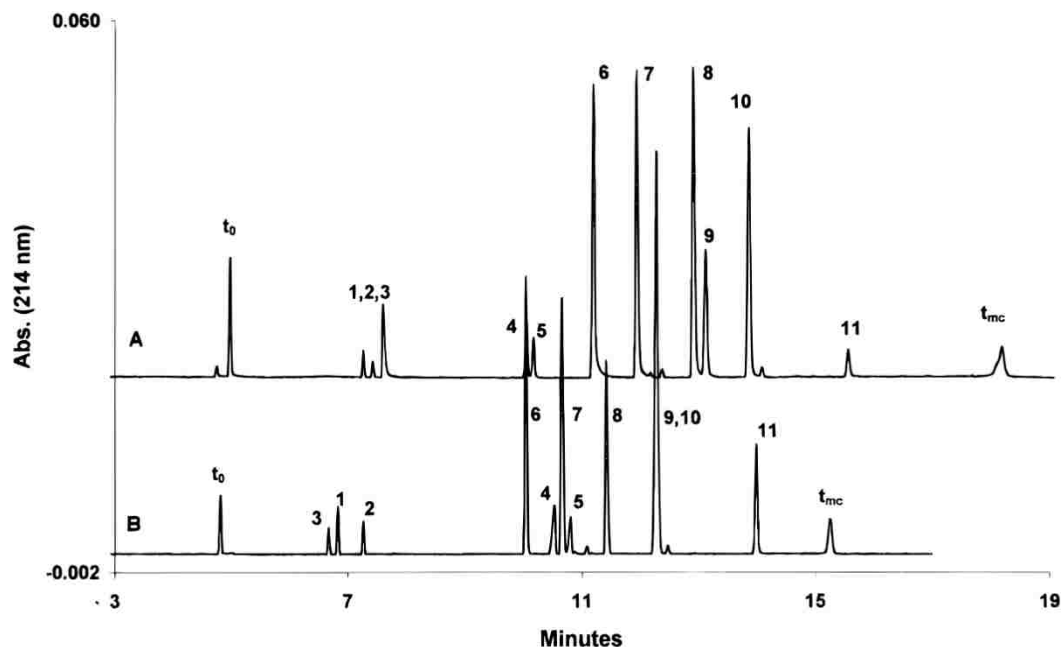
Figure 14 Separation of subsisted benzene and naphthalene compounds by SUS and SDS. Reproduced from [64].*"(A) 0.83% SUS polymer; (B) 30 mM SDS. Capillary was 50 cm effective length and 57 cm total length, 16.1 kV applied potential. A phosphate/borate buffer at pH 7.3 was employed. Key: (1) nitrobenzene; (2) anisole; (3) p-nitroaniline; (4) o-xylene; (5) m-xylene; (6) naphthylamine; (7) naphthalene methanol; (8) acenaphthenol; (9) naphthalene; (10) naphthaleneethanol; (11) diphenyl ether."*

While these initial reports of molecular micelles demonstrated their ability to solve the stability problems that had limited MEKC, the possibility to controlling selectivity as well by modification of the head groups rapidly became the primary area of investigation, although it was confirmed that different initiators incorporated into the core of the molecular micelle did not significantly alter the selectivity of the PSP [65].

The potential to control the selectivity of both molecular micelles and true micellar PSP systems is partially demonstrated through the use of mixed micelles of SUS and sodium 10-undecenyl leucinate (SUL). The addition of even 20% SUL to SUS micelles resulted in a dramatic shift in physicochemical properties of the PSP towards those of SUL micelles. Further addition of SUL up to 100% SUL micelles resulted in further gradual change amounting to less than half the change induced by the first 20% SUL [66].
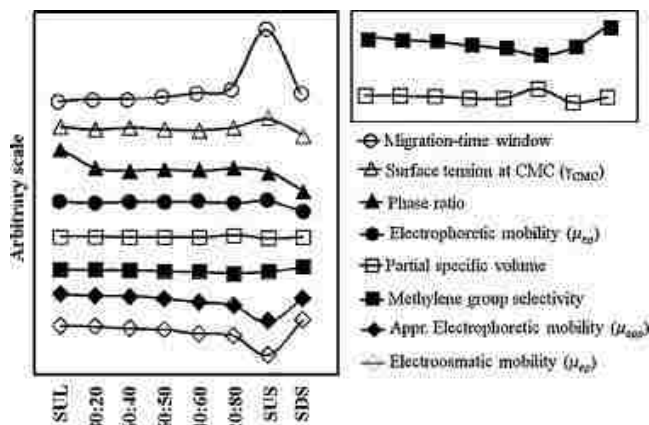
Figure 15 Changes in physicochemical properties from various compositions of SUL and SUS surfactant. Reproduced from [66]. *The presence of even small fractions of SLA surfactant has large impact on the MEKC properties. Further addition has limited impact.*

Variation of the alkyl chain length from eight to eleven carbons on SUS analogs has been seen to result in lower PSP polarity as well as providing a larger migration range, most likely due to effects on the shell of the molecular micelle [67]. Longer monomer chain length resulted in measureable, but not dramatic, variations in the relative strengths of interactions as measured by LSER. Longer chain PSPs were less cohesive, less polar, and better able to interact with nonbonding and π electrons. However, the correlation between the selectivity of the PSPs was better than 0.95 as measured by thirty-six solutes. Coupled with the LSER results this can be taken to indicate that while alkyl chain length can change the behavior of PSP, it is incapable of inducing a major shift in selectivity [67], [68]. Further studies comparing the performance of micellar PSPs formed of monomer to their polymerized analogs shows that the overall selectivity is often more dependent on the solute than whether or not the surfactants had been polymerized, although for most solutes the polymer form provided greater resolution [69].

2.2.1 Functionalization of shell
The only point on the molecular micelles available for functionalization is the ionic head group as exploited above. By switching out the head group to various alternate chemistries researchers have demonstrated the ability to alter the behavior of molecular micelle PSPs. Relatively simple modifications such as adding an amide moiety (Figure 16C) were shown to provide significantly higher mobility. Even employing a phosphate (Figure 16D) group still allowed the PSP to operate as low as pH 2.5 [70]. However, these modifications did not significantly alter the selectivity of the PSP from that of SUS.
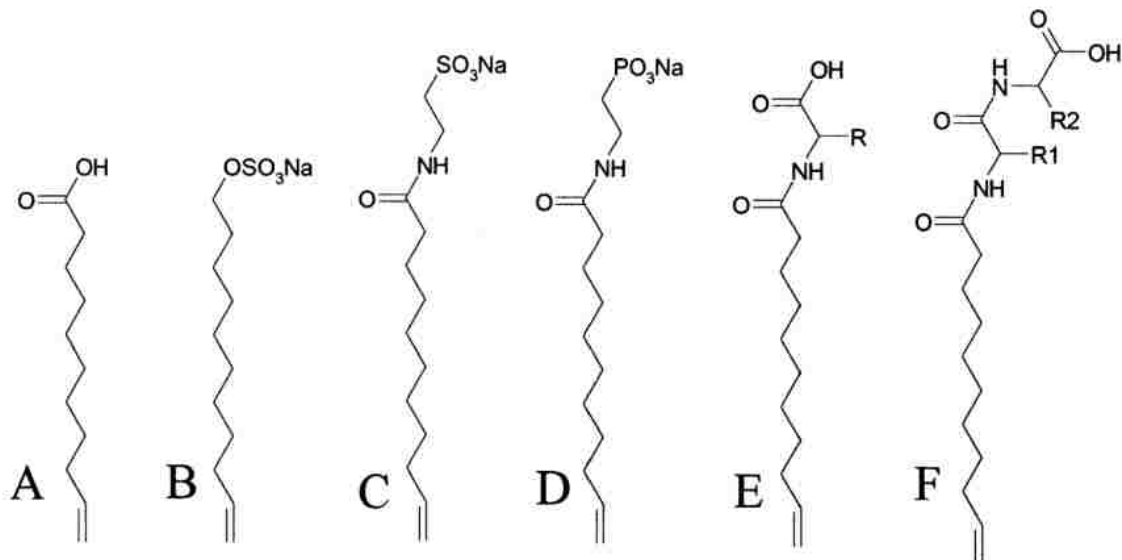
Figure 16 Selection of surfactant chemistries developed for use as molecular micelles. Adapted from [13]. (A) SUA; (B) SUS; (C) SUT; (D) SUP; (E) Amino Acid modified; (F) dipeptide modified.

In contrast, adding an amino acid group as the head group of the molecular micelle has been shown to not only alter the selectivity of the PSP, but to even provide chiral selectivity. A great deal of this work has been conducted by Prof. Shahab Shamsi, now of Georgia State University, and Prof. Issah Warner of Louisiana State University over several decades in papers utilizing molecular micelles functionalized by a wide range of amino acids (Figure 16E,F).

The use of poly(sodium undecenoly-L-valine) (poly-L-SUV) and a cationic amide version was patented in Japan in 1992 [71], [72] but results utilizing them were first published in 1994 by the Warner group [73]. The D-valine analog (poly-D-SUV) was shown to reverse the elution order of (±)-1,1′-di-2-napthal conformations, illustrating chiral selection by the chiral center of the amino acid. However, the addition of β- and γ-cyclodextrin (cyclodextrins are discussed in more detail in a on page 2-37) as a chiral selective additive provide greatly improved separations depending on the analyte [74], [75], and higher pH also improved the performance due to the PSP taking on a more open conformation at pH 10 [56].

In subsequent work the chiral recognition of the dipeptide version (poly-L-SUVV) was reported to be stronger, as shown in Figure 17, at the cost of some loss of chromatographic performance through lower mobility [76]. A large number of other dipeptide functionalized PSPs have been reported that confirm the behavior [77]–[83]. It is also shown that when different amino acids are used, their order in the dipeptide has a significant impact on the chiral selectivity as the selectivity is governed by the hydrophobic interactions and steric constraints of the PSP and analyte [78], [79], [84], [85]. Investigation of oligomer aggregation and temperature dependence of the aggregation shows that this class of PSP seems to be limited to 12000 g/mol or less [86].
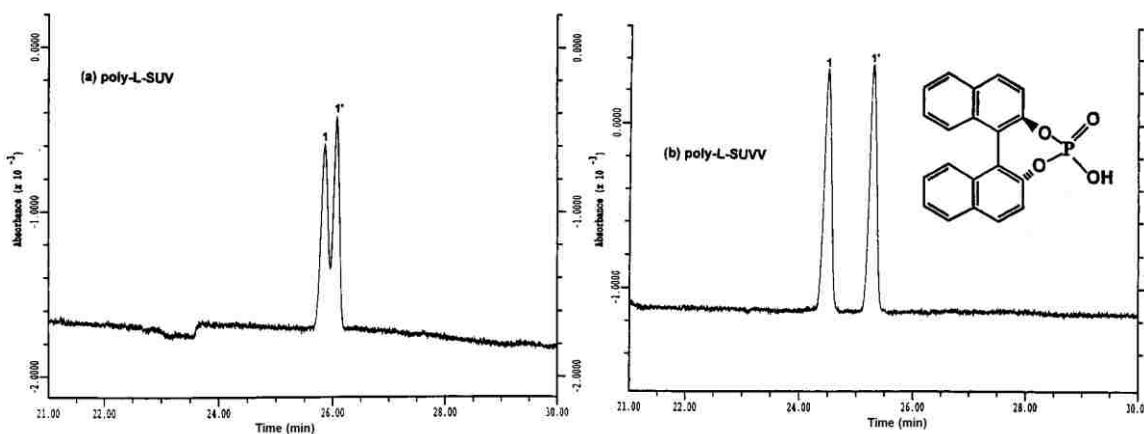
Figure 17 Chiral recognition by poly-L-SUV and poly-L-SUVV PSPs. The dipeptide form provides improved chiral resolution. Adapted from [76].

2.2.2 Detection

In addition to the improvements to PSP stability, and the new chiral selectivities molecular micelles enable, they also provide improvements to detector compatibility. Early work utilizing SUS successfully detected tricyclic antidepressants and β-blockers with low concentrations of SUS (0.1%), but saw the signal severely diminished by even 0.5% SUS [87]. The amino acid functionalized molecular micelle PSPs appear to perform much better. A large number of papers report the successful separations of chiral analytes utilizing a number of amino acid functionalized molecular micelle PSPs detected by ESI-MS [88]–[93]. There have also been reports demonstrating the functionality of APPI-MS with similar PSPs [94], [95].

2.3 Micro emulsions

While molecular micelles were developed to address the high conductivity of MEKC, other approaches focused on improving the selectivity. Microemulsion electrokinetic chromatography (MEEKC) was first reported in 1991 by Hitoshi Watarai of Akita University, Japan [96]. In MEEKC a stable microemulsion (ME) of immiscible solvents is dispersed and stabilized by a surfactant and co-surfactant to form a microemulsion whose droplets may then act as a PSP.

While less popular than MEKC, MEEKC has seen extensive research and method development, and many reviews are available on MEEKC methods and applications over the intervening decades [97]–[101]. Most microemulsions used for MEEKC are oil-in-water microemulsions. Producing such microemulsions relies on balancing the concentrations of the BGE, the immiscible solvent, and the surfactant and co-surfactant to provide the desired selectivity and stability. Additional organic modifiers may also be added to the BGE to further fine-tune the selectivity.
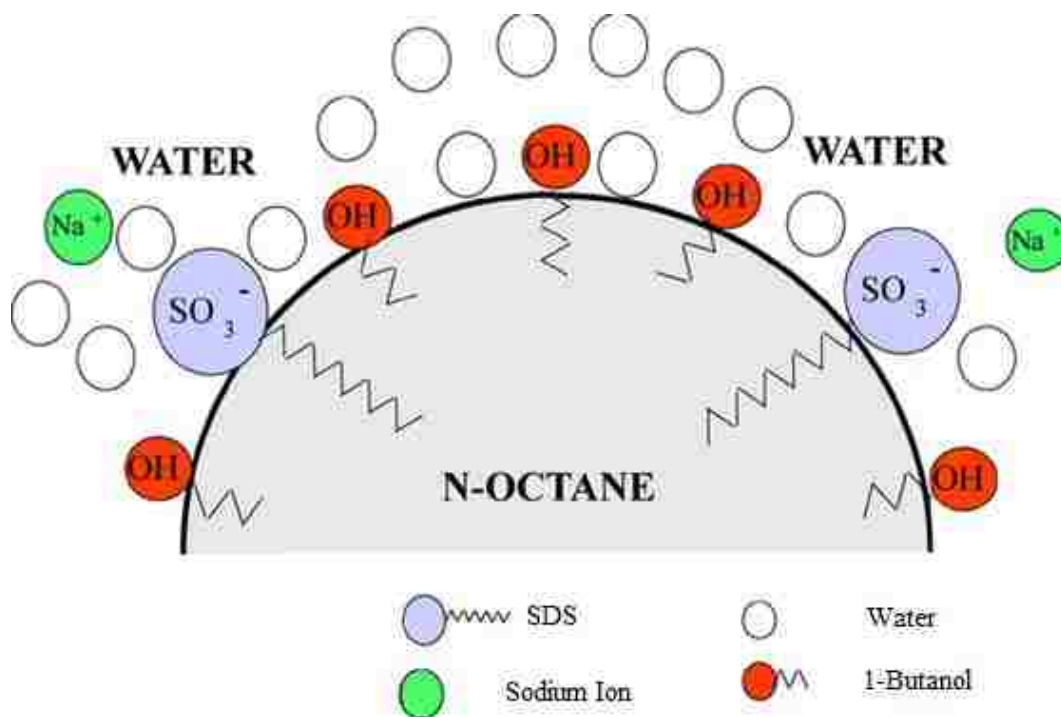
Figure 18 Schematic representation of an oil-in-water microemulsion. The nanometer scale immiscible n-octane droplets are stabilized in an aqueous BGE by SDS and 1-butanol. The SDS provides mobility to the droplets. Reproduced from [98].

Typical MEEKC utilizes a composition of about 0.70-0.90% w/v *n*-octane, 5-7% w/v butanol, and 100 mM SDS in a 10 mM borate or phosphate BGE. While the complicated nature of the phase behavior [102] is beyond the scope of this review, it has several impacts on MEEKC. The microemulsion droplets are less ridged than micelles [103]–[105] and can better solubilize many analytes, providing a higher rate of mass transfer and more efficient separation. This likely contributes to the prevalence of MEEKC in pharmaceutical analysis and other bio- or bio-focused work [106] where high molecular mass or low solubility analytes are common.

Unfortunately, the combination of many charged species and a high surfactant concentration lead to high conductivity in MEEKC, limiting it to low electric field strengthens to avoid loss of performance from Joule Heating. This further recommends MEEKC more for applications like the analysis of pharmaceuticals where its ability to precisely control selectivity is more valuable than minimizing analysis time [107].

The conductivity can be improved somewhat by preparing the microemulsion with a solvent like ethyl acetate that has a lower surface tension than oils like heptane or octane. The lower surface tension means that less surfactant is needed to stabilize the droplets, leading to lower conductivity and faster analysis for compatible analytes [108].

One of the primary tools MEEKC employs to control selectivity is the selection and concentration of the surfactant. While SDS is the most common surfactant for MEEKC, several others are used. Anionic bile salt surfactants like sodium cholate are shown to provide alternate selectivity [109], and many others (sulfosuccinic acid bis (2-ethylhexylester) sodium salt, dodecylsulfonate sodium salt, decylsulfonate sodium salt, sodium taurocholate, sodium cholate (SC) hydrate, and sodium deoxycholate) have been employed as well [110].

Cationic surfactants like cetyltrimethylammonium bromide (CTAB) have also been used [111], especially with cationic analytes, to avoid ionic interactions with the PSP [112]. Neutral surfactants like Triton X-100 have also been shown to provide alternate selectivity and solubility for analyzing charged analytes while avoiding any complications from charges on the PSP [113].

While surfactant concentrations under 2% w/v for SDS result in unstable microemulsions that degrade within hours [114], surfactant concentrations of even 3% w/v SDS are reported to be stable for months [101].

The pH of the BGE also has a significant effect on the performance of MEEKC as it affects both the ionization of the analytes and the strength of the EOF generated by the capillary. BGE at both pH extremes have been used. BGE as acidic as pH 1.2 has been used to fully neutralize acidic analytes and suppress EOF [96], [115] while pH 12 BGEs have been used to eliminate ionization of basic compounds [115].

Octane [116], [117] and heptane [118], [119] are generally used as the immiscible oil, although octane, hexane, and heptane have all been shown to give similar selectivity [120]. Less hydrophobic oils can also be used as already mentioned, but one of the most interesting modifications of the oil phase is the use of a chiral oil (2R,3R)-di-*n*-butyl tartrate to provide chiral selectivity [121].

The extreme contrast in analyte solubility between the aqueous BGE and the hydrophobic oil microemulsion can be moderated either through the use of less hydrophobic oils or by the addition of an organic modifier to the BGE. However, just as for MEKC, the organic modifier can only be used in moderate degrees (<<30% v/v) or it degrades the microemulsion.

Finally, 1-butanol is often used as the co-surfactant. It has little impact on the mobility of the microemulsion [122], but it does impact the droplet size and the EOF, as well as performing much the same role as an organic modifier in the BGE would [119], [123]. This provides control of droplet size (and thus charge density) as well as the ability of the analyte to partition between the BGE and PSP droplets [101].

These numerous components of the MEEKC system provide a large degree of control over MEEKC separations, but the large number of variables makes optimization quite

challenging. To overcome this, various experimental design strategies have been utilized to control the numerous interdependent variables. Many of these are reviewed in [101]. Despite the complexity of optimization and the limitations of high conductivity, MEEKC is capable of solvating and separating many analytes that are incompatible with MEKC. Proteins are a prime example. While they are generally too large to partition into a micellar PSP, they can partition into a microemulsion droplet because to its larger volume and less cohesive palisade layer of ionic groups. Analytes such as ribonuclease A, carbonic anhydrase II, lactoglobulin A and myoglobulin all show better resolution separations by MEEKC than by MEKC [124].

The value of MEEKC's compatibility with proteins and other compounds of biological importance is attenuated by MEEKC's incompatibility with mass spectra detectors. For example the attempt by Schappler et al. to conduct MEEKC-ESI-MS was unable to detected any peaks from a 20 µg/mL injection of doping agents (beta-blockers, etc.) due to ionization suppression from a minimal concentration of 2.33% SDS [44]. Just as in MEKC the surfactants suppress ionization in MS detection, a valuable tool for proteomics and metabolomics research.

2.4 Polymers
Within a few years of the introduction of molecular micelles, high-molecular mass copolymer chains were introduced to investigate the effects of polymer composition and mass on PSP performance. These polymers are in contrast to the molecular micelles discussed above: while the molecular micelles are formed by polymerization within the core of a micelle, the polymer PSPs in this section are polymerized in solution from a homogenous solution of free monomers.

While molecular micelles addressed the conductivity limitations of MEKC, like the micellar PSPs they are derived from, they must be capable of aggregating into a micelle. Thus they are intrinsically based on a ridged core, and the selectivity may only be controlled through functionalization of the ionic shell of the particle. This does not provide the breadth of selectivity options chromatographers could wish for.

By using random copolymers (in the sense of randomly ordered monomer units within the copolymer) as a polymeric PSP, researchers were able to create the desired type of PSP chemistries by selecting monomers with those chemistries. This control of PSP chemistry allowed for the systematic investigation of the effects of copolymer composition (ionic vs hydrophobic groups) on PSP performance as well as the effect of PSP hydrophobicity (short vs long alkyl chains on the hydrophobic monomers). This work has been summarized in several reviews of PSPs [12]–[16].
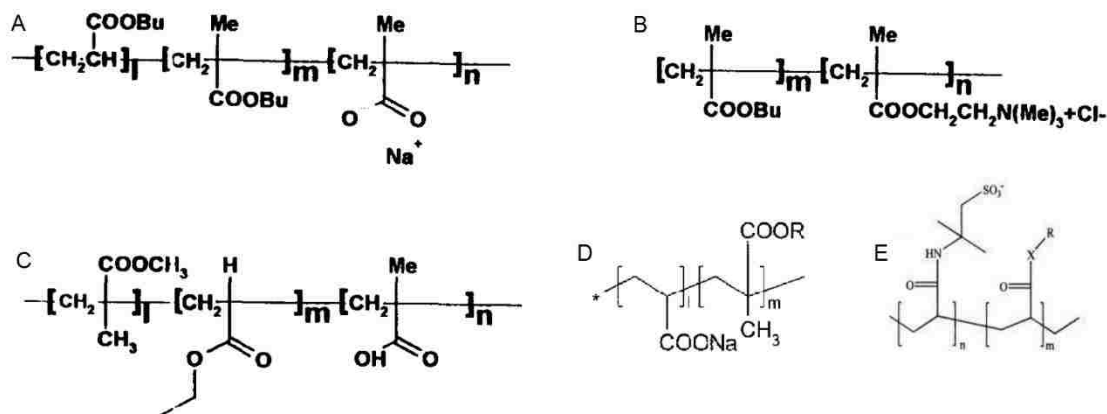
Figure 19 Polymer PSP configurations. A) BBMA; B) BMAC; C) Elvacite 2669; D) Acrylate polymers, R=C9, C13, C18; E) AMPS copolymers. X=N or O. Adapted from [12]–[14].

Copolymers of butyl acrylate and methacrylic acid (BBMA, Figure 19A) were the first acrylate copolymers to be reported by Terabe and Ozaki in 1994 [125], [126] and later used with methanol as an organic modifier [127] and even with MS detection [128]. A cationic version was also characterized (BMAC, Figure 19B) [127].

Elvacite 2669 is another early polymer PSP based on a poly-(methyl methacrylate-ethyl acrylate-methacrylic acid) (Figure 19C) [129]. It demonstrated stability in up to 70% methanol and was used for LSER studies [130], [131].

Fluorinated polymer PSPs have also been reported with similar behavior to the LiPFOS micellar PSPs [51]. As observed with the MEKC experiments the fluorocarbon species exhibited more cohesive and ridged behavior with more water-like solvation environments than their hydrocarbon analogs [51].

Moving closer to the idea of the NP PSPs investigated in this work, the impact of copolymer composition on PSP performance was studied in a series of reports of acrylate copolymers with differing alkyl chain lengths and molecular mass (Figure 19D) [13], [132], [133]. It was found that for a fixed acrylate/alkyl acrylate mole ratio and similar molar mass, methylene selectivity increased with increasing alkyl chain length. The shorter alkyl chain PSPs (C9) exhibited greater affinity for polar compounds while the polymers with longer alkyl chains (C18) had greater overall interaction with nonpolar or hydrophobic compounds [132]. This paper indicates that varying alkyl chain length on the monomers used for polymeric PSPs provides control of the methylene selectivity of the resulting polymer.

Further work with the acrylate copolymers demonstrated that mixtures of C9 and C18 phases provide intermediate selectivity in a predictable manner [133]. It was also noted that analytes with long alkyl chains were not solvated as well by polymer PSPs with short alkyl chains than they were by longer chain PSPs. This implies that polymer PSPs

comprised of short alkyl chain monomers are unable to create a large hydrophobic domain.

The second area of research on polymer PSPs relevant to this work is a body of literature on copolymers containing 2-acrylamido-2-methylpropane sulfonic acid (AMPS) with a variety of methacrylate and methacrylamide co-monomers [51], [134]–[138]. The effect of the mole fraction of AMPS to lauryl methacrylamide between 0.6 and 1 mole fraction AMPS showed increasing mobility with mole fraction of AMPS in the copolymer while hydrophobicity and peak symmetry decreased. A mole fraction of 0.8 AMPS was determined to provide the best compromise for overall PSP performance [136]. This suggests that an abundance of ionic groups are needed to provide the desired mobility, but the ionic monomer alone is unable to provide the necessary retention. Inclusion of even 20% composition of a hydrophobic monomer in the copolymer provides significant advantage as a PSP.

AMPS was also copolymerized with octyl (C8), lauryl (C12), and stearyl (C18) methacrylate, with lauryl and dihydrocholesteryl acrylate, with stearyl and *t*-octyl amide, and with lauryl methacrylamide [134], [138]. Significant differences in the selectivity of the methacryl*amide* and methacryl*ate* phases were observed, with acrylamide copolymers providing more hydrogen bonding and an overall more polar PSP than the acrylate copolymer PSPs [134]. However, the length of the alkyl chain on the hydrophobic monomers (C8 vs C12 vs C18) did not affect the overall selectivity of the PSP at the long chain lengths studied. This implies that there may be a threshold above which increasing alkyl chain length will not change methylene selectivity below C8. This is supported by this dissertation (Figure 47 on page 5-86).

In addition, the performance of the AMPS/*t*-octyl amide polymer and that of the AMPS/ dihydrocholesteryl acrylate was quite similar despite the tertiary versus semi-planer pendant chemistry of the two PSPs. The semi-planer configuration appeared to only provide unique selectivity towards planer polyaromatic hydrocarbon (PAH) compounds where it performed quite well with an acetonitrile modified BGE [138].

In combination with the body of copolymer PSP work cited above, this identified AMPS functionalized copolymers as a highly promising PSP that provided relatively high mobility, low conductivity, low cohesiveness, and low polarity. This combination provides good EKC performance for a large range of analytes including large molecules like peptides [51]. It is also compatible with higher electric field strengths and the organic modifiers needed for fast separations of highly retained compounds like the PAHs shown in Figure 20 [138].
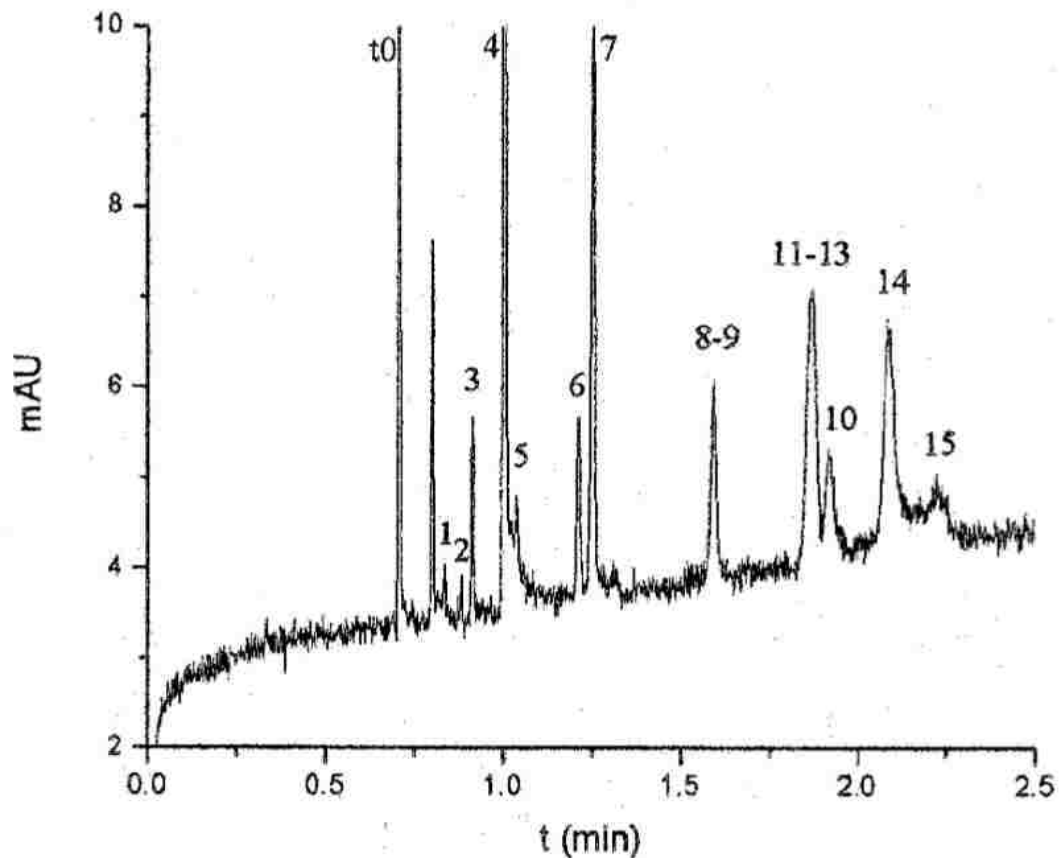
Figure 20 Separation of PAH compounds by polymer PSP. "1. acenaphthy-lene, 2. acenaphthene, 3. fluorene, 4. phenanthrene, 5.anthracene, 6. fluoranthene, 7. pyrene, 8. chrysene, 9.benz[a]anthracene, 10. benzo[a]pyrene, 11. benzo[e]pyrene,12. benzo[k]fluoranthene, 13. benz[e]acephenanthrylene,14. benzo[g,h,i]perylene, 15. dibenz[a,h]anthracene. The peak immediately after t0is an impurity." Separated by dihydrocholesteryl acrylate/AMPS polymer PSP (0.72% w/v) in 35 mM sodium borate with 29.6% v/v ACN on a 31.2 cm capillary. 30 kV at 38 μA. Reproduced from [137].

2.5 Cyclodextrin

While chiral selectivity has been demonstrated by molecular micelles functionalized by amino acids and by microemulsions with chiral surfactants as reported above, very few PSPs are capable of separating different chiral conformations from one another on their own. This is a severe limitation for many fields in which EKC would otherwise prove advantageous. To address this, cyclodextrins (CD) have long been used to provide, or enhance, chiral selectivity in the PSP.

Cyclodextrins are composed of units of D(+)-glucopyranose linked through an α(1,4)-glycosidic bonding that produces a molecule shaped like a truncated cone. Three varieties of CD are used in EKC: α, β, and γ-CD each having six, seven, or eight units respectively (Figure 21). The interior of a CD molecule is hydrophobic while the exterior is hydrophilic. This provides both solubility in aqueous BGE and hydrophobic interactions

for analytes. The hydroxal groups along the rim of the cone may be derivatized if desired to control the chiral selectivity of the CD or modify its mobility.
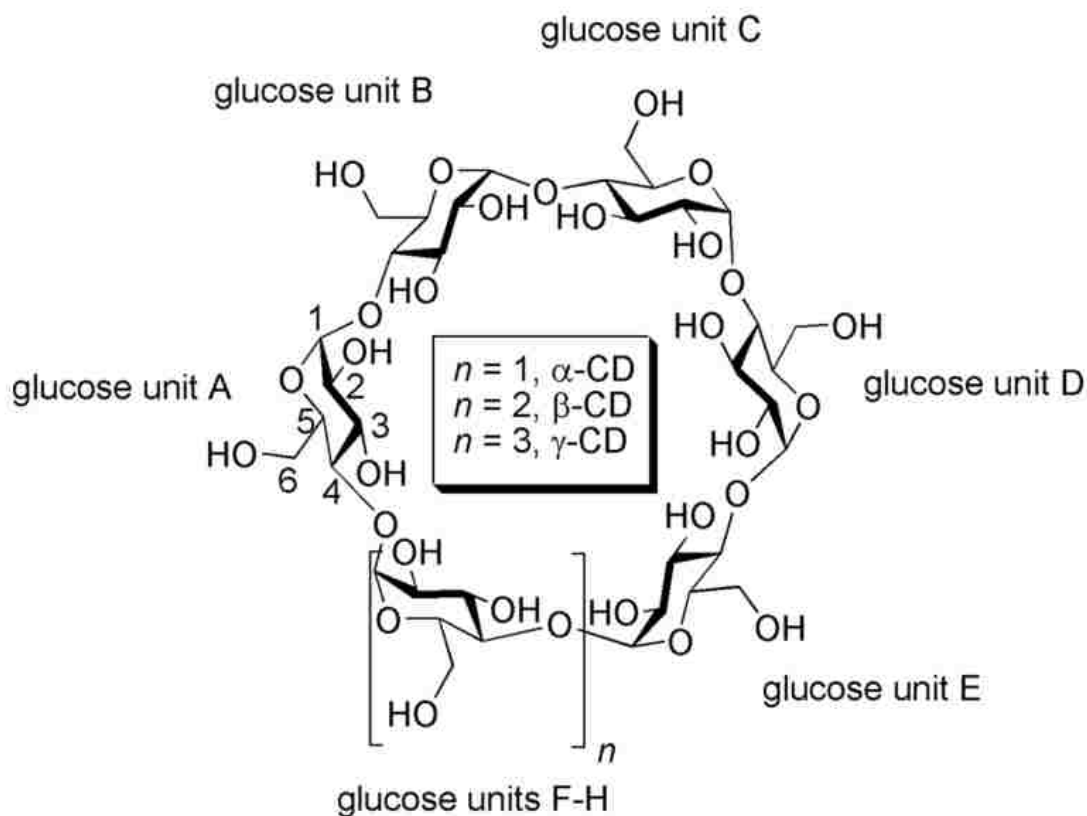
Figure 21 Structure and numbering of glucose units and atoms in CD derivatives. α, β, and γ-CD have six, seven, or eight units respectively. Reproduced from [139].

This ability to substitute any number of functional groups, either randomly or specifically, onto the CD by replacing the hydroxide groups on the rim of the CD allows the selectivity of the CD to be tuned to provide a practically infinite number of chiral selectivities by altering the substitutions [140], [141]. The reader is directed to the recent review by Rezanka et al. for a thorough examination of the modification and application of CD, as the wealth of information available is outside the scope of this dissertation [139].

Cyclodextrin is able to provide chiral selectivity for two primary reasons: first, that cyclodextrins provide a large number of chiral centers (β-CD has 35), and second, that interactions between the CD and analyte are based on "induced adaptation, that is, the shape of the CD is changed during the interaction [to conform to the analyte]" [139]. The consequence of this relatively low energy change in conformation is that CD usually exhibits little stability as a CD-analyte complex, resulting in a low binding constant relative to other more ridged PSP materials.

These weak interactions are ideal for providing the slight variations in selectivity needed to separate two different conformations of a chiral compound from one another, but are generally insufficient to separate a range of diverse compounds from one another. For this reason CD is most often used as an additive to CE or EKC. In this roll it provides additional selectivity to the primary electrophoretic or PSP driven separation.

The combined factors of CD sensitivity to BGE conditions (composition, ionic strength, pH), large number of CD types and substituents, and potential parallel system optimization for CE or EKC performance provides a challenging method development task for chromatographers. While experimental design strategies have been reported [142]–[144], some of which are quite detailed [145], method development remains a challenge for optimizing chromatography with CD.

Cyclodextrins are an important tool for CE and EKC that can be customized to provide specific selectivity. However, they lack the robustness and breadth of analyte compatibility needed in a general purpose PSP. Their "induced adaptation" to solvate analytes enhances their chiral selectivity, but limits both the retention they may provide as a PSP and the types of analytes they can solvate. Because the analyte must be capable of entering the hydrophobic interior of the conical CD to interact, analytes larger than di- or tripeptides are unable to interact with the CD.

2.6 Nanoparticles
The final class of PSPs to be discussed are nanoparticle (NP) PSPs comprised of polymer chains. The use of a polymer NP as a PSP was first reported by Wallingford and Ewing in 1989 with Eastman AQ-55 polymer particles as an aside in a review of other techniques [146]. While this first NP PSP was found to have significant limitations [12], [147], NP PSPs have advanced greatly through the years up to the latest generation reported in this work (Results 5-70).

2.6.1 Early examples
More extensive research on NP PSPs began to be reported in the last fifteen years. Early work was mostly focused on molecularly imprinted polymer (MIP) NPs with diameters ranging from 100 nm to 500 nm [148]–[152]. Precipitation polymerization was used to synthesize emulsifier-free NPs from 1,1-tris(hydroxymethyl)-propane trimethacrylate which were imprinted with S-propanolol [148] and (+)-ephedrine [151].

The synthetic and EKC conditions have been investigated [149] and generally show that these NPs require high levels of organic modifier in their BGE to maintain solubility, and even elevated separation temperatures as high as 60°C. Separations showed enantiomeric selectivity for several analytes, although highly retained analytes experienced lower efficiency and peak tailing.

This same pattern of lower efficiency for highly retained compounds was repeated in lauryl methacrylate, styrene, and divinylbenzene NPs synthesized by soap-free emulsion

polymerization with sodium persulfate [153], [154]. Although this yielded smaller 157±34 nm particles that provided better reproducibility, the authors suggest that the continuing loss of efficiency for highly retained compounds may be due to polydispersity in the NP size or chemistry. They also report a batch to batch reproducibility in retention factor of only 11%.

2.6.2 Detection

One of the first advantages of NP PSPs to be utilized was their compatibility with MS detection. The large size of the early MIP NPs resulted in light scattering in UV-VIS detectors and necessitated the use of non-spectrophotometric detectors. Nilsson and coworkers have repeatedly demonstrated NP PSPs to perform well with ESI-MS detection using an orthogonal ESI interface [150], [155], [156]. They have purposed that the large mass of the NP PSP provides sufficient momentum for the NPs to pass the skimmer cone of the MS without entering the spectrometer. This allows the MS to detect the less massive analytes without interference from the PSP. This is achieved without the need for complicated partial filling techniques or other systems to prevent the PSP from eluting alongside the analytes.

2.6.3 ACROSS work

Although early NP PSPs demonstrated some significant advantages, significant limitations remained. Precipitation polymerization and soap-free emulsion polymerization are unable to provide control of NP architecture, and ionic groups were only provided by the initiator (in the case of sodium persulfate initiated NPs) or through modification of the surface of the NPs after synthesis.

While the work with polymer PSPs had demonstrated the potential for control of PSP parameters by changing the composition and chemistry of the polymer, neither free-radical polymerization nor the techniques used for early NP PSPs could combine the two classes of PSP.

Combining the strengths of polymer PSPs with NP PSPs was finally made possible by the use of Reversible Addition-Fragmentation chain Transfer (RAFT) polymerization (described in its own chapter starting on page 3-43). NP PSPs synthesized by RAFT polymerization were first developed at the Australian Center for Research on Separations Science (ACROSS) at the University of Tasmania by Christopher Palmer and Emily Hilder in 2010.

As described in Chapter 3, RAFT provides control of both the chemistry of the NP through monomer selection and control of the architecture of the NP through the stoichiometry of the reactions. Using acrylic acid monomer for ionic/ hydrophilic character and butyl acrylate for hydrophobic character, Profs. Palmer and Hilder reported the synthesis and characterization of diblock copolymers that self-assembled into 63nm ± 26% NP PSP during synthesis [157].

This NP PSP consists of an approximate 5 mer ionic block of poly(acrylic acid) providing a charged "shell" around a hydrophobic "core" comprised of the poly(butyl acrylate) block of the copolymer. The behavior and selectivity of the NP PSP [158] has been reported along with demonstration of good ESI-MS performance [157].

However, the effects of NP architecture and chemistry on PSP performance have remained unexplored until this dissertation work. Research on RAFT NP synthesis conducted in parallel with this work has been reported in Andre Umansky's master's thesis [159] and some of the data in this dissertation has previously been published [160].

2.7 Conclusion

In the last 30 years extensive research has been conducted on pseudostationary phases (PSP) for electrokinetic chromatography (EKC) and many new PSPs have been introduced. These PSPs have expanded the capabilities of EKC and have individually addressed many of the limitations of EKC. Table 2 provides a subjective summary of the performance offered by each class of PSP in each of the seven categories of PSP performance introduced in chapter 1, 1.3 Pseudostationary phase properties, on page 1-14.

	Micelles	Molecular Micelles	Micro emulsions	Polymers	CD	NP
Mobility	+++	+++	++	++	-/+	+++
Stability	-	+++	-	+++	++	+++
Conductivity	-	++	--	++	++	+++
Mass transfer	+++	++	+++	++	++	+
Mono-dispersity	+++	+++	++	+++	+++	++
Detector Compatibility	+	++	-	++	++	+++
Selectivity	-	+	+++	++	++	++(+)

Table 2 Summary of relative qualities of each class of PSP. (-) Denotes an incompatibility, (+) functional performance, (++) good performance, and (+++) best performance to date.

Micelles remain the most widely employed class of PSP. They are often cheap, pure, and easy to work with, but they are incompatible with MS detection and have several other limitations.

Some of the limitations of micelles (for example, conductivity and stability) were addressed with molecular micelles, but limitations remain with controlling PSP selectivity and compatibility with large analytes.

Micro emulsions provide compatibility with even the largest and least soluble analytes, but suffer from high conductivity and complicated method development.

Polymer PSPs provided an ideal platform for the investigation of the effects of polymer composition and size on EKC performance, but have not seen application outside academia, most likely because there is no commercial source for the highly specific polymers required.

Cyclodextrins are a popular and widely employed additive that provides chiral selectivity or even size selectivity to CE and EKC. The ability to selectively modify them provides a capacity to fine-tuning selectivity. However, their relatively weak retention and sensitivity to analyte size prevents them from operating as a robust general-purpose PSP.

The latest generation of RAFT polymerized NP PSPs have been demonstrated to provide high mobility, stability in high organic modifier content, no significant contribution to conductivity, good mass transfer, limited dispersity, outstanding detector compatibility, and unique selectivity. Many of the advantages of polymer PSPs that were predicted to be available to NP PSPs are confirmed in this work including modifying selectivity and retention by monomer selection and high mobility provided by strongly ionic monomers. Additionally, the stability, detector compatibility, and negligible conductivity of molecular micelles are also replicated in NP PSPs.

The ESI-MS detector compatibility of molecular micelles and early NP PSPs has also been demonstrated with these NP PSPs, while the use of chromophore-free monomers and small NP sizes (<150 nm) ensures compatibility with spectrophotometric detectors.

Chapter 3 RAFT Synthesis

In traditional free-radical polymerization an initiator introduces a radical into the system and the reaction propagates by addition of monomer units to form a polymer chain as shown in Figure 22. The free-radical polymerization process is non-selective and continues until the monomer is either consumed or termination events consume the radicals. Termination events occur when two polymer chains bond to one another, consuming both radicals and producing a dead polymer. Because all growing polymer chains are active simultaneously, the probability of self-termination is high. The ongoing production of dead polymer throughout the reaction also results in high polydispersity in the products.
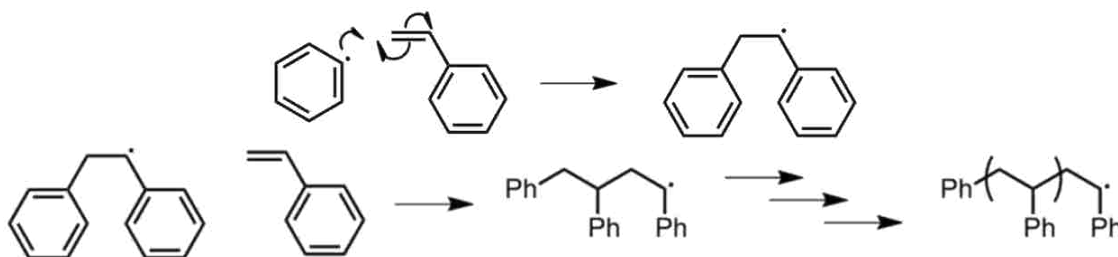
Figure 22 Free-radical polymerization mechanism: polymerization of styrene by benzyl peroxide initiator.

To synthesize NPs with rational and repeatable architecture, controlled polymerization is necessary to ensure that NP PSPs provide uniform and repeatable EKC performance. Polymerization techniques that provide control of polymer size and composition have revolutionized polymer chemistry since their introduction in the last several decades. A great deal of progress has been made expanding the techniques to work with a wide range of monomers and conditions. The most applicable controlled radical polymerization method for our work is reversible addition-fragmentation chain transfer (RAFT).

From its discovery in Australia at a Commonwealth Scientific and Industrial Research Organization (CSIRO) lab in 1998 [161], RAFT has been recognized as a powerful and versatile synthetic technique. The development and application of RAFT has been documented in several comprehensive reviews from CSIRO, first in 2006 [162], second in 2009 [163], and third in 2012 [164] by the inventing authors. As a general metric of the growth of the technique, the papers each contain 255, 552, and 721 citations respectively. A far more concise overview of the capabilities of RAFT is provided by H. Mori, a prominent author in the field [165].

RAFT polymerization was selected for this work for its compatibility with a wide range of monomers, its compatibility with aqueous solvents, its stability in storage and handling, its ease of purification and characterization, and its control of polydispersity even with diblock polymers. The availability of a sufficient body of work to guide the synthesis of our novel diblock polymer based NP PSPs was also a key asset for this work

as described below (page 3-52). The quantification of polydispersity is discussed in detail in Results on page 5-735-73.

3.1 RAFT

The widely accepted mechanism for RAFT polymerization operates by mediating free-radical polymerization in two ways: first, by rapid exchange of polymers between dormant and active states, and second, by carful stoichiometric control of the relative concentrations of all reactants in the synthesis.

At the heart of RAFT is the chain transfer agent (CTA), a molecule that initiates most of the polymers and then mediates their growth. The CTA consists of three domains as illustrated in Figure 23: a "Z" group that controls the reactivity of the CTA, a thiocarbonyl about which the RAFT process takes place, and an "R" group that can both act as a good leaving group and initiate polymerization of the monomer.
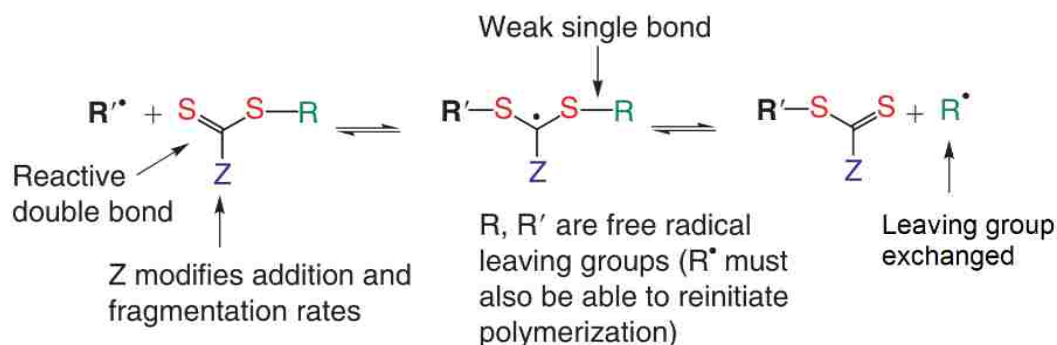
Figure 23 RAFT mechanism: The chain transfer agent (CTA) and its three domains in red, green, and blue. The polymerization is mediated by rapid exchange of leaving groups (R and R'). Adapted from [163].

A vast array of CTA molecules have been reported with various R and Z groups for different monomers and solvents [162]–[164]. Some are even commercially available (Figure 24), although they remain relatively expensive. The most common classes of CTA are the dithiobenzoate, trithiocarbonyl, and dithiocarbamates, each of which offers reaction kinetics and solubility suited to particular classes of monomer. For this work the trithiocarbonyl system was chosen for its improved resistance to hydrolysis and high transfer constants that provide rapid synthesis in aqueous solvent. The high reaction rate for trithiocarbonyl CTAs also allows us to utilize much lower initiator concentrations than required for slower CTAs like the dithiobenzoates. This reduces side reaction products, improving polymer purity to the point purification is not generally required until the final product is reached.
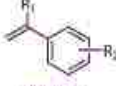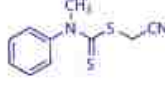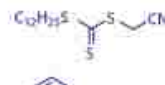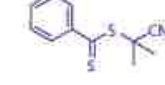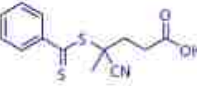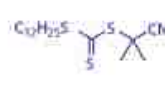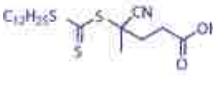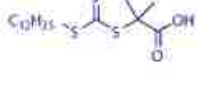
	styrenes	acrylates	acrylamides	methacrylates	methacrylamides	vinyl esters	vinyl amides
	—	—	—	—	—	+++	+++
	+++	+++	+++	—	—	—	—
	++	+	—	+++	+++	—	—
	++	+	+	+++	+++	—	—
	+++	++	++	+++	+++	—	—
	+++	++	++	+++	+++	—	—
	+++	+++	+++	+	+	—	—

Figure 24 Commercially available CTAs (left column) optimized for various monomers (top row). Reproduced from [166].

3.1.1 Polymerization Mechanism

The RAFT mechanism begins with the combination of a monomer, a CTA, and an initiator in a solvent (typically). Monomer concentration is set at least an order of magnitude higher than CTA concentration, with initiator concentration only a tenth or twentieth that of the CTA. Initiation can be induced by any number of methods such as thermal- or photo- degradation of the initiator or gamma irradiation. The newly formed radicals interact with the abundant monomer, forming active monomer-initiator adducts with a radical that initiates free-radical polymerization.

Figure 25 RAFT mechanism: Initiation. The initiator (I) is decomposed into radical ions (I˙) that react with monomer (M) and propagate to additional monomer to form polymer chains of n units (Pn˙). The radical is conserved on the polymer chain as denoted by the dot (•). Reproduced from [167].

In the second stage of the RAFT polymerization mechanism, growing (active) polymer $P_n^{\cdot}$ interacts with the thiocarbonyl group in a CTA molecule. The CTA undergoes β-scission shown in Figure 26 by formation of a P_n-S bond with the radical electron

3-45

contributed from the $P_n^{\bullet}$ polymer and a π electron from the S=C bond. The second π electron is left as a radical localized on the trithiocarbonyl group during the brief lifetime of the intermediate. With a properly selected R group the weak S-R bond ensures k_{β} is much faster than k_{-add}, resulting in the radical transferring to the R group with the formation of a new S=C π bond.

During the pre-equilibrium stage the the R$^{\bullet}$ groups are released from the CTA as radicals and the first polymers formed in solution are bound as a dormant polymers on the CTA molecules. The resulting combination of CTA and polymer is now called a macro-CTA (mCTA) as the R group of the CTA has been replaced by a much larger dormant polymer (P_n). As k_{add} is >> than k_{-add} (when R and Z groups are appropriately selected), this stage of the reaction will proceed until all R groups have been ejected from their parent CTA.

The new S-P_n bond is relatively weak, allowing the dormant polymer to still act as a leaving group if attacked by a group of equal or greater strength. This allows the mCTA to remain capable of continuing polymerization.
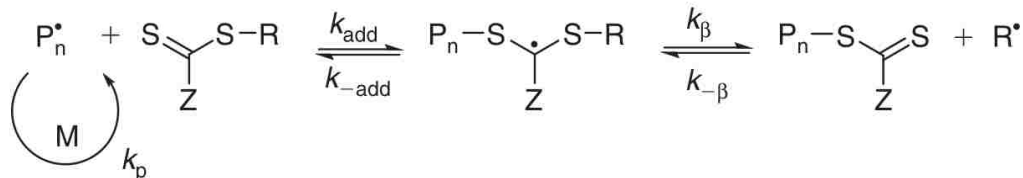
Figure 26 RAFT mechanism: Pre-equilibrium. Reproduced from [167].

The introduction of R$^{\bullet}$ radicals provides a new source of initiators for the reinitiation stage. This consists of the R$^{\bullet}$ radicals interacting with the monomer to form further radical monomer/R group adducts (R-M$^{\bullet}$) that begin free-radical polymerization. However, the much higher molar concentration of R$^{\bullet}$ radicals compared to I$^{\bullet}$ radicals ensures that most of the polymer chains will have been initiated by an R$^{\bullet}$ group rather than an I$^{\bullet}$ group.
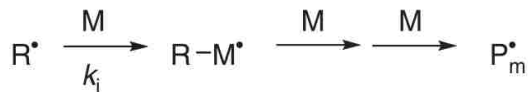
Figure 27 RAFT mechanism: Reinitiation. Reproduced from [94].

The first three stages of RAFT polymerization take place relatively quickly once initiation begins. While the kinetics are complex and depend on reaction temperature and concentration, as well as the reactivity of the monomer and CTA, within 30 minutes or so it is reasonable to expect the main equilibrium stage in Figure 28 to have begun.

In the fourth stage of RAFT polymerization, called Main Equilibrium or Chain Propagation, (shown in Figure 28) the active polymers in the solution and the dormant polymers bound to a CTA molecule are rapidly exchanged with one another. The rapid

3-46

exchange ensures that each of the individual polymers has an equal probability of propagating by reacting with monomer in solution while free as an active polymer in solution. Figure 28 shows this exchange as the transfer of $P_m^{\cdot}$ from the active state where it propagates at rate k_p, to the dormant state where it is attached to the thiocarbonyl of the CTA. This ejects the previously dormant P_n polymer as an active polymer that begins propagating at the same rate k_p.
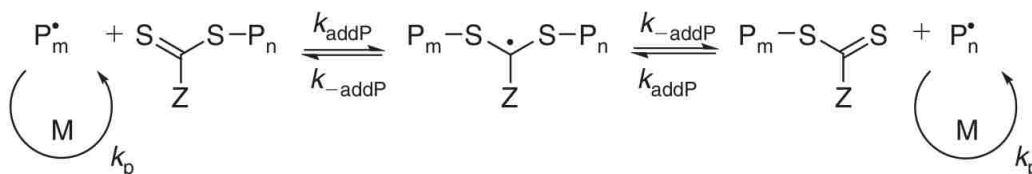
Figure 28 RAFT mechanism: Main equilibrium. Reproduced from [94].

However, at any given moment most polymers will be in the dormant state bound to a CTA molecule. Recall that each polymer chain was started by a single radical and that the only sources of radicals are the initiator (Figure 25) and the R$^{\cdot}$ groups (Figure 27). Because the CTA provides the R$^{\cdot}$ groups, there are exactly as many R$^{\cdot}$ groups as CTA molecules. Therefore the same number of polymers that are formed by R$^{\cdot}$ groups can be captured as dormant polymers by the CTA molecules. This means that the total number of active polymers in solution will be equal to the number of I$^{\cdot}$ groups. Stating the same thing mathematically:

$$\# \ active \ polymers = \# \ R^{\cdot} + \#I^{\cdot} - \#CTA$$
$$Where: \#R^{\cdot} = \#CTA \qquad \qquad 3\text{-}1$$
$$Therefore: \# \ active \ polymers = \#I^{\cdot}$$

Because the concentration of active polymer will only be equal to the original initiator concentration, the active polymer concentration may be controlled by the amount of initiator added. By using much less initiator than CTA the concentration of active polymer can be kept low. The low concentration of active polymers ensures that there is little probability of diffusion controlled self-termination from two active polymers reacting with one another in solution (Figure 29). This results in uniform polymers with little polydispersity as the large variations in chain length that arise from self-termination in free radical polymerization are not found in RAFT polymerization.
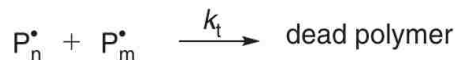
Figure 29 RAFT mechanism: Termination. Reproduced from [94].

The Main Equilibrium stage continues until either the reaction is stopped by quenching the radicals (typically by exposure to O_2) or all the monomer is consumed. The resulting

mCTA can then be purified and characterized. These mCTA polymers can be used in exactly the same way as a CTA to continue the polymerization with another monomer as they still contain the reactive thiocarbonyl moiety. The dormant polymer attached to the thiocarbonyl now acts as the R leaving group.

As with traditional free radical polymerization, RAFT polymerization is very sensitive to oxygen. Oxygen will react with both propagating radicals and intermediate radicals at diffusion-controlled rates [168]. These side reactions can be mitigated by taking the usual precautions to exclude air by sparging with an inert gas like N_2 or He, or by repeated freeze-pump-purge cycles.

3.1.2 Macro Chain Transfer Agent

The exact quantities of products that will be produced by RAFT polymerization is dependent on the relative concentrations of reactants involved, but in theory it will follow these ratios:

> Assuming 100 mol Monomer (M), 10 mol CTA, and 1 mol Initiator (I) are reacted under RAFT control to 90% conversion into polymer (P), then the products should be:
>
> 9 mol of R-$P_{(9-x)}$-CTA "living" polymer initiated by R groups
> 1 mol of I-$P_{(9-x)}$-CTA "living" polymer initiated by I groups
> 1-x mol of unreacted M
> 0.9 mol of R-$P_{(9-x)}$ "dead" polymer
> 0.1 mol of I-$P_{(9-x)}$ "dead" polymer
> x mol of $P_{(18-2)}$ self-terminated polymer

By keeping initiator concentrations low, the concentration of active polymers will also be kept low. This ensures that very few active polymers will react with one another, keeping "x" very small. Unreacted monomer can be easily removed by dialysis if needed. Unfortunately, "dead" polymer cannot be separated from the "living" mCTA by dialysis because the mass and chemistry are quite similar, but there is little need to do so when preparing polymers for further polymerization.

These reaction products can be used directly in the synthesis of additional blocks of polymer. The "living" mCTA can be expected to make up ~90% of the mass of solids collected from the RAFT polymerization of the mCTA depending on the initiator-to-CTA ratio. The other ~10% of the mass is dead polymer that will not react, and can be ignored as a spectator, until it is removed during subsequent dialysis of the diblock polymers.

The mCTA can then be utilized in further polymerization. The generation of block copolymers by sequential RAFT polymerization of different monomers enables the synthesis of many of the complex polymer architectures illustrated in Figure 30.
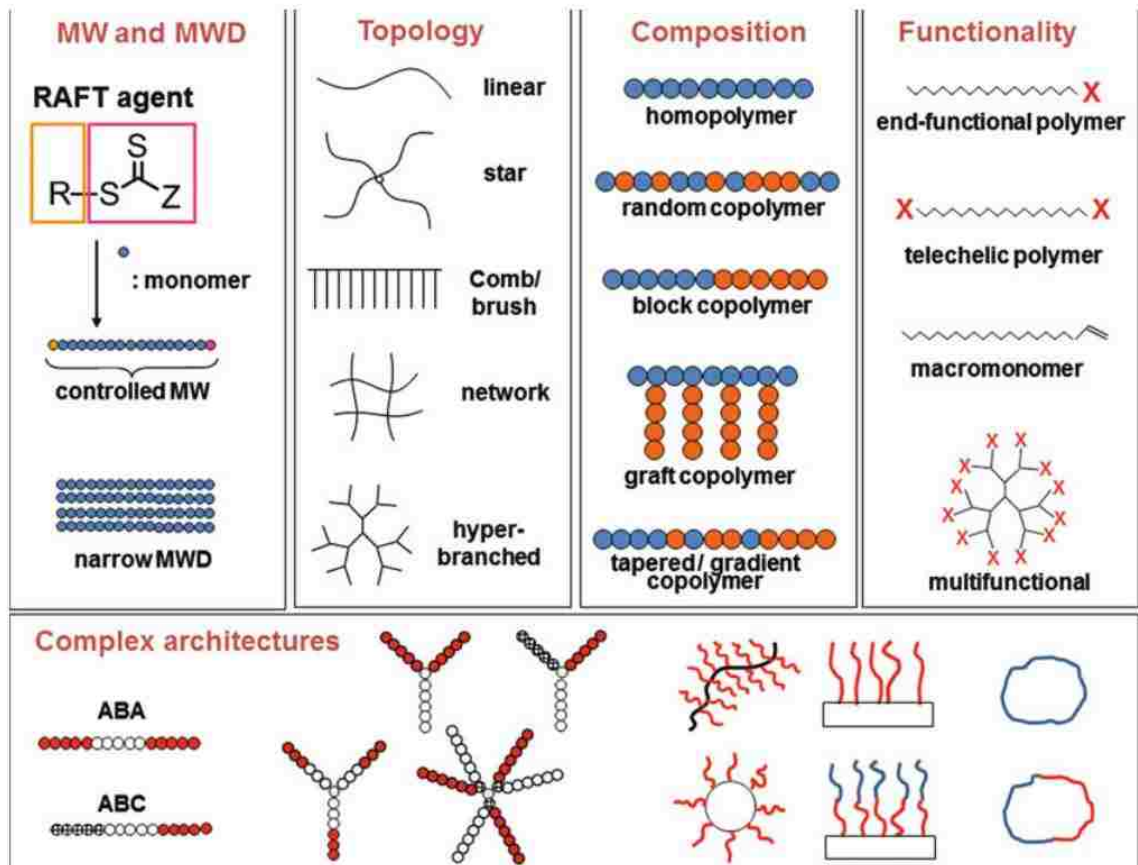
Figure 30 Polymer properties controlled or enabled by RAFT polymerization. Reproduced from [165]. *Narrow molecular weight dispersion (MWD) and block copolymer composition are the primary synthetic interest of this work.*

3.1.3 Diblock

To form NPs with controlled architecture block copolymers are needed. The synthesis of the diblock (literally two block polymer) proceeds by the same principles as for the mCTA. The resulting polymer is formally described to as an *AB-diblock copolymer*: *AB* denoting that monomers A and B are confined to discreet blocks in that order, *diblock* stating somewhat redundantly that there are two blocks composed of different monomers, and *copolymer* (also redundantly) conveying that the polymer is comprised of more than one monomer polymerized together into a polymer. While each of these terms provides a different level of specificity, "diblock" will generally be used in this work to describe the polymers that make up the NPs.

During diblock synthesis the presence of the second monomer does result in more complex polymers and a few additional side reactions, including the production of polymer chains containing only the second monomer ($P(M_2)_x$) shown in Figure 31.
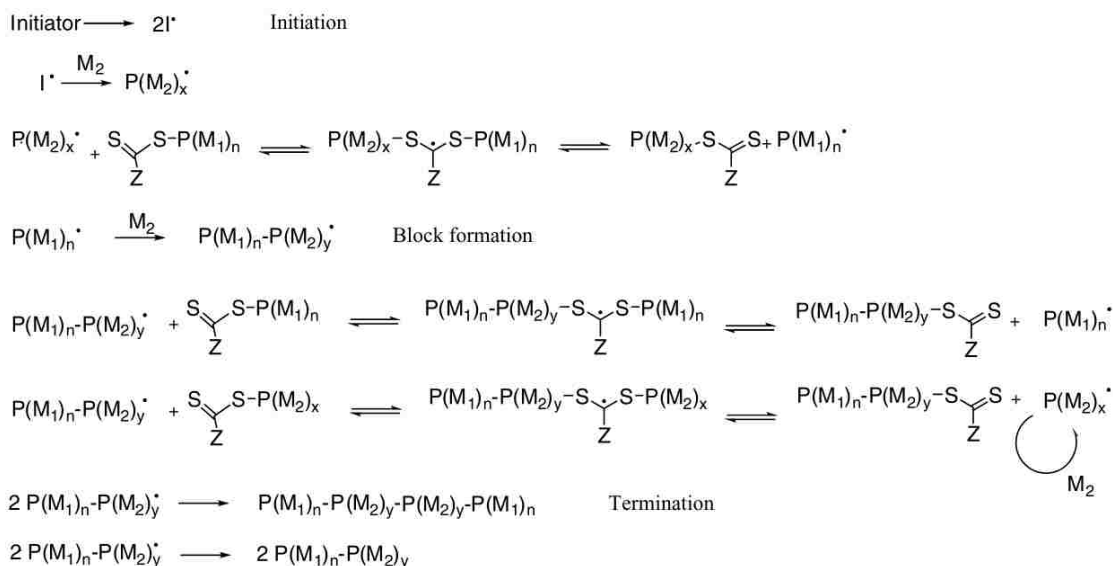
Figure 31 RAFT mechanism: Synthesis of block copolymer. Reproduced from [167].

Again, the concentration of $P(M_2)_x$ from this side reaction should only be equal to the concentration of initiator in the synthesis and can therefore be considered insignificant for a properly configured set of synthetic conditions[2].

3.2 Emulsion Polymerization

In this work the mCTA is polymerized in water from either acrylic acid or 2-acrylamido-2-methylpropane sulfonic acid (AMPS), both strongly hydrophilic monomers. Therefore these reactions take place in the bulk solution, and the reactants can be assumed to be uniformly distributed in solution. However, the polymerization of the diblock in water is more complex [169]. As the hydrophobic monomer of the second block adds to the mCTA, the hydrophobic nature of the amphiphilic copolymer increases until cohesive hydrophobic interactions drive the self-assembly of the copolymers into micelle-like particles.

From the point of self-assembly onwards, the RAFT polymerization effectively takes place in an emulsion polymerization environment. As depicted in Figure 32, this environment consists of three distinct phases: monomer droplets, monomer dissolved in the bulk aqueous solvent, and monomer-swollen micelles that will grow into polymer particles during the polymerization.

For a typical hydrophobic monomer like styrene, the monomer concentration in the droplets is ~9 M, in the solvent it is ~3.5 mM, and in the micelles it is ~2 M [170]. The relative concentration of monomer in each of these three environments, and the flux between them, is key to understanding the behavior of reaction and NP formation in the copolymer synthesis: polymerization will take place at much higher effective monomer

---

[2] Not all RAFT polymerizations in this work should be considered to be synthetically optimized.

concentrations (2 M) than for the mCTA, and; the monomer concentration at the location of the reaction is independent of the quantity of solvent the reaction takes place in.
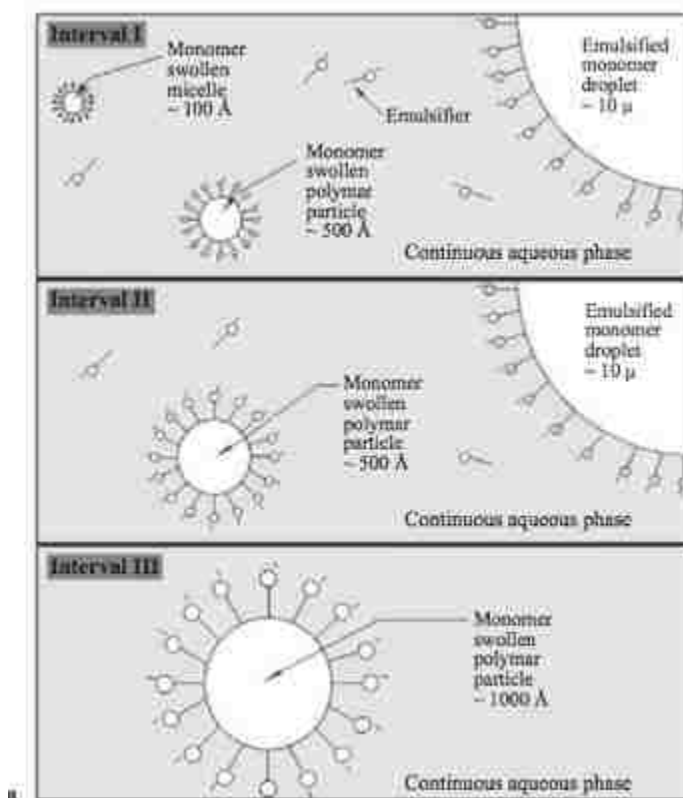
Under mechanical stirring the monomer will be dispersed into relatively few, and relatively large, monomer droplets that are in equilibrium with solubilized monomer in the bulk solvent. Within the micelles the growing hydrophobic chains of the copolymer are saturated with monomer because the hydrophobic monomer is better solvated by its polymer form than by water, and thus concentrates about the micelles of growing polymers.

The small size and relatively low aggregation number of the copolymer micelles means that there will be vastly more surface area on the numerous micelles than on the few monomer droplets, ensuring the flux of monomer and solubilized radicals into the micelles is statistically favored over flux into the droplets.

The monomer droplets act as a reservoir that replenishes the growing polymer particles with monomer by diffusion through the aqueous solvent. This ensures that so long as the flux of monomer from the droplets to the bulk solvent equals the rate of polymerization, the polymerization will progress as though at 2 M monomer concentration. For monomers such as methyl, ethyl, and butyl acrylate (that possess moderately high

solubility in water) this means a rapid growth phase is to be expected. However, monomers with very low solubility in water (for example, dodecyl acrylate) will polymerize at rates limited by the slow flux of monomer from the droplets into the solvent.

The use of water as a solvent, and the relatively benign substances and the low temperatures and pressures utilized in these syntheses further recommends RAFT as a synthetic technique that exemplifies many of the goals of green chemistry [172].

3.3 Guiding Literature

As described in detail in chapter 4, RAFT polymerization was used to synthesize AB diblock copolymers of poly(acrylic acid) or poly(AMPS) A blocks and poly(methyl, ethyl, butyl, or hexyl acrylate) B blocks that underwent self-assembly into latex NPs. The synthetic conditions were adapted from the RAFT polymerization of similar copolymers in the literature.

The use of RAFT polymerization to synthesize NPs from AB diblock copolymers has been demonstrated by Ferguson et al. [173]. Ferguson also reports the performance of several different CTAs with acrylates and acrylamides used or considered for this work. The process of NP formation proposed by Ferguson is shown in Figure 33 with acrylic acid based A blocks [poly(acrylic acid)] and butyl acrylate based [poly(BA)] B blocks.
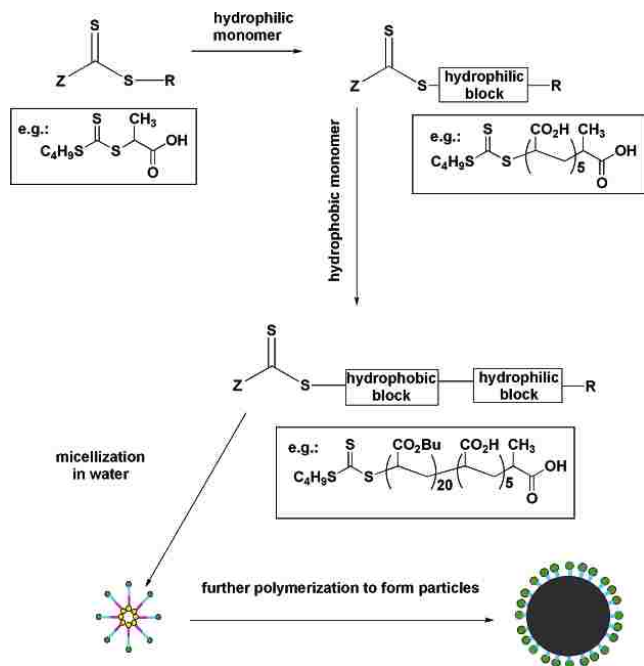
Figure 33 Formation of NPs from AB dobolck polymers synthisized by RAFT polymerizaton. Fergison discribes NPs as having an ionic "shell" and hydrophobic "core" with archatectural control provided by RAFT. Reproduced from [173].

The Ferguson paper provided the basis for the selection of 2-{((Butylsulfanyl)-carbonothioyl)sulfanyl}propanoic acid, shown in Figure 33 and here after called simply

3-52

"CTA," as the CTA for all the RAFT polymerizations in this work. The CTA was selected for its good performance with acrylate and acrylamide monomers as well the presence of a carboxylic acid moiety in the R group to match the chemistry of the ionic block, and a butyl alkyl chain on the Z group to mimic the hydrophobicity of the monomers used in the core.

The aqueous RAFT polymerization of AMPS-containing diblock polymers was demonstrated by McCormick [174] and the synthesis was adapted from Sumerlin [175]. The McCormick report details the RAFT polymerization of numerous monomers by a number of CTA agents and illustrates that AMPS can be used to provide improved ionization of the hydrophilic polymer blocks while still forming copolymers with monomers like butyl acrylate.

Further support for the formation of NPs of appropriate architecture for use as NP PSPs was provided by the use of RAFT polymerization to synthesize poly(acrylic acid) poly(styrene) copolymer based NPs of versus sizes by stoichiometric control of the monomer [176]. This work also utilized the same CTA employed here, further illustrating the practicality and compatibility of the CTA with various monomers.

Chapter 4 Materials and Methods

As we have seen in Chapter 2, latex nanoparticles provide a generational advancement over previous pseudostationary phases. This advancement is possible because of RAFT polymerization that provides synthetic control of the PSP as discussed in Chapter 3.

Characterization of polymer based NPs is challenging, and remains a developing area of research with many different techniques in use [177]–[181]. While the primary purpose of this work is to characterize the chromatographic behavior of NP PSPs in EKC, a basic understanding of the architecture of the NP is implicit in that characterization. In this chapter the instruments, methods, and materials utilized to make those determinations are described.

The materials and methods utilized to characterize the electrokinetic chromatographic performance are also reported.

4.1 Instrumentation

4.1.1 Synthetic characterization

Bruker NMR

NMR spectra were collected on a 400 MHz Bruker TopSpin instrument using 5 mg mCTA in 0.7 mL D_2O. The degree of polymerization was determined by comparison of the integrated area for the amide methylene (3.35 ppm) and terminal methyl group on the CTA (0.85 ppm).

500 MHz Varian NMR

NMR spectra were also collected on a 500 MHz Varian instrument controlled by Varian Mercury software. All NMR data processing was conducted with ACD Labs NMR Processor software.

HPLC

An Agilent 1260 HPLC with a Poroshell 120 C_{18} column and 90:10 acetonitrile:H_2O mobile phase running at 1 mL min^{-1} was used to measure CTA purity. The trithiocarbonyl moiety in the CTA was selectively detected by the PDA UV/VIS detector at 320 nm. Hydrocarbon species were detected at 210 nm.

GC

An Agilent 6890N gas chromatograph equipped with standard 30m DB-5 columns and an Agilent 5973N mass spectrometer was used to confirm the purity of any analytes with suspected contamination.

MALDI

MALDI analysis of mCTA was performed on a Bruker microFlex LRF instrument equipped with a 337 nm nitrogen laser. 2,5-Dihydroxybenzoic acid (DHB) was used as

matrix. Solutions of both DHB and mCTA were made at 10 mg/mL in 70:30 0.1% TFA/acetonitrile. Volumes of 1 µL mCTA solution and 1 µL DHB were co-applied on a Bruker MSP BigAnchor 96 target plate. Bruker Peptide Calibration Mix II consisting of Angiotensin II, Angiotensin I, Substance P, Bombesin, ACTH Clip 1-17, ACTH Clip 18-39, and Somatostatin 28 was used for mass calibration prior to analysis. Mass spectra were acquired in reflectron mode with a reflector gain of 50 and accelerating voltage of 19 kV. Laser power was set to 90% with a frequency of 60 Hz, and 500 shots were taken and summed per spectrum. Mass spectra were collected with Bruker FlexControl software, processed with Bruker FlexAnalysis software, and calculations were performed in Microsoft Excel.

MALDI-TOF is becoming more common for the analysis of synthetic polymers [182]–[184], and has been used to analyze polymers similar to AMPS such as polystyrene sulfonate [185], [186]. While work utilizing MALDI to characterize polymers has indicated that matrix effects can skew results for high molecular mass polymers towards lower masses, as MALDI-TOF can sometimes suffer from mass discrimination caused by either instrumental factors [187] or sample preparation [188], especially with high molecular weight and polydisperse polymer samples. However, the mCTA oligomers studied here have low dispersity and their molecular weights are low enough that this should not be a concern.

Dynamic Light Scattering

Malvern Zetasizer Nano ZS dynamic light scattering (DLS) provided the diameter of the NPs. The default method for latex NP sizing provided by Malvern was used in which the refractive index (RI) is set for polystyrene (1.590), absorption is 0.010, and parameters for water at 25.0°C are used for the dispersant: a viscosity of 0.8872 and RI 1.330 with dispersant viscosity set as the sample viscosity. Measurements were taken of latex NP suspensions prepared in 10 mM Tris buffer at pH 7.2 and 25.0°C to replicate EKC solvent conditions.

Chemical Ionization Mass Spectrometry

Mass spectra were collected with an Agilent 6320 Ion Trap MS with the Agilent Atmospheric Pressure Chemical Ionization (APCI) interface and custom 28 mm spacer as described in [189] to allow use of a capillary nebulizer assembly. Analytes were detected in positive ion mode between 50-350 m/z in Ultra Scan mode with an accumulation time of 20.00 ms and Smart Target of 200k ions. Skimmer 40.0V, Capillary Exit 102.3V, Octopoll 1 DC 12.00V, Octopoll 2 DC 1.70V, Trap Drive 37.3, Octopoll RF 118.3Vpp, Lens 1 -5.0V, Lens 2 -60.0V. The instrument was controlled with 6300 Series Ion Trap LC/MS software v6.1 (Build 90).

In the APCI source the capillary was maintained at -2000V, End plate Offset -500V, Corona +4000nA. The nebulizer settings are: 25.0 psi, Dry Gas 5.0 L/min, Dry Temp. 250°C, Vaporizer Temp. 350°C.

The coupled CE was an Agilent 61600AX CE. Injections were 100 mbar/s. 25kV was applied to a 80 cm × 50 µm capillary which was conditioned with 1 M NaOH for 10 min before use and flushed with BGE between runs.

4.1.2 Chromatographic characterization

Capillary Electrophoresis

All EKC separations were carried out on G1600 Agilent ³DCE instruments with on-column DAD controlled by Agilent Chemstation software.

A typical EKC run utilized the following procedure. Except when reported otherwise all EKC and LSER runs should be expected to follow this procedure: 10 mM Tris (ACROS, ≥99%%) adjusted to pH 7.20±0.05 using hydrochloric acid (EMD, GR ACS) was prepared daily using 18 MΩ nano-pure water (Barnstead D8991). Mixed standards were prepared at 4 mg/mL in acetone from analytes obtained in the highest purity available (≥98%) from Sigma-Aldrich or ACROS Organics. Analysis samples were prepared by dilution of the mixed standards in BGE to 100 µg/mL. 0.3% w/w suspensions of PSP were prepared by dilution of concentrated suspensions of PSP in the BGE.

Capillaries were prepared by flushing with 1.0 M NaOH for 10 min followed by BGE for 10 min before initial use, and re-conditioned as needed with the same method. Reconditioning was only required after 50+ runs. Capillaries were flushed with BGE for 1 min between each injection. The analysis samples were hydrodynamically injected at 35 mbar for 2 s onto 48.5 cm long 50 µm ID / 360 µm OD fused silica capillaries (Polymicro Technologies).

Analytes were detected at 210 nm or 245 nm, 8 cm from the outlet end of the capillary. Analyte peaks where identified by spectra and migration time. Ambiguous peaks were identified by spiking. The electrophoretic mobilities of the PSPs were measured from the elution times of acetone, as a marker for the EOF, and a homologous series of phenones; acetophenone, propiophenone, butyrophenone, valerophenone, heptanophenone, and hexanophenone, using the method of Bushey and Jorgenson [190] for all but the small MAAMPS NP.

The poor performance of the small MAAMPS NP precluded determination of the retention times of several of the phenones, so mobility was determined from the elution time of an injection of NPs in 50 mM borate BGE. When the other NPs were analyzed by this method their mobilities where found to be the same values as when measured by the retention method, but the measurement was less precise than the Bushey and Jorgenson method.

Linear Solvation Energy Relationships

The Linear Solvation Energy Relationship (LSER) model was used to investigate the solvation properties of the PSPs relative to the BGE. This model, which has been used previously to characterize and classify the solvation properties of dozens of PSPs [47], [48], [191], [192] including latex NPs [158], [160] provides information on the relative

strength of five types of chemical interactions between solutes and the PSP. In the current study, the retention times of 39 compounds (listed in Appendix A - LSER on page 8-136), and acetone as an unretained marker were measured in pentaplicate, and their retention factors were calculated. The retention factors were used to calculate the LSER parameters of each latex NP PSP by previously reported methods [160], [191].

4.2 Synthetic methods

4.2.1 Chemicals

Synthesis utilized:

2-Acrylamido-2-methylpropane sulfonic acid (AMPS) (Aldrich, 99%),
4,4′-Azobis(4-cyanovaleric acid) (V-501, Aldrich, ≥98.0%),
Hexyl acrylate (Aldrich, 98%),
Butyl acrylate (Aldrich, 99%),
Ethyl acrylate (Aldrich, 99%),
Methyl acrylate (Aldrich, 99%),
1-butanethiol (Aldrich, 99%),
Carbon disulfide (Aldrich, 99.9%),
2-bromopropionic acid (Aldrich, 99%),
Hexane (EMD, HPLC Grade),
Acetonitrile (EMD, HPLC)
Sodium hydroxide (EMD, GR ACS),
Hydrochloric acid (EMD, GR ACS),
Spectra/Por Regenerated Cellulose Dialysis Membrane of 500, 1000, and 2000 MWCO.

All water used in syntheses and chromatography was distilled and DI (18 MΩ) by a Barnstead D8991 or EMD Millipore SYNS0HF00.

4.2.2 Chain Transfer Agent

The chain transfer agent (CTA) is at the heart of RAFT polymerization. Its role is to mediate the radical polymerization by capturing and holding radical polymers as dormant polymers, while exchanging dormant polymers with active (radical) polymers to ensure all polymer chains have an equal degree of polymerization and to reduce the probability of self-termination.

Several batches of 2-{((butylsulfanyl)-carbonothioyl)sulfanyl}propanoic acid were synthesized as the CTA for this work utilizing the Ferguson procedure with minor variations [173]. This variation of the synthesis has been previously reported in the 2014 *Electrophoresis* article [160]. The method from this paper is included below (LH-67), and the specific variations from this synthesis for the other batches of CTA employed in this work are summarized in Table 3.

> "4.3 mL of 1-butanethiol (40 mmol), 6.5 mL of 25% NaOH (41 mmol),
> and 2.7 mL of carbon disulfide (61 mmol) were combined in 6.0 mL of

water and stirred for 30 min. In an ice bath, 3.7 mL of 2-bromopropionic acid (41 mmol) were added slowly with 6.0 mL of 25% NaOH (38 mmol). The mixture was stirred at room temperature for 18 h. The CTA was precipitated from solution with 10.0 mL of 10 M HCl and extracted into hexanes. The organic fraction was evaporated to dryness in vacuo. Powdery, bright-yellow CTA was recovered at 90.3% yield. Synthesis of the CTA is confirmed by proton NMR with chemical shifts that match literature values [32]. Powdery, bright yellow CTA was recovered at 90.3% yield. Synthesis of the CTA is confirmed by proton NMR with chemical shifts that match literature values [173]."

This representative synthesis was one of the several batches used in this work. The values for the rest are given in Table 3 below.

CTA Batch	Date Synthesized	BuThiol (mL)	CS$_2$ (mL)	BrProp (mL)	Rxn Time (Hr)	Total solvent (mL)	Purification	Yield
JSH 5A	6/14/2012	4.3	2.7	3.7	18	12.5 (no acetone)	Ppt oil w/ HCl, ext w/ hexanes. Evap. to dryness. NMR, HPLC	8.601g 90.3%
JSH 5B	8/2/2012	4.3	2.7	3.7	18	19.6	Ext w/ hexanes. Evap. to dryness.	9.24g 97%
JSH 5C	6/5/2013	13	8.1	11.1	Overnight	45.5	Ppt oil w/ HCl, ext w/ hexanes. Evap. to ½ vol, recry, filtered.	7.1g ~25%
JSH 28	7/27/2011	4.3	2.7	3.7	21	12.5	Ppt oil w/ HCl, ext w/ hexanes. Evap. to dryness. NMR, GC	7.969g 83.6%
HNC 22	6/4/2015	4.3	2.7	3.7	Overnight	12.5	Ppt oil w/ HCl, ext w/ hexanes. Evap. to dryness. NMR	3.438g 36%
LH 67	1/7/2013	4.3	2.7	3.7	Overnight	56.1	Ext. w/ hexanes, evap. To dryness, recy w/ hexane.	5.398g ~57%

Table 3 Nanoparticle synthetic conditions: CTA

4.2.3 Macro Chain Transfer Agent

The first polymerization stage is the synthesis of the macro CTA (mCTA) by RAFT polymerization of a monomer. 2-Acrylamido-2-methylpropane sulfonic acid (AMPS) was utilized as the monomer for the mCTA. AMPS was selected because the sulfonic acid group in AMPS remains ionized to very low pH, allowing the poly(AMPS) block to provide a charged, hydrophilic character to the final NP. The acrylamide moiety is also important as it compares well to the reactivity of the acrylate moieties of the hydrophobic monomers used in the core. This is necessary so that one CTA can mediate the polymerization of both monomers.

The four batches of mCTA employed in later synthesis are reported here. Ten of the NPs reported in the following section were synthesized from the same mCTA batch (JSH-26) to ensure uniform shell architecture. Polymerization of the mCTA was run to high percent conversion as measured by NMR and the reactions were quenched by freezing to prevent excess self-termination. The RAFT polymerization mechanism and synthetic concerns are discussed in detail in chapter 3.

Polymer length was stoichiometrically controlled by the ratio of CTA to monomer employed. The synthesis of JSH-26 is given as a representative synthesis. For this synthesis a 1:8 CTA-to-AMPS ratio was used. 24.030 g (115.95 mmol) AMPS, 3.4632 g (14.527 mmol) CTA, 213.9 mg (0.7632 mmol) V-501 (initiator), and 100 mL water were combined and sparged with nitrogen for an hour. The solution was heated to 70°C for 4.3 h while stirring and then quenched by freezing. After lyophilization, 28.490 g (105% yield) of yellow powder was recovered. The excess mass is attributed to incomplete removal of water due to the hydroscopic nature of the AMPS mCTA. NMR spectroscopy shows no hydrocarbon impurities. The mCTA was used without further purification.

mCTA	CTA	AMPS(g) AA(mL)	V-501 (mg)	Solvent (mL)	O_2 Removal	Rxn Time (hr)	Purification	Yield (%)
JSH-26	3.4632g LH-67	24.030g	213.9	100	60min N_2	5	None	105
JSH-33A	1.6036g JSH-5B	4 mL	199.2	16	40min N_2	7	NA	NA
JSH-33C	0.4951g JSH-5C	4 mL	62.9	16	45min N_2	5.25	Dialysis	88
JSH-42A	0.4670g JSH-28	7.253g	24.7	20	Pump/purge X3	Variable	NA	NA
JSH-42B	0.455g JSH-28	7.499g	25.4	20	Pump/purge X3	Variable	NA	NA
JSH-42C	0.450g JSH-28	7.517g	25.8	20	Pump/purge X3	Variable	NA	NA
LH-54C	1.237g JSH-5A	9.736	74	40	Pump/purge X3	4.5	None	NR
LH-43A	1.001g JSH-5A	14.772	60	40	Pump/purge X3	3.5	Dialysis	22
HNC-24	1.121g HNC-22	10.0	69	40	45+ min N_2	5	None	NR
HNC-29	0.3161g HNC-22	10.12g	45.5	34	45+ min N_2	5	None	NR

Table 4 Nanoparticle synthetic conditions for the mCTA used in this work.

4.2.4 Diblock / Nanoparticles

Copolymers were synthesized from mCTA and alkyl acrylates using modifications to the Sumerlin procedure [175] with stoichiometric control of polymer length providing control of particle diameter. Both round bottom flasks with magnetic stir bar stirrers (Figure 34B) and a small reaction vessel with overhead stirring (Figure 34A) were used. All dialysis was conducted with Spectra/Por 6 2000 molecular weight cut-off dialysis membrane with 20:1 ratio of dialysate-to-dialysis solution. The dialysate solution was changed at least twice over two or more days of dialysis for most NP synthesis.
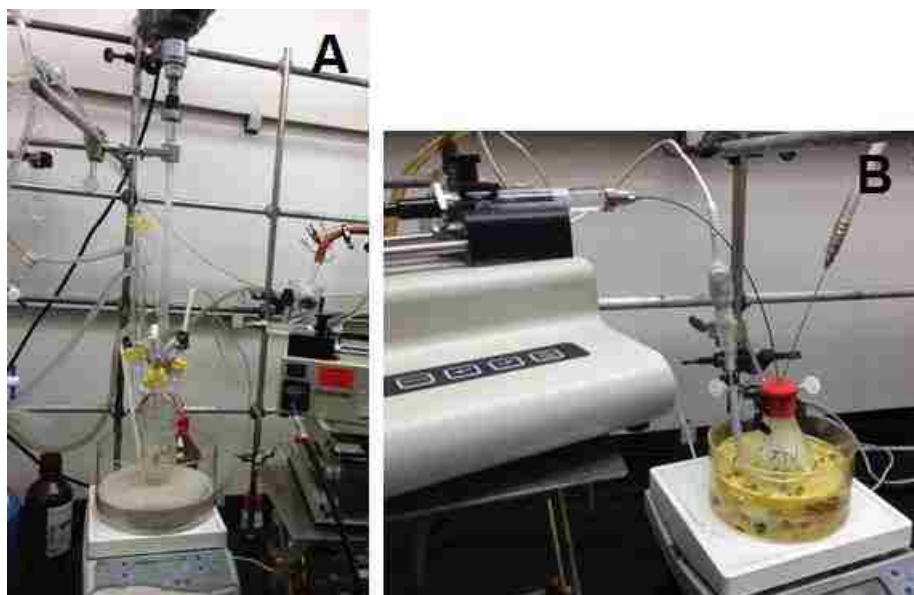
Figure 34 Synthetic apparatus for diblock synthesis. A) Overhead stirrer system B) Magnetic stirring system in round bottom flask.

LH-5 (BAAMPS, Large) was synthesized from 0.1676 g (0.0650 mmol) mCTA, 8.7 mg (0.060 mmol) V-501, and 30 mL water. This mixture was titrated to pH 6.89 and sparged with nitrogen for 1.5 hours. The mixture was heated to 70°C for 21 hours and 5.28 mL (36.9 mmol) butyl acrylate (569:1 monomer-to-mCTA ratio) were added at 1.0 mL/hour. The resulting white suspension was dialyzed. An average NP diameter of 139 nm ± 14% RSD was found by DLS in 10 mM pH 7.20 Tris buffer.

LH-111(BAAMPS, Small) was synthesized from 0.3374 g (0.1309 mmol) mCTA, 16.8 mg (0.031 mmol) V-501, and 30 mL water. This mixture was titrated to pH 7.32 and sparged with nitrogen for 1.5 hours. The mixture was heated to 70°C for 30 hours and 5.04 mL (35.3 mmol) butyl acrylate (270:1 monomer-to-mCTA ratio) were added at 1.0 mL/hour. The resulting yellow/white suspension was dialyzed. An average NP diameter of 17 nm ± 23% RSD was found by DLS in 10 mM pH 7.20 Tris buffer.

LH-12 (EAAMPS, Large) was synthesized from 0.3235 g (0.1255 mmol) mCTA, 16.8 mg (0.031 mmol) V-501, and 30 mL water. This mixture was titrated to pH 6.86 and sparged with nitrogen for an hour. The mixture was heated to 70°C for 22 hours and 2.57

mL (24.1 mmol) ethyl acrylate (192:1 monomer-to-mCTA ratio) were added at 1.0 mL/hour to the reaction vessel. The resulting white suspension was dialyzed. An average NP diameter of 115 nm ± 9.5% RSD was found by DLS in 10 mM pH 7.20 Tris buffer.

JSH-17A (EAAMPS, Small) was synthesized as reported [160] from 0.8756 g (0.2907 mmol) mCTA, 14 mg (0.050 mmol) V-501, and 10 mL water. This mixture was titrated to pH 6.94 and sparged with nitrogen for an hour. The mixture was heated to 70°C overnight and 1.62 mL (15.2 mmol) ethyl acrylate (51:1 monomer-to-mCTA ratio) were added at 1.0 mL/hour to the reaction vessel. The resulting yellow solution was dialyzed. An average NP diameter of 12 nm ± 23% RSD was found by DLS in 10 mM pH 7.20 Tris buffer.

LH-103 (MAAMPS, Large) was synthesized from 0.3372 g (0.1308 mmol) mCTA, 16.4 mg (0.059 mmol) V-501, and 25 mL water. This mixture was titrated to pH 6.69 and sparged with nitrogen for 2 hours. The mixture was heated to 70°C for ≥24 hours and 3.17 mL (35.2 mmol) methyl acrylate (269:1 monomer-to-mCTA ratio) were added at 1.0 mL/hour. The resulting yellow gel was sonicated into water to form a milky white suspension which was dialyzed. An average NP diameter of 123 nm ± 25% RSD was found by DLS in 10 mM pH 7.20 Tris buffer.

LH-11 (MAAMPS, Small) was synthesized from 0.3239 g (0.1257 mmol) mCTA, 16.9 mg (0.060 mmol) V-501, and 25 mL water. This mixture was titrated to pH 6.89 and sparged with nitrogen for 0.7 hour. The mixture was heated to 70°C for ≥20 hours and 1.59 mL (17.7 mmol) methyl acrylate (141:1 monomer-to-mCTA ratio) were added at 1.0 mL/hour to the reaction vessel. The resulting clear yellow suspension was dialyzed. An average NP diameter of 17 nm ± 19 % RSD was found by DLS in 10 mM pH 7.20 Tris buffer.

LH-13 (BAAMPS) was synthesized from 0.3214 g (0.1697 mmol) mCTA, 16.5 mg (0.0589 mmol) V-501, and 35 mL water. This mixture was titrated to pH 6.80 and sparged with nitrogen for 1 hour. The mixture was heated to 70°C overnight and 3.4 mL (24 mmol) butyl acrylate (140:1 monomer-to-mCTA ratio) were added at 1.0 mL/hour. The resulting cloudy white suspension was dialyzed. An average NP diameter of 50.77 nm ± 22% RSD was found by DLS in 10 mM pH 7.20 Tris buffer.

LH-14 (EAAMPS) was synthesized from 0.8709 g (0.4597 mmol) mCTA, 45 mg (0.16 mmol) V-501, and 35 mL water. This mixture was titrated to pH 6.76 and sparged with nitrogen for 1 hour. The mixture was heated to 70°C overnight and 3.43 mL (32 mmol) ethyl acrylate (68:1 monomer-to-mCTA ratio) were added at 1.0 mL/hour. The resulting clear yellow solution was dialyzed overnight. An average NP diameter of 58 nm ± 46 RSD was found by DLS in 10 mM pH 7.2 Tris buffer.

LH-7 (EAAMPS) was synthesized from 0.1673 g (0.0883 mmol) mCTA, 8.6 mg (0.031 mmol) V-501, and 30 mL water. This mixture was titrated to pH 6.91 and sparged with nitrogen for 0.7 hour. The mixture was heated to 70°C overnight and 4.01 mL (37.7

mmol) ethyl acrylate (427:1 monomer-to-mCTA ratio) were added at 1.0 mL/hour. The resulting off white solution was dialyzed. An average NP diameter of 116.1 nm ± 31 RSD was found by DLS in 10 mM pH 7.2 Tris buffer.

LH-15 (MAAMPS) was synthesized from 0.5526 g (0.2917 mmol) mCTA, 29.5 mg (0.1053 mmol) V-501, and 30 mL water. This mixture was titrated to pH 6.55 and sparged with nitrogen for 0.45 hour. The mixture was heated to 70°C overnight and 3.61 mL (40.1 mmol) methyl acrylate (137:1 monomer-to-mCTA ratio) were added at 1.0 mL/hour. The resulting clear yellow solution was dialyzed two days. An average NP diameter of 26.84 nm ± 25 RSD was found by DLS in 10 mM pH 7.2 Tris buffer.

LH-8B (MAAMPS) was synthesized from 0.3240 g (0.1710 mmol) mCTA, 19.8 mg (0.0706 mmol) V-501, and 40 mL water. This mixture was titrated to pH 6.88 and sparged with nitrogen for 0.7 hour. The mixture was heated to 70°C for 11 hours and 6.4 mL (71 mmol) methyl acrylate (413:1 monomer-to-mCTA ratio) were added at 1.0 mL/hour. The resulting solution was dialyzed. An average NP diameter of 87.73 nm ± 28 RSD was found by DLS in 10 mM pH 7.2 Tris buffer.

JSH-11A (BAAMPS) was synthesized from 0.496 g (0.262 mmol) mCTA, 8.0 mg (0.029 mmol) V-501, and 5 mL water. This mixture was titrated to pH 6.01 and sparged with nitrogen for 1+ hour. The mixture was heated to 70°C for 13 hours and 1.2 mL (8.4 mmol) butyl acrylate (28:1 monomer-to-mCTA ratio) were added at 1.0 mL/hour. The resulting cloudy white suspension was dialyzed. An average NP diameter of 14.2 nm ± 7.8% RSD was found by DLS in 10 mM pH 7.20 Tris buffer.

HNC-25 (BAAMPS) was synthesized from 0.2982 g (0.1157 mmol) mCTA, 4.5 mg (0.016 mmol) V-501, and 30 mL water. This mixture was titrated to pH 6.68 and sparged with nitrogen for 0.75 hour. The mixture was heated to 80°C overnight and 4.5 mL (32 mmol) butyl acrylate (272:1 monomer-to-mCTA ratio) were added at 1.0 mL/hour. The resulting cloudy white suspension was dialyzed. An average NP diameter of 89 nm ± 12% RSD was found by DLS in 10 mM pH 7.20 Tris buffer.

Table 5 and Table 6 (rotated landscape on page):

Core Chem	BA	BA	BA	BA	BA	EA	EA	EA	EA	MA	MA	MA	MA	HA	BA
Name	JSH-11A	LH-111	LH-13	HNC-25	LH-5	JSH-17A	LH-14	LH-12	LH-7	LH-11	LH-15	LH-8B	LH-103	KH-13	JSH-39
mCTA(g)	0.4960	0.3374	0.3214	0.2982	0.1676	0.8756	0.8709	0.3235	0.1673	0.3239	0.5526	0.3240	0.3372	0.5947	0.7360
Int (mg)	8.0	16.8	16.5	4.5	8.7	14.0	45.0	16.8	8.6	16.9	29.5	19.8	16.4	15.4	12.3
Mon. (g)	1.1	4.5	3.0	4.0	4.7	1.5	3.1	2.4	3.7	1.5	3.5	6.1	3.0	3.4	4.5
Size (nm)	14	17	51	89	139	12	58	115	116	17	27	88	123	68	44
PDI (RSD)	0.078	0.229	0.222	0.121	0.14	0.23	0.46	0.095	0.31	0.188	0.246	0.28	0.25	0.383	0.046
ionic:mer	7	8	8	11.3	8	13.4	8	8	8	8	8	8	8	8	20
pH	6.01	7.32	6.8	6.68	6.89	6.94	6.76	6.86	6.91	6.89	6.59	6.68	6.69	6.56	6.11
mCTA:Int	10.3	3.0	2.9	7.2	2.8	5.8	2.9	2.8	2.9	2.8	2.8	2.4	3.0	4.2	3.8
M:mCTA	28	197	139	272	417	51	68	138	417	103	138	413	198	69	208

Table 5 Nanoparticle synthetic conditions: NP.

CTA	JSH-28	HNC-22		JSH-5A							LH-67				
mCTA	JSH-33C	HNC-24	LH-43A	LH-54C2							JSH-26				
NP	JSH-39	HNC-25	JSH-17A	JSH-11A	LH-111	LH-13	LH-5	LH-14	LH-12	LH-7	LH-11	LH-15	LH-8B	LH-103	KH-13

Table 6 Synthetic flow chart denoting which CTA was used for which mCTA and NP in turn.

4.2.5 Nanoparticle Size Study

The RAFT polymerization method allows, in principle, the size of the NP to be systematically controlled by variation of the ratio of hydrophobic monomer to mCTA. To investigate the relationship between the monomer-to-mCTA ratio and NP diameter, sets of latex NPs were synthesized in batches of six reactions prepared and run simultaneously to ensure matching synthetic conditions. In a typical synthesis, AMPS mCTA (JSH-26) and 400 µg/mL solution of V-501 were titrated to pH 6.7±0.2 with NaOH before addition of varied amounts of monomer to separate glass vials.
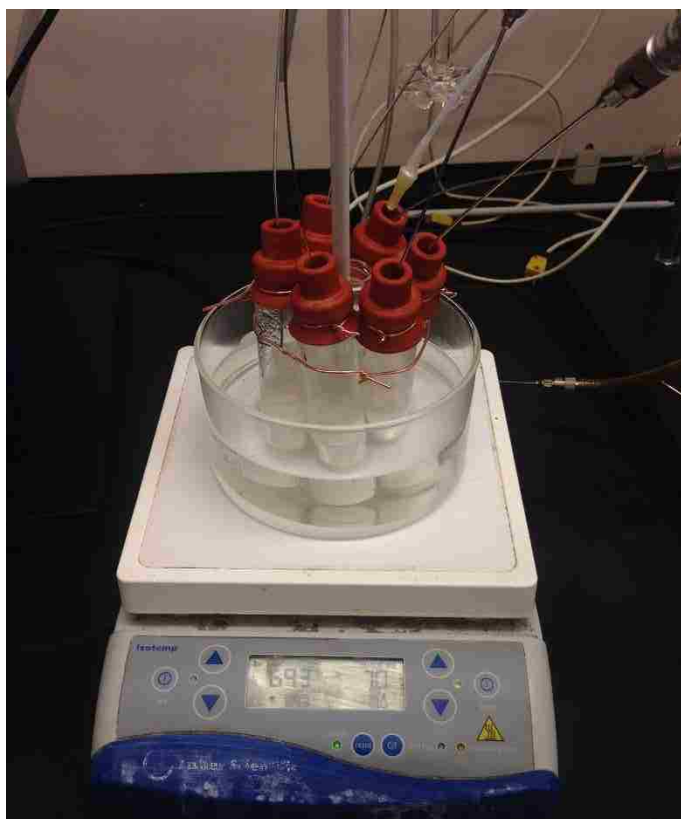
Figure 35 Synthetic apparatus for Size vs Mer studies.

The reactant quantities reported in Figure 36 below were calculated to produce a theoretical yield of 2 g of NPs at 90% conversion with a 10:1 mCTA-to-initiator ratio. Additional water was added as required to bring all reaction vials to an equal volume of 23±4 mL. Each set of vials was then simultaneously sparged with nitrogen for 30 min. The nitrogen flow was removed before heating to 70°C with magnetic stirring for 20±2 hours. NPs were characterized by DLS as prepared without additional purification. The results are discussed in 5.1.2 Hydrophobic Block Length on page 5-78.

BAAMPS

Core Chem	Vial 1	Vial 2	Vial 3	Vial 4	Vial 5	Vial 6	Vial 8	Vial 9	Vial 10	Vial 11	Vial 12
M:mCTA	100	100	150	200	500	500	100	100	700	800	800
JSH-26 mCTA (g)	0.2759	0.2759	0.1928	0.1482	0.0620	0.0620	0.2759	0.2759	0.0447	0.0392	0.0392
V-501 Init. (mg)	3.769403	3.769403	2.634047	2.024317	0.84739	0.84739	3.8	3.8	0.6	0.5	0.5
V-501 soluton (mL)	9.42	9.42	6.59	5.06	2.12	2.12	9.42	9.42	1.53	1.34	1.34
Monomer (mL)	1.93	1.93	2.02	2.07	2.17	2.17	1.93	1.93	2.19	2.19	2.19
DLS Size (nm)	20.78	22.74	33.47	38.15	99.88	103.4	22.99	28.24	130.90	158.60	133.00
DLS Size (%RSD)	15	17	9.9	8.8	7	4	19.00	23.00	2.70	1.20	1.30

EAAMPS

Core Chem	Vial 2	Vial 3	Vial 4	Vial 5	Vial 6
M:mCTA	200	200	400	600	800
JSH-26 mCTA (g)	0.1859	0.1859	0.0975	0.0661	0.0500
V-501 Init. (mg)	2.5393	2.5393	1.3315	0.9023	0.6824
V-501 soluton (mL)	6.35	6.35	3.33	2.26	1.71
Monomer (mL)	1.9762	1.9762	2.0725	2.1067	2.1242
DLS Size (nm)	31.35	52.51	107.2	154.8	228.3
DLS Size (%RSD)	5.9	9.3	1.7	2.2	1.9

MAAMPS

Core Chem	Vial 1	Vial 2	Vial 3	Vial 4	Vial 6	Vial 8	Vial 9	Vial 10	Vial 11	Vial 13	Vial 14	Vial 15	Vial 16	Vial 17	Vial 18	Vial 19	Vial 20
M:mCTA	100	200	200	400	800	100	150	200	300	400	500	600	700	800	800	400	500
JSH-26 mCTA (g)	0.3849	0.2130	0.2130	0.1125	0.0579	0.3402	0.2404	0.1859	0.1279	0.1125	0.0910	0.0764	0.0659	0.0579	0.0579	0.1125	0.0910
V-501 Init. (mg)	5.258379	2.90908	2.90908	1.536315	0.790375	4.6	3.3	2.5	1.7	1.5	1.2	1.0	0.9	0.8	0.8	1.5	1.2
V-501 soluton (mL)	13.15	7.27	7.27	3.84	1.98	11.62	8.21	6.35	4.37	3.84	3.11	2.61	2.25	1.98	1.98	3.84	3.11
Monomer (mL)	1.69	1.87	1.87	1.97	2.03	1.4930	1.5827	1.6317	1.6839	1.97	2.00	2.01	2.02	2.03	2.03	1.97	2.00
DLS Size (nm)	24.99	59.49	70.73	198.1	249	32.01	56.65	99.38	124	140.7	151.7	297.9	212.9	291	406	184.9	214
DLS Size (%RSD)	38	6.1	3.6	2.2	0.2	8.2	5.8	1.2	0.6	0.9	3.3	1.8	1.6	2.1	3.1	1.7	1.5

HAAMPS

Core Chem	Vial 1	Vial 2	Vial 3	Vial 5	Vial 6
M:mCTA	50	100	200	500	500
JSH-26 mCTA (g)	0.4962	0.2833	0.1524	0.0639	0.0639
V-501 Init. (mg)	13.4904	7.7004	4.1436	1.7368	1.7368
V-501 soluton (mL)	1.6935	1.9333	2.0806	2.1803	2.1803
Monomer (mL)	2.3685	1.3519	0.7275	0.3049	0.3049
DLS Size (nm)	16.90	19.65	38.17	58.87	130.4
DLS Size (%RSD)	31.00	31.00	24.00	15.00	7.5

Figure 36 Nanoparticle synthetic conditions: Size study.

4.3 Characterization

4.3.1 Chain Transfer Agent

The CTA was characterized by ^{1}H and ^{13}C NMR in CDCl$_3$, and the purity of many batches was checked by HPLC using the methods described in 4.1.1 Synthetic characterization on page 4-54. The NMR peak assignments are given below and match literature values [173].

^{1}H NMR: δ (ppm) 9.6 (br, 1H, CO$_2$**H**), 4.875 (q, J = 7.28 Hz, 1H, SC**H**), 3.38 (t, J = 7.28 Hz, 2H, C**H**$_2$S), 1.70 (pent, J = 7.63 Hz, 2H, C**H**$_2$CH$_2$CH$_2$S), 1.64 (d, J = 7.28 Hz, 3H, SCHC**H**$_3$), 1.45 (sext, J = 7.63 Hz, 2H, CH$_3$C**H**$_2$CH$_2$), 0.94 (t, J = 7.28 Hz, 3H, C**H**$_3$CH).

^{13}C NMR: δ (ppm) 221.9 (**C**=S), 177.7 (**C**=O), 47.7 (S**C**H), 37.3 (**C**H$_2$S), 30.1 (**C**H$_2$CH$_2$CH$_2$), 22.3 (CH$_3$**C**H$_2$), 16.8 (SCH**C**H$_3$), 13.8 (CH$_2$**C**H$_3$).

4.3.2 Macro Chain Transfer Agent

The number average degree of polymerization was measured by MALDI-TOF MS (method on page 4-54). Fifty spectra were collected for each mCTA characterized, and the degree of polymerization was calculated for each mCTA as described above. Calculations were done in house using a custom calculation program written and operated by Julie McGettrick in Microsoft Excel which will be available in an upcoming paper.

Degree of polymerization was also measured by ^{1}H NMR. NMR of polymers is inherently more imprecise than MS techniques and is heavily dependent on the selected integration ranges as anisotropy causes a great deal of broadening in the spectra of the motionally-restricted atoms. Both the MALDI-TOF and NMR found larger molecular weights than predicted by the reaction stoichiometry, but the NMR showed the largest discrepancy. The breadth of the ^{1}H NMR peaks lead to significant uncertainty in defining integration ranges. Due to this uncertainty the ^{1}H NMR should be considered semi-quantitative.

4.3.3 Diblock

The self-aggregated diblock polymers are very challenging to characterize. Traditional methods for determining polymer mass through size exclusion chromatography (SEC) are ineffective due to the aggregation of an unknown number of copolymers in each NP. Even when the aggregation number was known, there are no standards available with the same ionic character, so no quantitative measure could be made of diblock polymer mass by SEC.

Attempts to use MALDI to fragment NPs to analyze individual copolymers has so far proven futile using the conditions employed for mCTA analysis.

This leaves NMR as the only remaining option for probing the composition of the diblock copolymer within the structure of the NP. In this environment the copolymers are even

more motionally restricted, resulting in slow relaxation and anisotropic peak broadening. By using relaxation times of 5X T_1 relatively quantitative integration can be achieved [181]. However, the uncertainty in integration intervals remains a large source of error.

By comparing the peak area for CH_2 or CH_3 groups unique to each block of the polymer, general estimates of block length can be made. However, due to the uncertainty of the measurement, NMR estimates of relative block length should also be considered semi-quantitative at best.

4.3.4 Nanoparticles

Dynamic Light Scattering

As described above (page 4-55) DLS was used to determine the size of the NPs in typical buffer conditions. Z-average diameters are reported throughout this dissertation.

Residual mCTA in NPs

Several NPs were checked for residual mCTA by CE separation of an injection of NPs under conditions developed in the thesis work of Adam Sutton at the University of Western Sydney [193]. A capillary 48.5 cm long and 50 µm ID was flushed with 1 M NaOH for 10 min, water for 5 min, and 50 mM borate BGE for 10 min before 1.0% w/w NP solutions with acetone as a t_0 marker were hydrodynamicly injected at 35 mbar for 2 s and a potential of 20 kVDC was applied. The NPs eluted past the UV/VIS detector around 4-5 min into the run and the poly(AMPS) mCTA eluted around 6-7 min if it was detected. The details are in notebook JSH2-86 and chromatograms appear on page 5-90.

Mobility

The electrophoretic dispersity of the NPs was measured from the separation of an injection of NPs by CE (Figure 51). The peak width of the NPs provides the electrophoretic dispersity and the time of elution provides an approximant measure of the mobility using Equation 1-2. The electrophoretic mobility of the NPs was more often calculated by the Bushy and Jorgenson method [190]. The results from both methods was found to match each other closely.

The electrophoretic dispersity of the NPs corresponds strongly to the polydispersity in their size as measured by DLS. This is discussed on more detail below in 5.1.1 Ionic Block Length on page 5-73.

Chapter 5 Results

The goal of this research was to determine the effect of NP architecture on EKC performance. Since the NP architecture was defined by three factors, this research investigated the impact of those properties of the NP on performance as a PSP:

1. The ionic/hydrophilic polymer block chemistry
2. The degree of polymerization of hydrophobic polymer block and resulting changes in NP diameter
3. The hydrophobicity of the NP PSP core

With these structural features in mind, synthetic methods were optimized to allow multiple NP PSPs with systematic variation in architecture to be generated, characterized, and evaluated as PSPs. A novel ionic polymer block with strongly acidic sulfonate functionality was introduced, and the performance of these NPs in various buffer systems and at high and intermediate pH was evaluated. The bulk of the research is focused on six NP architectures; all synthesized using the same ionic polymer block as a mCTA but with variations in hydrophobic block chemistry and degree of polymerization. These six NPs comprise hydrophobic cores consisting of monomers of increasing hydrophobicity (methyl-, ethyl-, and butyl-acrylates), each generated with "large" and "small" diameters of approximately 126 nm and 15 nm respectively.

The chromatographic performance of the PSPs is described by the parameters of electrophoretic mobility, methylene selectivity, number of theoretical plates generated, and the peak capacity of the separation [191], [194]. LSER analysis was also conducted for each of the materials that exhibited practical performance in these categories in order to more fully characterize structure-induced changes in the solvation environment and separation selectivity of the PSPs. The utility of the NP PSPs in various background electrolytes (BGE), including BGE containing up to 30% acetonitrile, is demonstrated, as is a representative practical application to the analysis of nitroaromatic explosives.

5.1 Structural Properties
5.1.1 Ionic Block

The primary considerations in selecting a desired length and chemistry of the ionic polymer block are that it: A) provide charge to give mobility to the NP PSP; B) electrostatically shield NPs from one another; and C) that it not degrade the EKC performance of the NP PSP.

The charge provided by a polymer in solution is complex and not fully understood. Once polymerized, ionic moieties do not necessarily behave the same as they did in the monomer form. It seems reasonable to expect the presence of a large number of ionic sites within a relatively small volume along a polymer chain to generate a peculiar solvent environment where counter ions are able to be rapidly exchanged or even be

shared between ionic moieties. In water it is also expected that the solvent will form a hydrating shell around the polymer that further distributes the charge into what will be measured as a zeta potential distributed over the stern layer (see 2.1 Micelles section on page 2-20) of the polymer or polymeric particle.

Electrostatic shielding of NPs is important as soft colloidal materials like polymer NPs should be expected to undergo flocculation (defined by IUPAC as "a process of contact and adhesion whereby the particles of a dispersion form larger-size clusters." [195]). Much like Oswald ripening in liquid/liquid emulsions where Laplace pressure drives small particles to infuse into larger ones, flocculation will cause instability in the NP suspension. In this case the ionic section of the diblock provides electrostatic repulsion that inhibits NP PSPs from impinging on one another, thus suppressing flocculation.

Finally, while electrostatic repulsion between NPs is required to maintain stable NP suspensions, it must not shield the hydrophobic core of the NP from analytes or otherwise interfere with the partitioning of a solute between the NP and bulk solution. This can be, in large part, achieved by conducting the analysis at a pH where the analyte is not ionized. However, this is not always possible or even desired.

As has been shown for poly(acrylic acid) functionalized NP PSPs in the literature [158], and will be shown in the 5.5 LSER Characterization
 section on page 5-92 for poly(AMPS) NP PSPs, the ionic block appears to have little to no impact on mass transfer (the partitioning of the analyte between the PSP and bulk phase) or to provide any major contribution to NP PSP selectivity.

Chemistry
The ionic block of the copolymer NPs provides the charge needed for the NP to have electrophoretic mobility as shown in Equation 1-2. It was also shown in Figure 7 and further explored in the section on 1.3.1 Mobility on page 1-15 how higher mobility improves the capability of the PSP to provide good resolution. Latex NP PSPs developed in the past employed poly(acrylic acid) as the ionic block, but it has also been reported that poly(acrylic acid) has an effective pKa of ~7.4 at 25°C [196]. While the polymer has a complex system of conformational and ionic changes associated with neutralization of the polymer, poly(acrylic acid) based PSPs can be expected to be limited to neutral or basic buffers for EKC to avoid loss of ionization [158].

To improve the mobility and operational pH range of NP PSPs the first aim of this research was to replace the poly(acrylic acid) block with a poly(AMPS) block. AMPS provides a sulfonic acid moiety with low pKa to ensure that the ionic block of the copolymer remains ionized even in acidic buffers.
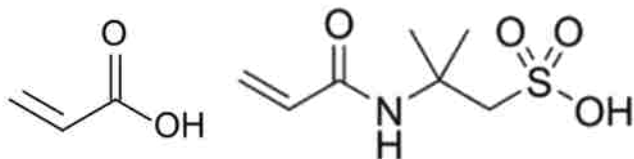
Figure 37 Acid form of ionic monomers. Acrylic acid (left) and AMPS (right).

RAFT polymerization of AMPS was conducted as reported above in the 4.2.3 Macro Chain Transfer Agent section starting on page 4-60. Several batches of mCTA were produced and used to synthesize diblocks over the course of this work. It was found that so long as great care was taken to remove oxygen from the reaction flask, the RAFT polymerization of AMPS was facile and repeatable.

The poly(AMPS) mCTAs were found to reach high conversion within 2-3 hours (Figure 38) at practically the same rate as poly(acrylic acid) (Figure 39). The overall conversion rate was investigated by polymerization of AMPS under identical conditions in three separate reactions. Aliquots were analyzed for percent conversion by ^{1}H NMR. Despite some variation in time needed for the reaction to start up, all runs illustrate that high conversion is reached in two hours and little benefit is had by running a reaction for more than three hours under these conditions.
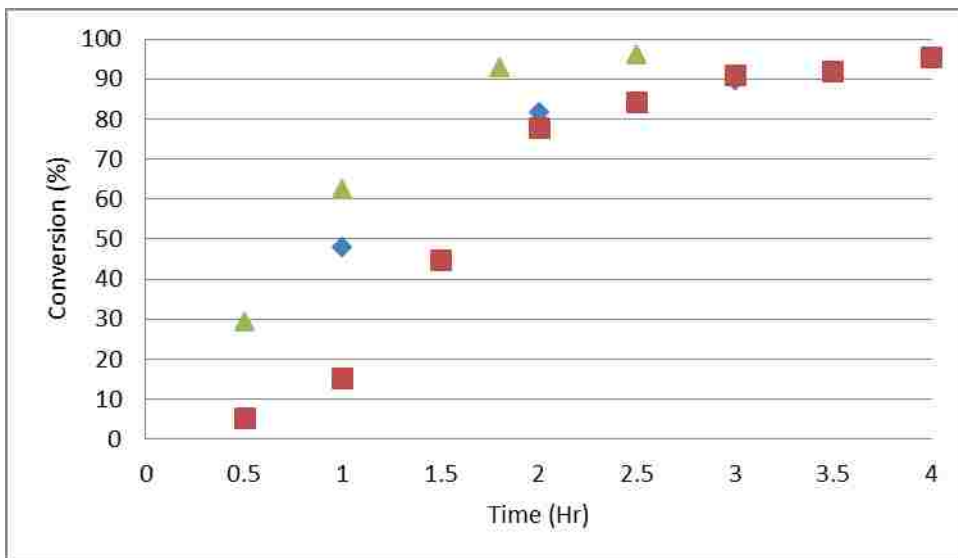

Figure 38 RAFT polymerization of poly(AMPS) mCTA: % conversion vs reaction time. Reaction started with 1.75M monomer at 400:20:1 molar ratio of Monomer:CTA:Initiator. (♦) JSH-42A, (■) JSH-42B, (▲) JSH-42C.

For poly(acrylic acid) a single RAFT polymerization was monitored to confirm a very similar overall reaction time. The slightly longer time needed to reach ~90% conversion may be due to a slightly lower molar concentration of acrylic acid in JSH-33A than of AMPS in the JSH-42A-C reactions despite a higher relative initiator concentration.
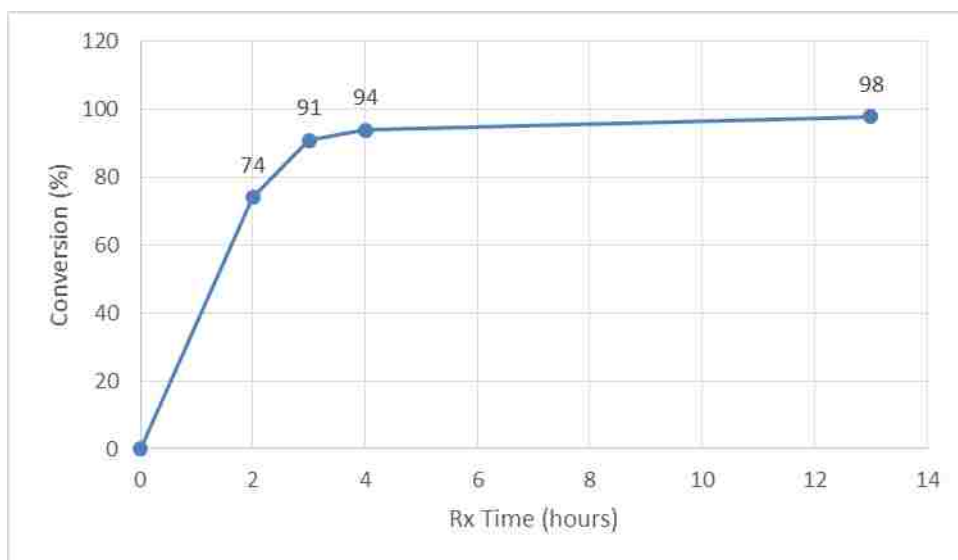
Figure 39 RAFT polymerization of poly(acrylic acid) mCTA: % conversion vs reaction time. Reaction started with 1.375M monomer at 82:9.5:1 molar ratio of Monomer:CTA:Initiator. Reaction JSH-33A.

Because self-termination of polymers occurs at a diffusion limited rate, it will slow slightly as polymer mass increases. However, the reaction should be halted as soon as possible to reduce the amount of self-terminated polymers that may be formed. In addition to the loss of polymer to self-termination, the CTA is known to lose activity either through hydrolysis [174] or side reactions with the polymer [197]. To minimize these negative effects, the general understanding of the conversion rate provided by these studies was used to limit mCTA reaction times to minimize the formation of unwanted species.

Length

The lengths of the ionic polymer blocks were measured by MALDI-TOF MS and NMR as described on page 4-68. MALDI-TOF analysis generates an envelope of the polymer masses that are produced by RAFT polymerization. The dispersion of this envelope of masses is quantified by the polydispersity index (PDI) of the polymer based on the ratio of mass averaged molecular mass (M_w) to the number averaged molecular mass (M_n).

The M_n, M_w, and PDI are defined in Equations 5-1, 5-2, and 5-3 respectively as:

$$\bar{M}_n = \frac{\sum_i N_i M_i}{\sum_i N_i} \tag{5-1}$$

$$\bar{M}_w = \frac{\sum_i N_i M_i^2}{\sum_i N_i M_i} \tag{5-2}$$

5-73

$$PDI = \frac{M_w}{M_n} \qquad\qquad 5\text{-}3$$

Where N_i is the number or abundance of polymer of mass M_i. The M_n value will emphasize the average number of each mass of polymer while the M_w value will emphasize the mass distribution among the polymers. The PDI provides a measure of how nearly the two values match. A PDI of 1.00 would mean that the envelope of polymer masses was perfectly symmetrical as indicated by M_n and M_w being equal. However, this is never the case. Polydispersity always results in M_w being larger than M_n as self-termination events increase the mass of the resulting polymers by as much as twice the mass of the parent polymers. The average degree of polymerization for a given polymer can be calculated by subtracting the mass of the end groups from M_n and dividing the result by the formula weight of the monomer.
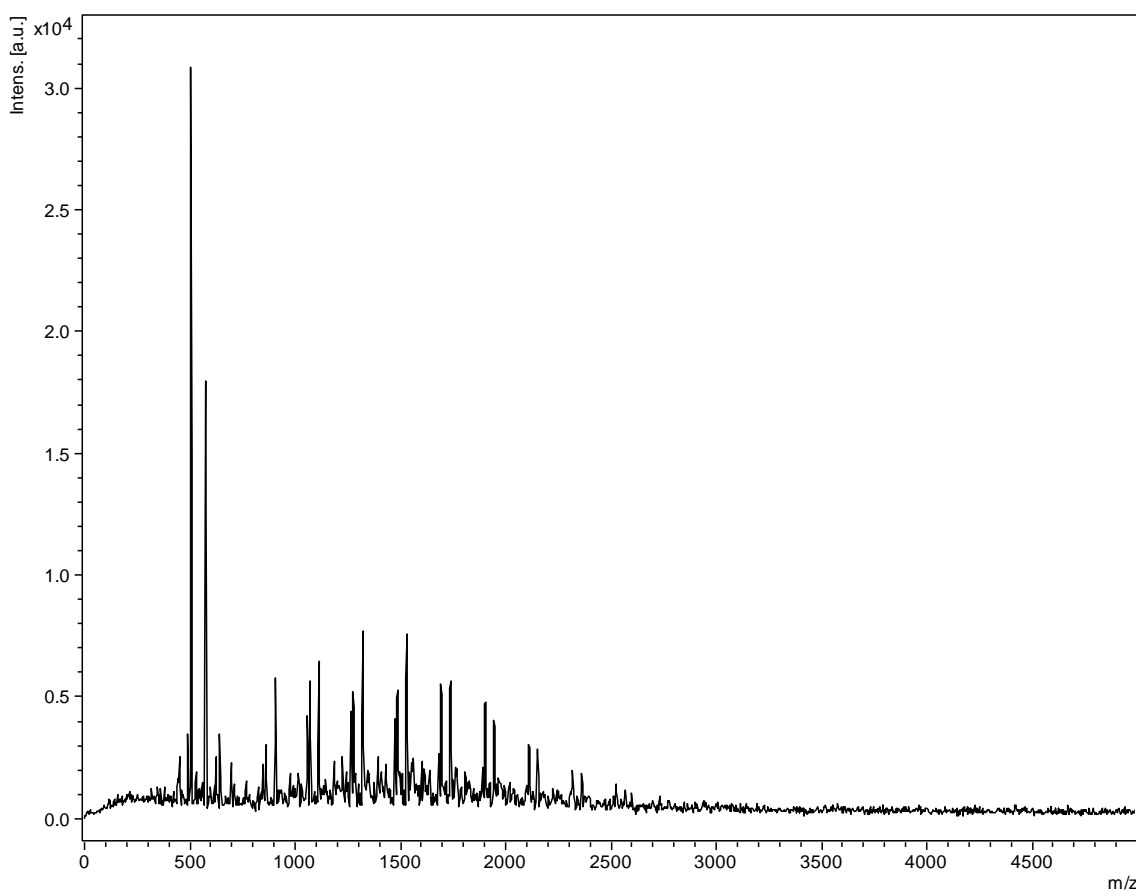

Figure 40 MALDI-TOF MS spectra of poly(AMPS) mCTA JSH-26. Collected in reflectron mode. DP=8±12% PDI=1.05 Mn=1980. High intensity peaks around 500m/z are matrix components. The paired peaks are mCTA with and without the CTA attached from fragmentation during ionization.

Figure 40 shows a representative MALDI-TOF analysis of a poly(AMPS) mCTA. This polymer is calculated to have a M_n=1980 g/mol, M_w=2079 g/mol and PDI of 1.05. The poly(acrylic acid) mCTA synthesized for the kinetic study was also characterized by

5-74

MALDI as shown in Figure 41. Considering the polymer distribution in Figure 41, we can calculate an M_n of 916.7 u an M_w of 957.8 u and a PDI of 1.045. The low PDI values observed here are a further indication that the polymerization proceeded under RAFT control; uncontrolled free radical polymerizations typically give much higher PDI ~1.5-2.0. In contrast, RAFT polymerization can typically provide a PDI of ≤1.1, especially for extremely short chain polymers like the mCTA in this work.
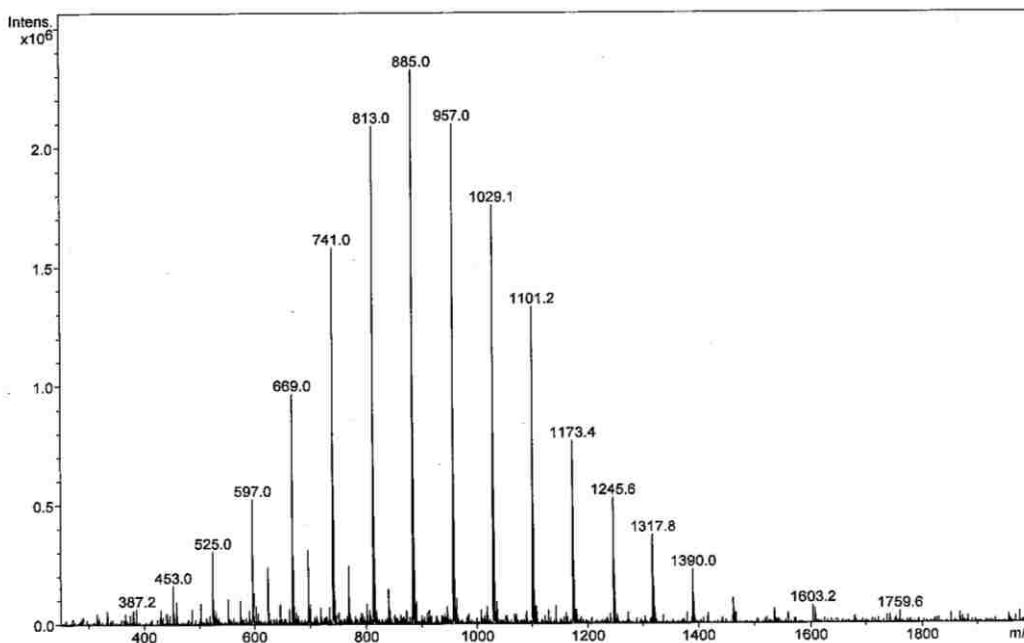

Figure 41 MALDI-TOF MS spectra of poly(acrylic acid) mCTA JSH-33A. Poly(acrylic acid) mCTA is also easily characterized by MALDI, although it may be less prone to loss of the CTA during ionization. Mn=916.7m/z, Mw=957.8m/z, PDI=1.045, DP=9.41mer.

Capillary electrophoresis was also used to study the degree of polymerization and its effect on the electrophoretic mobility of the poly(AMPS) mCTA used in most of the NP syntheses in this project. This approach was introduced, developed and explained in the Masters work of Adam Sutton at the University of Western Sydney [193]. In that work the separation of charged polymers (polyelectrolytes) was studied under so-called "critical conditions" where the mobility of the polyelectrolyte chain is independent of molecular mass. Sutton describes this behavior at the critical conditions as coiling of the polymer to better utilize shielding from counter ions:

> "These critical conditions arise in CE due to interactions of the counter ion with the polymer chain [198]. The polymer likely adopts a coiled conformation so that the electrostatic friction outweighs the hydrodynamic friction [199]. With the addition of each monomer unit the addition of the charge is offset by the screening of the counter ion adding to the electrostatic friction [200]. In this situation, separation of polyelectrolytes can occur according to structure or end groups."
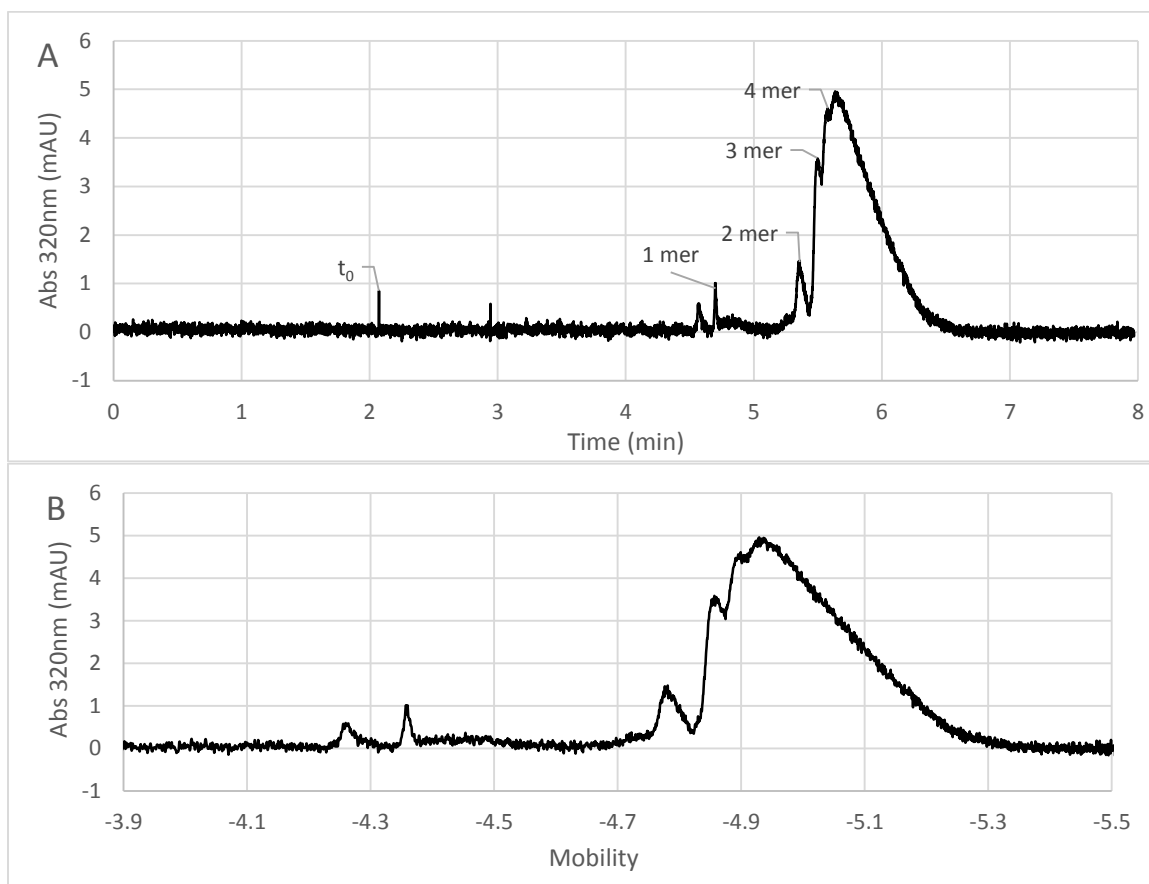
Figure 42 CE separation of JSH-26 poly(AMPS) mCTA in 50mM Borate on a 48.5cm x 50μm (40cm effective) capillary. 5g L^{-1} sample injected for 70 mbar s^{-1}. A) Absorbance vs time, B) Expanded view plotted vs mobility. No more than five of the eight dominate chain lengths are resolved: chains with more than 4-5 mer have indistinguishable mobility under EKC conditions. Chain length was found to provide even less variation in mobility at lower buffer concentrations.

The CE separation of poly(AMPS) JSH 26 is shown in Figure 42, conducted under buffer conditions identical to that used in EKC experiments. Above approximately five mer the poly(AMPS) reach the critical condition, no further separation of mCTA is observed, and individual polymer chains provide relatively consistent mobility. Based on signal strength, the majority of the polymer is 5 mer or greater. The breadth of the peak in Figure 42B illustrates that there is indeed ~10% variability in mobility of the mCTA under EKC conditions.

Nanoparticles synthesized using AMPS mCTAs of differing length and butyl acrylate cores were characterized by EKC, and the results are presented in Table 7. The NPs also vary in the degree of polymerization of butyl acrylate, complicating interpretation of the results. Alterations in the degree of polymerization of the poly(AMPS) block in the range of 6 to 11 mers appear to have no dramatic impact on primary EKC characteristics such as mobility or methylene selectivity compared to the effects of the size of the NP. The data for JSH-26 in Table 7 are of particular note as the mCTA was prepared as a large

batch (25 g) and was used in the synthesis of many of the NPs characterized here. The use of a single batch of mCTA for the preparation of NPs was preferred when investigating the roll of the NP core, as this eliminates any variability that could be introduced by variations in mCTA from NP to NP.

BAAMPS NP	poly(AMPS) mCTA	Poly(AMPS) DP	Size (nm)	μ_{ep} $-10^{-4}(cm^2/V*s)$	α_{CH2} (AU)
JSH-11A	LH-54C2	6-7*	14.2	3.818	3.104
LH-5	JSH-26	8	139	4.396	3.285
LH-111	JSH-26	8	17.1	4.005	3.130
HNC-25	HNC-21	11.3	89	3.946	3.287

*Table 7 Effect of DP of poly(AMPS) mCTA on PSP mobility. At the chain lingths studied here DP has no significant impact on mobility compared to the far larger effects of NP size. *Degree of polymerizaton is measureed by MALDI except for LH-54C2 where DP is estamated from reaction stoichiometry.*

That variations of a few mer have no little impact on NP PSP mobility of a ~10 mer polymer block is not surprising. The variability in mobility between different NPs is no greater than the variability observed for an individual polymer synthesis (Figure 42B). Although EKC conditions are not true critical conditions for poly(AMPS), the ionic polymer block will provide sufficiently uniform mobility for the NP PSP for uniform EKC behavior. This uniformity is further ensured by individual NPs containing a random sample of the available poly(AMPS) chain lengths, which further averages the mobility between all NPs.

The data presented here indicate that the synthetic conditions yield poly(AMPS) mCTA reproducibly under RAFT control, and that at chain lengths above 5, the electrophoretic mobility is independent of degree of polymerization. These results also suggest that the length of the ionic polymer block has relatively minor effects on EKC selectivity and performance of NP PSPs. Results to be presented below also demonstrate relatively minor differences in EKC selectivity for NP PSPs with poly(AMPS) vs poly(acrylic acid) shells. Given all of these results, changes in the length of the ionic polymer block was not expected to have substantial effects on the EKC selectivity of performance of NP PSPs, and this was not studied further.

5.1.2 Hydrophobic Block
Because past work [157], [158], [160] has suggested that analytes are solvated by the hydrophobic block of the diblock polymer nanoparticles, and have little to no interaction with the ionic block, most of this work focuses on the hydrophobic block. To understand the effect the hydrophobicity of the hydrophobic block has on selectivity, a number of monomers, each providing different degrees of hydrophobicity, were employed to synthesize NP PSPs.

While butyl acrylate has been used for diblock based NP PSPs in the past [158], this work compares NPs containing butyl acrylate with ethyl acrylate and methyl acrylate hydrophobic blocks to investigate the effects of reducing hydrophobicity, and hexyl acrylate to investigate the effect of increased hydrophobicity. Each of these NPs was synthesized and characterized with a different degree of polymerization of the hydrophobic block, resulting in different NP diameters.

Length and NP Diameter
To investigate the capacity of RAFT polymerization to control and systematically vary NP size, a significant number of NPs were synthesized with various molar ratios of monomer to CTA (4.2.5 Nanoparticle Size Study, page 4-66). The results of these studies are presented in Figure 43. These results indicate that it is indeed possible to systematically control the degree of polymerization of the hydrophobic block, and, in turn, the diameter of the resulting NP by control of the synthetic conditions.

There are two additional striking results observed from the results in Figure 43. First, there is a linear relationship between NP diameter and the ratio of hydrophobic monomer to mCTA. Second, the slope of the linear regression shows that the longer alkyl chain butyl acrylate core monomer results in a smaller NP per mer than do the shorter alkyl chain ethyl acrylate or methyl acrylate monomers. The synthetic reproducibility is relatively poor for the MAAMPS NPs, resulting in significant scatter in that plot, but the trend is apparent. However, limited results with hexyl acrylate based HAAMPS NPs exhibited the same relationship between polymer length and NP size as BAAMPS, suggesting that extending alkyl chain length beyond four methylene units may not provide any increase in cohesive intra-polymer forces.

The result that the NP diameter measured by DLS increases linearly with the monomer ratio (M-to-mCTA) is highly significant as it illustrates that the polymers do not experience sufficient inter-polymer forces within the NP to collapse the polymer chains onto one another and exclude the aqueous BGE. If cohesive forces dominated the inter-polymer interactions, the polymers would be expected to collapse into a relatively dense spherical NP composed primarily of polymer chains. In that configuration, NP size should correlate to the cube root of monomer ratio; a doubling in monomer would produce a doubling of volume and therefore increase the diameter by $\sqrt[3]{2}$.
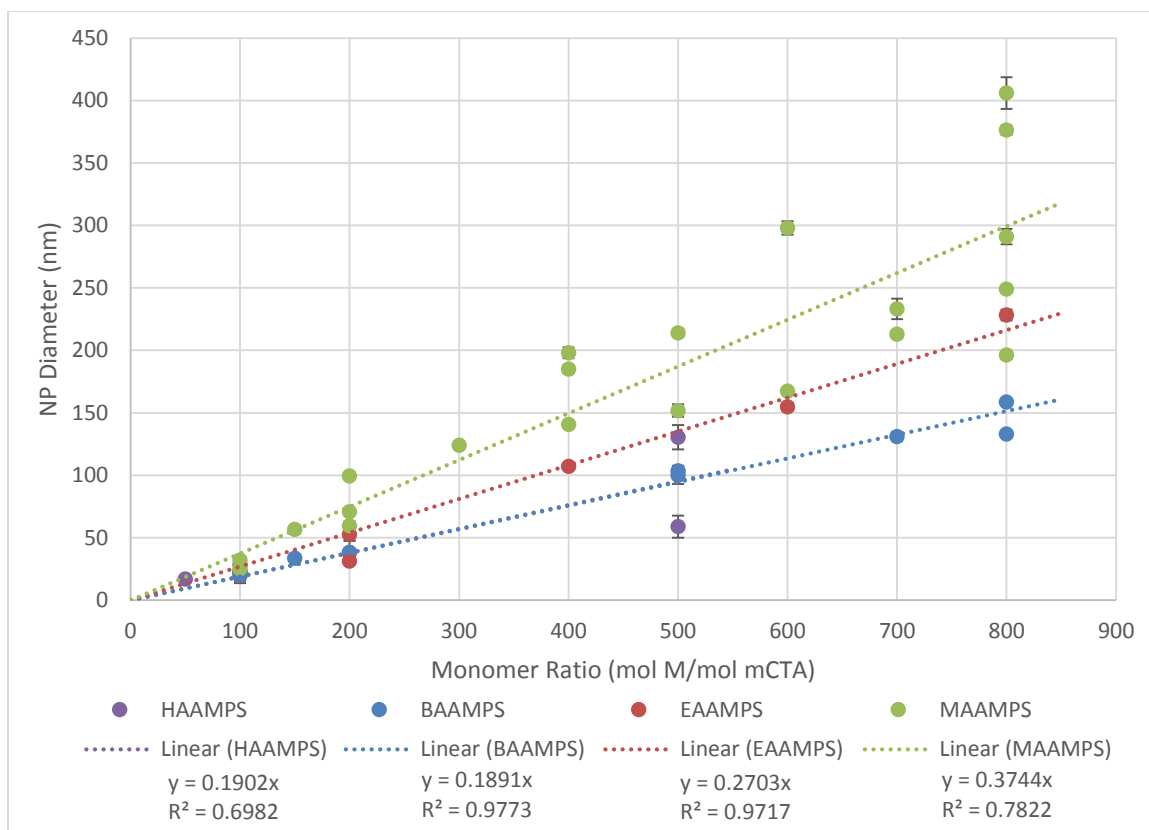
*Figure 43 NP diameter measured by DLS vs moles of monomer per polymer. Plotted for hexyl- (HAAMPS)-
(BAAMPS), ethyl- (EAAMPS), and methyl- (MAAMPS) acrylate monomers.*

It can be inferred from the observed *linear relationships* that the polymer di-blocks remain as relatively straight chains within the NP at the monomer-to-mCTA ratios investigated here. The consequence of this is that the NPs should be expected to have significant water content within the core. The aqueous content of the NPs should be greater for the less hydrophobic core monomers (MAAMPS) than for the more hydrophobic core monomers (BAAMPS). A more open, water-solvated, structure for the less hydrophobic cores could explain the greater size of those NPs relative to the more hydrophobic counterparts. This water-solvated structure does in fact have significant impacts on the observed solvation properties of the NP PSPs (page 5-92).

With these data we can begin to visualize the NP structure more accurately. The typical NP architecture that is proposed, or at least inferred, in the literature is a relatively dense, anhydrous polymer particle. The particle is typically imagined as polymer version of the molecular micelles in Figure 13 on page 2-27: an ionic shell surrounding a hydrophobic core of polymer collapsed onto its self by the dominance of cohesive forces.

The data shown in Figure 43 confirms earlier suspicions [158] that this model does not apply to either the poly(AMPS) or poly(acrylic acid) based NP PSPs. Instead, the NP PSPs should rather be visualized as an open and hydrated three dimensional mesh,

network, or raft of polymer chains. This structure is currently best envisioned as small domains of polymer gel. These rafts of polymer chains are suspected to have a relatively homogenous distribution of ionic polymer blocks throughout rather than the earlier core/shell model where ionic blocks were believed to be localized on the outer surface or "shell" of the NP.

Chemistry
Six NPs were selected in methyl, ethyl, and butyl acrylate chemistries and in small and large sizes for further characterization as EKC PSPs and analysis by LSER (methods: page 4-56, results: page 5-92). These six NPs were selected for their consistency in size, and all but one (EAAMPS (Small), JSH-17A) were synthesized with the same mCTA (JSH-26) to eliminate variations that could arise from the ionic block of the diblocks. The synthetic conditions and general properties of the NPs are presented in Table 8.

Two other batches of BAAMPS NPs are also widely employed in this work: JSH-11A and HNC-25. Both are used to investigate the effects of pH on mobility (the work with JSH-11A has been published in [160]) and HNC-25 is also used extensively to demonstrate performance with different buffers and analytes. JSH-11A may be classified as a "Small" BAAMPS NP, while the larger 89 nm HNC-25 BAAMPS NP is still smaller than the "Large" LH-5 NP used for LSER studies.

The AMPS based NPs are also compared to the BAAA NP from earlier work [157], [158] and to JSH-39, a BAAA NP synthesized for this research.

NP	PSP	Ionic Block Mer	Hydrophobic Block Mer	Diameter
	SDS[a]	N/A	N/A	1.84nm[b]
	BAAA[c]	5	159	63nm±26%
JSH-39	BAAA	~20[d]	~208[d]	44nm±4.6%
JSH 11A	BAAMPS	7	28	14nm±7.8%
HNC-25	BAAMPS	8.76	272	89nm±12%
KH 13	HAAMPS	8	95?	68nm±38%
LH 5	BAAMPS (Large)	8	417	139nm±14%
LH 111	BAAMPS (Small)	8	197	17nm±23%
LH 12	EAMPS (Large)	8	138	115nm±9.5%
JSH 17A	EAAMPS (Small)	13.4	51	12nm±23%
LH 103	MAAMPS (Large)	8	198	123nm±25%
LH 11	MAAMPS (Small)	8	103	17nm±19%

Table 8 Pseudostationary phase properties of various PSPs. [a][25] [b][170] [c][157] from literature. [d]Estimated from stoichiometry.

NP	PSP	Diameter (nm)	Mobility -10^{-4}(cm²/V*s)	Variance in NP mobilities (4σ)	Methylene Selectivity	Average Efficiency (plates/m)	Peak Capacity
	SDS[a]	1.84[b]	4.05±0.041		2.33±0.040	311000±93000	120
ACROSS	BAAA[c]	63nm±26%	4.06±0.041		3.25±0.030	205000±39000	98
JSH-39	BAAA	44nm±4.6%	3.656±0.01[d]		3.254±0.01[d]	126000[d]	77
JSH 11A	BAAMPS	14nm±7.8%	3.818±0.031		3.104±0.005	204000±91000	98
HNC-25	BAAMPS	89nm±12%	3.946±0.094		3.287±0.12	214000±24000	100
KH 13	HAAMPS	68nm±38%	4.048±0.10		3.233±0.067	45488±3500	47
LH 5	BAAMPS (Large)	139nm±14%	4.396±0.010	1.08	3.285±0.067	197610±14000	103
LH 111	BAAMPS (Small)	17nm±23%	4.005±0.015	1	3.13±0.046	543929±17000	138
LH 12	EAMPS (Large)	115nm±9.5%	3.793±0.007	0.4	2.98±0.017	198543±6500	79
JSH 17A	EAAMPS (Small)	12nm±23%	3.735±0.023	0.4	2.769±0.033	248125±11000	105
LH 103	MAAMPS (Large)	123nm±25%	3.642±0.027	0.9	2.615±0.063	282671±3000	85
LH 11	MAAMPS (Small)	17nm±19%	3.887[d]±0.029	0.5	2.389±0.009	78621±4900	51

Table 9 Pseudostationary phase properties of various PSPs. [a][25] [b][170] [c][157] from literature. [d]The JSH-39 BAAA NP parameters are derived from a single run, errors are calculated from the fit of the mobility calculation while the rest are the SD in N=5 measurements.

5.2 EKC Properties and Performance

The goal of this research to determine the effects of NP chemistry and size on the properties and performance of NPs as PSPs for EKC. Each of the NPs presented in Table 8 has been characterized by multiple EKC experiments to quantify and compare performance, selectivity, and solvation properties. The results of these studies are presented in Table 9 and are discussed in detail below.

5.2.1 Electrophoretic Mobility

The electrophoretic mobility of the PSP provides the velocity differential that allows separations in the EKC system. As such, greater mobility is directly related to better chromatographic performance (Figure 7 on page 1-13); a higher mobility PSP provides a larger migration range between the elution time of an unretained analyte and a fully retained analyte [201], [202]. A greater migration range also allows for the separation of more complex mixtures by providing a higher peak capacity.

Table 9 (above) and Figure 44 (below) present the mobilities of SDS micelles [25], 60 nm latex NP PSPs with acrylic acid shell and butyl acrylate core (BAAA) [157], and the AMPS functionalized NPs. The electrophoretic mobilities of the AMPS NPs, with the noteworthy exception of the large BAAMPS NP, are generally somewhat lower than that of SDS and are comparable to that of the acrylic acid NP. In general, the sulfonate moieties on the anionic NP shell provide comparable mobility and migration range to SDS. The size and chemistry of the hydrophobic block are the primary source of variation in mobility.

With the exception of the smaller MAAMPS NPs (whose mobility was measured by an alternate method discussed on page 4-56), the magnitude of the electrophoretic mobility appears to increase with hydrophobic block length and with the hydrophobicity of the monomer constituting the hydrophobic core. As discussed above, the electrophoretic mobility of the NPs are presumed to be a complex function of the packing structure and extent of ionization of the sulfonate moieties in the ionic block which lead to differences in charge and charge density on the NP.

While the set of six NP PSPs used for LSER analysis exhibit strong trends in mobility, the HAAMPS NP does not continue the trend towards greater mobility with increasing hydrophobicity of the hydrophobic block. In addition, the JSH-11A BAAMPS NP exhibits somewhat less mobility than the similarly sized LH-111 BAAMPS (Small) NP despite having identical hydrophobic chemistry. This difference is highlighted in Table 7, and while it may be attributable to the different batch of mCTA employed in the syntheses, it is most likely more indicative of the variability from synthesis to synthesis that may be expected from variations in both the mCTA and diblock.
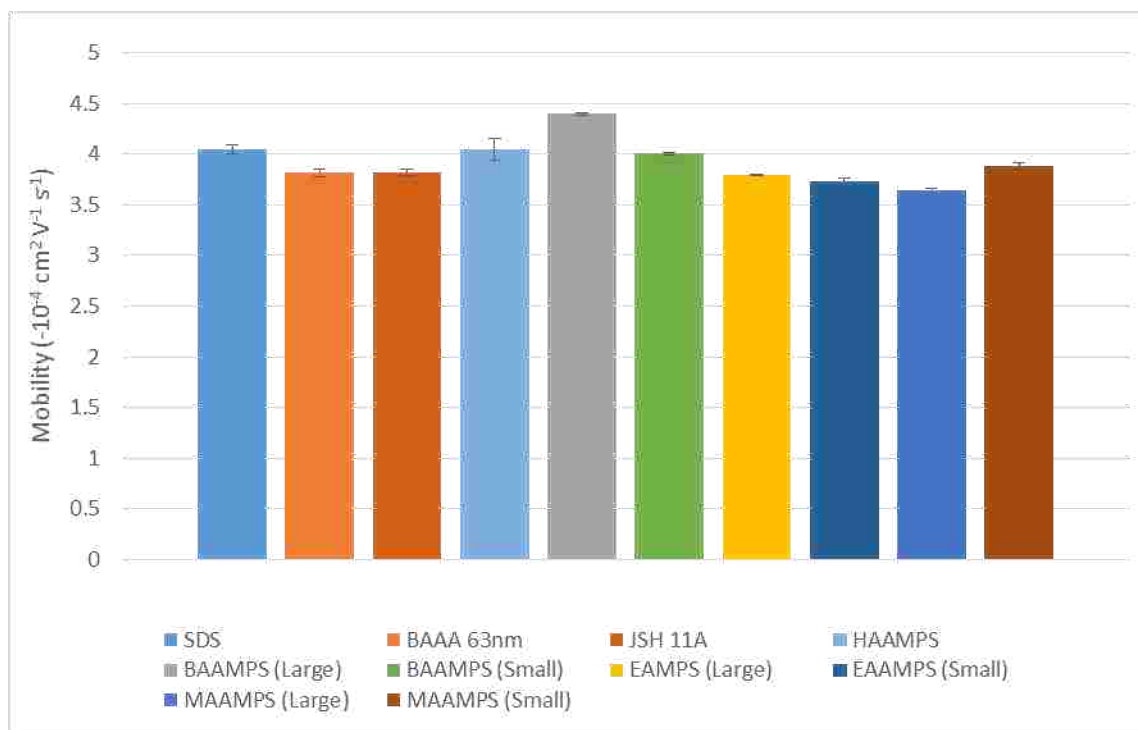
Figure 44 Mobility of NP PSPs determined by retention of a homologues series of alkyl-phenones in 10mM pH 7.20 Tris BGE. Standard errors shown based on variance in five sequential measurements.

These trends are consistent with the trends in NP cohesivity and overall degree of hydration observed in the following sections. More cohesive and more aqueous NPs seem to have lower mobility than do less cohesive and hydrophobic architectures. The mobility of HAAMPS is one piece of data among many that suggests that the extra methylene groups of hexyl acrylate provide little further advantage over butyl acrylate as a PSP.

Effects of BGE Composition and pH on Mobility

Further study of the effects of BGE composition, ionic strength and pH on mobility reveal that the composition and ionic strength of the BGE have as much or more impact than pH, as illustrated in Figure 45. The sharp discontinuity in mobility for both BAAA and BAAMPS chemistries around pH 7 is attributed to the change in BGE composition from Tris to MES buffers. The change in ionic strength between pH~7 Tris buffer (S_{BAAA}=8.5 mM, S_{BAAMPS}=9.1 mM) and MES buffer (S_{BAAA}=8.6 mM, S_{BAAMPS}=5.8 mM) does not appear to explain the change in mobility as the change in ionic strength between Tris at pH~8 (S_{BAAA}=4.9 mM, S_{BAAMPS}=4.3 mM) and pH~7 is much larger yet little change in mobility is observed. The effects of buffers on a BAAMPS NP PSP is explored in more detail in 5.6.1 BGE and Sample on page 5-97.
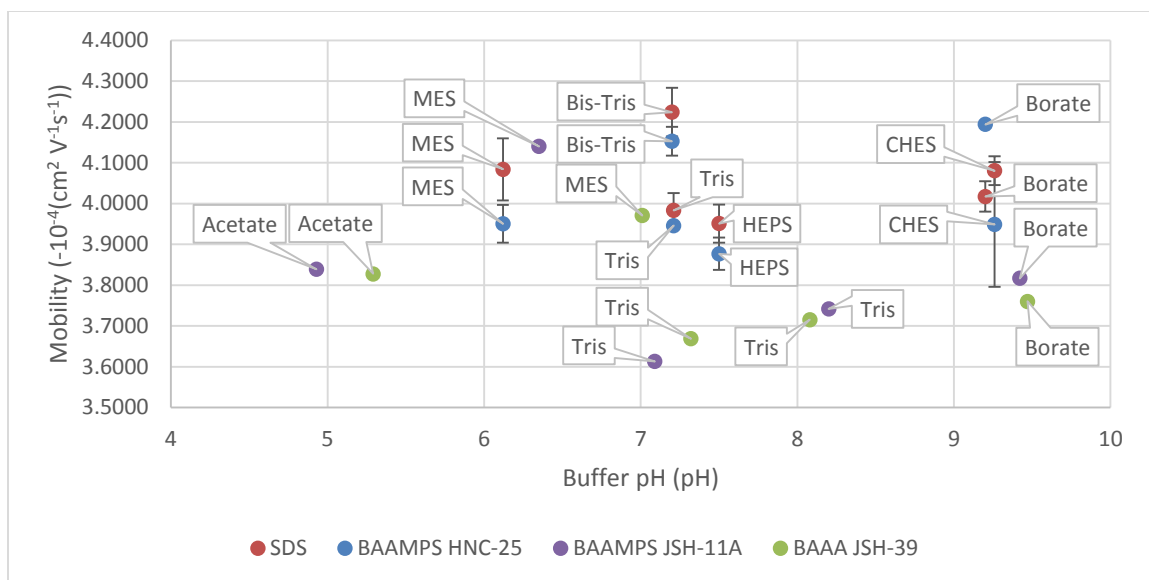
5-84

Figure 45 Variation in mobility in different buffers and pH. Neither BAAA (JSH-39) nor BAAMPS (JSH-11A) NP PSPs lose mobility at low pH. However, both see strong changes around pH 7 between Tris and MES buffers. This suggests that the BGE composition and ionic strength does meaningfully effect the ionic shielding available to the ionic polymer block. BAAMPS (HNC-25) and SDS show a similar discontinuity between Tris and Bis-Tris. JSH-11A results also reported in [160].

Part of the motivation for synthesizing NPs with AMPS ionic blocks was to improve PSP mobility and performance relative to those with acrylate ionic blocks, particularly at low pH. The overall mobility of poly(AMPS) functionalized NP PSPs is seen to match or exceed that of poly(acrylic acid) functionalized NP PSPs (BAAA) of the same hydrophobic block chemistry at neutral to high pH (Figure 44). This might be expected if the more acidic sulfonate moieties are ionized to greater extent than the less acidic carboxylate groups.
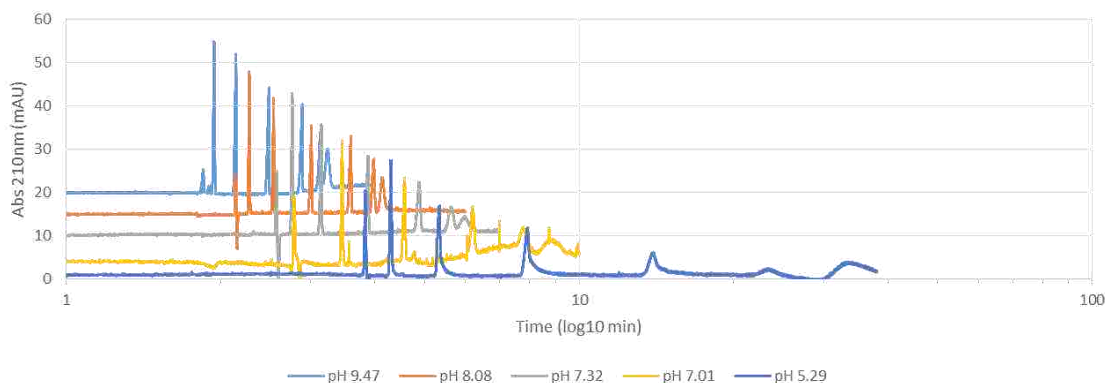

Figure 46 Mobility of JSH-39 BAAA NP shown in separations of six phenones in 10mM buffers: Borate (pH 9.47), Tris (pH 8.08), Tris (pH 7.32), acetic (5.29). Time is plotted on log scale to retain the visibility of the faster separations, but it should be noted that as the EOF drops off the analysis time increases by an order of magnitude or more.

However, the mobility of the BAAA NP does not diminish significantly even at the lower end of the operational pH range in EKC, suggesting that the extent of ionization remains constant. This is demonstrated by the separation of the six phenones by JSH-39 BAAA NP PSP in various buffers as shown in Figure 46. At high pH separations are fast and highly efficient, but as the pH decreases the EOF drops off and the analysis time balloons from just a few minutes to over half an hour. However, there is no overall loss of mobility from the BAAA NP; the mobility at pH 9.47 is -3.84×10^{-4} (cm^2 V^{-1} s^{-1}) and it remains unchanged at pH 5.29 even as the EOF drops from 8.7×10^{-4} (cm^2 V^{-1} s^{-1}) to 4.2×10^{-4} (cm^2 V^{-1} s^{-1}). Below a pH of 5.29 the mobility of the NP PSP will be greater than that of the EOF and the migration direction will reverse for highly retained analytes while analytes with a retention factor of ~1 will be retained indefinitely in the capillary. BAAA NPs are also reported to lose ionization below this pH [158], but this does not have a significant effect in practice.

5.3 Methylene Selectivity

The relative strength of the hydrophobic interactions between NP PSPs and solutes is quantified by methylene selectivity, which is the chromatographic selectivity between adjacent solute homologs differing in structure by only one methylene. It was expected that increases in the alkyl chain length of the acrylate monomers constituting the core would result in increasing hydrophobic character analogous to reversed-phase HPLC stationary phases.
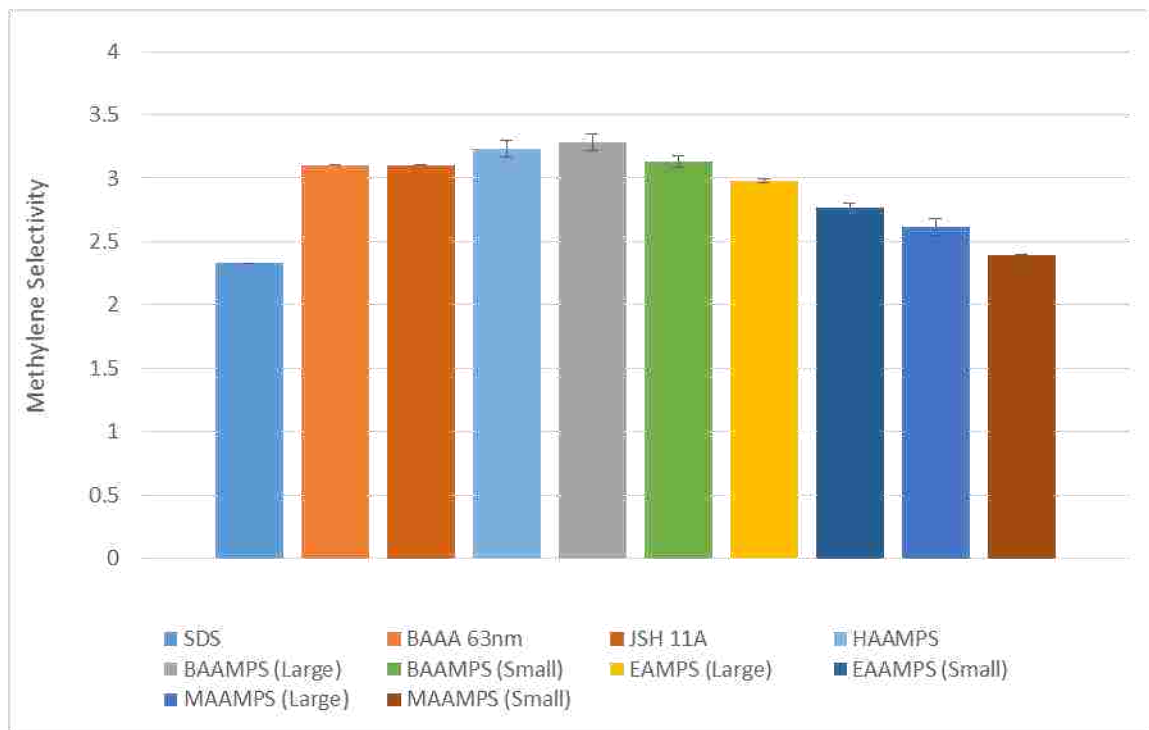

Figure 47 Methylene Selectivity of NP PSPs determined by retention of a homologues series of alkyl-phenones in 10mM pH 7.20 Tris BGE. Methylene Selectivity is derived from the slope of the relationship between the log of retention factor (k) and the alkyl chain length of the series of alkyl-phenones by taking the anti-log of the slope. Standard errors shown based on variance in five sequential measurements.

The methylene selectivities for SDS and the NP PSPs are presented in Table 9 and Figure 47. All of the NP PSPs, with the possible exception of the smallest MAAMPS, have significantly higher methylene selectivity and are significantly more hydrophobic than SDS micelles. Methylene selectivity does increase with both the alkyl chain length of the hydrophobic monomers and with the size of the NP, with the chemistry of the core having a greater impact than the diameter of the NP. It is clearly possible to vary the hydrophobic character of NP PSPs via systematic variation in size or core chemistry.

5.3.1 Selectivity

The retention factors of three acids, three bases, three arenes, and three polar compounds for five NP PSPs of varied chemistry and size are shown in Figure 48. These compounds have been selected to provide some qualitative indication of how the NP PSPs behave towards different types of compounds. Changes in selectivity are apparent where the connecting lines cross. There are clearly some differences in separation selectivity afforded by the different PSP structures. Toluene and 3-chlorophenol in particular have markedly different retention with BAAMPS (Small) than with the other NP PSPs. It is difficult to see or describe any particular trends or patterns in the results, however. A quantitative measure of the differences in selectivity of NP PSPs is reported in the 5.5 LSER Characterization
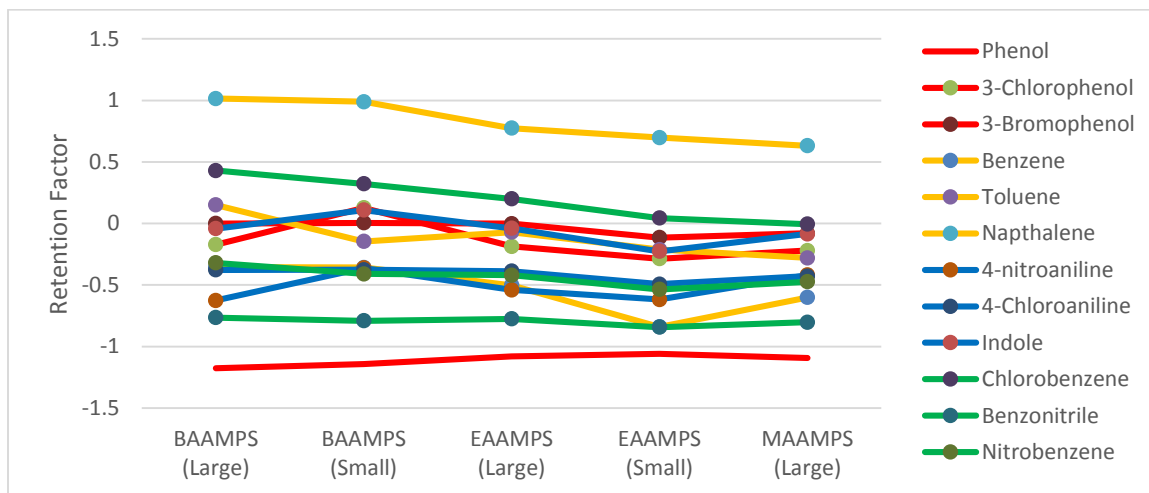 section starting on page 5-92.

Figure 48 Variations in retention between NP PSPs for various classes of analytes from LSER work. Sets in red are acidic, yellow are arene, blue are basic, and green are polar. While some variations in selectivity are obvious for specific analytes like toluene, most analytes show similar trends in selectivity between NP PSPs.

5.4 Efficiency

The average plate counts, and resulting peak capacities, for each of the PSPs was quantified for the homologous series of alkyl phenones and the results are presented in Table 8 and Figure 49. The size and chemistry of the NPs has a significant effect on plate numbers and peak asymmetry, with the smaller BAAMPS (LH-111) and EAAMPS (JSH-

17A) particles generating higher plate numbers than their larger counterparts, and the smaller BAAMPS NPs generating the highest plate numbers overall. The NP PSPs in general provide somewhat lower plate counts than SDS micelles, with the exception of the smaller BAAMPS, which provides significantly higher plate counts. The plate number for the smaller MAAMPS (LH-11) is very poor relative to other PSPs.
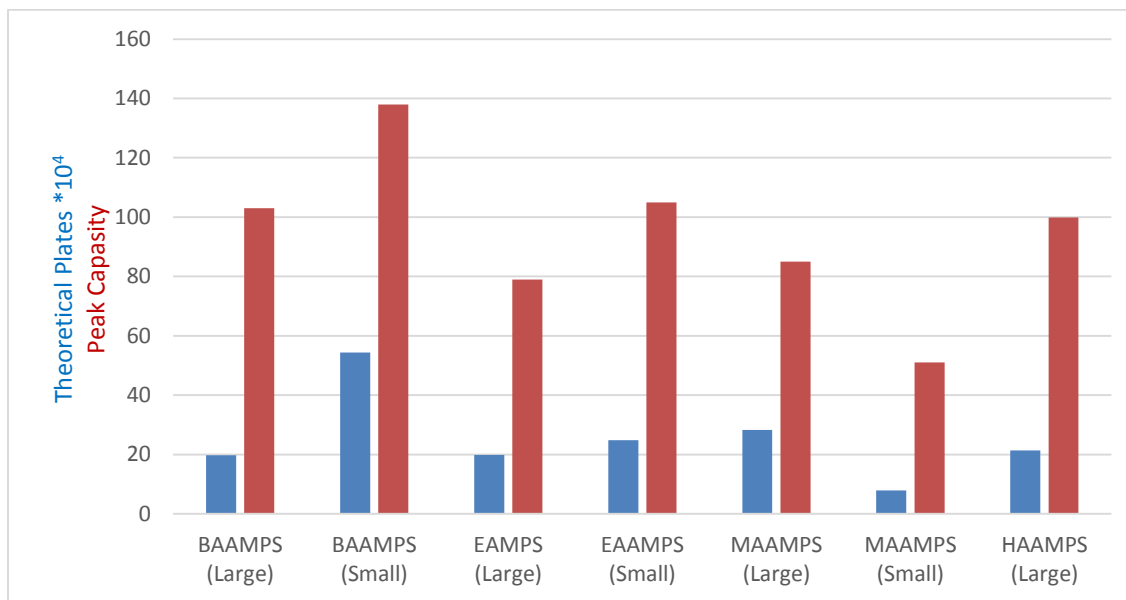

Figure 49 Effect of core chemistry on Efficiency (x10⁴) and Peak Capacity. BAAMPS(Large) LH-5, BAAMPS(Small) LH-111, EAAMPS(Large) LH-12, EAAMPS(Small) JSH-17A, MAAMPS(Large) LH-103, MAAMPS(Small) LH-11, HAAMPS(Large) HNC-46.

Typical separations for the alkyl phenones using the NP PSPs are presented in Figure 50. There are several common features in the separations of these compounds observed with all of the NP PSPs. The peaks are often asymmetrical, with significant peak fronting observed particularly for phenones with intermediate affinity for the PSPs. Similar behavior was previously observed with the BAAA NP PSP [157]. Fronting is either not present or is significantly less pronounced for early eluting phenones, and is either less pronounced or is less apparent, relative to other broadening mechanisms, for late eluting phenones. Fronting is universally observed for alkyl-phenones, but not for all solute chemistries; several other solutes were observed to have tailing peaks. The observed peak assymetry is the primary cause of lower plate counts observed for most of the NP PSPs relative to SDS micelles. Fronting of alkyl phenones is a greater problem for EAAMPS (LH-12 and JSH-17A) and MAAMPS materials (LH-103 and LH-11) and is very severe for the small MAAMPS (LH-11) material, causing very low plate counts and rendering it ineffective as a PSP.

The observed fronting is less severe at higher PSP concentrations and lower solute concentrations. This is consistent with solute concentration overload being the cause of the peak asymmetry. Williamson and Davis observed that anti-Langmuir isotherm models and concentration overloading could explain observed peak fronting in EKC

[203], [204]. Tailing peaks are expected for concentration overload and solutes with non-linear Langmuir-type isotherms [205]. The affinities of the NP PSPs for all solutes are very high, resulting in low NP concentrations for effective separations but making concentration overload a common problem. Concentration overload effects appear to be more severe for NPs with cores composed of less hydrophobic acrylates with short alkyl side chains, and are particularly severe for the small MAAMPS NP (LH-11).
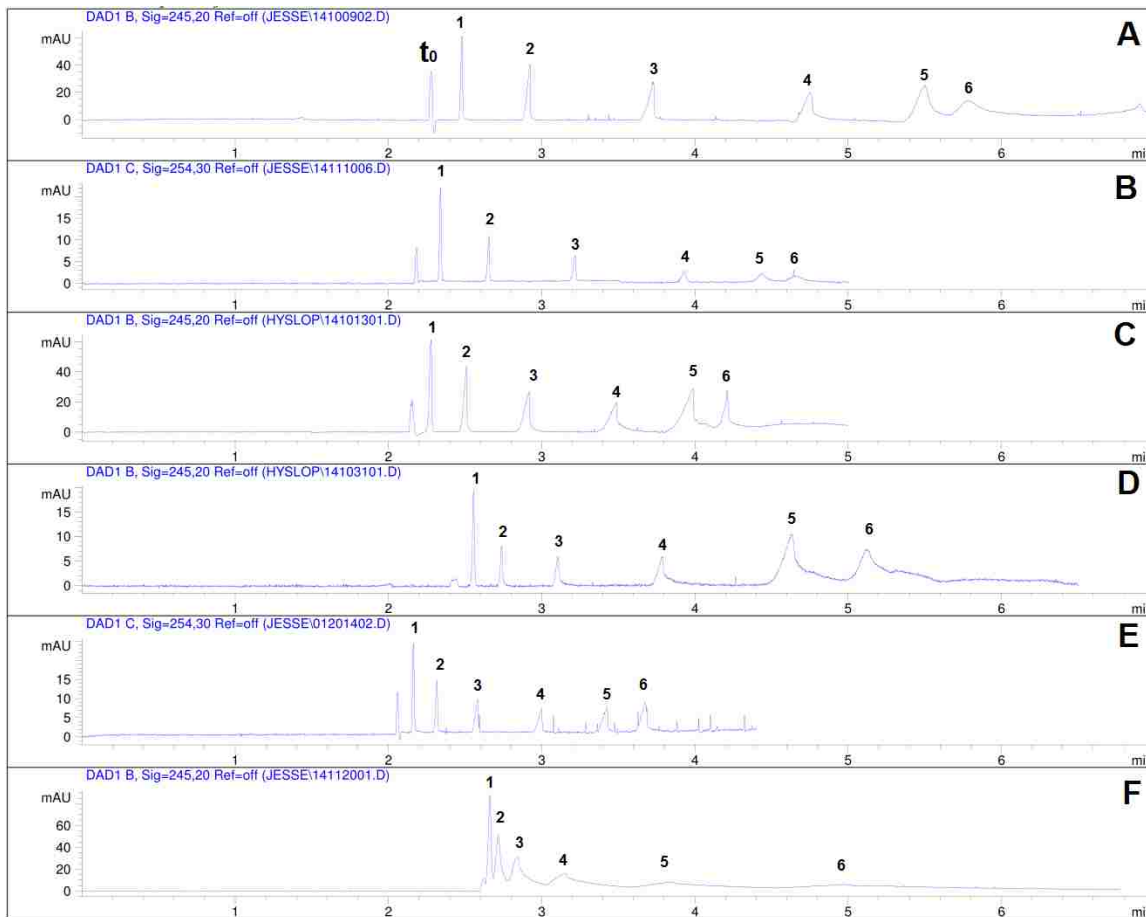

Figure 50 EKC chromatograms of the separation of t_0. Acetone 1. acetophenone, 2. propiophenone, 3. butyrophenone, 4. valerophenone, 5. hexanophenone, 6. heptanophenone in 10 mM TRIS buffer at pH 7.2 by A. LH-5 BAAMPS(Large), B. LH-111 BAAMPS(Small), C. LH-12 EAAMPS(Large), D. JSH-17A EAAMPS(Small), E. LH-103 MAAMPS(Large), F. LH-11 MAAMPS(Small).

In the absence of concentration overloading and Joule heating effects, band broadening in EKC is expected to be dominated by longitudinal diffusion [9], [30], [206], [207]. However, while the late eluting peaks in Figure 50 are relatively symmetrical, they are also broad and have relatively low plate counts. The plate counts for late eluting compounds are also significantly lower with the larger BAAMPS NP (LH-5) than for the smaller BAAMPS NP (LH-111). Broad and often asymmetrical peaks are generally observed for late eluting compounds separated by EAAMPS and MAAMPS NPs. These observations are not consistent with longitudinal diffusion being the dominant broadening mechanism, since late eluting compounds should have higher plate counts in that case.

5-89

The current is very low in these systems (<10 µA, see Figure 66 on page 5-109), so Joule heating is not significant, and does not explain the low plate counts or the differences in plate counts between large and small NPs.

Terabe et al. [10] considered several other potential broadening mechanisms, but generally found these to be negligible for micellar systems. Two of these, which are expected to result in greater broadening for later-eluting compounds, may need to be reconsidered for NP PSPs.

Inter-micellar diffusion is a broadening effect that is expected to scale as the square of the inter-NP distance. Using the theoretical mass of the diblock and DLS diameters, the calculated inter-NP distances are about 100 nm for small nanoparticles and 700 nm for large nanoparticles. These values are ten to seventy times greater for the NP PSPs than for SDS micelles due to the lower NP PSP concentrations relative to SDS micelles. The inter-NP distances are also greater for larger NPs than for smaller NPs because the number concentration of larger NPs is smaller. However, our estimates of broadening from inter-NP diffusion for the highly retained phenones, using equation 25 from [10] indicate that this should be an insignificant contribution (<10%) to broadening relative to longitudinal diffusion.

A second broadening mechanism that has a greater effect for late-eluting compounds is the microheterogeneity of the PSP. Polymer NPs have greater microheterogeneity than SDS micelles, and there could be significant differences in microheterogeneity between large and small NPs. The contribution to broadening from NP microheterogeneity is estimated to be about seven or eight times greater than that estimated for SDS micelles generated by [10].
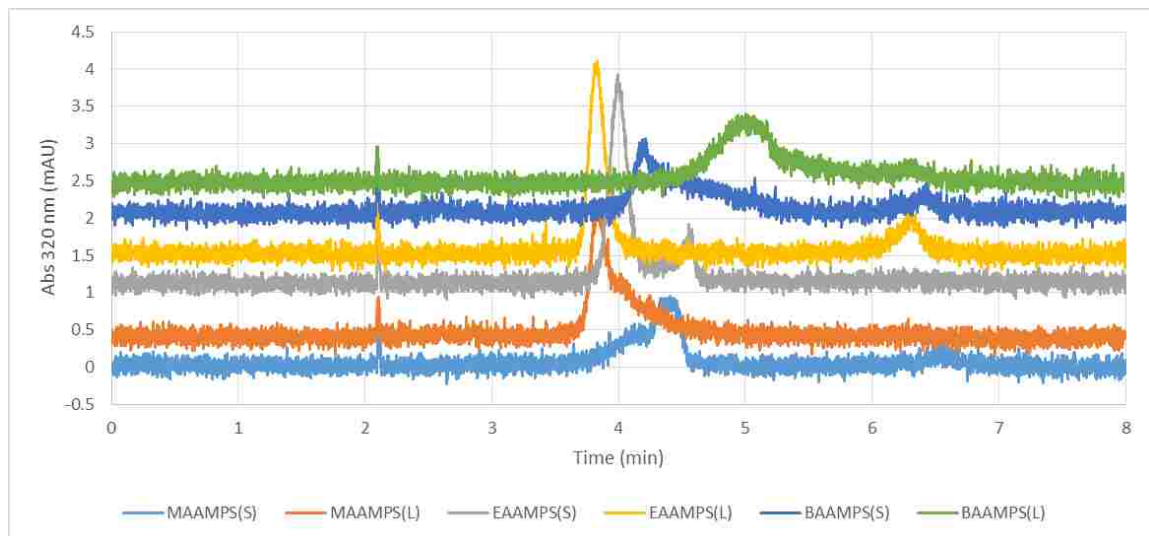

Figure 51 Separations of NPs by CE. 1.0% NP in 50 mM Borate buffer, 20KV, 48.5cm x 50 um capillary. t₀ at 2 min, NPs at 3.5-5 min, unreacted mCTA at 6-7 min.

The stability of the NPs allows the magnitude and variance in electrophoretic mobility to be measured by CE separation just as for the mCTA on page 5-76. Doing so shows that the relative standard deviations in NP electrophoretic mobilities are 20% or less, with no significant difference between NPs of different average size. The 20% variation in mobility is similar to the variation in NP diameter from light scattering studies.

Using equation 38 from [10] the effect of NP electrophoretic polydispersity can be estimated. This analysis shows that while there is dispersion in the electrophoretic mobility of the NP PSPs, it is not clear that this will translate into significant band broadening of the analyte. The analyte is expected to rapidly partition between the PSP and bulk solution, averaging the mobility of each NP PSP the analyte interacts with over a large number of NPs.

However, there is uncertainty in this analysis because the plate height is also inversely proportional to the rate constant for desorption of the solute from the PSP, and this value is not known for the NP PSPs. Still, calculations indicate that NP electrophoretic polydispersity would contribute 20% or less to the overall band broadening even if the desorption kinetics are ten times slower for the NP PSPs than for SDS micelles. The RSD in electrophoretic mobility is the same for large and small BAAMPS NPs, so this mechanism does not explain our observations unless desorption rates from the NP PSP (mass transfer rate or partitioning rate) are also significantly slower for large NPs.
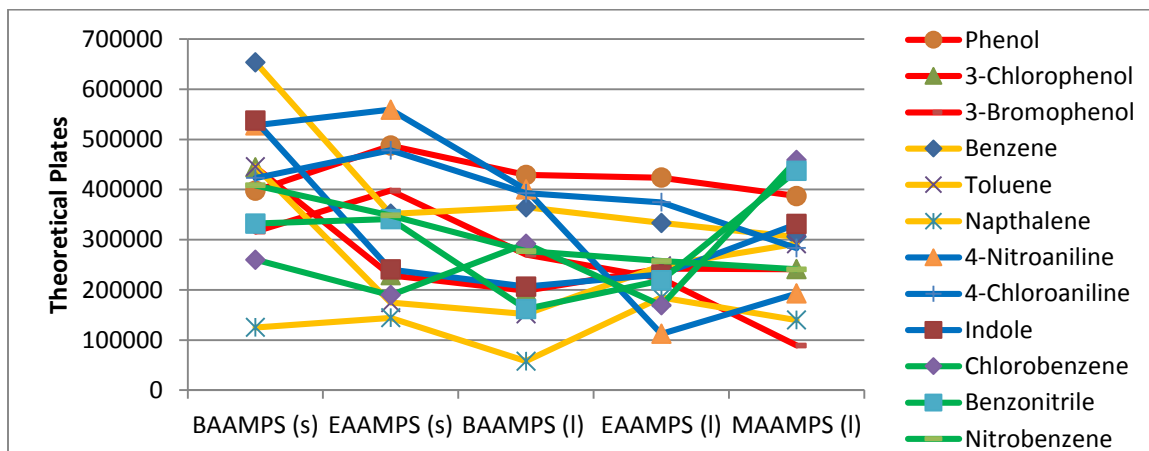

Figure 52 Efficiency as a function of NP PSP for analytes of various chemistry from LSER work. Overall efficiency of a PSP seems to be influenced by large changes in efficiency of a few analytes. However, the variations do not strongly correlate to a given type class of compound. Sets in red are acidic, yellow are arene, blue are basic, and green are polar.

While the broadening and loss of efficiency are shown in Figure 50 to correlate strongly with increasing retention of a homologous series of alkyl phenones, the effects between NP PSPs are also noteworthy. In Figure 52 the efficiency of a number of compounds representing acidic, basic, arene, and polar chemistries are shown for various NP PSPs. The smaller (and better performing) NP PSPs show significantly better efficiency for a few of the compounds, but there is little to no consistency in which compounds

experience different levels of performance. The most evident pattern is in the higher theoretical plate count for highly polar compounds (4-nitroanaline and 4-chloroaniline) when run with smaller NP PSPs.

Peak asymmetry was calculated as a pseudo-moment by the ChemStation software integrator for these compounds. The full method of calculation and relevant equations are available in [208]. The calculation effectively compares the ratio of the area in front of the maxima to that behind: values greater than one indicate fronting of the peak and values less than 1 indicate tailing.
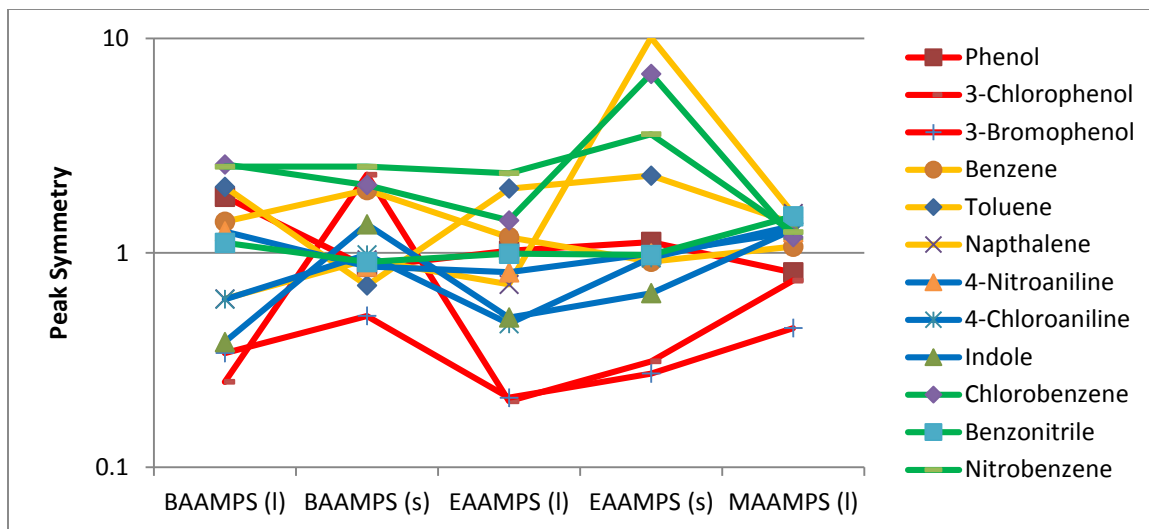

Figure 53 Peak Symmetry of twelve compounds from LSER work. The symmetry values (plotted on a log axis) show the magnitude of fronting (>1) or tailing (<1) in each NP PSP based on the ratio of the peak area in front of the peak maxima divided by the peak area behind (longer retention time) the maxima.

The peak symmetry of these compounds does show consistency between NP PSPs with acidic compounds often tailing, and both polar and arene compounds fronting, for all NP PSPs. The tailing of 3-bromophenol and 3-chlorophenol is the most consistent among the 39 compounds used in the LSER studies, suggesting that the halogens, more than the phenol moiety, may be the commonality to distinct tailing. Whether this is because the halogens lower the pKa of the phenol or because of a direct interaction with the halogen is unknown.

5.5 LSER Characterization

Linear Solvation Energy Relationships (LSER) have long been used in EKC to describe the strength and nature of interactions between analytes and the PSP [47], [48], [191], [192]. The logarithm of the retention factor provides a measure of the free energy of transferring an analyte between the BGE and the PSP. The LSER model allows this to be attributed to differences in the free energies of cavity formation and various solute-solvent interactions in the BGE and PSP respectively.

These free energies are modeled by five solute descriptors: the McGowan characteristic volume (V), excess molar refraction (E), dipolarity/polarizability (S), and hydrogen bond acidity and basicity (A and B respectively). By correlating the known solute descriptors V,E,S,A, and B in Equation 5-4 with the logarithm of the experimentally determined solute retention factor (log(k)) for a large number of solutes, the relative strength of each interaction provided by a PSP is determined.

The strength of each interaction is described by the system descriptors v,e,s,a,b calculated by the multiple linear regression between the log(k) measured for each solute and the solute descriptors provided in [20], [191], [192], [204], [205], [209], [210] and also summarized in Appendix A - LSER on page 8-136.

$$\log(k) = c + vV + eE + sS + aA + bB \qquad\qquad 5\text{-}4$$

The magnitude of the system descriptors describe the difference in free energy of solvation, either positive or negative, between the bulk BGE and the PSP *relative to a given BGE composition*. For LSER results to be fully comparable they must be generated in the same BGE conditions.

The LSER results for SDS [53] and five of the AMPS NPs are presented in Figure 54 and Table 10. In many cases, the NP phases show significantly different system parameters relative to SDS and to one another.
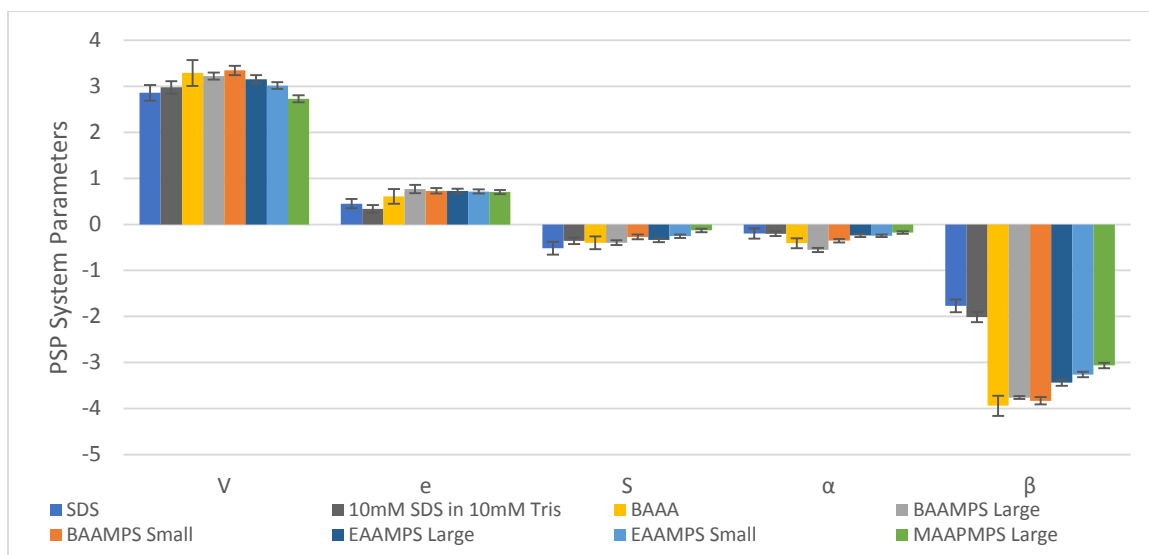

Figure 54 LSER system parameters. SDS reported from [25] *and as determined in analogous EKC conditions with the NP PSPs shows only insignificant variations from BGE composition. EKC of 39 solutes ran in 10 mM triss at pH 7.20±0.05 with 0.3% w/w NP PSP. System descriptors are: McGowan characteristic volume (v), excess molar refraction (e), dipolarity/ polarizability (s), and hydrogen bond acidity and basicity (a and b respectively).*

The NP phases have significantly more positive e, less negative s, and much more negative b values than SDS. Parameter v varies from being significantly more positive to

5-93

being indistinguishable from SDS, while parameter a varies from being more negative to being indistinguishable, depending on NP size and chemistry. The results relative to SDS indicate that these PSPs provide very different solvation environments, which should result in very different separation selectivities, relative to SDS micelles. Additionally, the extent of these differences varies between different NP chemistries.

Another interesting observation is that the LSER parameters for the NPs, particularly v, s, a, and b, show consistent trends with systematic variation in the NP structure and chemistry. In general, the magnitude of these values decreases with reduced alkyl chain length of the core monomer and with reduction in the size of the NP core. This demonstrates that the synthetic control offered by the RAFT polymerization approach allows for methodical variation in the chromatographic selectivity of NP PSPs.

The McGowan characteristic volume system constant (v) represents the difference in free energy of cavity formation between the BGE and PSP, as well as any differences in residual dispersion interactions between the two phases [211]. The aqueous BGE is a relatively cohesive environment due to strong dipole-dipole and hydrogen bonding interactions between water molecules. The system descriptor v is positive in all cases, indicating that the PSPs are less cohesive then water. Less cohesive PSPs are more easily deformed to solvate an analyte and produce higher v terms than do more cohesive PSPs that require more energy to form a solvation cavity.

The NP PSPs show a uniform drop in v with alkyl chain length from BAAMPS to MAAMPS NPs, consistent with the shorter alkyl chains resulting in more cohesive, water-like, NP character. This is consistent with the observations in 5.1.2 Hydrophobic Block Length on page 5-78 that water is incorporated into the core of the NPs, with greater water incorporation possible for less hydrophobic core chemistries. The v term is equivalent to SDS or larger for all tested NPs. This indicates that the nanoparticle cores are relatively non-cohesive, and that hydrogen bonding and dipole-dipole interactions between water molecules incorporated into the NP core must be relatively weak.

Of course, these results also reflect the nature of interactions with SDS micelles, which in many cases may occur by different methods at the micelle-water interfacial region of the micelle. The size of the NP also produces significant, though minor, variations in the v term with smaller BAAMPS NPs shown to be less cohesive, while inversely, the small EAAMPS is more cohesive than their larger counterparts. This variation is not fully understood and the results are insufficient to explain the effect.

Excess molar refraction (e) represents the difference between the tendency of the BGE and the PSP to interact with polarizable n- and π-electrons on the analyte. The solute descriptor is derived from the difference between the molar refraction of the solute and an imaginary n-alkane of the same characteristic volume [191]. All measured NP PSPs provide double the capacity for these interactions than does SDS with no significant difference between the NP PSPs. This illustrates a unique selectivity from SDS provided

by the NP PSPs. The increase in (e) might be attributed to the ester moieties in the NP PSP core provided by the acrylate monomers.

The dipolarity/polarizability term (s) characterizes the dipole-dipole and induced dipole-dipole interactions relative to those provided by the BGE [212], [213]. While all the PSPs provide weaker dipole type interactions than the aqueous BGE, the NP PSPs do provide significant, if limited, increases relative to SDS and as the alkyl chain length of the core monomer decreases. This is also consistent with a more water-like environment for NP core monomers with shorter alkyl chains, and with greater access to polar or polarizable ester moieties in the NP core.

The relative energy of interactions with hydrogen bond acids (a) and bases (b) are a measure of the difference in hydrogen bond basicity and acidity, respectively, of the PSP vs the aqueous BGE [212], [214]. Note that the analyte parameters A and B are based on the acidity and basicity of the analytes, so the complementary system descriptors for the PSP necessarily describe the inverse behavior: the (a) term represents the basicity of the PSP while (b) represents the acidity.

Water is a strong hydrogen bond donor and acceptor, so most PSPs have negative a and b terms. The PSPs, including SDS micelles, prove only slightly less basic than water, suggesting that ionic head groups, amide, ester, ketone, or associated water, are able to accept hydrogen bonds with only slightly less free energy of solvation than the BGE. The (b) term shows that the NP PSPs are far less acidic than the aqueous BGE, and also that the NP PSPs are less acidic than SDS. The b term strongly reflects the inverse relationship between alkyl chain length and aqueous character with MAAMPS providing much less negative b-term than the BAAMPS NP PSPs.

Although there are amide functionalities on the AMPS shell, the NP cores do not have hydrogen bond donors. Interactions of hydrogen bond bases, then, would necessarily be with NP-associated water. This water is apparently much less able to donate a hydrogen bond than water in the BGE or water associated with the sulfate head groups of SDS.

PSP		v	e	s	a	b	R^2
SDS [53]	Regression Values:	2.86 (0.17)	0.45 (0.10)	-0.52 (0.14)	-0.20 (0.11)	-1.77 (0.14)	nr
	Normalized Values:	0.83	0.13	-0.15	-0.058	-0.51	
BAAMPS Large	Regression Values:	3.222 (0.090)	0.767 (0.054)	-0.398 (0.047)	-0.554 (0.036)	-3.762 (0.074)	0.98
	Normalized Values:	0.64	0.15	-0.079	-0.11	-0.74	
BAAMPS Small	Regression Values:	3.34 (0.10)	0.728 (0.060)	-0.271 (0.052)	-0.351 (0.039)	-3.832 (0.081)	0.97
	Normalized Values:	0.65	0.14	-0.053	-0.068	-0.74	
EAAMPS Large	Regression Values:	3.155 (0.089)	0.725 (0.052)	-0.338 (0.045)	-0.242 (0.034)	-3.439 (0.071)	0.97
	Normalized Values:	0.67	0.15	-0.071	-0.051	-0.73	
EAAMPS Small	Regression Values:	3.016 (0.075)	0.715 (0.046)	-0.254 (0.037)	-0.243 (0.028)	-3.262 (0.059)	0.97
	Normalized Values:	0.67	0.16	-0.056	-0.054	-0.72	
MAAMPS Large	Regression Values:	2.731 (0.076)	0.705 (0.045)	-0.131 (0.039)	-0.176 (0.030)	-3.065 (0.062)	0.97
	Normalized Values:	0.65	0.17	-0.032	-0.042	-0.73	

Table 10 LSER parameters for NP PSPs.

5.6 Practical Performance

5.6.1 BGE and Sample Composition

The performance of NP PSPs in various buffers, broadly described as the background electrolyte (BGE), is rarely reported. Even in this work the performance of a given NP PSP was rarely compared between different BGE solutions because the performance must be measured in a consistent BGE for results to remain comparable between PSPs.

While some limited comparisons have been conducted with multiple NP PSPs run in different BGEs at different pHs as in Figure 45, that work focused on mobility as a function of pH, and so some buffers were pushed to the limits of their buffering range. This introduced ionic strength as an estimated, but uncontrolled, variable. Careful control of each parameter is critical to producing data that can be compared between analyses.

To study the impact of the buffer on EKC performance 100 μg mL^{-1} (ppm) samples of the six alkyl phenones (acetophenone – hexanophenone) in the BGE solution were prepared from a single 50 mg mL^{-1} (ppt) standard in acetone and separated by a BAAMPS NP PSP (HNC-25) in six different buffers near their pK_a except for Tris (pKa 8.07) which was run at pH 7.21 to match most previous work with Tris buffer. All other parameters are as reported in the 4.1.2 Chromatographic characterization - Capillary Electrophoresis section on page 4-56.

Borate (pH ~9.2), CHES (pH 9.26), HEPES (pH 7.5), Bis-Tris (pH 7.20), Tris (pH 7.21), and MES (pH 6.12) buffers were used for the BGE at a buffer concentration of 10 mM (Bis-Tris therefore was at a molar concentration of 2 mM and borate was 2.5 mM). Samples were sequentially spiked with acetone and the increasing acetone concentration was found to flatten the baseline for buffers that had abnormal and unstable baselines. Abnormal baselines were observed for the NP PSP in CHES, Bis-Tris, and HEPES analogous to the chromatogram of CHES shown in Figure 55.

Why changes to the sample composition have such a pronounced effect on the baseline of the entire separation is not entirely clear. However, it is hypothesized that the poor baseline may be due to adsorption of either analytes or buffer to the capillary wall. It has been observed during the LSER studies that 1-napthal and biphenyl will degrade EOF, requiring the capillary to be flushed with an organic solvent like ACN to restore the EOF. It is likely that the acetone content in the sample performs that roll here, and increasing the acetone content provides a more complete reconditioning of the capillary during each run.
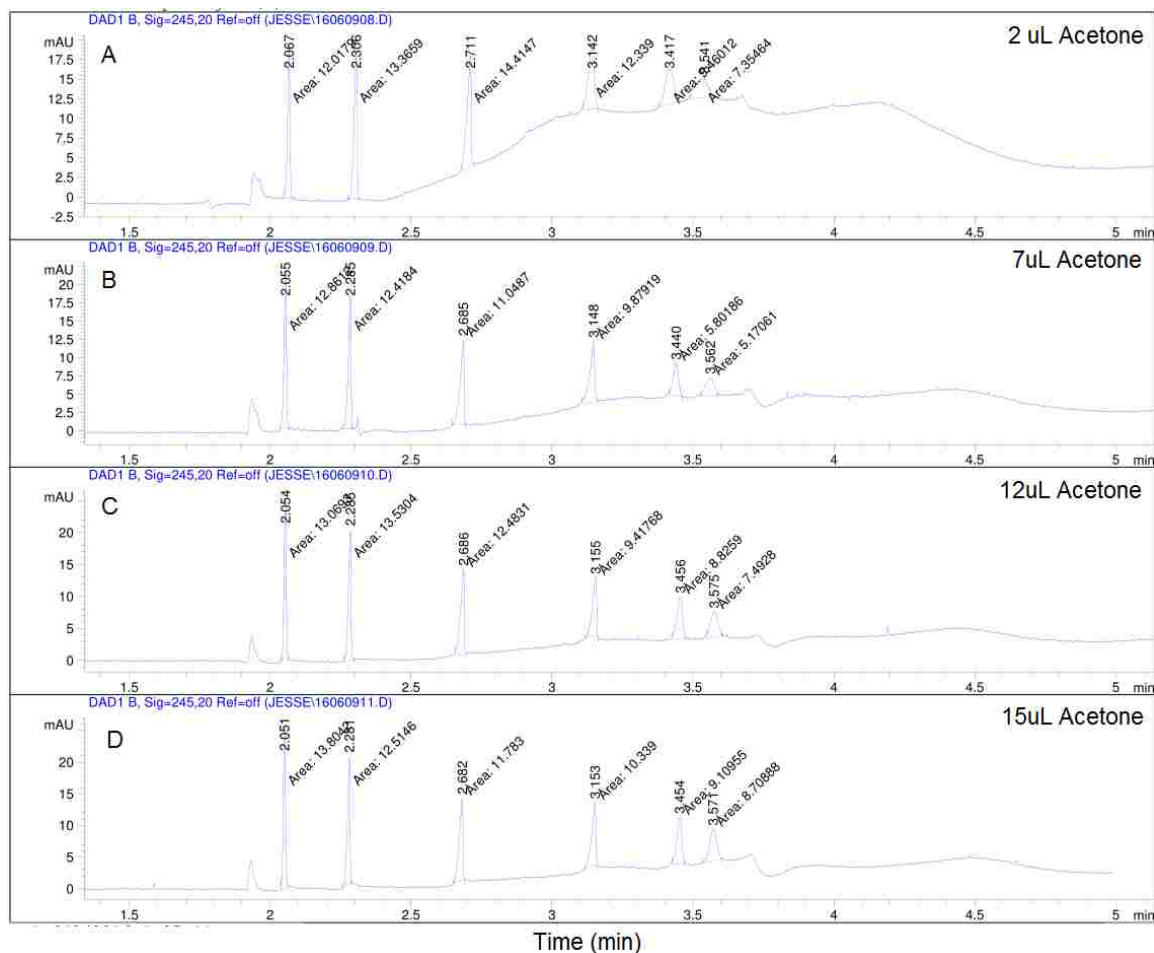
Figure 55 Representative separation of phenones with abnormal baseline in CHES buffer. The baseline was dramatically improved by increasing acetone concentration as shown in 1 mL of sample.

The NP PSP performance was compared to that of SDS micelles that were run concurrently using injections of the same samples. The NP PSP mobility, methylene selectivity, t_{PSP}, efficiency, and the signal to noise ratio of butyrophenone were calculated for each run. Mobility remained remarkably consistent and the NP demonstrate consistently higher methylene selectivity than SDS micelles in all buffers. However, acetone concentration did produce some minor variations that are most likely due to different peak shapes at different acetone concentrations shifting the retention times of the peaks very slightly.

The measurement of t_{PSP} illustrates that the same separation took much longer with SDS than with the NP PSP. Since there is no significant difference in the mobility of the NPs vs SDS, this difference in t_{psp} is due to lower electroosmotic flow, likely caused by higher ionic strength, in SDS systems. Note that these terms are plotted on a log scale in Figure 56, and thus the NP PSP demonstrates much faster analysis times than the SDS. Finally, the signal to noise ratio of butyrophenone illustrates the degree of noise and background absorbance provided by each buffer.

Figure 56 Relative performance of HNC-25 BAAMPS NP to 50mM SDS micelles in different buffers. Tris at pH 7.2 is shown provide the most consistent performance between NP PSPs and SDS micelles. Bis-Tris, Borate, and CHES buffers all provide better performance with SDS micelles. The high mobility recorded for the NP PSP with 2uL acetone in CHES is attributed to uncertainty in the measurement due to poor baseline rather than a chromatographic cause.
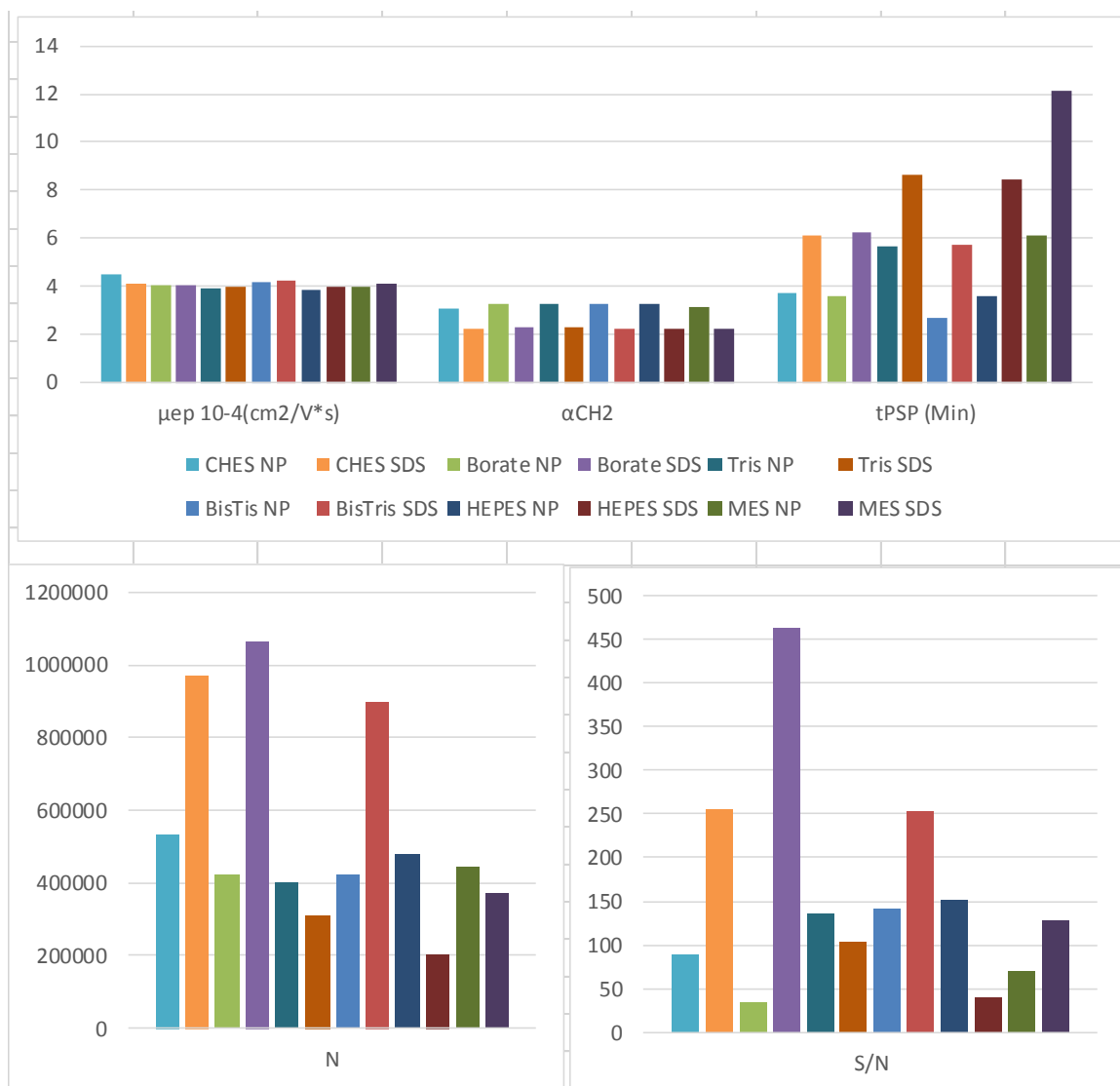
Figure 57 Relative performance of 0.3% w/w BAAMPS NP PSP HNC-25 and 50mM SDS in different buffers. Values are averages of the four runs in differing amounts of acetone shown above. SDS has higher efficiency and S/N for three of the six buffers. However, SDS also requires much longer analysis times as shown by t_{PSP} and offers lower methylene selectivity ($\alpha CH2$) than the NP PSPs.

This work shows that despite the ease of preparing and working with borate buffer, it provides much lower performance as illustrated by the low S/N than even CHES provides at the same pH. Tris at pH 7.21 is shown to be the most consistent performer between the BAAMPS NP PSP and the SDS micelles. This reaffirms the choice of Tris as the buffer used for all LSER work.

Curiously, all buffers experience a pattern of change in efficiency with varying acetone content in the sample, but the patterns are not consistent. Whether this means that there is

an optimum concentration of organic sample modifier for each buffer remains an open question.
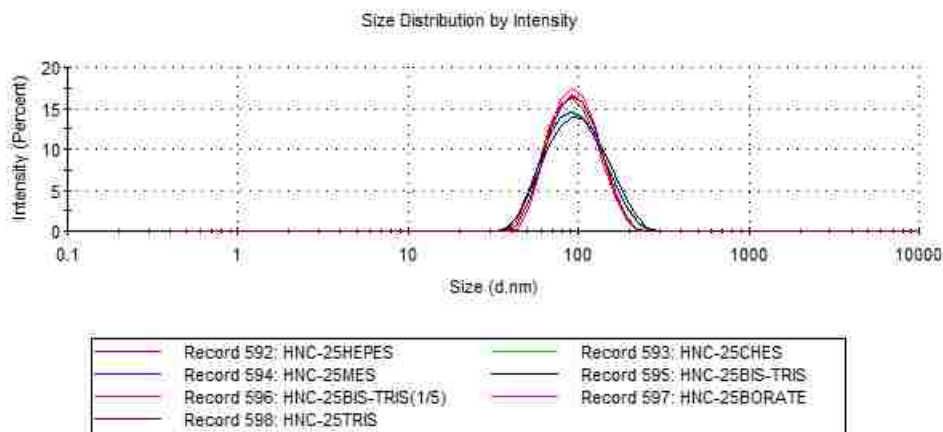
Figure 58 The BGE composition has minimal effect on NP size as measured by DLS in the 10 mM buffer used in the experiments above.

It is also important to note that the BAAMPS NP PSP experienced minimal change in its size in the various buffers at the low BGE concentrations needed for EKC. This further illustrates that the architecture of the NP remains consistent between buffers.

5.6.2 Organic Solvent stability/ modifiers

One of the primary categories in which NP PSPs outperform most other classes of PSP is stability in the presence of organic modifiers in the BGE. As shown in Figure 10 on page 2-22, organic modifiers cause high CMC for micellar PSPs leading to other deleterious effects. To illustrate the stability of NP PSPs in the presence of organic modifiers, the retention factors of many LSER compounds were measured at various concentrations of acetonitrile (ACN). The resulting plot (Figure 59) and chromatogram (Figure 60) show the NP PSP retention decreases consistently with increasing ACN content while the selectivity remains the same.
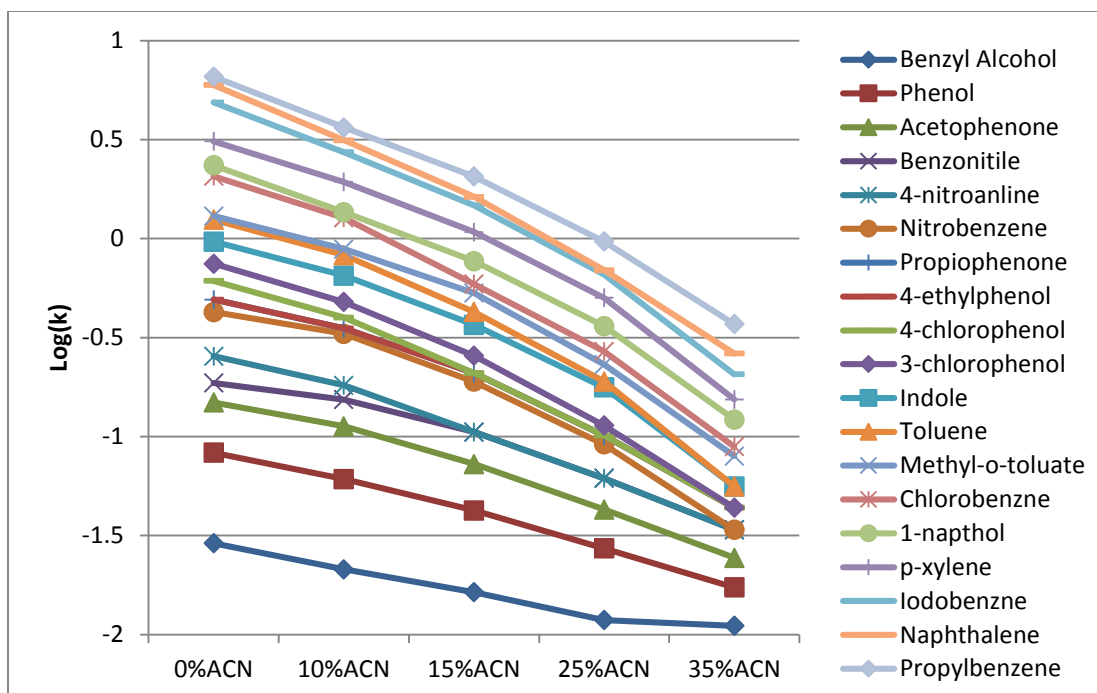
Figure 59 Retention factor vs % acetonitrile in BGE for BAAMPS (HNC-25) NP PSP. The reduction in retention is uniform and consistent to at least 35% acetonitrile content in the BGE. While the linear relationship between log k and % organic modifier that characterizes reversed-phase behavior is not fully observed here, a consistent decrease in retention with no change in selectivity is observed.

The data illustrate the capability to control retention with organic modifier content in the BGE. Little degradation of the baseline occurs until high ACN concentrations are reached (>15%). At high modifier concentrations loss of resolution between compounds with low retention is observed, but the reduced retention for highly retained compounds like propylbenzene and naphthalene provides improved resolution as predicted in Figure 7 on page 1-13 for compounds with more intermediate retention factors.
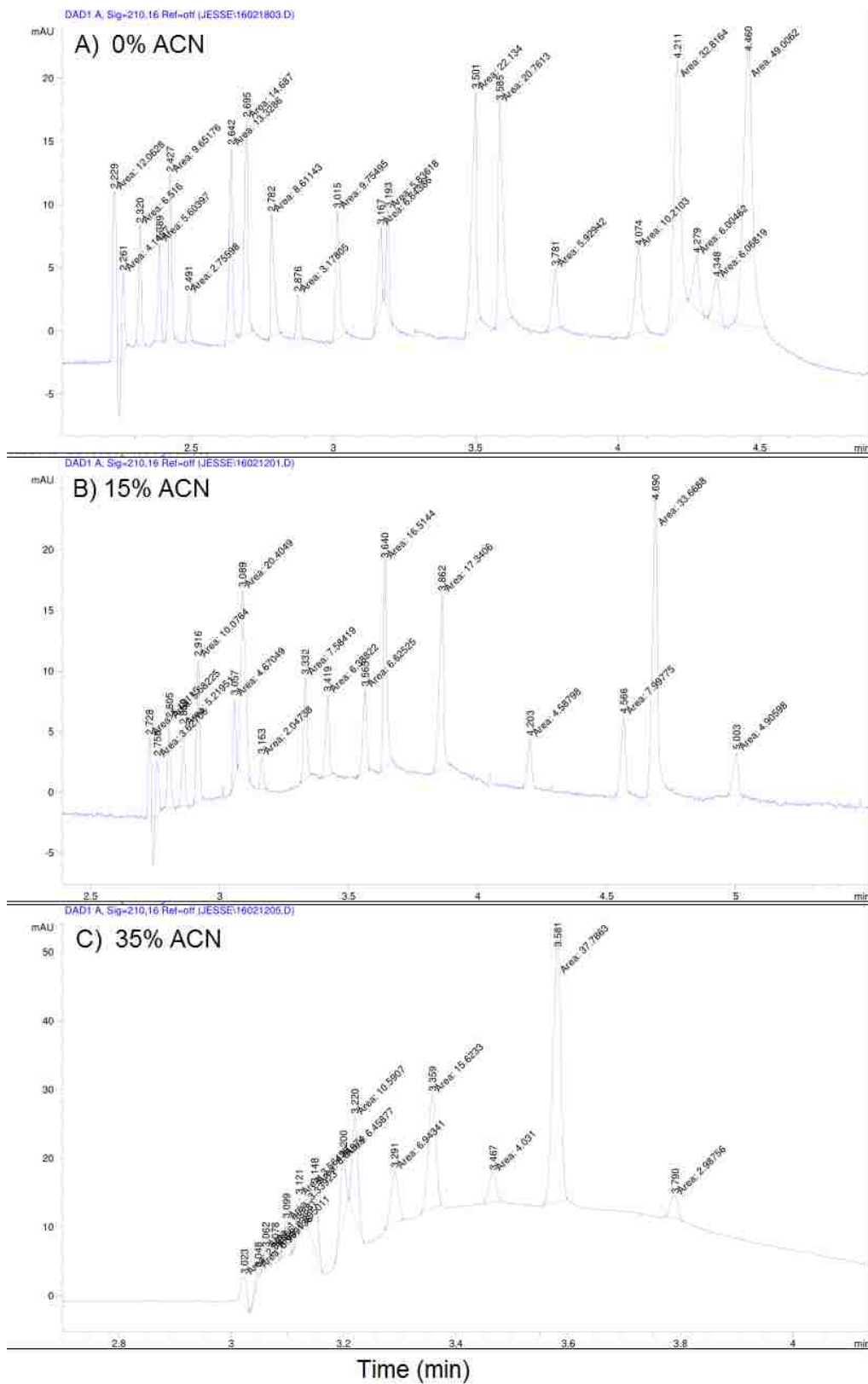
Figure 60 Separations of selected LSER compounds by BAAMPS (HNC-25) in A) 0%, B) 15%, and C) 35% acetonitrile organic modifier in 10mM Tris BGE. Compounds used are listed in Figure 59.

5-103

While some rise in baseline is observed at high modifier percentages, the signal to noise ratio and peak shapes remain excellent even at very high ACN content.
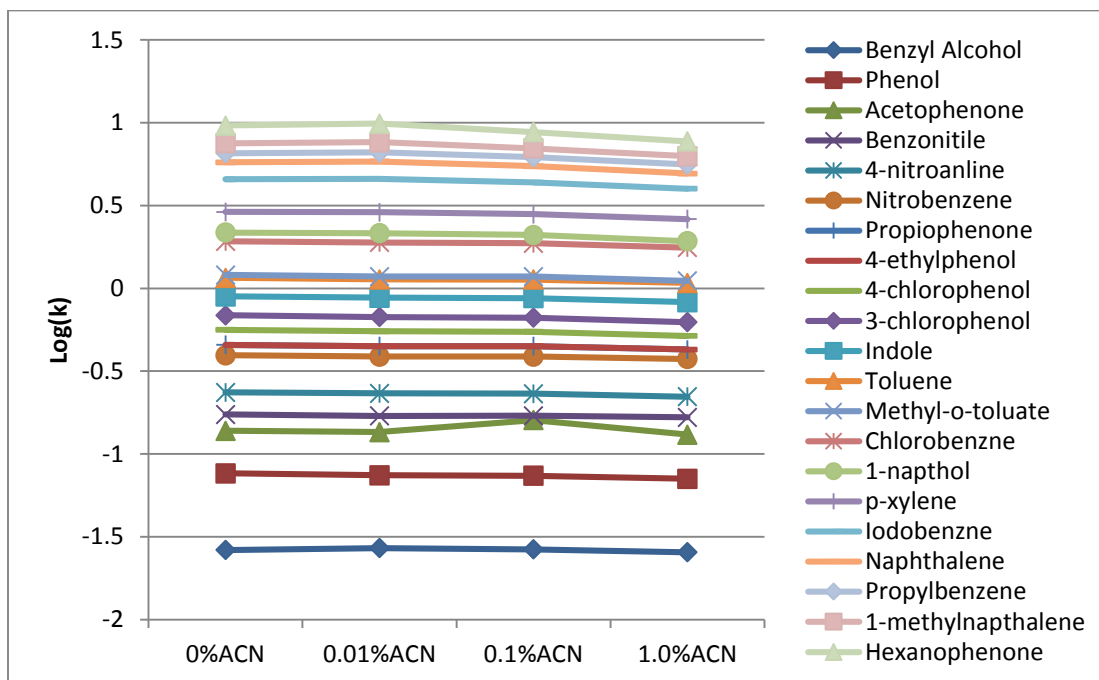

Figure 61 Change in retention from low levels of organic modifier. Extremely low concentrations of ACN were tested to check for concentration of the modifier in the NPs. The lack of any meaningful change in log(k) suggests that the modifier is not concentrated in the NPs but remains as a homogenous solution in the BGE..

In section 3.2 Emulsion Polymerization, the ability of hydrophobic polymers like butyl acrylate to better solvate their own monomer than water resulted in the saturation of polymer particles with monomer. The behavior of the NP PSPs at very low concentrations of ACN in the BGE was investigated to determine if NP PSPs provide a hydrophobic environment capable of extracting an organic modifier from the BGE, thus modifying the selectivity of the NP by changing the internal solvation environment within the NP.

It was found that of the many compounds that were tested only acetophenone showed even a slight anomalous response to the modifier concentration before the concentration was high enough to provide a significant impact on the solute-solvent interactions available in the BGE. This suggests that the organic modifier does not significantly alter the environment within the NP PSP and that the changes in retention factor achieved by addition of an organic modifier may be attributed to its effects on the BGE rather than the NP PSP.

5.6.3 Detector Compatibility

Mass Spectrometer

Another context in which PSP stability is necessary for good performance is during ionization and MS detection. While this is not a research focus of the work reported here, some preliminary data has been generated through collaboration with Emily Hilder and the Australian Center for Research on Separations Science (ACROSS) at the University of Tasmania. Jesse Hyslop spent several months studying the behavior of NP PSPs with MS detection at the University of Tasmania in 2014 through the award of an East Asia Pacific Summer Institutes (EAPSI) fellowship from the NSF in collaboration with the Australian Academy of Science (AAS).

In this research several beta-blockers were analyzed by CE and EKC separations with Atmospheric Pressure Chemical Ionization Mass Spectroscopy (APCI-MS). This represents the first known report of APCI with NP PSPs, although some similar CE-APCI-MS work has been reported in the past [189]. More information on the APCI device, its history, and integration with CE can be found in the excellent review by Hommerson et al. [215].
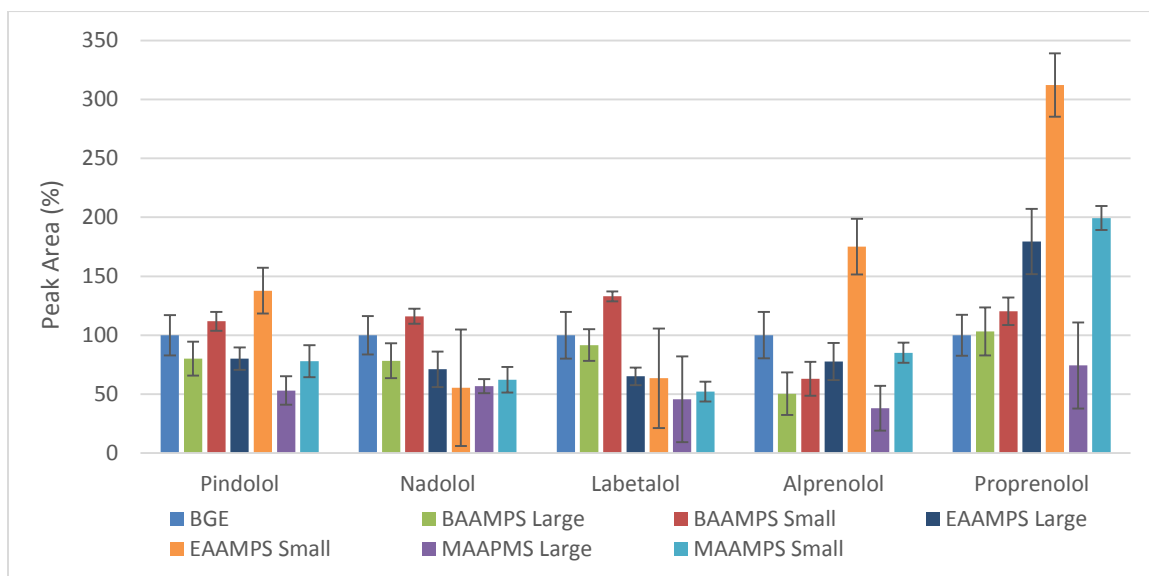
Figure 62 Effects of 0.3% w/w NP PSPs on MS detection of beta-blocker compounds. The peak area of the most abundant ion for each compound is reported as a percentage of the peak area in BGE without NP PSP. Despite relatively low sensitivity, the superiority of the small NPs over large NP PSPs is evident, as well as the compatibility of all five beta-blockers with the six NP PSPs in EKC-APCI-MS.

While all five beta-blockers can be detected and quantified by NP EKC-APCI-MS, some NP PSPs show significantly better peak area arising from better ionization efficiency and from better peak shape under the effects of EKC than during elution without the NP PSP. Within uncertainty, the small NP PSPs match or exceed the performance of the large NP PSP. The BAAMPS NPs provided the most consistent performance, and the enhanced signal exhibited by half of the beta-blockers with the small EAAMPS NPs is intriguing and warrants further investigation.
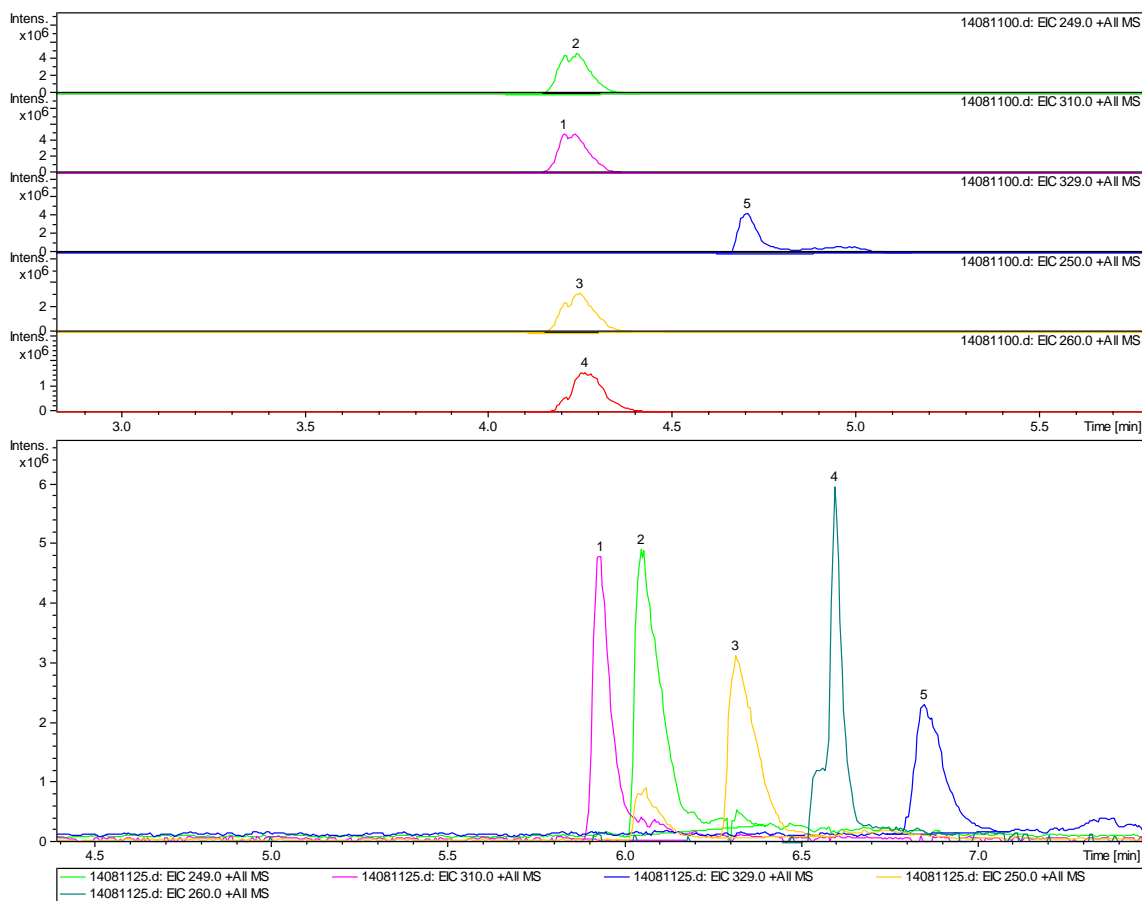
Figure 63 Extracted ion chromatograms of beta-blockers run in BGE (Top) and separated by Small BAAMPS (LH-11) NP PSP (Bottom) and detected with APCI-MS. Note that the NP PSP has little effect on peak height. 80cm x 50μm capillary with 50/2 mbar/sec injection 100 ppm samples. EKC at 25kV with 0.3% w/w NP PSP. Peak 1 Nadolol (310m/z); Peak 2 Pindolol (249m/z); Peak 3 Alprenolol (250m/z); Peak 4 Proprenolol (260m/z); Peak 5 Labetalol (329m/z).

The 20 mM ammonium carbonate buffer (pH 9.99, 10% ACN) did not appear to produce excessive noise or interference, but the sensitivity of the analysis was lower than expected. Although the APCI parameters were optimized, it is probable that significant improvement in sensitivity could be achieved with further optimization of the MS settings and sheath flow composition.

While this work should not be construed to demonstrate a rigorous investigation of NP PSP performance in NP EKC-APCI-MS, it does represent a robust demonstration of the compatibility of these NP PSPs with APCI ionization.

UV-VIS Spectrometer

To be compatible with UV/VIS detectors NP PSPs must produce minimal light scattering from the NPs at the analytical wavelengths and avoid any strong absorbance at those wavelengths. Light scattering appears to cause little signal loss as all NPs are relatively

small relative to the analytical wavelengths. Most NP PSPs exhibit very similar absorbance properties to one another.
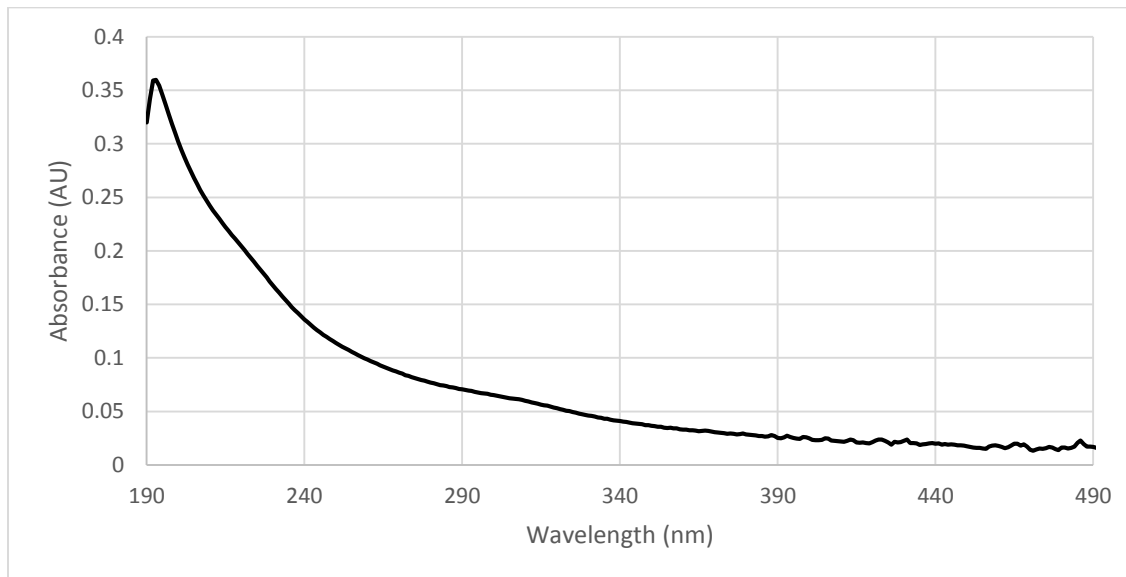

Figure 64 UV/VIS spectra of BAAMPS (LH-5) 0.00245% w/w in 1 cm cuvette.

The calibration curves used to measure the molar absorptivity of the primary NP components and products are available in Appendix B – Molar Absorptivity on page 8-140. While the NP has very strong absorbance, its presence in EKC at μM concentrations (assuming a molar mass of 40,000 u), mitigates its impact on UV-VIS detection sufficiently for the analysis of small molecules down to 1-10 ppm LOD.

	200nm	210nm	245nm	310nm	320nm	400nm
CTA (AU/M*cm)	6651	4946	1543	13399	11884	30
mCTA (AU/M*cm)	30642	11855	1828	9386	8029	335
NP (AU/M*cm)	48656661	39776957	20641263	10054435	8977863	4237660

Table 11 Molar Absorptivity of CTA, AMPS mCTA, and BAAMPS (LH-5) NP. The NP is assumed to have a molar mass of 40,000 u.

5.7 Conductivity

One of the key advantages of NP PSPs is that they do not significantly change the conductivity of a BGE. Unlike MEKC where there is always a concentration of surfactant equal to the CMC of the surfactant in solution, NP PSPs do not have any associated free surfactant to raise the conductivity. Additionally, these NP PSPs operate at lower concentrations than most other PSPs due to their strong hydrophobic character and high affinity for solutes. Because much less material is needed than for other classes of PSP, there are even fewer ionic groups to carry charge introduced by the NP PSP.

The conductivity of the BGE and PSP solution is easily measured by the current conducted at a given electric field strength in the capillary. Conductivity, the reciprocal of resistance, is equal to the ratio of the current to the voltage. Therefore current is a direct measure of conductivity in fixed-voltage EKC in capillaries of equivalent dimensions.
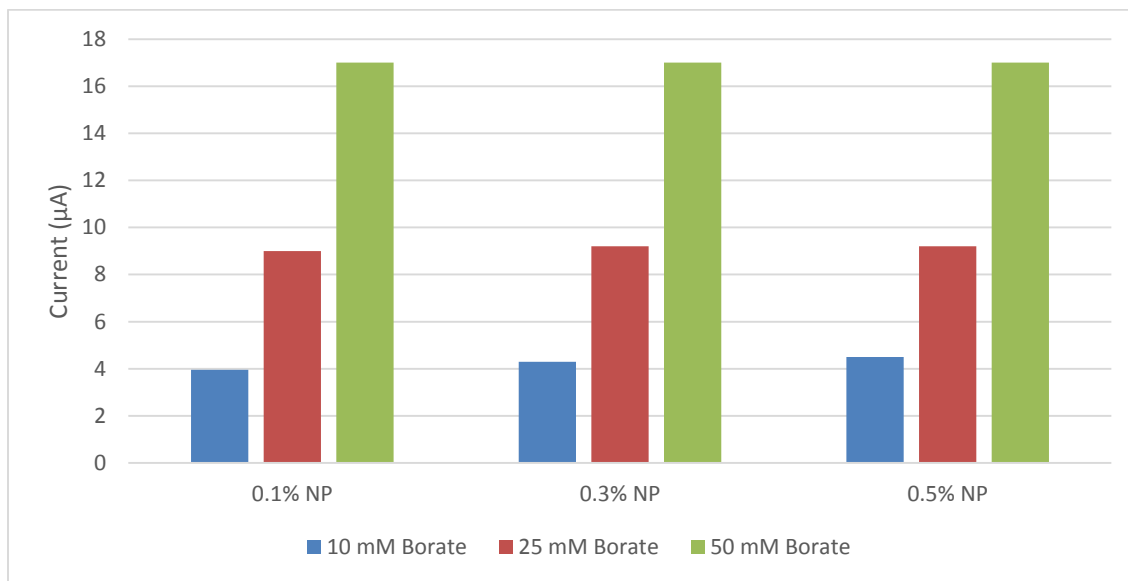

Figure 65 Conductivity of NP PSP (HNC-25) in 10mM Borate as a function of NP concentration and Buffer concentration. The conductivity is shown to be dominated by the BGE concentration will only minor contributions from the NP PSP. 48.5 cm x 50 μm capillary, 20kV, pH 9.2, 25°C.

The very low conductivity increase associated with a NP PSP is reflected in the extremely small increases in current observed with increasing NP PSP concentration compared to the current observed from the BGE alone as shown in Figure 65. The additional current carried by the NPs is negligible at these typical NP concentrations.
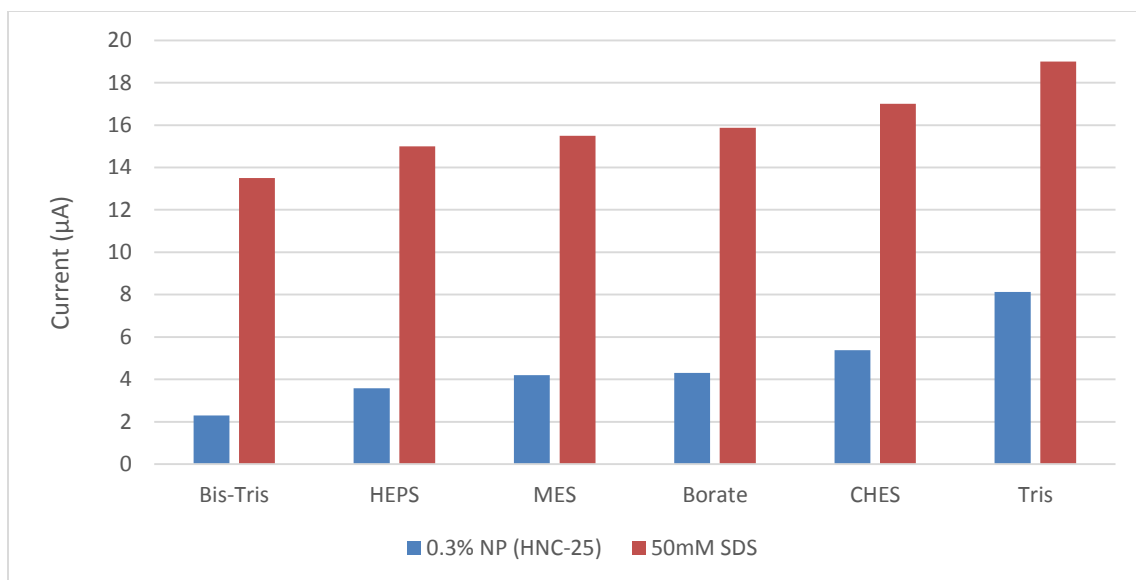
Figure 66 Current with NP PSP (HNC-25) and SDS micelles in various 10mM BGEs. 48.5 cm x 50 μm capillary, 20kV, 25°C. All buffers but Tris (pH 7.2) are at their pKa.

The observed current in several EKC BGEs containing typical concentrations of a NP PSP and SDS are shown in Figure 66. In all cases, the NP PSP system carries significantly less current, with an average absolute difference in current of 11.3±0.3 µA. Depending on the background conductivity of the BGE, this represents a 2.3 to 5.9 fold decrease in current when using the NP PSP. The overall conductivity of the BGE is the sum of the background BGE conductivity and the conductivity of the added PSP. The background conductivity is a function of the concentration and extent of ionization of the buffer components.

The polyprotic buffers Bis-Tris and Borate both provide somewhat lower conductivity than zwitterionic buffers of the same pH (HEPES and CHES respectively) despite providing identical 10 mM buffer capacity. This suggests that polyprotic buffers do run "cooler" than monoprotic buffers. Tris was tested at pH 7.2 where most of the buffer is in its conjugate base form, resulting in the observed elevated current over that of the other buffers.

5.8 Mixed PSP Separations

As shown above, each size and chemistry of NP PSP has its own degree of selectivity. This suggests that the selectivity could be controlled by mixing two NP PSPs to "tune" the selectivity.

A pilot study has been conducted by determining the retention factors of several LSER compounds in 0.3% w/w solutions of BAAMPS (LH-5) and EAAMPS (LH-12) NP PSP under typical 10 mM Tris conditions as well as in mixed solution of 0.15% BAAMPS and 0.15% EAAMPS NP PSP.

Analyte retention (k) in:	0.3% BAAMPS	0.15% BAAMPS 0.15% EAAMPS	0.3% EAAMPS	Calculated Mobility	Measured Mobility	% Error in Mobility
Acetophenone	0.144	0.131	0.118	-0.455	-0.460	1.1
Propiophenone	0.525	0.455	0.377	-1.230	-1.244	1.2
Butyrophenone	1.577	1.339	1.037	-2.249	-2.277	1.2
Valerophenone	4.770	4.174	3.053	-3.165	-3.208	1.3
Hexanophenone	13.561	13.223	9.469	-3.644	-3.697	1.4
Heptanophenone	32.021	35.416	26.521	-3.802	-3.867	1.7
Benzonitrile	0.191	0.165	0.167	-0.596	-0.563	-5.8
4-Chloroaniline	0.440	0.410	0.399	-1.157	-1.157	-0.1
3-Chlorophenol	0.686	0.665	0.647	-1.564	-1.588	1.5
Chlorobenzene	2.616	2.054	1.821	-2.730	-2.674	-2.1
Napthalene	8.855	8.165	7.804	-3.501	-3.543	1.2

Table 12 Variation from modeled retention for mixed NP PSPs shows an average 0.24% error from predicted analyte mobility. The average of the absolute values of percent error is 1.7%.

Given the measured retention factors for an individual analyte on each PSP and the electrophoretic mobilities for each of the PSPs, an expected electrophoretic mobility for that analyte can be predicted and calculated using Equation 5-5. In this approach, the mobility of the analyte is effectively weighted to the affinity and mobility of each PSP by summing the fractions of the analyte in each PSP times the mobility of each PSP. The approach assumes that the two PSPs act as independent phases and not as a single mixed phase.

$$\Delta\mu_{r(calc)} = \frac{1}{1 + k_{PSP1} + k_{PSP2}}(\mu_{PSP1}k_{PSP1} + \mu_{PSP2}k_{PSP2}) \qquad \text{5-5}$$

The effect on the mobility of each of eleven analytes was determined from individual retention times of the analytes using measured NP PSP mobilities of -4.24×10^{-4} cm^2 V^{-1} S^{-1} for BAAMPS and -3.56×10^{-4} cm^2 V^{-1} S^{-1} for EAAMPS. Experimental μ_{EOF} values were calculated with Equation 1-6 and μ_r was calculated by Equation 1-8 (see page 1-11). The experimental analyte mobility by the mixed NP PSP was calculated with Equation 5-6 and compared to the calculated mobility from Equation 5-5 using the mobility and retention factors of the analytes with each of the NP PSPs. This method is reproduced from [133]. The measured analyte mobilities are reported in the measured mobility column in Table 12 and the effect predicted by the retention of the analytes in the pure NP PSPs using Equation 5-5 is shown in the calculated mobility column.

$$\mu_{ep,r(measured)} = \mu_{EOF} - \mu_r \qquad \text{5-6}$$

The low average error of 0.24% between calculated and measured mobilities shows that EKC with a mixture of two NP PSPs performs very much as expected with retention operating as a weighted sum of the retention by two independent phases. However, it

must be noted that if the two analytes with the greatest errors (benzonitrile and chlorobenzene) are excluded, the remaining analytes have a consistent +1.3±0.2% error, implying a bias towards the more retentive phase.

Based on this pilot study we may expect consistent retention behavior within mixtures of NP PSPs. This allows the expected analyte mobilities provided by a mixture of NP PSPs to be calculated *a priori*, allowing the model to be used to predict conditions that maximize resolution between analytes or otherwise optimize the chromatographic performance of a mixed NP PSP system. This illustrates an additional method of selectivity control provided by NP PSPs.

5.9 Separations

Separations of compounds of interest to several fields that employ chromatography are briefly reported here to demonstrate the application of NP PSPs to practical chromatographic tasks. By utilizing the fundamental principles developed in this work, future research should be expected to produce even better results.

Explosives

The rapid detection and identification of explosives is important for a multitude of safety and security applications. To illustrate the potential capability of NP PSPs to the analyses of these types of compounds a representative separation of seventeen explosive compounds and degradation products is shown in Figure 67. These compounds were separated by a BAAMPS NP PSP (HNC-25) under typical conditions. A complete study of the application of NP PSPs to the analysis of explosives and explosive residues will be reported in detail by Julie McGettrick in her forthcoming publications and dissertation.
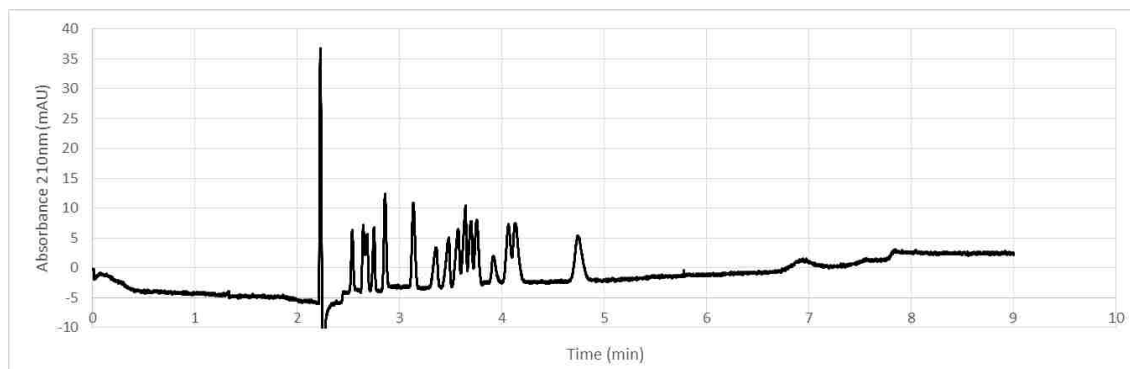

Figure 67 EKC separation of 17 explosive compounds and residues in 5 minutes by BAAMPS (HNC-25) NP PSP. From left to right: Acetone, RDX, Nitrobenzene, Dinitrobenzene, Trinitrobenzene, HMX, Dinitroaniline, 4-Nitrotoluene, 3-Nitrotoluene, 2-Nitrotoluene, 2,6-Dinitrotoluene, 2,4- Dinitrotoluene, 2-Amino, 4,6- Dinitrotoluene, Nitroglycerin, Trinitrotoluene, 4-Amino-2,6-Dinitrotoluene, Tetryl.

Figure 67 demonstrates the separation of 16 of 17 compounds, including the 2/3/4-nitrotoluene series and the nitro-, dinitro-, and trinitrobenzene series in under five minutes. Explosives such as RDX, HMX, TNT, and Nitroglycerin are easily resolved. No organic solvents were needed aside from acetone to mark t_0.

The compatibility of NP PSPs with organic modifiers allows the retention factor of highly hydrophobic analytes to be controlled with modifier content. To demonstrate this a number of polynuclear aromatic hydrocarbons (PAH) were separated by NP EKC as shown in Figure 68. The relatively low plate counts in this separation are apparently characteristic for these large multi-ring PAHs. This behavior requires further investigation to determine whether it is endemic to the NP PSPs. Separations of other compounds in BGEs containing up to 35% acetonitrile showed much higher plate counts, suggesting that the low plate counts in Figure 68 are associated with the analytes and not the addition of acetonitrile.
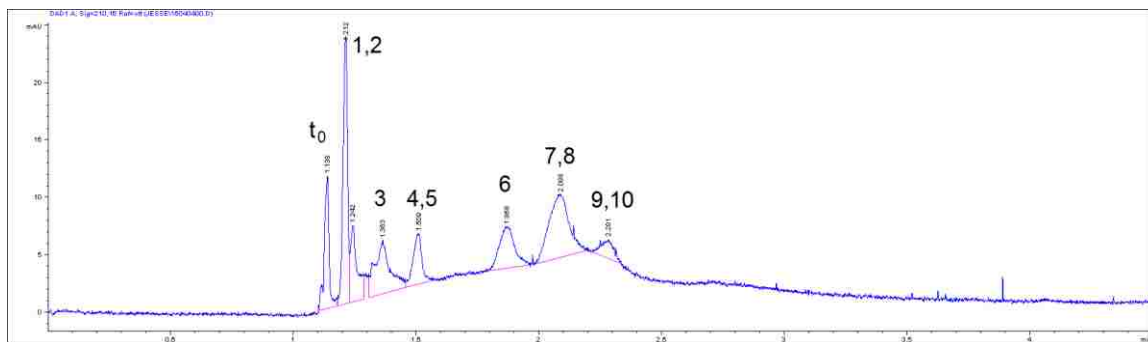
Figure 68 Separation of 10 PAH compounds by NP EKC in 3 min. 0.3% BAAMPS (HNC-25) in pH 7.23 10mM Tris with 30% ACN. 20kV on 32 cm 50 µm ID capillary. 20 ppm sample injected with 70mbar/s pressure. 1) Anthracene, 2) Acenaphthylene, 3) Retene, 4) Pyrene, 5) Chrysene, 6) Benz(a)anthracene, 7) Dibenz[a,h]anthracene, 8) Benz[e]Acephenanthrylen, 9) Benzo(k)fluoranthene, 10) Benzo(e)pyrene

5.10 Principal Component Analysis

How NP PSPs are related to other classes of PSP is illustrated by including the NP PSPs analyzed by LSER alongside 54 other PSPs from the literature in the Principal Component Analysis (PCA) of PSPs recently published by Khaledi and coworkers [47]. Khaledi identified four "clusters" of PSPs characterized by similar behavior as described by their LSER parameters (Figure 69). Including the five NP PSP parameters from this work in in Khaledi's analysis produces an identical classification of the 54 PSPs and 16 decoy systems from [47] with the five NP PSPs bridging between Cluster II and IV.
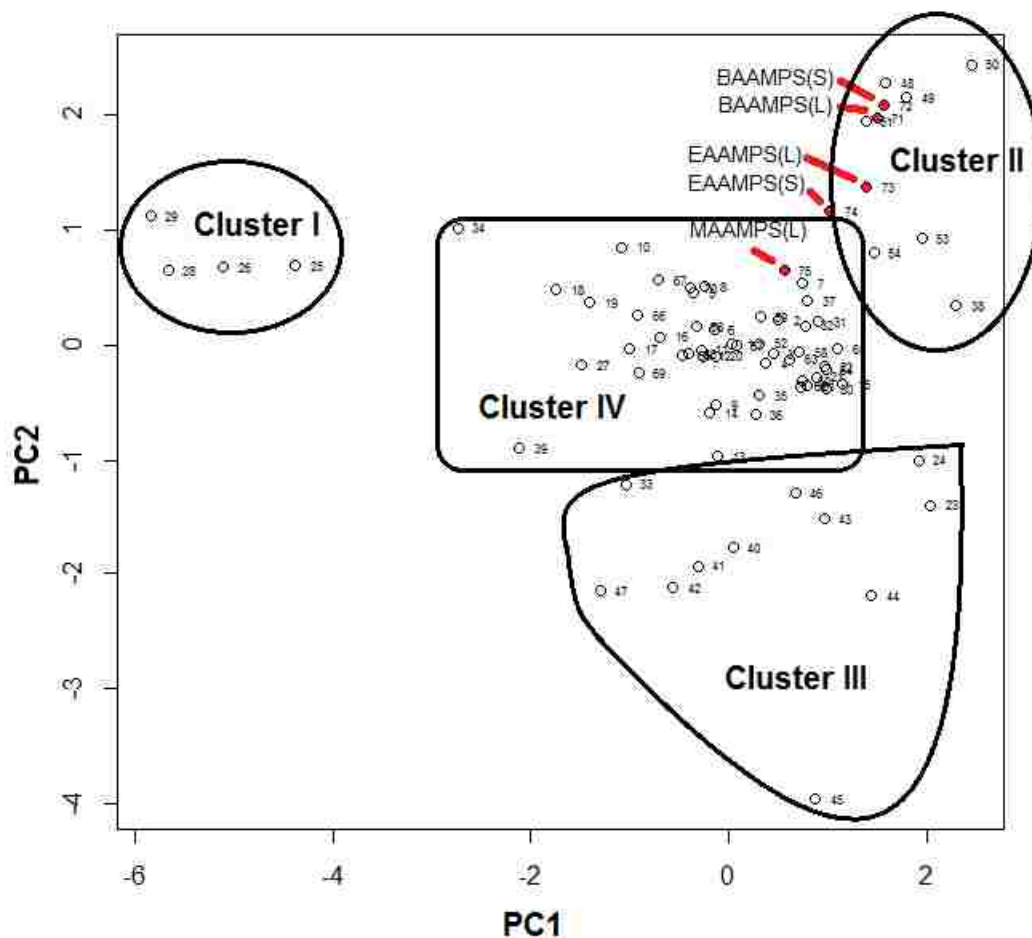
Figure 69 PCA of 54 PSPs, 16 dummy PSPs(replicate data of SDS), and 5 NP PSPs using the procedures and data from [47] with the NP PSP LSER data from this work. The NP PSPs bridge Clusters II and IV. This demonstrates both the centrality of the hydrophobic block to the behavior of the PSP and the broad range of behavior that can be controlled by monomer selection in NP PSPs.

Khaledi reports that Cluster I consists of a series of fluorinated surfactants (illustrating the unique behavior of fluorinated materials as PSPs), Cluster II spans from the cationic surfactant hexadecyltrimethyl ammonium bromide (#38) to a group of alkyl methacrylate-based polymer PSPs. Clusters III and IV have no clear boundary, indicating comparable selectivity. They are therefore differentiated by PSP types: Cluster III is mostly comprised of polymer PSPs including Elvacite 2669 (#33) and siloxane-based polymers (#40-47). Cluster IV primarily contains micellar PSPs including the "dummy PSPs" consisting of SDS parameters measured by many laboratories under various conditions. PSP #34 midway between Cluster I and IV is noteworthy as a mixed micelle of LiPFOS fluorinated surfactant and LiDS hydrocarbon surfactant that demonstrates hybrid behavior.

5-113

The NP PSPs are primarily distributed by their core chemistry between Clusters II and IV indicating that their characteristics are most consistent with the chemically similar alkyl methacrylate-based polymer PSPs. However, the more cohesive NPs with shorter alkyl chains have behavior that approaches or enters the domain of surfactant based PSPs.

This PCA demonstrates that the NP PSPs provide consistent behavior with polymers chemically similar to the hydrophobic block of the NPs as well as demonstrating the breath of synthetic control provided by the NP PSP approach. This provides further evidence that solute interactions are localized to the hydrophobic block of the polymers comprising the NPs.

Chapter 6 Summary and Conclusions

Chromatography is a fundamental tool used in most fields of chemistry and biochemistry as well as some fields of engineering and physics. As such it is a critical enabling technology. Advances in chromatography are rapidly brought into use to speed the development of technologies as diverse as drug development in pharmacology, flavor analysis in the food sector, and water quality monitoring in environmental monitoring and compliance.

Among the many chromatographic systems available today, Capillary Electrophoresis (CE) stands out for its simple and rugged instrumental design coupled with unique properties that greatly enhance the performance of CE over other chromatographic systems like HPLC and IC that can be used for similar tasks. CE's use of electroosmotic flow (EOF) (page 1-4) to provide bulk transport through the capillary column without band broadening from parabolic flow profiles intrinsic to pressure driven systems like HPLC (page 1-6) is a key advantage. Another is the extremely small injection volumes needed—on the order of a few nanoliters. Many other properties are discussed in section 1.1.3 Capillary Electrophoresis on page 1-4.

However, CE is unable to separate neutral compounds on its own. Electrokinetic Chromatography (EKC) is a technique developed in 1984 [7] to separate neutral compounds by their retention in a Pseudostationary Phase (PSP), analogous to retention chromatography in HPLC (1.2 Electrokinetic Chromatography page 1-8). The PSP is the heart of EKC separations and much research has been conducted in the intervening years (see Chapter 2: The Development of the PSP).

The advantages of several of the different classes of PSPs that have been previously developed have been united in the most recent generation of Nanoparticle (NP) PSPs (page 2-40). The synthesis of these NP PSPs is made possible by the use of recent advancements in Reversible Addition-Fragmentation chain Transfer (RAFT) polymerization (See Chapter 3: RAFT Synthesis). RAFT allows the synthesis of copolymers with control of both polymer block chemistry and length, providing control over the architecture of the resulting polymer NP PSP (4.2 Synthetic methods page 4-57).

While the performance of this latest generation of NP PSPs has been demonstrated in two earlier papers [157], [158] using a single batch of poly(butyl acrylate) /poly(acrylic acid) (BAAA) based NP PSP, this work reports the relationship between NP architecture and their performance as a PSP in EKC for the first time (Chapter 5: Results page 5-70).

Each component of NP architecture was sequentially investigated. For the ionic block of the polymer poly(acrylic acid) and poly(AMPS) (AMPS described on page 4-57) were both used with five to ten mer block lengths (Table 7 page 5-77) as measured by MALDI (pages 4-54 and 4-60). Poly(butyl acrylate) hydrophobic blocks were used to demonstrate that the BAAA and BAAMPS NPs respectively showed little variation in mobility with ionic block length between 6 and 11 mer AMPS, and no major difference between the

BAAA and BAAMPS chemistries (5.1.1 Ionic Block page 5-70). NPs with AMPS ionic blocks were used for the characterization of the remaining architectural properties.

The hydrophobic block of the copolymers was synthesized with hexyl-, butyl-, ethyl-, and methyl-acrylate monomers to yield HAAMPS, BAAMPS, EAAMPS, and MAAMPS NPs. The hypothesis that increasing the hydrophobicity of the monomer would produce a more hydrophobic NP with increased retention for non-polar compounds was confirmed up to an alkyl chain length of four (5.3 Methylene Selectivity page 5-86). Methylene selectivity, the metric for the strength of hydrophobic interaction, shows that increasing alkyl chain length of the monomer increased the strength of the interactions up to BAAMPS, where the methylene selectivity seems to plateau (see Figure 47 on page 5-86), as HAAMPS provides analogous results and the increasing insolubility of the monomer makes synthesis more difficult.

The final architectural variable was the size of the NP. This may be controlled by the amount of monomer used during the synthesis of the hydrophobic block (5.1.2 Hydrophobic Block page 5-77 and Figure 43 page 5-79). Using this stoichiometric control BAAMPS, EAAMPS, and MAAMPS NPs were synthesized in small (average 15 nm) and large (average 126 nm) sizes. The EKC performance of this set of six NP PSPs was then investigated. The results of this work makes up much of the sections 5.2.1 Electrophoretic Mobility (page 5-83), 5.3 Methylene Selectivity (page 5-86), 5.4 Efficiency (page 5-87), and 5.5 LSER Characterization (5-92) as well as being used to demonstrate compatibility with APCI-MS detection (page 5-105).

The Linear Solvation Energy Relationship (LSER) studies (page 5-92) show that the less hydrophobic or smaller NP demonstrates more aqueous-like solvent behavior than a larger NP of the same chemistry or than a NP of more hydrophobic character. This pattern is reflected throughout this work, with smaller or less hydrophobic NP PSPs exhibiting behavior nearer to the Back Ground Electrolyte (BGE) than larger or more hydrophobic NP PSPs.

One peculiar behavior observed in the efficiency of both these NPs and the previously reported BAAA NP is that efficiency deteriorates with increasing retention. The degree of broadening is greater than that projected for diffusion, and although all major theories related to broadening in EKC have been considered (section 5.4 Efficiency page 5-87), none of the existing models of band broadening fully explain the observed behavior.

Despite this broadening, the NP PSPs were capable of efficiencies of over half a million theoretical plates for a separation taking only a few minutes (Table 9 page 5-82). This equates to an average efficiency of more than a million plates per meter during the separation of acetophenone, propiophenone, butyrophenone, valerophenone, heptanophenone, and hexanophenone. These six phenones span the entire separation window and experience the same broadening other compounds do. This peak efficiency was obtained with the small BAAMPS NP. Larger and less hydrophobic NP PSPs trend around a quarter million theoretical plates on 48.5 cm capillaries.

While the smaller NPs typically exhibit better performance than their larger counterparts, NP chemistry has greater influence over selectivity than size (Figure 49 page 5-88 and Figure 47 page 5-86).

With this in mind, the overall finding is that smaller and more hydrophobic NP PSPs are preferred as a general purpose PSP. Specifically, NPs less than 25 nm in diameter and with the hydrophobic block of the copolymer comprised of poly(butyl acrylate) give the best overall performance.

The NP PSPs are fully compatible with organic modifiers in the BGE (page 5-101) and provide no significant contribution to the conductivity of the system (page 5-107). These properties enable NP PSPs to be employed in a broad range of separations applications because the selectivity of the system can be modified by changing the BGE composition without needing many different types of PSP. The low conductivity of NP PSPs allows high electric field strengths to be used, reducing the total analysis time.
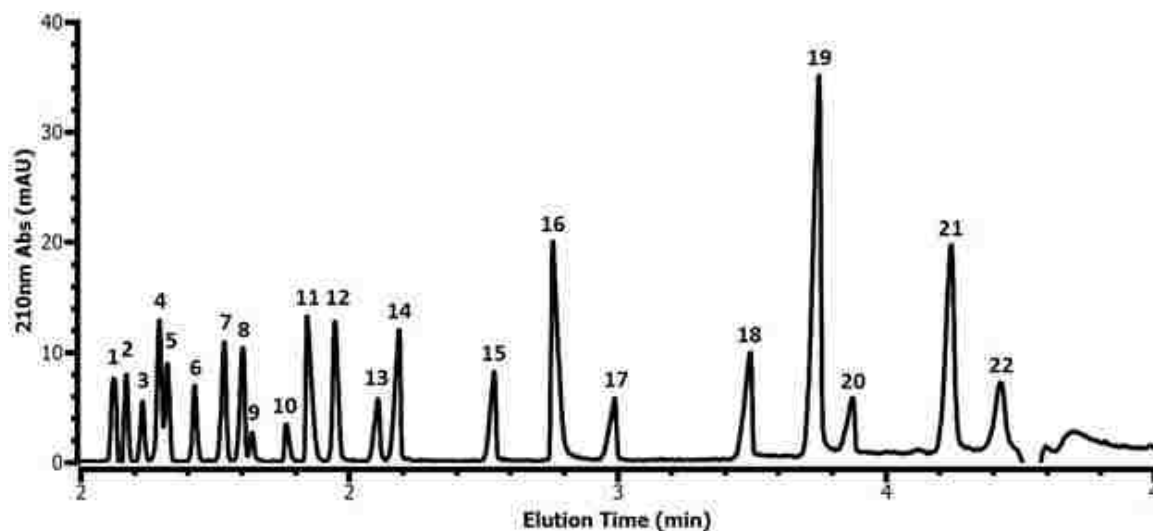
Figure 70 Separation of 22 compounds in under 5 min by NP EKC using BAAMPS (JSH-11A). Peak assignments in Figure 71 of Appendix A - LSER. Reproduced from authors paper [160].

6.1 Future Work

This work has laid a quantitative foundation to the understanding the behavior of polymer NPs as PSPs in EKC that will inform future research and production of NP PSPs. It also illuminates where some of the most promising variations on the chemistries employed here may be found.

Cationic NP PSPs are a natural extension of this technology. While the anionic NPs used in this work function well with neutral analytes, cationic analytes may have unwanted interactions with the PSP or may adsorb to the anionic capillary walls. Cationic NP PSPs offer to broaden the compatibility of EKC by operating in capillaries coated with cationic

material (potentially the PSP its self) to reverse the EOF and prevent adsorption of positively charged analytes. This work is currently being pursued in the Palmer research group by Julie McGettrick.

The ability to incorporate any desired chemistry into the NP PSPs that can be acquired as a monomer and is compatible with RAFT opens up many opportunities to synthesize NP PSPs with specific selectivity for a given task. One of the most challenging types of selectivity to produce is chiral selectivity for the separation of enantiomers.

By utilizing the methyl ester of amino acids as the hydrophobic monomer in the synthetic scheme reported here, it should be possible to synthesize NP PSPs with amino acids providing both hydrophobic interactions and chiral centers to provide enantiomeric selectivity. Amino acids and dipeptides have been demonstrated to provide chiral resolution before (Chapter 2 page 2-29), so this is a promising opportunity. The increased methylene selectivity and large number of chiral centers that would be provided by a NP comprised of amino acids should greatly improve the magnitude of chiral selectivity. This would merge the advantages of CD with those of the NP PSPs reported here. This project is currently being pursued in the Palmer research group by Derek Schultz.

Aromatic character is another chemistry that could be incorporated into NP PSPs. Styrene NPs (StAMPS) were attempted during this work and synthesis was identified as a challenge that will require more optimization. The arene is expected to provide stronger π-π and induced dipole interactions. However, the strong absorption of aromatic compounds in the UV means that a StAAMPS NP may have limited compatibility with UV-VIS detection and require fluoresce or MS detection.

Fluorinated NPs are another alternate chemistry that may provide useful selectivity. Fluorinated compounds are known to have higher affinity for fluorinated solvents than for the protonated versions of the same solvents [216] and it may be possible to leverage this to provide fluorous selectivity. Beyond the several specific selectivities outlined here, any number of monomers may be incorporated into polymer NP PSPs.

Moving beyond the development of new selectivities, bringing NP PSPs to the chromatography market will require further development of the synthesis to scale up synthesis from the 4 g batches in this work to production quantities of tens of kg. As RAFT polymerization has become more widely understood and employed throughout the polymer industry, no difficulty is anticipated in scaling up synthesis to commercial quantities.

The characterization of the RAFT copolymers in terms of molecular mass or degree of polymerization is extremely challenging as the copolymers aggregate into particles. This precludes traditional approaches such as size exclusion chromatography (SEC) from being used to determine the molecular mass. Even if SEC could be applied, no standards are available for the unique amphiphilic diblock copolymers that comprise these NP PSPs. This provides a novel research opportunity for polymer chemists utilizing alternate

instrumentation like NMR or CE and techniques including Melt-State NMR to investigate the properties of the copolymer materials [178], [179], [181], [217]–[219].

Finally, the broadening mechanics of NP PSPs have already been noted as an area for further investigation and modeling.

Chapter 7 References

[1]   C. W. Gehrke, R. L. Wixom, and E. Bayer, *chromatography a century of discovery 1900–2000 - the bridge to the sciences/technology*, vol. 64. Elsevier, 2001.

[2]   N. Tanaka, K. Sakagami, and M. Araki, "Effect of alkyl chain length of the stationary phase on retention and selectivity in reversed-phase liquid chromatography," *J. Chromatogr. A*, vol. 199, pp. 327–337, Oct. 1980.

[3]   J. L. Rafferty, J. I. Siepmann, and M. R. Schure, "A molecular simulation study of the effects of stationary phase and solute chain length in reversed-phase liquid chromatography," *J. Chromatogr. A*, vol. 1223, pp. 24–34, 2012.

[4]   Apblum, "File:Capillaryelectrophoresis.png - Wikimedia Commons," *Wikimedia* , 2007. [Online]. Available: https://commons.wikimedia.org/wiki/File:Capillaryelectrophoresis.png. [Accessed: 11-Aug-2016].

[5]   B. (Brian J. . Kirby, *Micro- and nanoscale fluid mechanics transport in microfluidic devices*. Cambridge University Press, 2010.

[6]   D. Harvey, "Electrophoresis," *UC Davis ChemWiki*, 2016. [Online]. Available: http://chemwiki.ucdavis.edu/Core/Analytical_Chemistry/Analytical_Chemistry_2.0/12_Chromatographic_and_Electrophoretic_Methods/12G%3A_Electrophoresis. [Accessed: 10-May-2016].

[7]   S. Terabe, K. Otsuka, K. Ichikawa, A. Tsuchiya, and T. Ando, "Electrokinetic separations with micellar solutions and open-tubular capillaries," *Anal. Chem.*, vol. 56, no. 1, pp. 111–113, Jan. 1984.

[8]   C. P. Palmer, "Electrokinetic Chromatography: An Historical Review of Developments in Theory and Practice," *Sci. Chromatogr.*, vol. 7, no. 1, pp. 7–29, Oct. 2015.

[9]   J. M. Davis, "New assessments of dispersion in micellar electrokinetic chromatography," *J. Microcolumn Sep.*, vol. 10, no. 6, pp. 479–489, 1998.

[10]   S. Terabe, K. Otsuka, and T. Ando, "Band broadening in electrokinetic chromatography with micellar solutions and open-tubular capillaries," *Anal. Chem.*, vol. 61, no. 3, pp. 251–260, Feb. 1989.

[11]   K. Kleparník and F. Foret, "Recent advances in the development of single cell analysis—A review," *Anal. Chim. Acta*, vol. 800, pp. 12–21, 2013.

[12]   C. P. Palmer, "Micelle polymers, polymer surfactants and dendrimers as pseudo-stationary phases in micellar electrokinetic chromatography," *J. Chromatogr. A*, vol. 780, no. 1–2, pp. 75–92, Sep. 1997.

[13]   C. P. Palmer, "Polymeric and polymer-supported pseudostationary phases in micellar electrokinetic chromatography: performance and selectivity.," *Electrophoresis*, vol. 21, no. 18, pp. 4054–72, Dec. 2000.

[14]   C. P. Palmer, "Recent progress in the development, characterization and application of polymeric pseudophases for electrokinetic chromatography," *Electrophoresis*, vol. 23, no. 22–23, pp. 3993–4004, Dec. 2002.

[15]   C. P. Palmer and J. P. McCarney, "Recent progress in the use of soluble ionic polymers as pseudostationary phases for electrokinetic chromatography.," *Electrophoresis*, vol. 25, no. 23–24, pp. 4086–94, Dec. 2004.

[16] C. P. Palmer, "Recent progress in the use of ionic polymers as pseudostationary phases for EKC.," *Electrophoresis*, vol. 28, no. 1–2, pp. 164–73, Jan. 2007.

[17] C. P. Palmer, "Recent progress in the use of ionic polymers as pseudostationary phases for electrokinetic chromatography," *Electrophoresis*, vol. 30, no. 1. WILEY-VCH Verlag, pp. 163–168, Jan-2009.

[18] P. Hommerson, A. M. Khan, G. J. de Jong, and G. W. Somsen, "Comparison of electrospray ionization and atmospheric pressure photoionization for coupling of micellar electrokinetic chromatography with ion trap mass spectrometry," *J. Chromatogr. A*, vol. 1204, no. 2, pp. 197–203, 2008.

[19] M. J. Blandamer, P. M. Cullis, L. G. Soldi, J. B. F. N. Engberts, A. Kacperska, N. M. Van Os, and M. C. S. Subha, "Thermodynamics of micellar systems: Comparison of mass action and phase equilibrium models for the calculation of standard Gibbs energies of micelle formation," *Adv. Colloid Interface Sci.*, vol. 58, no. 2, pp. 171–209, 1995.

[20] C. F. Poole and S. K. Poole, "Interphase model for retention and selectivity in micellar electrokinetic chromatography," *J. Chromatogr. A*, vol. 792, no. 1–2, pp. 89–104, Dec. 1997.

[21] M. M. Ghahremanpour, S. S. Arab, S. B. Aghazadeh, J. Zhang, and D. van der Spoel, "MemBuilder: a web-based graphical interface to build heterogeneously mixed membrane bilayers for the GROMACS biomolecular simulation program.," *Bioinformatics*, vol. 30, no. 3, pp. 439–41, Feb. 2014.

[22] J. Šteflová, M. Štefl, S. Walz, M. Knop, and O. Trapp, "Comprehensive study on critical micellar concentrations of sds in acetonitrile-water solvents," *Electrophoresis*, vol. 37, no. 10, pp. 1287–1295, Feb. 2016.

[23] N. J. Chang and E. W. Kaler, "The structure of sodium dodecyl sulfate micelles in solutions of water and deuterium oxide," *J. Phys. Chem.*, vol. 89, no. 14, pp. 2996–3000, Jul. 1985.

[24] F. M. Menger, "The structure of micelles," *Acc. Chem. Res.*, vol. 12, no. 4, pp. 111–117, Apr. 1979.

[25] Katz, E., Schoenmakers, P. and N. Miller, *Handbook of HPLC*. New York: Marcel Dekker, 1998.

[26] W. M. Nelson, Q. Tang, A. K. Harrata, and C. S. Lee, "On-line partial filling micelllar electrokinetic chromatography-electrospray ionization mass spectrometry," *J. Chromatogr. A*, vol. 749, no. 1–2, pp. 219–226, Oct. 1996.

[27] P. G. Muijselaar, K. Otsuka, and S. Terabe, "On-line coupling of partial-filling micellar electrokinetic chromatography with mass spectrometry," *J. Chromatogr. A*, vol. 802, no. 1, pp. 3–15, Apr. 1998.

[28] L. K. Amundsen, J. T. Kokkonen, and H. Sirén, "Comparison of partial filling MEKC analyses of steroids with use of ESI-MS and UV spectrophotometry.," *J. Sep. Sci.*, vol. 31, no. 5, pp. 803–13, Mar. 2008.

[29] W. M. Nelson and C. S. Lee, "Mechanistic Studies of Partial-Filling Micellar Electrokinetic Chromatography," *Anal. Chem.*, vol. 68, no. 18, pp. 3265–3269, Jan. 1996.

[30] L. Yu, T. H. Seals, and J. M. Davis, "Reexamination of Dependence of Plate Number on SDS Concentration in Micellar Electrokinetic Chromatography.,"

Anal. Chem., vol. 68, no. 23, pp. 4270–80, Dec. 1996.

[31]   R. Nagarajan and E. Ruckenstein, "Theory of surfactant self-assembly: a predictive molecular thermodynamic approach," *Langmuir*, vol. 7, no. 12, pp. 2934–2969, Dec. 1991.

[32]   A. Pan, B. Naskar, G. K. S. Prameela, B. V. N. P. Kumar, A. B. Mandal, S. C. Bhattacharya, and S. P. Moulik, "Amphiphile behavior in mixed solvent media I: self-aggregation and ion association of sodium dodecylsulfate in 1,4-dioxane-water and methanol-water media.," *Langmuir*, vol. 28, no. 39, pp. 13830–43, Oct. 2012.

[33]   L. Sepulveda, E. Lissi, and F. Quina, "Interactions of neutral molecules with ionic micelles," *Adv. Colloid Interface Sci.*, vol. 25, pp. 1–57, 1986.

[34]   G. J. Duns, L. W. Reeves, D. W. Yang, and D. S. Williams, "Measurement of the Solubility of Benzene in Micellar Solution by NMR," *J. Colloid Interface Sci.*, vol. 173, no. 2, pp. 261–264, 1995.

[35]   R. E. Wasylishen, J. C. T. Kwak, Z. Gao, E. Verpoorte, J. B. MacDonald, and R. M. Dickson, "NMR studies of hydrocarbons solubilized in aqueous micellar solutions," *Can. J. Chem.*, vol. 69, no. 5, pp. 822–833, May 1991.

[36]   G. E. A. Aniansson, "The mean lifetime of a micelle," in *Surfactants, Adsorption, Surface Spectroscopy and Disperse Systems*, Darmstadt: Steinkopff, 1985, pp. 2–5.

[37]   F. M. Kuni, A. I. Rusanov, A. P. Grinin, and A. K. Shchekin, "Thermodynamic and Kinetic Foundations of the Micellization Theory: 5. Hierarchy of Kinetic Times," *Colloid J.*, vol. 63, no. 6, pp. 723–730, 2001.

[38]   S. G. Oh and D. O. Shah, "The effect of micellar lifetime on the rate of solubilization and detergency in sodium dodecyl sulfate solutions," *J. Am. Oil Chem. Soc.*, vol. 70, no. 7, pp. 673–678, Jul. 1993.

[39]   J. Zhao and B. M. Fung, "NMR study of the transformation of sodium dodecyl sulfate micelles," *Langmuir*, vol. 9, no. 5, pp. 1228–1231, May 1993.

[40]   K. L. Rundlett and D. W. Armstrong, "Mechanism of signal suppression by anionic surfactants in capillary electrophoresis-electrospray ionization mass spectrometry.," *Anal. Chem.*, vol. 68, no. 19, pp. 3493–7, Oct. 1996.

[41]   H. L. Cheng, M.-C. Tseng, P.-L. Tsai, and G. R. Her, "Analysis of Synthetic chemical drugs in adulterated Chinese medicines by capillary electrophoresis/electrospray ionization mass spectrometry," *Rapid Commun. Mass Spectrom.*, vol. 15, no. 16, pp. 1473–1480, Aug. 2001.

[42]   G. W. Somsen, R. Mol, and G. J. de Jong, "On-line micellar electrokinetic chromatography–mass spectrometry: feasibility of direct introduction of non-volatile buffer and surfactant into the electrospray interface," *J. Chromatogr. A*, vol. 1000, no. 1, pp. 953–961, 2003.

[43]   R. Mol, E. Kragt, I. Jimidar, G. J. de Jong, and G. W. Somsen, "Micellar electrokinetic chromatography–electrospray ionization mass spectrometry for the identification of drug impurities," *J. Chromatogr. B*, vol. 843, no. 2, pp. 283–288, 2006.

[44]   J. Schappler, D. Guillarme, S. Rudaz, and J.-L. Veuthey, "Microemulsion electrokinetic chromatography hyphenated to atmospheric pressure photoionization mass spectrometry," *Electrophoresis*, vol. 29, no. 1, pp. 11–19,

Jan. 2008.

[45] A. Wuethrich, P. R. Haddad, and J. P. Quirino, "Online Sample Concentration in Partial-Filling Chiral Electrokinetic Chromatography - Mass Spectrometry," *Chirality*, vol. 26, no. 11, pp. 734–738, Nov. 2014.

[46] L. Yang, A. K. Harrata, and C. S. Lee, "On-Line Micellar Electrokinetic Chromatography−Electrospray Ionization Mass Spectrometry Using Anodically Migrating Micelles," *Anal. Chem.*, vol. 69, no. 10, pp. 1820–1826, May 1997.

[47] C. Fu and M. G. Khaledi, "Characterization and classification of pseudo-stationary phases in micellar electrokinetic chromatography using chemometric methods.," *Anal. Chem.*, vol. 86, no. 5, pp. 2371–9, Mar. 2014.

[48] C. Fu and M. G. Khaledi, "Micellar selectivity triangle for classification of chemical selectivity in electrokinetic chromatography.," *J. Chromatogr. A*, vol. 1216, no. 10, pp. 1891–900, Mar. 2009.

[49] M. D. Trone and M. G. Khaledi, "Statistical evaluation of linear solvation energy relationship models used to characterize chemical selectivity in micellar electrokinetic chromatography," *J. Chromatogr. A*, vol. 886, no. 1, pp. 245–257, 2000.

[50] E. Fuguet, C. Ràfols, E. Bosch, M. H. Abraham, and M. Rosés, "Solute–solvent interactions in micellar electrokinetic chromatography: III. Characterization of the selectivity of micellar electrokinetic chromatography systems," *J. Chromatogr. A*, vol. 942, no. 1, pp. 237–248, 2002.

[51] S. Schulte, A. K. Singh, E. Rauk, and C. P. Palmer, "Performance and selectivity of polymeric pseudostationary phases for the electrokinetic separation of amino acid derivatives and peptides," *Anal. Bioanal. Chem.*, vol. 382, no. 3, pp. 777–782, Jun. 2005.

[52] C. P. Palmer and H. M. McNair, "Novel pseudostationary phase for micellar electrokinetic capillary chromatography," *J. Microcolumn Sep.*, vol. 4, no. 6, pp. 509–514, Nov. 1992.

[53] C. P. Palmer, M. Y. Khaled, and H. M. McNair, "A monomolecular pseudostationary phase for micellar electrokinetic capillary chromatography," *J. High Resolut. Chromatogr.*, vol. 15, no. 11, pp. 756–762, Nov. 1992.

[54] K. Arai, Y. Maseki, and Y. Ogiwara, "Behavior of poly(sodium 10-undecenoate) as surfactant," *Die Makromol. Chemie, Rapid Commun.*, vol. 8, no. 11, pp. 563–567, Nov. 1987.

[55] K. Arai, J. Sugita, and Y. Ogiwara, "Polymerization of sodium 10-undecenoate under irradiation of UV light," *Die Makromol. Chemie*, vol. 188, no. 11, pp. 2511–2516, Nov. 1987.

[56] D. Y. Chu and J. K. Thomas, "Photophysical characterization of polyelectrolytes in the form of polymerized micelles from an ionic surfactant with a terminal double bond," *Macromolecules*, vol. 24, no. 9, pp. 2212–2216, Apr. 1991.

[57] C. E. Larrabee and E. D. Sprague, "Radiation-induced polymerization of sodium 10-undecenoate in aqueous micelle solutions," *J. Polym. Sci. Polym. Lett. Ed.*, vol. 17, no. 12, pp. 749–751, Dec. 1979.

[58] E. D. Sprague, D. C. Duecker, and C. E. Larrabee, "Association of spin-labeled substrate molecules with poly(sodium 10-undecenoate) and the sodium 10-

undecenoate micelle," *J. Am. Chem. Soc.*, vol. 103, no. 23, pp. 6797–6800, Nov. 1981.

[59]   E. D. Sprague, D. C. Duecker, and C. . Larrabee, "The effect of a terminal double bond on the micellization of a simple ionic surfactant," *J. Colloid Interface Sci.*, vol. 92, no. 2, pp. 416–421, Apr. 1983.

[60]   B. Durairaj and F. D. Blum, "Synthesis and dynamics of oligomeric micelles," *Langmuir*, vol. 5, no. 2, pp. 370–372, Mar. 1989.

[61]   C. M. Paleos, C. I. Stassinopoulou, and A. Malliaris, "Comparative studies between monomeric and polymeric sodium 10-undecenoate micelles," *J. Phys. Chem.*, vol. 87, no. 2, pp. 251–254, Jan. 1983.

[62]   T. W. Moy, P. L. Ferguson, A. H. Grange, W. H. Matchett, V. A. Kelliher, W. C. Brumley, J. Glassman, and J. W. Farley, "Development of separation systems for polynuclear aromatic hydrocarbon environmental contaminants using micellar electrokinetic chromatography with molecular micelles and free zone electrophoresis," *Electrophoresis*, vol. 19, no. 12, pp. 2090–2094, Sep. 1998.

[63]   C. P. Palmer and S. Terabe, "A Novel Sulfate Polymer as a Pseudo-Stationary Phase for Micellar Electrokinetic Chromatography," *J. Microcolumn Sep.*, vol. 8, no. 2, pp. 115–121, 1996.

[64]   C. P. Palmer and S. Terabe, "Micelle Polymers as Pseudostationary Phases in MEKC: Chromatographic Performance and Chemical Selectivity," *Anal. Chem.*, vol. 69, no. 10, pp. 1852–1860, May 1997.

[65]   C. P. Palmer and K. T. Tellman, "Poly(sodium 10-undecylenate) as a pseudo-stationary phase for micellar electrokinetic chromatography: Effects of polymerization initiator," *J. Microcolumn Sep.*, vol. 11, no. 3, pp. 185–191, 1999.

[66]   D. M. Ahlstrom, Y. M. Hoyos, H. Arslan, and C. Akbay, "Binary mixed micelles of chiral sodium undecenyl leucinate and achiral sodium undecenyl sulfate: I. Characterization and application as pseudostationary phases in micellar electrokinetic chromatography.," *J. Chromatogr. A*, vol. 1217, no. 3, pp. 375–85, Jan. 2010.

[67]   C. Akbay and S. A. Shamsi, "Polymeric sulfated surfactants with varied hydrocarbon tail: I. Synthesis, characterization, and application in micellar electrokinetic chromatography," *Electrophoresis*, vol. 25, no. 45, pp. 622–634, Feb. 2004.

[68]   C. Akbay and S. A. Shamsi, "Polymeric sulfated surfactants with varied hydrocarbon tail: II. Chemical selectivity in micellar electrokinetic chromatography using linear solvation energy relationships study," *Electrophoresis*, vol. 25, no. 45, pp. 635–644, Feb. 2004.

[69]   F. H. Billiot, E. J. Billiot, and I. M. Warner, "Comparison of monomeric and polymeric amino acid based surfactants for chiral separations," *J. Chromatogr. A*, vol. 922, no. 1, pp. 329–338, 2001.

[70]   K. T. Tellman and C. P. Palmer, "Polymers of sodium-N-undec-10-ene-1-oyl taurate and sodium-N-undec-10-ene-1-oyl aminoethyl-2-phosphonate as pseudostationary phases for electrokinetic chromatography," *Electrophoresis*, vol. 20, no. 1, pp. 152–161, Jan. 1999.

[71]   S. Hara and A. Dobashi, "No Title," # 92, 149, 205, 1992.

[72]   S. Hara and A. Dobashi, "No Title," # 92, 149, 206, 1992.

[73]   J. Wang and I. M. Warner, "Chiral Separations Using Micellar Electrokinetic Capillary Chromatography and a Polymerized Chiral Micelle," *Anal. Chem.*, vol. 66, no. 21, pp. 3773–3776, Nov. 1994.

[74]   J. Wang and I. M. Warner, "Combined polymerized chiral micelle and γ-cyclodextrin for chiral separation in capillary electrophoresis," *J. Chromatogr. A*, vol. 711, no. 2, pp. 297–304, Sep. 1995.

[75]   B. C. Valle, F. H. Billiot, S. A. Shamsi, X. Zhu, A. M. Powe, and I. M. Warner, "Combination of cyclodextrins and polymeric surfactants for chiral separations," *Electrophoresis*, vol. 25, no. 45, pp. 743–752, Feb. 2004.

[76]   S. A. Shamsi, J. Macossay, and I. M. Warner, "Improved Chiral Separations Using a Polymerized Dipeptide Anionic Chiral Surfactant in Electrokinetic Chromatography: Separations of Basic, Acidic, and Neutral Racemates," *Anal. Chem.*, vol. 69, no. 15, pp. 2980–2987, Aug. 1997.

[77]   E. Billiot, S. Thibodeaux, S. Shamsi, and I. M. Warner, "Evaluating Chiral Separation Interactions by Use of Diastereomeric Polymeric Dipeptide Surfactants," *Anal. Chem.*, vol. 71, no. 18, pp. 4044–4049, Sep. 1999.

[78]   E. Billiot, R. A. Agbaria, S. Thibodeaux, S. Shamsi, and I. M. Warner, "Amino Acid Order in Polymeric Dipeptide Surfactants: Effect on Physical Properties and Enantioselectivity," *Anal. Chem.*, vol. 71, no. 7, pp. 1252–1256, Apr. 1999.

[79]   E. Billiot, J. Macossay, S. Thibodeaux, S. A. Shamsi, and I. M. Warner, "Chiral Separations Using Dipeptide Polymerized Surfactants: Effect of Amino Acid Order," *Anal. Chem.*, vol. 70, no. 7, pp. 1375–1381, Apr. 1998.

[80]   F. Haddadian Billiot, E. J. Billiot, and I. M. Warner, "Depth of penetration of binaphthyl derivatives into the micellar core of sodium undecenoyl leucyl-leucinate surfactants," *J. Chromatogr. A*, vol. 950, no. 1, pp. 233–239, 2002.

[81]   K. A. Agnew-Heard, S. A. Shamsi, and I. M. Warner, "Optimizing enantioseparation of phenylthiohydatoin amino acids with polymerized sodium n-undecanoyl l-valinate in chiral electrokinetic chromatography," *J. Liq. Chromatogr. Relat. Technol.*, vol. 23, no. 9, pp. 1301–1317, May 2000.

[82]   J. K. Rugutt, E. Billiot, and I. M. Warner, "NMR Study of the Interaction of Monomeric and Polymeric Chiral Surfactants with (*R*)- and (*S*)-1,1'-Binaphthyl-2,2'-diyl Hydrogen Phosphate," *Langmuir*, vol. 16, no. 7, pp. 3022–3029, Apr. 2000.

[83]   S. A. Shamsi, B. C. Valle, F. Billiot, and I. M. Warner, "Polysodium *N* -Undecanoyl- l -leucylvalinate: A Versatile Chiral Selector for Micellar Electrokinetic Chromatography," *Anal. Chem.*, vol. 75, no. 3, pp. 379–387, Feb. 2003.

[84]   S. J. Thibodeaux, E. Billiot, E. Torres, B. C. Valle, and I. M. Warner, "Enantiomeric separations using polymeric L-glutamate surfactant derivatives: Effect of increasing steric factors," *Electrophoresis*, vol. 24, no. 6, pp. 1077–1082, Mar. 2003.

[85]   S. J. Thibodeaux, E. Billiot, and I. M. Warner, "Enantiomeric separations using poly(l-valine) and poly(l-leucine) surfactants: Investigation of steric factors near the chiral center," *J. Chromatogr. A*, vol. 966, no. 1, pp. 179–186, 2002.

[86]   H. H. Yarabe, S. A. Shamsi, and I. M. Warner, "Characterization and Thermodynamic Studies of the Interactions of Two Chiral Polymeric Surfactants with Model Substances: Phenylthiohydantoin Amino Acids," *Anal. Chem.*, vol. 71, no. 18, pp. 3992–3999, Sep. 1999.

[87]   W. Lu, S. A. Shamsi, T. D. McCarley, and I. M. Warner, "On-line capillary electrophoresis-electrospray ionization mass spectrometry using a polymerized anionic surfactant," *Electrophoresis*, vol. 19, no. 12, pp. 2193–2199, Sep. 1998.

[88]   S. A. Shamsi, "Micellar Electrokinetic Chromatography−Mass Spectrometry Using a Polymerized Chiral Surfactant," *Anal. Chem.*, vol. 73, no. 21, pp. 5103–5108, Nov. 2001.

[89]   C. Akbay, S. A. A. Rizvi, and S. A. Shamsi, "Simultaneous enantioseparation and tandem UV-MS detection of eight beta-blockers in micellar electrokinetic chromatography using a chiral molecular micelle.," *Anal. Chem.*, vol. 77, no. 6, pp. 1672–83, Mar. 2005.

[90]   J. Hou, S. A. A. Rizvi, J. Zheng, and S. A. Shamsi, "Application of polymeric surfactants in micellar electrokinetic chromatography-electrospray ionization mass spectrometry of benzodiazepines and benzoxazocine chiral drugs.," *Electrophoresis*, vol. 27, no. 5–6, pp. 1263–75, Mar. 2006.

[91]   J. Hou, J. Zheng, S. A. A. Rizvi, and S. A. Shamsi, "Simultaneous chiral separation and determination of ephedrine alkaloids by MEKC-ESI-MS using polymeric surfactant I: method development.," *Electrophoresis*, vol. 28, no. 9, pp. 1352–63, May 2007.

[92]   J. Hou, J. Zheng, and S. A. Shamsi, "Simultaneous chiral separation of ephedrine alkaloids by MEKC-ESI-MS using polymeric surfactant II: application in dietary supplements.," *Electrophoresis*, vol. 28, no. 9, pp. 1426–34, May 2007.

[93]   J. Hou, J. Zheng, and S. A. Shamsi, "Separation and determination of warfarin enantiomers in human plasma using a novel polymeric surfactant for micellar electrokinetic chromatography-mass spectrometry.," *J. Chromatogr. A*, vol. 1159, no. 1–2, pp. 208–16, Aug. 2007.

[94]   J. He and S. A. Shamsi, "Chiral micellar electrokinetic chromatography-atmospheric pressure photoionization of benzoin derivatives using mixed molecular micelles," *Electrophoresis*, vol. 32, no. 10, pp. 1164–1175, May 2011.

[95]   J. He and S. A. Shamsi, "Application of Polymeric Surfactants in Chiral Micellar Electrokinetic Chromatography (CMEKC) and CMEKC Coupled to Mass Spectrometry," 2013, pp. 319–348.

[96]   H. Watarai, "Microemulsion capillary electrophoresis.," *Chem. Lett.*, vol. 20, no. 3, pp. 391–394, 1991.

[97]   S. H. Hansen, "Recent applications of microemulsion electrokinetic chromatography," *Electrophoresis*, vol. 24, no. 2223, pp. 3900–3907, Dec. 2003.

[98]   R. Ryan, S. Donegan, J. Power, E. McEvoy, and K. Altria, "Recent advances in the methodology, optimisation and application of MEEKC," *Electrophoresis*, vol. 30, no. 1, pp. 65–82, Jan. 2009.

[99]   R. Ryan, S. Donegan, J. Power, and K. Altria, "Advances in the theory and application of MEEKC," *Electrophoresis*, vol. 31, no. 5, pp. 755–767, Mar. 2010.

[100]   R. Ryan, E. McEvoy, J. Sheila Donegan, J. Power, and K. Altria, "Recent

developments in the methodology and application of MEEKC," *Electrophoresis*, vol. 32, no. 1, pp. 184–201, Jan. 2011.

[101] R. Ryan, K. Altria, E. Mcevoy, S. Donegan, and J. Power, "A review of developments in the methodology and application of microemulsion electrokinetic chromatography," *Electrophoresis*, vol. 34, no. 1. pp. 159–177, 2013.

[102] K. Altria, M. Broderick, S. Donegan, and J. Power, "Preliminary Study on the Use of Water-in-Oil Microemulsion Eluents in HPLC," *Chromatographia*, vol. 62, no. 7–8, pp. 341–348, Oct. 2005.

[103] T. Wen, X. Zhao, G. Luo, Y. Wang, J. Wang, J. Zhu, and Z. Yu, "Comparison of the performance of microemulsion electrokinetic chromatography and 1-butanol modified micellar electrokinetic chromatography on the separations of amphetamine and it's ephedra alkaloid impurities," *Chinese J. Anal. Chem.*, vol. 34, no. 11, pp. 1529–1534, 2006.

[104] T. Wen, X. Zhao, G. Luo, J. Wang, Y. Wang, B. Yao, J. Zhao, J. Zhu, and Z. Yu, "Comparison of microemulsion electrokinetic chromatography and solvent modified micellar electrokinetic chromatography on rapid separation of heroin, amphetamine and their basic impurities," *Talanta*, vol. 71, no. 2, pp. 854–860, 2007.

[105] X. Yang, Y. Xia, C. Tao, Y. Liao, Y. Zuo, and H. Liu, "A comparative study of micellar and microemulsion EKC for the analysis of benzoylurea insecticides and their analogs," *Electrophoresis*, vol. 28, no. 11, pp. 1744–1751, Jun. 2007.

[106] K. D. Altria, "Background theory and applications of microemulsion electrokinetic chromatography," *J. Chromatogr. A*, vol. 892, no. 1, pp. 171–186, 2000.

[107] P. E. Mahuzier, M. S. A. Prado, B. J. Clark, E. R. M. Kedor-Hackmann, and K. D. Altria, "An introduction to the theory and application of microemulsion electrokinetic chromatography," *Lc Gc Eur.*, vol. 16, no. 1, p. 22–+, 2003.

[108] P.-E. Mahuzier, B. J. Clark, S. M. Bryant, and K. D. Altria, "High-speed microemulsion electrokinetic chromatography," *Electrophoresis*, vol. 22, no. 17, pp. 3819–3823, Sep. 2001.

[109] I. Mikšík and Z. Deyl, "Microemulsion electrokinetic chromatography of fatty acids as phenacyl esters," *J. Chromatogr. A*, vol. 807, no. 1, pp. 111–119, 1998.

[110] M. Haunschmidt, K. Ortner, K. Hainz, E. Bradt, L. Sternbauer, W. Buchberger, and C. W. Klampfl, "Investigations on the migration behavior of insulin and related synthetic analogues in CZE, MEKC and MEEKC employing different surfactants," *Electrophoresis*, vol. 31, no. 9, pp. 1560–1564, Mar. 2010.

[111] R. L. Boso, M. S. Bellini, I. Mikšík, and Z. Deyl, "Microemulsion electrokinetic chromatography with different organic modifiers: separation of water- and lipid-soluble vitamins," *J. Chromatogr. A*, vol. 709, no. 1, pp. 11–19, Aug. 1995.

[112] Y. Ishihama, Y. Oda, K. Uchikawa, and N. Asakawa, "Evaluation of Solute Hydrophobicity by Microemulsion Electrokinetic Chromatography," *Anal. Chem.*, vol. 67, no. 9, pp. 1588–1595, 2002.

[113] H. Watarai and I. Takahashi, "Comparison of three different microemulsion systems as the run buffer for the capillary electrophoretic separation of ketone test solutes," *Anal. Commun.*, vol. 35, no. 9, pp. 289–292, 1998.

[114] M. F. Miola, M. J. Snowden, and K. D. Altria, "The use of microemulsion

electrokinetic chromatography in pharmaceutical analysis," *J. Pharm. Biomed. Anal.*, vol. 18, no. 4, pp. 785–797, 1998.

[115] S. J. Gluck, M. H. Benkö, R. K. Hallberg, and K. P. Steele, "Indirect determination of octanol-water partition coefficients by microemulsion electrokinetic chromatography," *J. Chromatogr. A*, vol. 744, no. 1–2, pp. 141–146, Sep. 1996.

[116] H. Watarai, "Microemulsions in separation sciences," *J. Chromatogr. A*, vol. 780, no. 1–2, pp. 93–102, Sep. 1997.

[117] K. . Altria, "Application of microemulsion electrokinetic chromatography to the analysis of a wide range of pharmaceuticals and excipients," *J. Chromatogr. A*, vol. 844, no. 1, pp. 371–386, 1999.

[118] H. Watarai, K. Ogawa, M. Abe, T. Monta, and I. Takahashi, "Capillary Electrophoresis with O/W Microemulsions of water/SDS/1-butanol/heptane," *Anal. Sci.*, vol. 7, no. Supple, pp. 245–248, 1991.

[119] R. Szücs, E. Van Hove, and P. Sandra, "Micellar and microemulsion electrokinetic chromatography of hop bitter acids," *J. High Resolut. Chromatogr.*, vol. 19, no. 4, pp. 189–192, Apr. 1996.

[120] X. Fu, J. Lu, and A. Zhu, "Microemulsion elektrokinetic chromatographic separation of antipyretic analgesic ingredients," *J. Chromatogr. A*, vol. 735, no. 1–2, pp. 353–356, May 1996.

[121] J. H. Aiken and C. W. Huie, "Use of a microemulsion system to incorporate a lipophilic chiral selector in electrokinetic capillary chromatography," *Chromatographia*, vol. 35, no. 7–8, pp. 448–450, Apr. 1993.

[122] L. Song, Q. Ou, W. Yu, and G. Li, "Separation of six phenylureas and chlorsulfuron standards by micellar, mixed micellar and microemulsion electrokinetic chromatography," *J. Chromatogr. A*, vol. 699, no. 1–2, pp. 371–382, May 1995.

[123] N. Gorski, M. Gradzielski, and H. Hoffmann, "The influence of ionic charges on the structural and dynamical behavior of O/W microemulsion droplets," *Berichte der Bunsengesellschaft für Phys. Chemie*, vol. 100, no. 7, pp. 1109–1117, Jul. 1996.

[124] G.-H. Zhou, G.-A. Luo, and X.-D. Zhang, "Microemulsion electrokinetic chromatography of proteins," *J. Chromatogr. A*, vol. 853, no. 1, pp. 277–284, 1999.

[125] S. Terabe, H. Ozaki, and Y. Tanaka, "New Pseudostationary Phases for Electrokinetic Chromatography: A High-Molecular Surfactant and Proteins," *J. Chinese Chem. Soc.*, vol. 41, no. 3, pp. 251–257, Jun. 1994.

[126] H. Ozaki, S. Terabe, and A. Ichihara, "Micellar electrokinetic chromatography using high-molecular surfactants use of butyl acrylate-butyl methacrylate-methacrylic acid copolymers sodium salts as pseudo-stationary phases," *J. Chromatogr. A*, vol. 680, no. 1, pp. 117–123, Sep. 1994.

[127] H. Ozaki, A. Ichihara, and S. Terabe, "Micellar electrokinetic chromatography using high-molecular-mass surfactants: comparison between anionic and cationic surfactants and effects of modifiers," *J. Chromatogr. A*, vol. 709, no. 1, pp. 3–10, Aug. 1995.

[128] H. Ozaki, N. Itou, S. Terabe, Y. Takada, M. Sakairi, and H. Koizumi, "Micellar

electrokinetic chromatography—mass spectrometry using a high-molecular-mass surfactant on-line coupling with an electrospray ionization interface," *J. Chromatogr. A*, vol. 716, no. 1–2, pp. 69–79, Nov. 1995.

[129] S. Yang, J. G. Bumgarner, and M. G. Khaledi, "Separation of highly hydrophobic compounds in MEKC with an ionic polymer," *J. High Resolut. Chromatogr.*, vol. 18, no. 7, pp. 443–445, Jul. 1995.

[130] S. Yang, J. G. Bumgarner, and M. G. Khaledi, "Chemical selectivity in micellar electrokinetic chromatography II. Rationalization of elution patterns in different surfactant systems," *J. Chromatogr. A*, vol. 738, no. 2, pp. 265–274, Jul. 1996.

[131] S. K. Wiedmer, H. Tenhu, P. Vastamäki, and M.-L. Riekkola, "Elvacite 2669 as pseudostationary phase: Electrokinetic capillary chromatography and light scattering study," *J. Microcolumn Sep.*, vol. 10, no. 7, pp. 557–565, 1998.

[132] C. P. Palmer, "No Title," in *9th International Symposium on HPCE*, 1997.

[133] C. P. Palmer, C. J. Watson, W. Shi, and K. T. Tellman, "Performance and Selectivity of Polymeric Pseudo-Stationary Phases for Electrokinetic Chromatography," in *International Symposium on Capillary Chromatography and Electrophoresis*, 1999.

[134] W. Shi, D. S. Peterson, and C. P. Palmer, "Effect of pendant chain lengths and backbone functionalities on the chemical selectivity of sulfonated amphiphilic copolymers as pseudo-stationary phases in electrokinetic chromatography," *J. Chromatogr. A*, vol. 924, no. 1–2, pp. 123–135, Jul. 2001.

[135] W. Shi and C. P. Palmer, "On-column sample preconcentration in electrokinetic chromatography by sweeping with polymeric pseudo-stationary phases," *J. Sep. Sci.*, vol. 25, no. 4, pp. 215–221, Mar. 2002.

[136] W. Shi, C. J. Watson, and C. P. Palmer, "Sulfonated acrylamide copolymers as pseudo-stationary phases in electrokinetic chromatography," *J. Chromatogr. A*, vol. 905, no. 1, pp. 281–290, 2001.

[137] W. Shi and C. P. Palmer, "High-speed separations by electrokinetic chromatography using polymeric pseudostationary phases," *J. Sep. Sci.*, vol. 25, no. 8, pp. 543–546, Jun. 2002.

[138] W. Shi and C. P. Palmer, "Effect of pendent group structures on the chemical selectivity and performance of sulfonated copolymers as novel pseudophases in electrokinetic chromatography," *Electrophoresis*, vol. 23, no. 9, pp. 1285–1295, May 2002.

[139] P. Řezanka, K. Navrátilová, M. Řezanka, V. Král, and D. Sýkora, "Application of cyclodextrins in chiral capillary electrophoresis," *Electrophoresis*, vol. 35, no. 19, pp. 2701–2721, Oct. 2014.

[140] K. A. Kahle and J. P. Foley, "Two-chiral-component microemulsion electrokinetic chromatography–chiral surfactant and chiral oil: Part 1. Dibutyl tartrate," *Electrophoresis*, vol. 28, no. 11, pp. 1723–1734, Jun. 2007.

[141] Z. Juvancz and J. Szejtli, "The role of cyclodextrins in chiral selective chromatography," *TrAC Trends Anal. Chem.*, vol. 21, no. 5, pp. 379–388, 2002.

[142] C.-E. Lin, H.-T. Cheng, I.-J. Fang, Y.-C. Liu, C.-M. Kuo, W.-Y. Lin, and C.-H. Lin, "Strategies for enantioseparations of catecholamines and structurally related compounds by capillary zone electrophoresis using sulfated β-cyclodextrins as

chiral selectors," *Electrophoresis*, vol. 27, no. 17, pp. 3443–3451, Sep. 2006.

[143] U. Schmitt, S. K. Branch, and U. Holzgrabe, "Chiral separations by cyclodextrin-modified capillary electrophoresis - Determination of the enantiomeric excess," *J. Sep. Sci.*, vol. 25, no. 15–17, pp. 959–974, Nov. 2002.

[144] T. Sokoließ and G. Köller, "Approach to method development and validation in capillary electrophoresis for enantiomeric purity testing of active basic pharmaceutical ingredients," *Electrophoresis*, vol. 26, no. 12, pp. 2330–2341, Jun. 2005.

[145] H. Ates, D. Mangelings, and Y. Vander Heyden, "Fast generic chiral separation strategies using electrophoretic and liquid chromatographic techniques," *J. Pharm. Biomed. Anal.*, vol. 48, no. 2, pp. 288–294, 2008.

[146] A. G. Wallingford, R. A., Ewing, "No Title," *Adv. Chromatogr.*, vol. 29, pp. 65–67, 1989.

[147] C. P. Palmer, K. Hancock, H. . McNair, W. Tyndall, and S. Morris, "No Title," in *15th International Symposium on Capillary Chromatography*, 1993.

[148] L. Schweitz, P. Spégel, and S. Nilsson, "Molecularly imprinted microparticles for capillary electrochromatographic enantiomer separation of propranolol," *Analyst*, vol. 125, no. 11, pp. 1899–1901, 2000.

[149] P. Spégel, L. Schweitz, and S. Nilsson, "Molecularly imprinted microparticles for capillary electrochromatography: Studies on microparticle synthesis and electrolyte composition," *Electrophoresis*, vol. 22, no. 17, pp. 3833–3841, Sep. 2001.

[150] P. Viberg, M. Jornten-Karlsson, P. Petersson, P. Spégel, and S. Nilsson, "Nanoparticles as Pseudostationary Phase in Capillary Electrochromatography/ESI-MS," *Anal. Chem.*, vol. 74, no. 18, pp. 4595–4601, Sep. 2002.

[151] T. de Boer, R. Mol, R. A. de Zeeuw, G. J. de Jong, D. C. Sherrington, P. A. G. Cormack, and K. Ensing, "Spherical molecularly imprinted polymer particles: A promising tool for molecular recognition in capillary electrokinetic separations," *Electrophoresis*, vol. 23, no. 9, pp. 1296–1300, May 2002.

[152] P. Spégel, L. Schweitz, and S. Nilsson, "Selectivity toward Multiple Predetermined Targets in Nanoparticle Capillary Electrochromatography," *Anal. Chem.*, vol. 75, no. 23, pp. 6608–6613, 2003.

[153] P. Spégel, P. Viberg, J. Carlstedt, P. Petersson, and M. Jörntén-Karlsson, "Continuous full filling capillary electrochromatography: Nanoparticle synthesis and evaluation," *J. Chromatogr. A*, vol. 1154, no. 1, pp. 379–385, 2007.

[154] P. Viberg, P. Spégel, J. Carlstedt, M. Jörntén-Karlsson, and P. Petersson, "Continuous full filling capillary electrochromatography: Chromatographic performance and reproducibility," *J. Chromatogr. A*, vol. 1154, no. 1, pp. 386–389, 2007.

[155] C. Nilsson and S. Nilsson, "Nanoparticle-based pseudostationary phases in capillary electrochromatography.," *Electrophoresis*, vol. 27, no. 1, pp. 76–83, Jan. 2006.

[156] C. Nilsson, P. Viberg, P. Spégel, M. Jörntén-Karlsson, P. Petersson, and S. Nilsson, "Nanoparticle-based continuous full filling capillary

electrochromatography/electrospray ionization-mass spectrometry for separation of neutral compounds.," *Anal. Chem.*, vol. 78, no. 17, pp. 6088–95, Sep. 2006.

[157] C. P. Palmer, E. F. Hilder, J. P. Quirino, and P. R. Haddad, "Electrokinetic chromatography and mass spectrometric detection using latex nanoparticles as a pseudostationary phase.," *Anal. Chem.*, vol. 82, no. 10, pp. 4046–54, May 2010.

[158] C. P. Palmer, A. Keeffer, E. F. Hilder, and P. R. Haddad, "Retention behavior and selectivity of a latex nanoparticle pseudostationary phase for electrokinetic chromatography.," *Electrophoresis*, vol. 32, no. 5, pp. 588–94, Feb. 2011.

[159] A. Umansky, "AB DIBLOCK COPOLYMER NANOPARTICLES VIA RAFT-MEDIATED POLYMERIZATION AS A PSEUDOSTATIONARY PHASE FOR ELECTROKINETIC CHROMATOGRAPHY," Jun. 2013.

[160] J. S. Hyslop, L. M. G. Hall, A. A. Umansky, and C. P. Palmer, "RAFT polymerized nanoparticles: influences of shell and core chemistries on performance for electrokinetic chromatography.," *Electrophoresis*, vol. 35, no. 5, pp. 728–35, Mar. 2014.

[161] J. Chiefari, Y. K. (Bill) Chong, F. Ercole, J. Krstina, J. Jeffery, T. P. T. Le, R. T. A. Mayadunne, G. F. Meijs, C. L. Moad, G. Moad, E. Rizzardo, and S. H. Thang, "Living Free-Radical Polymerization by Reversible Addition−Fragmentation Chain Transfer: The RAFT Process," *Macromolecules*, vol. 31, no. 16, pp. 5559–5562, Aug. 1998.

[162] G. Moad, E. Rizzardo, and S. H. Thang, "Living Radical Polymerization by the RAFT Process—A First Update," *Aust. J. Chem.*, vol. 59, no. 10, p. 669, 2006.

[163] G. Moad, E. Rizzardo, and S. H. Thang, "Living Radical Polymerization by the RAFT Process – A Second Update," *Aust. J. Chem.*, vol. 62, no. 11, p. 1402, 2009.

[164] G. Moad, E. Rizzardo, S. H. Thang, and Et al., "Living Radical Polymerization by the RAFT Process - A Third Update," *Aust. J. Chem.*, vol. 65, no. 8, p. 985, 2012.

[165] H. Mori, "Living Radical Polymerization: Reversible Addition-Fragmentation Chain Transfer (RAFT) Polymerization," in *Encyclopedia of Polymeric Nanomaterials*, Berlin, Heidelberg: Springer Berlin Heidelberg, 2014, pp. 1–9.

[166] Sigma-Aldrich Co. LLC., "RAFT: Choosing the Right Agent to Achieve Controlled Polymerization." [Online]. Available: http://www.sigmaaldrich.com/materials-science/polymer-science/raft-polymerization.html. [Accessed: 13-Jun-2016].

[167] C. Barner-Kowollik, Ed., *Handbook of RAFT Polymerization*. Weinheim, Germany: Wiley-VCH Verlag GmbH & Co. KGaA, 2008.

[168] B. Maillard, K. U. Ingold, and J. C. Scaiano, "Rate constants for the reactions of free radicals with oxygen in solution," *J. Am. Chem. Soc.*, vol. 105, no. 15, pp. 5095–5099, 1983.

[169] J. M. O'Donnell, "Reversible addition-fragmentation chain transfer polymerization in microemulsion," *Chem. Soc. Rev.*, vol. 41, no. 8, p. 3061, 2012.

[170] S. Bon, "bonlabTV," 2015. [Online]. Available: https://www.youtube.com/playlist?list=PL249969D6F103CB4B. [Accessed: 15-Jun-2016].

[171] F. J. Schork, Y. Luo, W. Smulders, J. P. Russum, A. Butté, and K. Fontenot, "Miniemulsion Polymerization," Springer Berlin Heidelberg, 2005, pp. 129–255.

[172] M. Semsarilar and S. Perrier, "'Green' reversible addition-fragmentation chain-transfer (RAFT) polymerization," *Nat. Chem.*, vol. 2, no. 10, pp. 811–820, Oct. 2010.

[173] C. J. Ferguson, R. J. Hughes, D. Nguyen, B. T. T. Pham, R. G. Gilbert, A. K. Serelis, C. H. Such, and B. S. Hawkett, "Ab Initio Emulsion Polymerization by RAFT-Controlled Self-Assembly §," *Macromolecules*, vol. 38, no. 6, pp. 2191–2204, Mar. 2005.

[174] C. L. McCormick and A. B. Lowe, "Aqueous RAFT Polymerization: Recent Developments in Synthesis of Functional Water-Soluble (Co)polymers with Controlled Structures [†]," *Acc. Chem. Res.*, vol. 37, no. 5, pp. 312–325, May 2004.

[175] B. S. Sumerlin, M. S. Donovan, Y. Mitsukami, A. B. Lowe, and C. L. McCormick, "Water-Soluble Polymers. 84. Controlled Polymerization in Aqueous Media of Anionic Acrylamido Monomers via RAFT," *Macromolecules*, vol. 34, no. 19, pp. 6561–6564, Sep. 2001.

[176] D. E. Ganeva, E. Sprong, H. de Bruyn, G. G. Warr, C. H. Such, and B. S. Hawkett, "Particle Formation in ab Initio RAFT Mediated Emulsion Polymerization Systems," *Macromolecules*, vol. 40, no. 17, pp. 6181–6189, Aug. 2007.

[177] E. Uliyanchenko, S. van der Wal, and P. J. Schoenmakers, "Challenges in polymer analysis by liquid chromatography," *Polym. Chem.*, vol. 3, no. 9, pp. 2313–2335, 2012.

[178] M. Jacquin, P. Muller, G. Lizarraga, C. Bauer, H. Cottet, and O. Théodoly, "Characterization of Amphiphilic Diblock Copolymers Synthesized by MADIX Polymerization Process," *Macromolecules*, vol. 40, no. 8, pp. 2672–2682, Apr. 2007.

[179] P. Castignolles, M. Gaborieau, E. F. Hilder, E. Sprong, C. J. Ferguson, and R. G. Gilbert, "High-Resolution Separation of Oligo(acrylic acid) by Capillary Zone Electrophoresis," *Macromol. Rapid Commun.*, vol. 27, no. 1, pp. 42–46, Jan. 2006.

[180] P. Castignolles and M. Gaborieau, "Viscosimetric detection in size-exclusion chromatography (SEC/GPC): The Goldwasser method and beyond," *J. Sep. Sci.*, vol. 33, no. 22, pp. 3564–3570, Nov. 2010.

[181] M. Gaborieau, R. Graf, and H. W. Spiess, "Investigation of Chain Dynamics in Poly(*n* -alkyl methacrylate)s by Solid-State NMR: Comparison with Poly(*n* -alkyl acrylate)s," *Macromol. Chem. Phys.*, vol. 209, no. 20, pp. 2078–2086, Oct. 2008.

[182] M. W. F. Nielen, "Maldi time-of-flight mass spectrometry of synthetic polymers," *Mass Spectrom. Rev.*, vol. 18, no. 5, pp. 309–344, 1999.

[183] G. Montaudo, F. Samperi, and M. S. Montaudo, "Characterization of synthetic polymers by MALDI-MS," *Prog. Polym. Sci.*, vol. 31, no. 3, pp. 277–357, Mar. 2006.

[184] N. A. Mautjana and H. Pasch, "Matrix-Assisted Laser Desorption Ionization Mass Spectrometry of Synthetic Polymers," *Macromol. Symp.*, vol. 313–314, no. 1, pp. 157–161, Mar. 2012.

[185] P. O. Danis and D. E. Karr, "Analysis of Poly(styrenesulfonic acid) by Matrix-Assisted Laser Desorption/Ionization Time-of-Flight Mass Spectrometry," *Macromolecules*, vol. 28, no. 25, pp. 8548–8551, Dec. 1995.

[186] R. Arakawa, S. Watanabe, and T. Fukuo, "Effects of sample preparation on

matrix-assisted laser desorption/ionization time-of-flight mass spectra for sodium polystyrene sulfonate," *Rapid Commun. Mass Spectrom.*, vol. 13, no. 11, pp. 1059–1062, Jun. 1999.

[187] D. C. Schriemer and L. Li, "Mass Discrimination in the Analysis of Polydisperse Polymers by MALDI Time-of-Flight Mass Spectrometry. 2. Instrumental Issues," *Anal. Chem.*, vol. 69, no. 20, pp. 4176–4183, Oct. 1997.

[188] D. C. Schriemer and L. Li, "Mass Discrimination in the Analysis of Polydisperse Polymers by MALDI Time-of-Flight Mass Spectrometry. 1. Sample Preparation and Desorption/Ionization Issues," *Anal. Chem.*, vol. 69, no. 20, pp. 4169–4175, Oct. 1997.

[189] P. Hommerson, A. M. Khan, G. J. de Jong, and G. W. Somsen, "Capillary Electrophoresis-Atmospheric Pressure Chemical Ionization-Mass Spectrometry Using an Orthogonal Interface: Set-Up and System Parameters," *J. Am. Soc. Mass Spectrom.*, vol. 20, no. 7, pp. 1311–1318, 2009.

[190] M. M. Bushey and J. W. Jorgenson, "Separation of dansylated methylamine and dansylated methyl-d3-amine by micellar electrokinetic capillary chromatography with methanol-modified mobile phase," *Anal. Chem.*, vol. 61, no. 5, pp. 491–493, Mar. 1989.

[191] W. Faubel, S. Heissler, and U. Pyell, *Electrokinetic Chromatography*. Chichester, UK: John Wiley & Sons, Ltd, 2006.

[192] C. F. Poole, S. K. Poole, and M. H. Abraham, "Recommendations for the determination of selectivity in micellar electrokinetic chromatography," *J. Chromatogr. A*, vol. 798, no. 1–2, pp. 207–222, Mar. 1998.

[193] A. T. Sutton, "Characterisation of double hydrophilic block copolymers," University of Western Sydney, 2014.

[194] J. C. Giddings, "Maximum number of components resolvable by gel filtration and other elution chromatographic methods," *Anal. Chem.*, vol. 39, no. 8, pp. 1027–1028, Jul. 1967.

[195] S. Slomkowski, J. V. Alemán, R. G. Gilbert, M. Hess, K. Horie, R. G. Jones, P. Kubisa, I. Meisel, W. Mormann, S. Penczek, and R. F. T. Stepto, "Terminology of polymers and polymerization processes in dispersed systems (IUPAC Recommendations 2011)," *Pure Appl. Chem.*, vol. 83, no. 12, pp. 2229–2259, Jan. 2011.

[196] M. Sakurai, T. Imai, F. Yamashita, K. Nakamura, T. Komatsu, and late T. Nakagawa, "Temperature Dependence of Viscosities and Potentiometric Titration Behavior of Aqueous Poly(acrylic acid) and Poly(methacrylic acid) Solutions," *Polym. J.*, vol. 25, no. 12, pp. 1247–1255, Dec. 1993.

[197] B. A. Abel and C. L. McCormick, "Mechanistic Insights into Temperature-Dependent Trithiocarbonate Chain-End Degradation during the RAFT Polymerization of N-Arylmethacrylamides," *Macromolecules*, vol. 49, no. 2, pp. 465–478, 2016.

[198] M. Muthukumar, "Theory of electrophoretic mobility of a polyelectrolyte in semidilute solutions of neutral polymers," *Electrophoresis*, vol. 17, no. 6, pp. 1167–1172, 1996.

[199] D. Long, J.-L. Viovy, and A. Ajdari, "Simultaneous Action of Electric Fields and

Nonelectric Forces on a Polyelectrolyte: Motion and Deformation," *Phys. Rev. Lett.*, vol. 76, no. 20, pp. 3858–3861, May 1996.

[200] J.-L. Barrat and F. Joanny, "Theory of Polyelectrolyte Solutions," in *Polymeric Systems*, 1st ed., John Wiley & Sons, Inc., 2007, pp. 1–66.

[201] E. S. Ahuja, K. R. Nielsen, J. P. Foley, and E. L. Little, "Infinite Elution Range in Micellar Electrokinetic Capillary Chromatography Using a Nonionic/Anionic Mixed Micellar System," *Anal. Chem.*, vol. 67, no. 1, pp. 26–33, Jan. 1995.

[202] J. P. Foley, "Optimization of micellar electrokinetic chromatography," *Anal. Chem.*, vol. 62, no. 13, pp. 1302–1308, Jul. 1990.

[203] Y. Williamson and J. M. Davis, "Modeling of anti-Langmuirian peaks in micellar electrokinetic chromatography: benzene and naphthalene.," *Electrophoresis*, vol. 26, no. 21, pp. 4026–42, Nov. 2005.

[204] Y. Williamson and J. M. Davis, "Origin of peak asymmetry and isotherm nonlinearity in micellar electrokinetic chromatography: variation of peak shape with buffer concentration.," *Electrophoresis*, vol. 27, no. 3, pp. 572–83, Feb. 2006.

[205] K. W. Smith and J. M. Davis, "Quantitative Study of Concentration Overload, Peak Asymmetry, and Efficiency Loss in Micellar Electrokinetic Chromatography," *Anal. Chem.*, vol. 74, no. 23, pp. 5969–5981, Dec. 2002.

[206] J. M. Davis, "Dispersion in micellar electrokinetic chromatography," *Adv. Chromatogr. (New York)*, vol. 40, pp. 115–157, 2000.

[207] L. Yu and J. M. Davis, "Study of high-field dispersion in micellar electrokinetic chromatography," *Electrophoresis*, vol. 16, no. 1, pp. 2104–2120, 1995.

[208] Agilent Technologies, "Evaluating System Suitability CE, GC, LC and A/D ChemStation Revisions: A Evaluating System Suitability." pp. 1–17.

[209] S. K. Poole and C. F. Poole, "Characterization of Surfactant Selectivity in Micellar Electrokinetic Chromatography," *Analyst*, vol. 122, no. 3, pp. 267–274, Jan. 1997.

[210] R. Pascoe and J. P. Foley, "Effect of class I and II organic modifiers on retention and selectivity in vesicle electrokinetic chromatography.," *Electrophoresis*, vol. 23, no. 11, pp. 1618–27, Jun. 2002.

[211] M. H. Abraham and J. C. McGowan, "The use of characteristic volumes to measure cavity terms in reversed phase liquid chromatography," *Chromatographia*, vol. 23, no. 4, pp. 243–246, Apr. 1987.

[212] M. H. Abraham, "Scales of solute hydrogen-bonding: their construction and application to physicochemical and biochemical processes," *Chem. Soc. Rev.*, vol. 22, no. 2, p. 73, Jan. 1993.

[213] M. H. Abraham, M. H. Abraham, A. Ibrahim, and A. M. Zissimos, "Determination of sets of solute descriptors from chromatographic measurements," *J. Chromatogr. A*, vol. 1037, no. 1–2, pp. 29–47, May 2004.

[214] A. M. Zissimos, M. H. Abraham, M. C. Barker, K. J. Box, and K. Y. Tam, "Calculation of Abraham descriptors from solvent–water partition coefficients in four different systems; evaluation of different methods of calculation," *J. Chem. Soc. Perkin Trans. 2*, no. 3, pp. 470–477, Feb. 2002.

[215] P. Hommerson, A. M. Khan, G. J. de Jong, and G. W. Somsen, "Ionization techniques in capillary electrophoresis-mass spectrometry: Principles, design, and application," *Mass Spectrom. Rev.*, vol. 30, no. 6, pp. 1096–1120, Nov. 2011.

[216] J. A. Gladysz, D. P. Curran, and I. T. Horváth, Eds., *Handbook of Fluorous Chemistry*. Weinheim, FRG: Wiley-VCH Verlag GmbH & Co. KGaA, 2004.

[217] M. Beiner, "Relaxation in Poly(alkyl methacrylate)s: Crossover Region and Nanophase Separation," *Macromol. Rapid Commun.*, vol. 22, no. 12, pp. 869–895, Aug. 2001.

[218] P. Castignolles, R. Graf, M. Parkinson, M. Wilhelm, and M. Gaborieau, "Detection and quantification of branching in polyacrylates by size-exclusion chromatography (SEC) and melt-state 13C NMR spectroscopy," *Polymer (Guildf).*, vol. 50, no. 11, pp. 2373–2383, 2009.

[219] M. Gaborieau, R. Graf, S. Kahle, T. Pakula, and H. W. Spiess, "Chain Dynamics in Poly(*n* -alkyl acrylates) by Solid-State NMR, Dielectric, and Mechanical Spectroscopies," *Macromolecules*, vol. 40, no. 17, pp. 6249–6256, Aug. 2007.

Chapter 8 Appendices
Appendix A - LSER
Parameters

Peak	Solute	V	E	S	α	β
21	1-methylnapthalene	1.226	1.344	0.9	0	0.2
16	1-Napthol	1.1441	1.52	1.08	0.61	0.4
	3,5-Dimethylphenol	1.057	0.82	0.84	0.57	0.36
	3-Bromophenol	0.95	1.06	1.15	0.7	0.16
11	3-Chlorophenol	0.898	0.909	1.06	0.69	0.15
	3-methyl benzyl Alcohol	1.057	0.815	0.9	0.33	0.59
	4-Bromophenol	0.95	1.08	1.17	0.67	0.2
	4-Chloroacetophenone	1.136	0.955	1.09	0	0.44
	4-Chloroaniline	0.939	1.06	1.13	0.3	0.31
10	4-Chlorophenol	0.898	0.915	1.08	0.67	0.2
	4-Chlorotoluene	0.98	0.705	0.67	0	0.07
9	4-ethylphenol	1.057	0.8	0.9	0.55	0.36
	4-fluorophenol	0.793	0.67	0.97	0.63	0.23
6	4-nitroaniline	0.9904	1.22	1.91	0.42	0.38
	4-Nitrotoluene	1.032	0.87	1.11	0	0.28
4	Acetophenone	1.014	0.818	1.01	0	0.48
	Anisole	0.916	0.708	0.75	0	0.29
	Benzene	0.716	0.61	0.52	0	0.14
5	Benzonitrile	0.871	0.742	1.11	0	0.33
2	Benzyl Alcohol	0.916	0.803	0.87	0.33	0.56
	biphenyl	1.324	1.36	0.99	0	0.22
15	Chlorobenzene	0.839	0.718	0.65	0	0.07
	Ethylbenzene	0.998	0.613	0.51	0	0.15
	Ethylbenzoate	1.214	0.689	0.85	0	0.46
12	Indole	0.946	1.2	1.12	0.44	0.22
18	Iodebenzene	0.975	1.188	0.82	0	0.12
	M-Cresol	0.916	0.822	0.88	0.57	0.34
	Methyl benzoate	1.073	0.733	0.85	0	0.46
14	Methyl-o-toluate	1.214	0.772	0.87	0	0.43
19	Napthalene	1.085	1.36	0.92	0	0.2
7	Nitrobenzene	0.891	0.871	1.11	0	0.28
	p-Cresol	0.916	0.82	0.87	0.57	0.31
3	Phenol	0.775	0.805	0.89	0.6	0.3
	Phenyl Acetate	1.073	0.661	1.13	0	0.54
8	propiophenone	1.155	0.804	0.95	0	0.51
20	Propylbenzene	1.139	0.604	0.5	0	0.15
17	p-Xylene	0.998	0.613	0.52	0	0.16
	Resorcinol	0.834	0.98	1	1.1	0.58
13	Toluene	0.857	0.601	0.52	0	0.14
1	Acetone	N/A	N/A	N/A	N/A	N/A
22	Hexanophenone	N/A	N/A	N/A	N/A	N/A

Figure 71 Thirty nine solutes and LSER solute descriptors and retention order in Figure 70.

8-137

Structures

4-nitroaniline
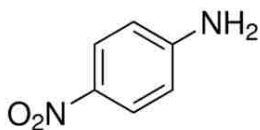
4-Chloroaniline
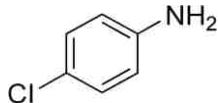
3-Chlorophenol
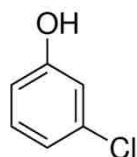
3-Bromophenol
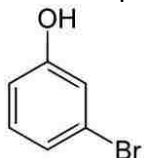
4-Bromophenol
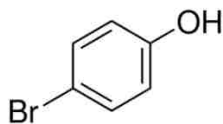
1-Naphthol
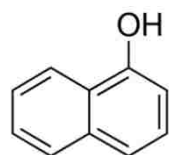
Resorcinol
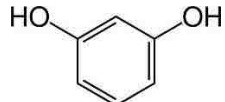
4-Chlorophenol
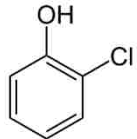
Phenol
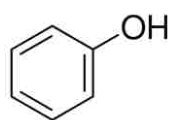
4-fluorophenol
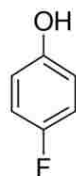
m-Cresol
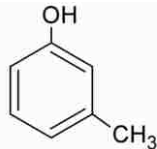
3,5-Dimethylphenol
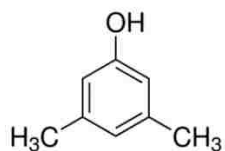
p-Cresol
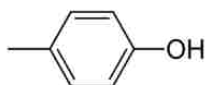
4-ethylphenol
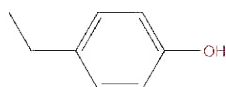
Benzyl Alcohol
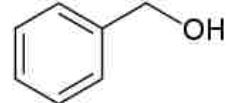
3-methyl benzyl Alcohol
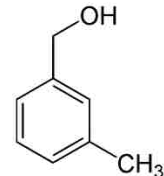
Indole
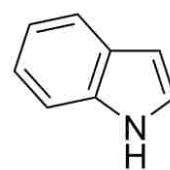
Ethylbenzoate
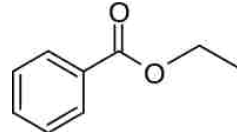
Benzene

p-Xylene
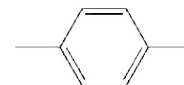
Methyl benzoate

Toluene

Anisole

Chlorobenzene
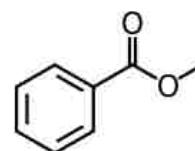
Ethylbenzene
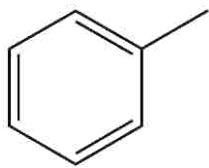
Biphenyl

Iodebenzene

4-Chlorotoluene
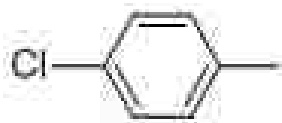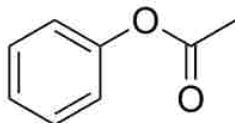
Acetophenone
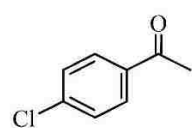
Benzonitrile

Phenyl Acetate
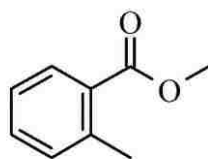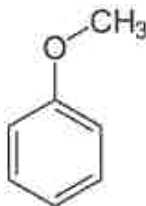
Propiophenone
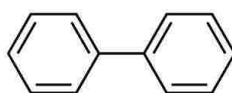
4-Nitrotoluene
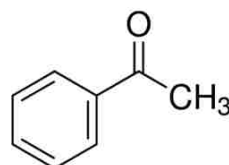
4-Chloroacetophenone

Propylbenzene
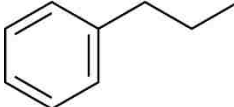
Napthalene
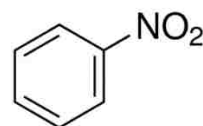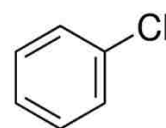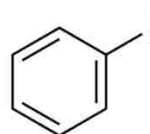
Methyl-o-toluate

Nitrobenzene

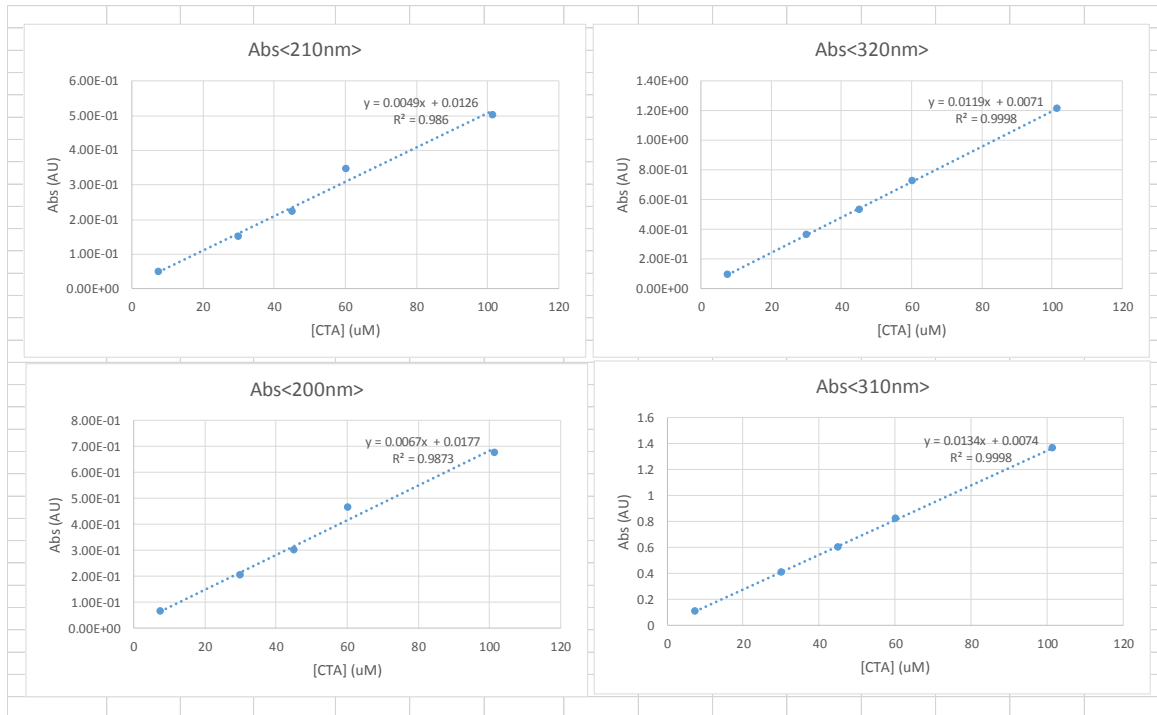1-methylnapthalene

8-139
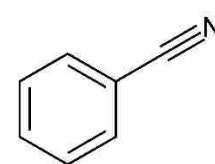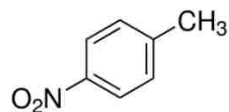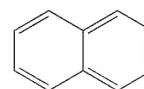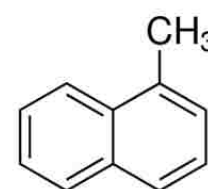
Appendix B – Molar Absorptivity

Figure 72 Molar Absorptivity of CTA calibration curves.

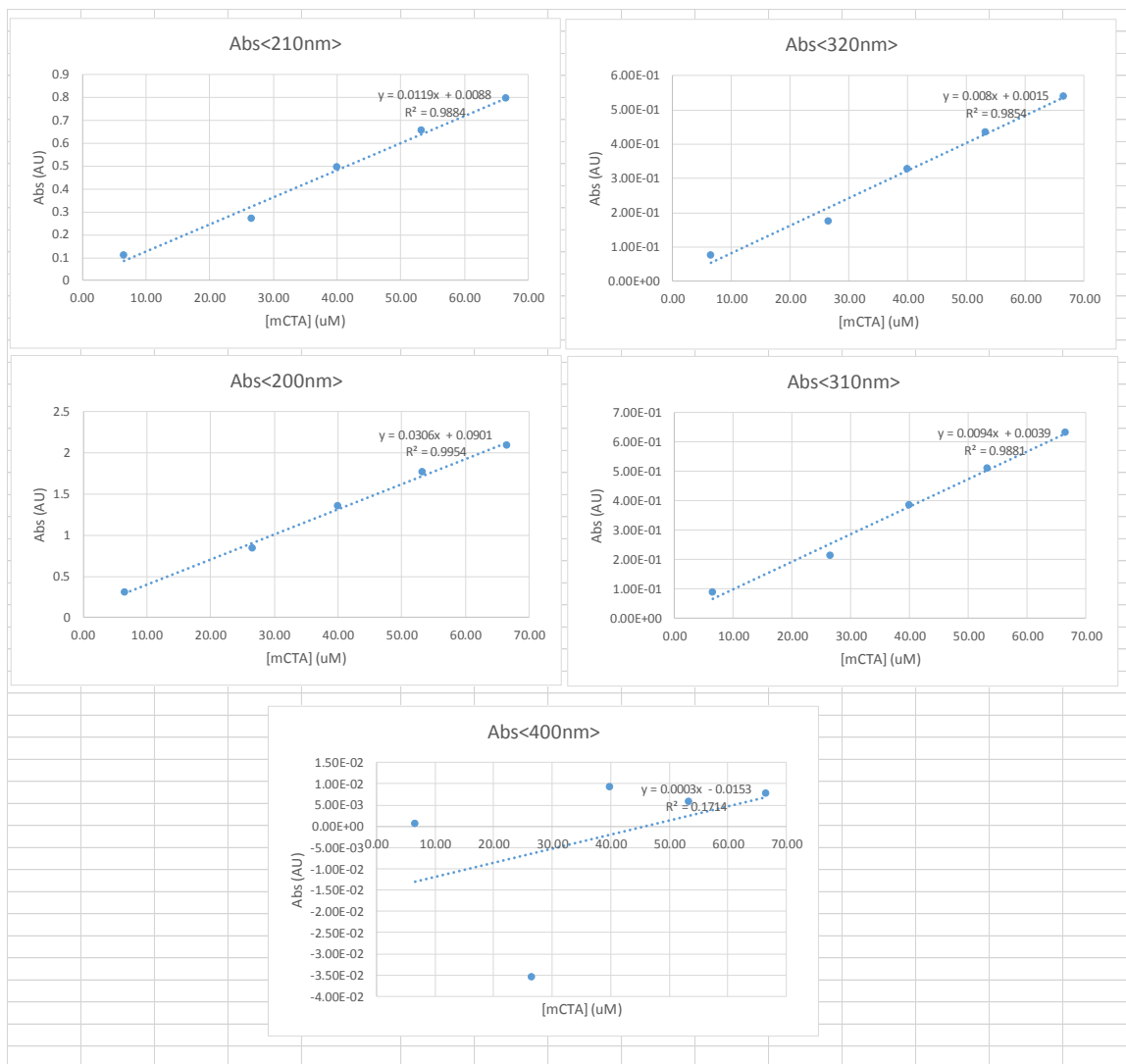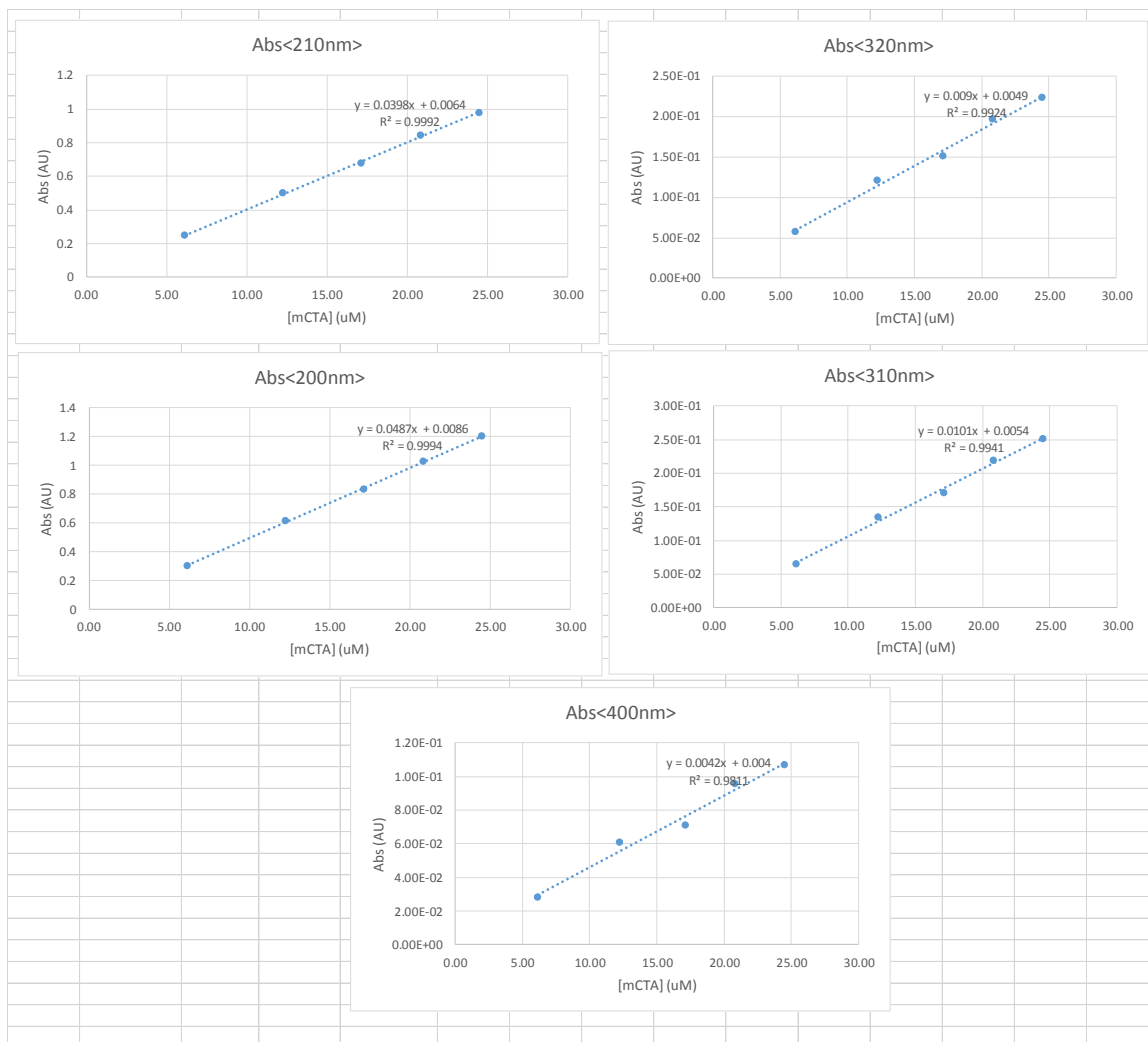*Figure 73 Molar Absorptivity of AMPS mCTA calibration curves.*

Figure 74 Molar Absorptivity of BAAMPS (LH-5) NP calibration curves.

Appendix C – SEM Images

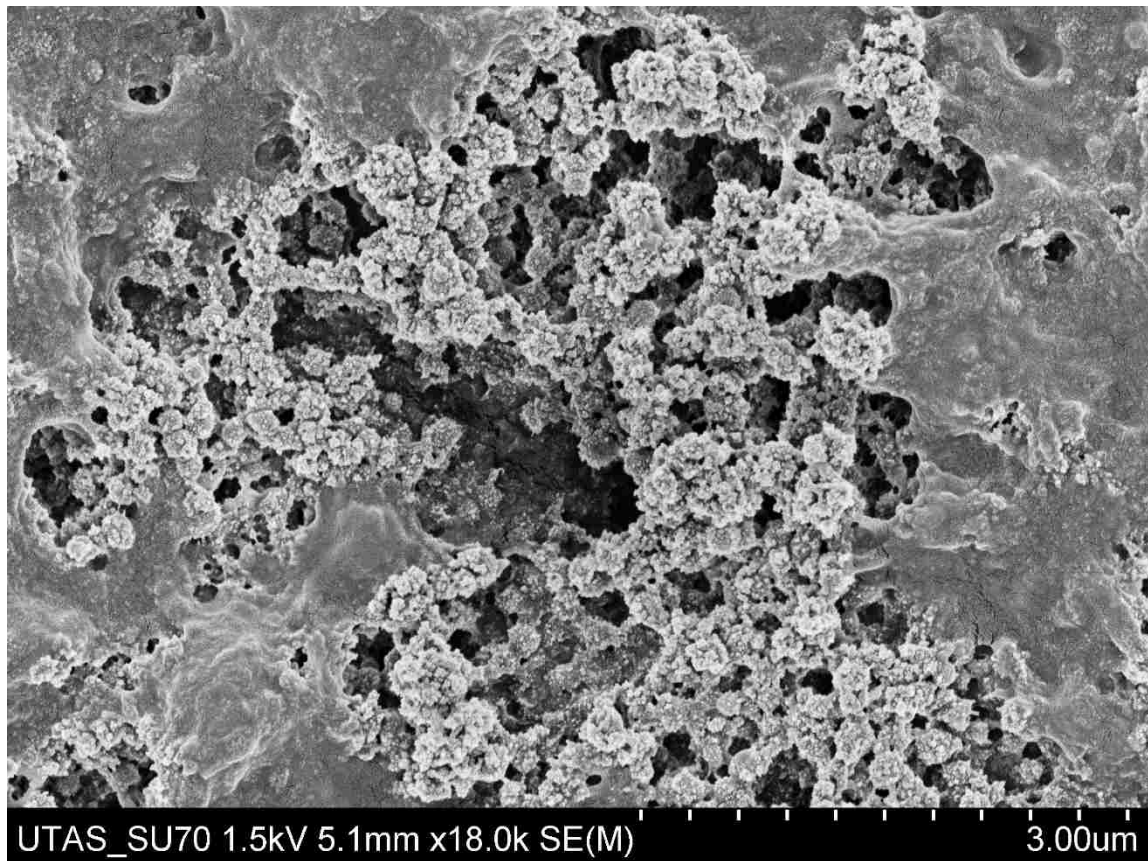
UTAS_SU70 1.5kV 5.1mm x18.0k SE(M) 3.00um

Figure 75 SEM image of dried large BAAMPS (LH-5) material. The micro structures are similar in diameter to DLS measurements, although desolation appears to have resulted in the flocculation of most of the polymer NPs into an amorphous solid.
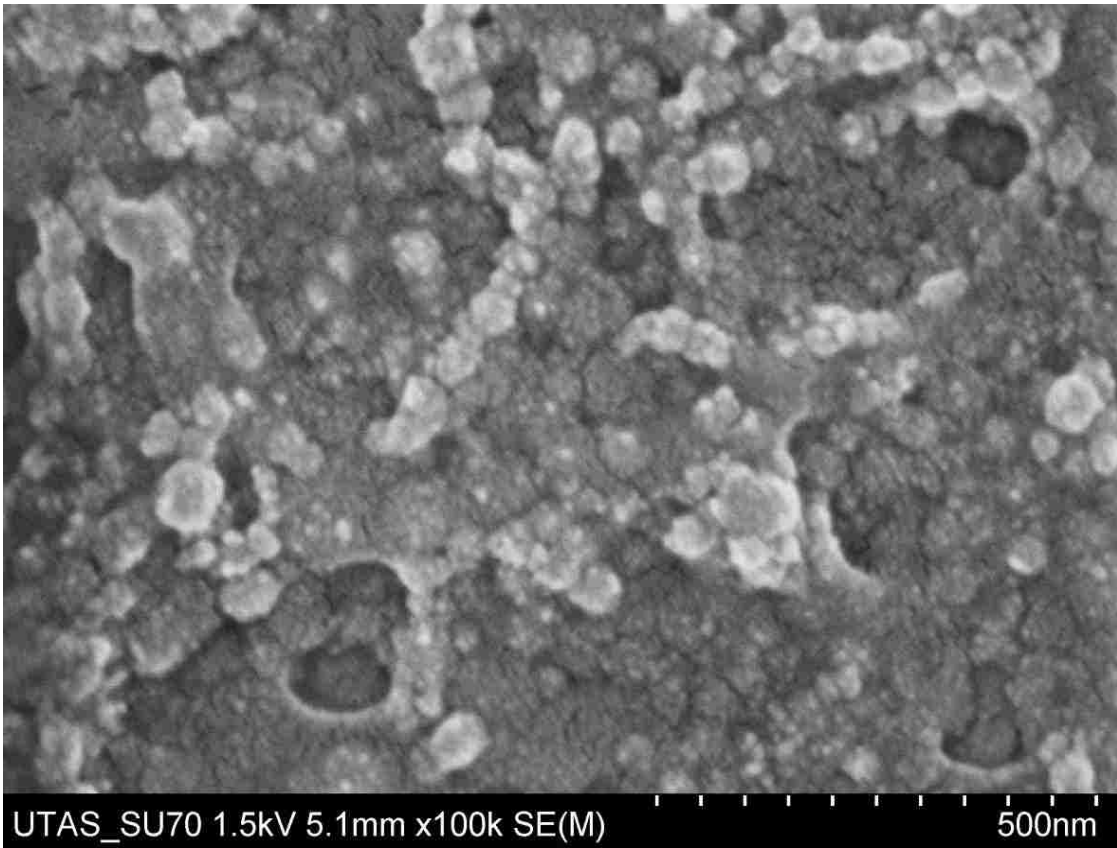
Figure 76 SEM image of large MAAMPS (LH-103) material. If the blobs are infact deslovated NPs they have droped to about half the size measured by DLS.

…happily ever after.